Theoretical Studies of Quantum Electrodynamics for Local Picture of Electron Spin and Time-evolution Simulation Method of Operators

Masahiro Fukuda

2016

Theoretical Studies of Quantum Electrodynamics for Local Picture of Electron Spin and Time-evolution Simulation Method of Operators

Masahiro Fukuda

Department of Micro Engineering

Kyoto University

2016

Contents

General Introduction

Recently, advances in atom- and nano-technology are remarkable. It is now possible to measure, fabricate, and control structures on the atomic and molecular scale. Even a single photon and a single electron spin can be measured and manipulated by the current technology of photonics and spintronics. Considering such progress in experiments, as for the theoretical side, theoretical prediction of physical phenomena and evaluation of physical properties in a local region have been growing in importance. In order to treat spin properties in a local region theoretically, it is essential to discuss them on the basis of relativistic quantum field theory. In particular, in atomic and molecular scales, it is important to discuss systems consisted of electrons, nuclei and photons on the basis of quantum electrodynamics (QED). In the field of quantum chemistry, relativistic theory and QED have been regarded as only a slight correction. However, the concept of "locality" based on relativistic theory gives novel images to physical phenomena and mechanisms of chemical reactions. Hence, in this study, the local picture of electron spin and the first principle calculation method based on QED are discussed.

The following three things are needed to calculate physical quantities numerically in the framework of QED. The first one is to define local physical quantity operators. The second one is to compute time evolution of quantum field operators. The last one is to compute the time evolution of a wavefunction, which corresponds to the state vector of quantum field theory, as is done in quantum mechanics of point particles. In this study, since it is difficult to prepare the state vector by quantum field theory as the first step, a quantum mechanical wave packet of the steady electronic state is used as an approximation. Under the approximation, numerical calculations of local physical quantities for spin are performed in order to discuss local distributions of spin-related physical quantities which are derived from operators by relativistic quantum field theory. Moreover, a formulation of a numerical

simulation method of the time evolution of the quantum field operators is discussed with aim for preparation of a state of QED.

This thesis is organized as follows. PART I (Chapter 1-3) is devoted to the theoretical studies of the local picture of electron spin. In the framework of QED, the electron has mainly three fundamental properties: charge, spin and mass. Strictly speaking, local physical quantities for the electron are given by three symmetries. The first one is the electric charge current density derived from the gauge symmetry. This is a famous quantity which consists of the electric charge density and conventional charge current density. The second one is the chiral current density derived from the chiral symmetry, which is partially conserved approximately symmetry for the electron. The chiral current density consists of the zeta potential and the spin angular momentum density. The last one is the energy-momentum tensor density derived from the general principle of relativity. The energy-momentum tensor density consists of the energy density, momentum density and stress tensor density. Recently, the "quantum spin vorticity theory" is proposed as a consequence of the general relativistic symmetry of the energy-momentum tensor. The quantum spin vorticity theory can give the time evolution equations of the electronic momentum density and the spin angular momentum density as equations which relate local mechanical physical quantities derived from the energy-momentum tensor density. These local images of an electronic state by the quantum spin vorticity theory can help us to understand spin phenomena in condensed matter and molecular systems from a unified viewpoint.

In Chapter 1, local physical quantities for spin are investigated on the basis of the four- and two-component relativistic quantum theory. In the quantum field theory, two types of the torque densities appear in the equation of motion of the spin angular momentum density operator. One is the "spin torque density", which has the same form as the torque derived by the quantum mechanics. The other torque density is called as the "zeta force density" operator, which originates from the spatial distribution of the chiral component of the electron density. The zeta force, which is the gradient of the zeta potential, does not appear in the quantum mechanical Heisenberg equation for spin due to the definition of the inner product including the integration over the whole region, the zeta force density can have nonzero local contribution. The spin torque density, the zeta force density and the zeta potential, which are significant physical quantities for spin to describe a local picture of spin

dynamics based on the quantum field theory, are studied by using Li atom and C_6H_6 in the steady ground states. In addition, a calculation method of these local physical quantities based on the two-component relativistic quantum theory is discussed. Some different types of relativistic numerical calculations of local physical quantities in Li atom and C_6H_6 are demonstrated and compared. Local physical quantities for each orbital are also discussed, and it is shown that a total zeta potential is given as a result of some cancellation of large contributions from each orbital.

In Chapter 2, the local spin dynamics of the electron is studied from the viewpoint of the electric dipole moment (EDM) of the electron in the framework of quantum field theory. Heavy polar diatomic molecules are known as the most promising candidates for experiments of the EDM of the electron, which is a hopeful and inexpensive probe of physics beyond the standard model of particle physics. The improvements of the computational accuracy of the effective electric field ($\mathcal{E}_{\rm eff}$) for the EDM and understanding of spin precession are important for experimental determinations of the upper bound of the EDM. In this chapter, calculations of $\mathcal{E}_{\rm eff}$ in YbF ($^2\Sigma_{1/2}$), BaF ($^2\Sigma_{1/2}$), ThO ($^3\Delta_1$), and HF^+ ($^2\Pi_{1/2}$) are performed on the basis of the restricted active space configuration interaction approach by using the four-component relativistic electronic structure calculation. The spin precession is also discussed from the viewpoint of the local spin torque dynamics. It is shown that a new contribution to the torque density for spin is brought into by the EDM. In addition, distributions of the local spin angular momentum density and torque densities induced by external fields in the above molecules are calculated and a property related with large $\mathcal{E}_{\rm eff}$ is discussed.

In Chapter 3, the spin Hall effect as an application of the spin vorticity theory is discussed. It is proposed that the dynamical picture of the spin Hall effect can be explained as the generation of the spin vorticity by the applied electric field on the basis of the "quantum spin vorticity theory", which describes the equation of motion of local spin and the vorticity of spin in the framework of the quantum field theory. Similarly, it is proposed that the dynamical picture of the inverse spin Hall effect can be explained as the acceleration of the electron by the rotation of the spin torque density as driving force accompanying the generation of the spin vorticity. These explanations by the spin vorticity defined in the quantum spin vorticity theory can help us to understand spin phenomena in condensed matter and molecular systems from a unified viewpoint.

PART II (Chapter 4-6) is devoted to studies of the time-evolution simulation method of operators in QED. As mentioned in PART I, QED is significant to analyze electronic structures by local physical quantities. Furthermore, QED plays an important role even in the long range intermolecular interactions since QED is best suited to account for the finite speed of propagation of the photon automatically. In this part, a formulation of time evolution of a system which consists of the electrons, nuclei and photons is discussed in the framework of QED.

In Chapter 4, a formulation of time evolution of physical quantities is discussed in the framework of the Rigged QED. The Rigged QED is a theory which has been proposed to treat dynamics of electrons, photons and atomic nuclei in atomic and molecular systems in a quantum field theoretic way. To solve the dynamics in the Rigged QED, different techniques from those developed for the conventional QED are needed. As a first step toward this issue, a procedure to expand the Dirac field operator, which represents electrons, by the electron annihilation/creation operators and solutions of the Dirac equation for electrons in nuclear potential is proposed. Similarly, the Schrödinger field operators, which represent atomic nuclei, are expanded by nucleus annihilation/creation operators. Then, time evolution equations for these annihilation and creation operators are derived and a calculation method of time evolution of the operators for physical quantities is discussed. In addition, a method to approximate the evolution equations of the operators by the evolution equations for the density matrices of electrons and atomic nuclei is proposed. By solving the equations numerically under this approximation, it is found that "electron-positron oscillations", the fluctuations originated from virtual electron-positron pair creations and annihilations, appear in the charge density of a hydrogen atom.

In Chapter 5, the discussion in Chapter 4 is advanced by including the effect of the self-energy process, in which the electron emits a photon and then absorbs it again. As a result, the period of the electron-positron oscillations becomes shorter by including the self-energy process, and it can be interpreted as the increase in the electron mass due to the self-energy.

In Chapter 6, the method to compute integrals which appear in the retarded potential term for a real-time simulation based on QED is discussed. These integrals do not appear in the quantum chemistry computation using the electrostatic Hamiltonian, and they are

oscillatory integrals over the infinite interval, which are in general difficult to make converge. Therefore, the retarded potential term is ignored in the previous chapter. In this chapter, it is found that the oscillatory integrals over the infinite interval involved in them can be efficiently performed by the method developed by Ooura and Mori based on the double exponential formula.

Part I

Theoretical Studies of Local Picture of Electron Spin in Quantum Electrodynamics

Chapter 1

Local Physical Quantities for Spin Based on the Relativistic Quantum Field Theory in Molecular Systems

1.1 Introduction

Spin is one of the most significant nature of electron. Recently, a considerable number of studies for spin are reported in various fields such as spintronics, multiferroics and molecular spin science. The materials used in these fields are already in nano-scale. Therefore, the unified understanding of the nature of local spin in the electronic state of condensed matter and molecular systems based on the fundamental theory is desired.

A number of equations which describe the spin dynamics have been already proposed. For example, the Landau-Lifshitz-Gilbert equation [1], which is introduced phenomenologically, is widely used in the field of the spintronics. Larmor precession, Thomas precession and BMT (Bargmann-Michel-Telegdi) equation are also known as the text book matters [2]. More generally, the time derivative of the spin angular momentum is treated by the Heisenberg equation for a given Hamiltonian in the relativistic quantum mechanics [3].

A physical quantity in the framework of the quantum mechanics is defined only after integrating over the whole region. As for the spin, the spin torque is defined as the time derivative of the spatial integration of the spin angular momentum density by using the quantum mechanical Heisenberg equation, $d\vec{s}_e/dt = \frac{i}{\hbar}[H, \vec{s}_e\,]$. On the other hand, in the

framework of the quantum field theory, a physical quantity is defined as an expectation value of a density operator at each space-time. Since the local spin angular momentum density operator, $\hat{s}_e^i(x) = \hat{\psi}(x)\frac{\hbar}{2}\Sigma^i\hat{\psi}(x)$, is described by continuum field operators, the torque density operator for spin defined by $\partial\hat{s}_e^i(x)/\partial t$ can include the internal torque which originates from the internal structure of the electronic state, besides one induced by the external fields. Hence, the time derivative of the spin angular momentum density operator, $\partial\hat{s}_e^i(x)/\partial t = \hat{t}_e^i(x) + \hat{\zeta}_e^i(x)$, gives a new torque density operator $\hat{\zeta}_e^i(x)$. It is different from the "spin torque density" operator, $\hat{t}_e^i(x) = -\epsilon_{ijk}\frac{c}{2}\left[\hat{\psi}^\dagger(x)\gamma^0\gamma^k\left(-i\hbar\hat{D}_e^j(x)\right)\hat{\psi}(x) + h.c.\right]$, which has the same form as the torque derived by the quantum mechanics. This new torque density operator is called the "zeta force density" operator [4, 5], $\hat{\zeta}_e^i(x) = -\partial_i\left(\frac{\hbar c}{2}\hat{\psi}(x)\gamma_5\hat{\psi}(x)\right)$. Due to the existence of the zeta force density, the spin torque density can have non-zero contribution even in a steady state. Moreover their torque density can exist even if the spin angular momentum density is zero over the whole region. Thus, local physical quantities and their related equations help us to understand physical properties of a local region in a molecule and an atom and chemical reaction mechanisms from a new point of view.

In order to investigate the nature of the local physical quantities in a molecular system, the state vector should be prepared apart from the definition of the quantum field theoretic density operator. It is so difficult to prepare the state vector by the quantum field theory that we use a quantum mechanical wave packet as an approximation. Even if we use the quantum mechanical wave packet, we need to rely on the *ab initio* calculation. In particular, the relativistic electronic structure calculation is necessary to calculate the local physical quantities for spin. Our group has already discussed the local physical quantities for spin by using the four-component relativistic calculations for spin stationary state of diatomic system of alkali atoms [6], transition element atoms [7], and allene type molecules with chiral and achiral structures [8]. However, the four-component relativistic calculations consume enormous computational time and cost. Therefore, in this paper we also discuss how to treat the local physical quantities for spin by two-component relativistic wave packets.

This paper is organized as follows. At first, in order to clarify the nature of spin from the viewpoint of the fundamental theory, we show that the equation of the local spin dynamics under the external gravity in the quantum field theory is derived naturally as a consequence of the general principle of relativity. This equation is called the "spin vorticity principle".

We also explain how the spin vorticity principle gives the equation of motion of local spin and the vorticity of spin in the limit to the Minkowski space-time. After explaining the feature of local physical quantities for spin, we mention problems for applying the two-component relativistic wave packet to calculations of local physical quantities. We discuss the formulation of the two-component expressions of the local physical quantities for spin in a steady state. Finally, some different types of relativistic numerical calculations of local physical quantities in Li atom and C_6H_6 are demonstrated and compared. Then the distributions of local physical quantities for each orbital are discussed and we find that total local physical quantities are given as a result of some cancellation of large contributions from each orbital.

1.2 Theory

1.2.1 Spin vorticity theory

In this section, we review the spin vorticity theory [9–12]. First of all, we assume the quantum electrodynamics system under external gravity. To treat the Dirac field under the external gravity we have to use vierbein formulation [13]. This formulation enables us to construct the gravitational covariant derivative of the Dirac field

$$\hat{D}_{e\mu}(g) = \hat{D}_{e\mu} + i\frac{1}{2\hbar}\gamma_{ab\mu}J^{ab}, \tag{1.1}$$

$$\hat{D}_{e\mu} = \partial_\mu + i\frac{Z_e e}{\hbar c}\hat{A}_\mu, \tag{1.2}$$

where $\hat{D}_{e\mu}$ is the gauge covariant derivative, $J^{ab} = \frac{i\hbar}{4}\left[\gamma^a, \gamma^b\right]$, γ^a are the gamma matrices, $\gamma_{ab\mu}$ is the spin connection [14], e is the electron charge ($e > 0$), $Z_e = -1$, and $\hat{A}_\mu$ is the gauge field. Here, Greek indices and Latin indices a and b run over 0 to 3. The former refers to the general coordinate indices, while the latter refers to the local Lorentz frame indices. We adopt the Einstein summation convention. We put a hat to indicate a quantum operator to distinguish it from a c-number. The gravitational covariant derivative of the Dirac spinor of the electron $\hat{D}_{e\mu}(g)\hat{\psi}$ transforms covariantly under both of the general coordinate and local Lorentz transformations. Then, the Lagrangian density $\hat{\mathcal{L}}$ for the quantum electrodynamics

system under external gravity is written as

$$\hat{\mathcal{L}} = \hat{\mathcal{L}}_e + \hat{\mathcal{L}}_{\rm EM}, \tag{1.3}$$

$$\hat{\mathcal{L}}_e = \frac{c}{2}\left[\hat{\bar{\psi}}(i\hbar\gamma^a e_a{}^\mu \hat{D}_{e\mu}(g) - m_e c)\hat{\psi} + h.c.\right], \tag{1.4}$$

$$\hat{\mathcal{L}}_{EM} = -\frac{1}{16\pi}\hat{F}_{\mu\nu}\hat{F}_{\rho\sigma}g^{\mu\rho}g^{\nu\sigma}, \tag{1.5}$$

where $\hat{\bar{\psi}} = \hat{\psi}^\dagger\gamma^0$, $e_a{}^\mu$ the vierbein field, m_e the electron mass, c the speed of light in vacuum and $g^{\mu\nu}$ the metric tensor. The electromagnetic field strength tensor is $\hat{F}_{\mu\nu} = \partial_\mu\hat{A}_\nu - \partial_\nu\hat{A}_\mu$.

The symmetric energy-momentum tensor is defined as [13]

$$\hat{T}_{\mu\nu} = \frac{1}{\sqrt{-g}}\eta_{ab}e^b{}_\nu\frac{\delta\left(\hat{\mathcal{L}}\sqrt{-g}\right)}{\delta e_a{}^\mu} = \hat{T}_{e\mu\nu} + \hat{T}_{{\rm EM}\mu\nu}, \tag{1.6}$$

$$\hat{T}_{e\mu\nu} = -\hat{\varepsilon}^\Pi_{\mu\nu} - \hat{\tau}^\Pi_{e\mu\nu}(g) - g_{\mu\nu}\hat{\mathcal{L}}_e = \hat{T}_{e\nu\mu}, \tag{1.7}$$

$$\hat{T}_{{\rm EM}\mu\nu} = -\frac{1}{4\pi}g^{\rho\sigma}\hat{F}_{\mu\rho}\hat{F}_{\nu\sigma} - g_{\mu\nu}\hat{\mathcal{L}}_{\rm EM} = \hat{T}_{{\rm EM}\nu\mu}, \tag{1.8}$$

where $g = \det g_{\mu\nu}$ and $\eta_{\mu\nu} = {\rm diag}(1,-1,-1,-1) = \eta^{\mu\nu}$. In Eq. (1.7), the symmetry-polarized stress tensor $\hat{\tau}^\Pi_{e\mu\nu}(g)$ originates from the direct derivative with respect to the vierbein field $e_a{}^\mu$. The other term $\hat{\varepsilon}^\Pi_{\mu\nu}$ is called the symmetry-polarized geometrical tensor, which originates from the existence of the spin connection [9].

These anti-symmetric parts, $\hat{\varepsilon}^A_{\mu\nu}$ and $\hat{\tau}^A_{e\mu\nu}$, should cancel with each other since the energy-momentum tensor is symmetric. Thus,

$$\hat{\varepsilon}^{A\mu\nu} + \hat{\tau}^{A\mu\nu}_e(g) = 0. \tag{1.9}$$

Eq. (1.9) is called the quantum spin vorticity principle. This equation can describe the spin dynamics even in non-inertial frame. In the limit to the Minkowski space-time, it is revealed that Eq. (1.9) describes spin dynamics. In the limit of $e^a{}_\mu \to \delta^a{}_\mu$ and $g_{\mu\nu} \to \eta_{\mu\nu}$, the symmetry-polarized tensors $\hat{\varepsilon}^\Pi_{\mu\nu}$ and $\hat{\tau}^\Pi_{e\mu\nu}(g)$ are reduced to

$$\hat{\varepsilon}^{\Pi\mu\nu} = -\frac{\hbar}{4Z_e e}\epsilon^{\mu\nu\lambda\sigma}\partial_\lambda\hat{j}_{5\sigma}, \tag{1.10}$$

$$\hat{\tau}^{\Pi\mu\nu}_e = \frac{c}{2}\left[\hat{\psi}^\dagger\gamma^0\gamma^\nu\left(-i\hbar\hat{D}^\mu_e\right)\hat{\psi} + h.c.\right], \tag{1.11}$$

where $\epsilon^{\mu\nu\lambda\sigma}$ is the Levi-Civita tensor, $\hat{j}^\mu_5 = Z_e ec\hat{\bar{\psi}}\gamma^\mu\gamma_5\hat{\psi}$ is the chiral current density and $\gamma_5 = i\gamma^0\gamma^1\gamma^2\gamma^3$. The Levi-Civita tensor $\epsilon^{\mu\nu\lambda\sigma}$ is totally antisymmetric in all the indices and $\epsilon^{0123} = 1$. Substituting Eq. (1.10) and Eq. (1.11) for Eq. (1.9), the equation of motion of

spin and the equation for the vorticity of spin are derived as follows:

$$\frac{\partial}{\partial t}\hat{\vec{s}}_e = \hat{\vec{t}}_e + \hat{\vec{\zeta}}_e, \tag{1.12}$$

$$\mathrm{rot}\hat{\vec{s}}_e = \frac{1}{2}\left[\hat{\bar{\psi}}\vec{\gamma}\left(i\hbar\hat{D}_{e0}\right)\hat{\psi} + h.c.\right] - \hat{\vec{\Pi}}_e, \tag{1.13}$$

where the spin angular momentum density $\hat{\vec{s}}_e$, the spin torque density $\hat{\vec{t}}_e$, the zeta force density $\hat{\vec{\zeta}}_e$, and the kinetic momentum density $\hat{\vec{\Pi}}_e$ are defined as

$$\hat{s}_e^i = \hat{\psi}^\dagger\frac{\hbar}{2}\Sigma^i\hat{\psi} = \frac{\hbar}{2Z_e ec}\hat{j}_5^i, \tag{1.14}$$

$$\hat{t}_e^i = -\epsilon_{ijk}\hat{\tau}_e^{Ajk}, \tag{1.15}$$

$$\hat{\zeta}_e^i = -\partial_i\hat{\phi}_5, \quad \hat{\phi}_5 = \frac{\hbar}{2Z_e e}\hat{j}_5^0, \tag{1.16}$$

$$\hat{\Pi}_e^i = \frac{1}{2}\left[\hat{\bar{\psi}}\gamma^0\left(i\hbar\hat{D}_e^i\right)\hat{\psi} + h.c.\right]. \tag{1.17}$$

In the equations above, Σ^i is the 4×4 Pauli matrix, and ϵ_{ijk} is the Levi-Civita tensor. Hereafter, Latin letters run from 1 to 3.

The spin angular momentum density $\hat{\vec{s}}_e$ and the zeta potential $\hat{\phi}_5$ correspond to the spatial components and the zero-th component of the chiral current density $\hat{j}_5^\mu$, respectively. This fact indicates that the zeta potential is as significant as the spin angular momentum density. Another expression of the zeta potential is $\hat{\phi}_5 = \frac{\hbar c}{2}\left(\hat{\psi}_R^\dagger\hat{\psi}_R - \hat{\psi}_L^\dagger\hat{\psi}_L\right)$, where the right-handed and left-handed spinors are $\hat{\psi}_R = [(1+\gamma_5)/2]\hat{\psi}$ and $\hat{\psi}_L = [(1-\gamma_5)/2]\hat{\psi}$, respectively. Similarly, the Lagrangian of the electron can rewritten with these spinors as

$$\hat{\mathcal{L}}_e = \frac{c}{2}\left[\hat{\bar{\psi}}_L(i\hbar\gamma^\mu\hat{D}_{e\mu})\hat{\psi}_L + \hat{\bar{\psi}}_R(i\hbar\gamma^\mu\hat{D}_{e\mu})\hat{\psi}_R - m_e c\left(\hat{\bar{\psi}}_L\hat{\psi}_R + \hat{\bar{\psi}}_R\hat{\psi}_L\right)\right] + h.c. \tag{1.18}$$

This mass term, which originates from the Yukawa interaction between the Dirac field and the Higgs field according to the standard model [14], mixes $\hat{\bar{\psi}}_L$ and $\hat{\bar{\psi}}_R$. Hence, the zeta potential is not conserved due to this mixing.

As shown in Eq. (1.16), the gradient of the zeta potential is the zeta force density, which compensates the spin torque density derived by the stress tensor. Apparently the spin torque density is the same form as the torque derived by the Heisenberg equation of spin in the relativistic quantum mechanics [3]; concretely,

$$\frac{d}{dt}\langle\langle\psi|\frac{\hbar}{2}\Sigma^i|\psi\rangle\rangle = \langle\langle\psi|\frac{1}{2}\left(-i\hbar c\epsilon_{ijk}\gamma^0\gamma^k D_{ej}\right)|\psi\rangle\rangle, \tag{1.19}$$

where $|\psi\rangle\rangle$ is a quantum mechanical ket vector. Here, we mention that the definitions of the physical quantities are different between the quantum mechanics and the quantum field

theory. While the quantum field theory gives the physical quantities as an expectation value for a time-independent state vector in the Heisenberg picture $|\Phi\rangle$, the physical quantity of the quantum mechanics is defined only after integrating over the whole region. Namely,

$$\langle\langle\psi|\frac{\hbar}{2}\vec{\Sigma}|\psi\rangle\rangle \leftrightarrow \int \langle\Phi| : \hat{\psi}^{\dagger}(x)\frac{\hbar}{2}\vec{\Sigma}\hat{\psi}(x) : |\Phi\rangle d^3\vec{r}, \tag{1.20}$$

where we represent normal ordering with colons. In the quantum field theory, the state vector should be prepared for calculations of physical quantities apart from the definition of the quantum field theoretic density operator. When we use a relativistic quantum mechanical wave packet as an approximation of a state vector of the quantum field theory, we can discuss local physical quantities by reading the electron field operator $\hat{\psi}$ as the quantum mechanical wave packet ψ. This approximation is used in later sections. Let us now return to Eq. (1.19). The zeta force density does not appear in Eq. (1.19) since the zeta force is lost due to the definition of the inner product in the quantum mechanics as we mentioned above. Nevertheless, the zeta force can exist in a local region and its contribution is significant for spin control in a molecular scale. Actually, the zeta potential is observable as the difference of the chirality components of the electron density. The zeta force is its gradient and also observable. Therefore this novel torque contribution is potentially important for spin phenomena.

In addition, the spin vorticity in Eq. (1.13) plays a crucial role as a component of the momentum density in spin dynamical phenomena. The electronic momentum density $\hat{P}_e^i = \frac{1}{c}\hat{T}_e^{i0}$ is given as

$$\hat{\vec{P}}_e = \hat{\vec{\Pi}}_e + \frac{1}{2}\mathrm{rot}\hat{\vec{s}}_e. \tag{1.21}$$

We discuss these local physical quantities in a benzene molecule by numerical calculations in the later section.

1.2.2 Zeta potential and spatial symmetry

As we mentioned above, the zeta potential is the source of the zeta force density, which plays an important role for spin control in the local region. We explain here a relation between the zeta potential and the spatial symmetry of a concerning system in order to grasp a feature of the zeta potential. For simplicity, we discuss hereafter in the framework of

the relativistic quantum mechanics except for the definition of the local physical quantities. The spatial rotation operator around k-axis and the parity operator for four-component relativistic electronic state ψ are given as $S_{\rm R}(\omega) = \cos\frac{\omega}{2} + i\Sigma^k \sin\frac{\omega}{2}$ and $S_{\rm P} = \eta\gamma^0$ ($|\eta|^2 = 1$), respectively [3]. The reflection operator can be written as $S_{\rm m} = S_{\rm R}(\pi)S_{\rm P}$

As for the zeta potential $\phi_5 \propto \psi^\dagger\gamma_5\psi$, it is easy to derive following equations,

$$\left(S_{\rm P}\psi\right)^\dagger \gamma_5 S_{\rm P}\psi = -\psi^\dagger\gamma_5\psi, \tag{1.22}$$

$$\left(S_{\rm R}(\omega)\psi\right)^\dagger \gamma_5 S_{\rm R}(\omega)\psi = \psi^\dagger\gamma_5\psi, \tag{1.23}$$

$$\left(S_{\rm m}\psi\right)^\dagger \gamma_5 S_{\rm m}\psi = -\psi^\dagger\gamma_5\psi. \tag{1.24}$$

These equations mean the following two relations between the zeta potential and the symmetry of ψ. (i) If ψ has n-fold rotational symmetry (excluding the phase factor), the zeta potential has the same symmetry. (ii) If ψ has reflection symmetry (excluding the phase factor), the sign of the zeta potential is reversed with the reflection plane. From these relations, the interesting features for atoms and molecules are revealed. While the zeta potential of single atoms and linear molecules is zero due to their C_∞ symmetry, more complex molecules can have the nonzero zeta potential. This fact means the zeta potential can be generated by breaking of some symmetry in ψ along with the formation process of the complex molecules.[1]

1.2.3 Local picture change errors

In order to investigate the local physical quantities in large molecular systems, the relativistic two-component formulation is suitable in comparison with the four-component formulation, which consumes much time and cost. However, local physical quantities cannot be derived rigorously by a two-component wave function. Here, we mention this problem with local physical quantities calculated from two-component relativistic wave packets. The Foldy-Wouthuysen-Tani transformation [15] is widely applied to construct a relativistic

[1]Incidentally, this explanation is apparently in contradiction with the previous works [6, 7], where the calculated zeta potential in atoms and linear molecules had finite values. However, this is because the symmetries of the ψ used in the previous works were broken a little. We emphasize that the local physical quantities such as the zeta potential are more sensitive to the accuracy of ψ than integrated quantities such as the total energy.

two-component formulation. The large and small components of the Hamiltonian can be decoupled by a unitary operator U as

$$H_{4c} = \begin{bmatrix} h_{LL} & h_{LS} \\ h_{SL} & h_{SS} \end{bmatrix}, \quad U H_{4c} U^\dagger = \begin{bmatrix} h_{++} & 0 \\ 0 & h_{--} \end{bmatrix}. \tag{1.25}$$

The wave packet is transformed as

$$\psi_{2c} = U\psi_{4c} = \begin{pmatrix} \psi_{2c+} \\ \psi_{2c-} \end{pmatrix}. \tag{1.26}$$

This transformation does not change integrated value of the energy density:

$$\int \psi_{4c}^\dagger H_{4c} \psi_{4c} d^3\vec{r} \;=\; \int \psi_{2c+}^\dagger h_{++} \psi_{2c+} d^3\vec{r} + \int \psi_{2c-}^\dagger h_{--} \psi_{2c-} d^3\vec{r}. \tag{1.27}$$

Integrated physical quantities are often approximated as

$$\begin{aligned} \int \psi_{4c}^\dagger \Omega_{4c} \psi_{4c} d^3\vec{r} \;&=\; \int \psi_{2c}^\dagger U \Omega_{4c} U^\dagger \psi_{2c} d^3\vec{r} \\ &\approx\; \int \psi_{2c+}^\dagger [\Omega_{4c}]_{LL} \psi_{2c+} d^3\vec{r}, \end{aligned} \tag{1.28}$$

where Ω_{4c} is an arbitrary operator. This approximation causes the so-called picture change error [16]. Besides the picture change error, there is another problem when we treat local physical quantities by the two-component wave packets. Since the unitary operator U includes some differential operators, local quantities are not conserved before and after the transformation:

$$\psi_{4c}^\dagger \Omega_{4c} \psi_{4c} \neq \psi_{2c}^\dagger U \Omega_{4c} U^\dagger \psi_{2c}. \tag{1.29}$$

This means that local physical quantities cannot be derived rigorously by the two-component wave function defined by this unitary transformation with the existence of the Dirac mass term. This difficulty is characteristic of evaluation of local physical quantities. For this reason, we calculate local physical quantities by using the two-component relativistic wave function as an approximation of the large component of the four-component relativistic wave function.

1.2.4 Two-component expressions of the local physical quantities

Next, we discuss how to express the local physical quantities by using the large component of the four-component relativistic wave function. The time-independent Dirac equation

neglecting the vector potential is written as

$$\left(Z_e eA_0 - E\right)\psi^L - i\hbar c\sigma^m \partial_m \psi^S = 0, \tag{1.30}$$

$$-i\hbar c\sigma^m \partial_m \psi^L + \left(Z_e eA_0 - E - 2m_e c^2\right)\psi^S = 0, \tag{1.31}$$

where E is the energy, $\psi = \begin{pmatrix} \psi^L \\ \psi^S \end{pmatrix}$ is a relativistic four-component wave function, σ^m are the 2×2 Pauli matrices.

It is easy to be derived from Eq. (1.31)

$$\psi^S = \frac{-i\hbar K}{2m_e c}\sigma^m \partial_m \psi^L, \tag{1.32}$$

$$K = \frac{2m_e c^2}{(2m_e c^2 + E - Z_e eA_0)}. \tag{1.33}$$

We can write Eq. (1.30) using Eq. (1.32) as

$$-\frac{\hbar^2}{2m_e}\left[K\partial_n\partial_n\psi^L + (\partial_n K)\partial_n\psi^L + i\varepsilon_{mnl}\sigma^l(\partial_m K)\partial_n\psi^L\right] + Z_e eA_0\psi^L = E\psi^L. \tag{1.34}$$

Considering the non-relativistic limit $c \to \infty$, then $K \to 1$, and Eq. (1.34) is reduced to

$$-\frac{\hbar^2}{2m}\partial_n\partial_n\psi^L + Z_e eA_0\psi^L = E\psi^L, \tag{1.35}$$

which has the same form of the Schrödinger equation. The local physical quantities are also reduced to

$$s_e^k = \frac{\hbar}{2}\psi^{L\dagger}\sigma^k\psi^L, \tag{1.36}$$

$$\phi_5 = -\frac{i\hbar^2}{4m}\psi^{L\dagger}\sigma^m\partial_m\psi^L + h.c.\ , \tag{1.37}$$

$$\zeta_e^k = \frac{i\hbar^2}{4m}\partial_k\left(\psi^{L\dagger}\sigma^m\partial_m\psi^L\right) + h.c.\ , \tag{1.38}$$

$$\tau_e^{\Pi kl} \approx \frac{\hbar^2}{4m}\left[i\varepsilon_{lmn}\partial_m\left(\psi^{L\dagger}\sigma^n\partial_k\psi^L\right) - (\partial_k\psi^L)^\dagger\partial_l\psi^L + \psi^{L\dagger}\partial_k\partial_l\psi^L\right] + h.c.\ , \tag{1.39}$$

$$t_e^k = -\frac{i\hbar^2}{4m}\left[\partial_k\left(\psi^{L\dagger}\sigma^m\partial_m\psi^L\right) - \psi^{L\dagger}\sigma^k\partial_m\partial_m\psi^L\right] + h.c. \tag{1.40}$$

Using Eq. (1.35), the spin torque density is reduced to

$$t_e^k = -\frac{i\hbar^2}{4m}\partial_k\left(\psi^{L\dagger}\sigma^m\partial_m\psi^L\right) + h.c. \tag{1.41}$$

Therefore, the spin torque density and the zeta force density, which exist even in the limit of $c \to \infty$, are exactly canceled with each other in the steady state.

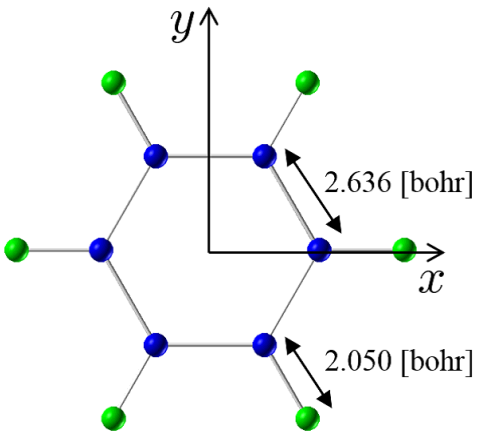

Figure 1.1: Molecular structure of benzene (C_6H_6).

In other words, the difference between Eq. (1.40) and Eq. (1.41),

$$\Delta_e^k = \frac{i\hbar^2}{4m}\psi^{L\dagger}\sigma^k\partial_m\partial_m\psi^L + h.c. \tag{1.42}$$

is zero if the ψ^L obeys Eq. (1.35). Although Eq. (1.42) is not zero when the relativistic interaction contribution is large, this value enables us to estimate roughly the accuracy of the local physical quantities.

1.3 Computational details

We demonstrate calculations of local physical quantities for spin in Li and C_6H_6, whose structure is shown in FIG. 1.1, by using the four- and two-component wave functions of the relativistic quantum mechanics as approximations of state vectors of the quantum field theory. The electronic state for Li is calculated by the Full-Configuration Interaction (FCI) method. For C_6H_6, CISD, Dirac-Hartree-Fock (DHF), Exact-2-Component (X2C) method [17–26] and the Dyall's spin-free Hamiltonian [27] method are employed. The Dyall's spin-free Hamiltonian means the four-component Dirac-Coulomb Hamiltonian without the spin-orbit interaction. These wave functions are derived by using DIRAC13 program package [28]. The uncontracted Dyall's quadruple zeta (QZ) basis set [29] for the Li and double zeta (DZ) basis sets for C_6H_6 are used in our calculations. These basis sets have correlating functions for all shells. Calculations of the local physical quantities are performed by the QEDynamics program package [30] developed in our group. As another example of the two-component method for the benzene, we also employ a local spin density approx-

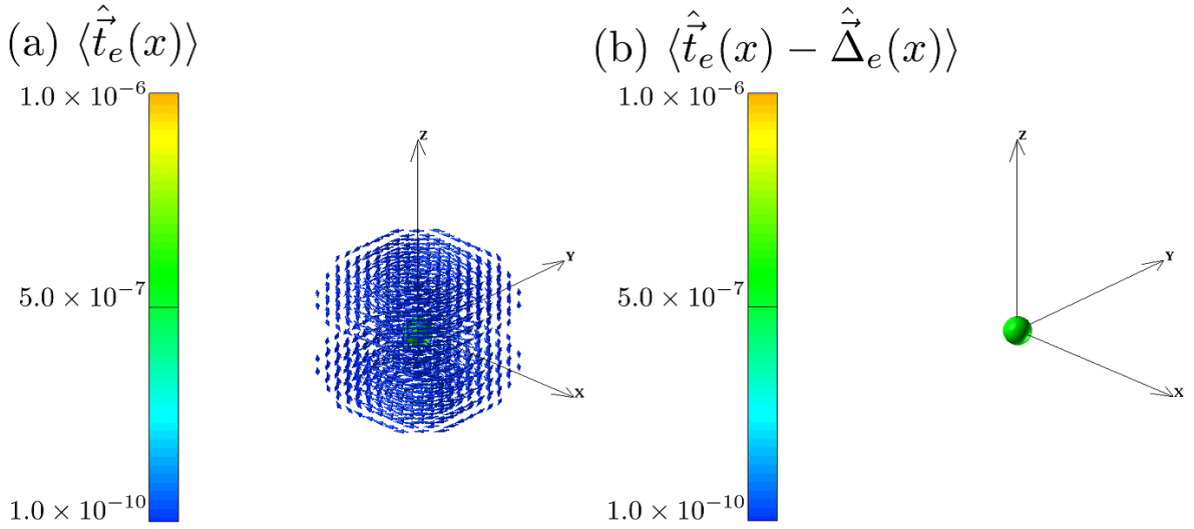

Figure 1.2: The distribution of (a) the spin torque density and (b) $\langle \hat{\vec{t}}_e - \hat{\vec{\Delta}}_e \rangle$ (Eq. (1.42)) in the Li atom.

imation [31] in the density-functional theory (DFT) [32] including the spin-orbit coupling within the pseudopotential scheme. This calculation is performed by an *ab initio* DFT code, OPENMX [33]. We made some modifications on the program code for our purpose of calculating local physical quantities, which are calculated by using the two-component relativistic wave function as a substitute for the large component of the four-component relativistic wave function. Pseudoatomic orbitals centered on atomic sites are used as the basis sets [34]. We use the pseudoatomic orbitals specified by H7.0-$s2p1$ and C7.0-$s3p2d1$, where H and C stands for the atomic symbol, 7.0 represents the cutoff radius (bohr), and $s3p2d1$ means the employment of three, two, and one orbitals for the s, p, and d component, respectively.

1.4 Results and Discussion

At first, the spatial distribution of the spin torque density in the Li atom by the full CI calculation is shown in FIG. 1.2. While the spin torque density is distributed with nonzero values, the spatial distribution of the zeta force density is zero over the whole region as the computational result. This results in inconsistency with Eq. (1.12). As we mentioned in Sec. 1.2.2, the spin torque density and zeta force density in single atoms should be zero due to C_∞ symmetry. For this reason, the spin torque density shown in FIG. 1.2(a) is considered

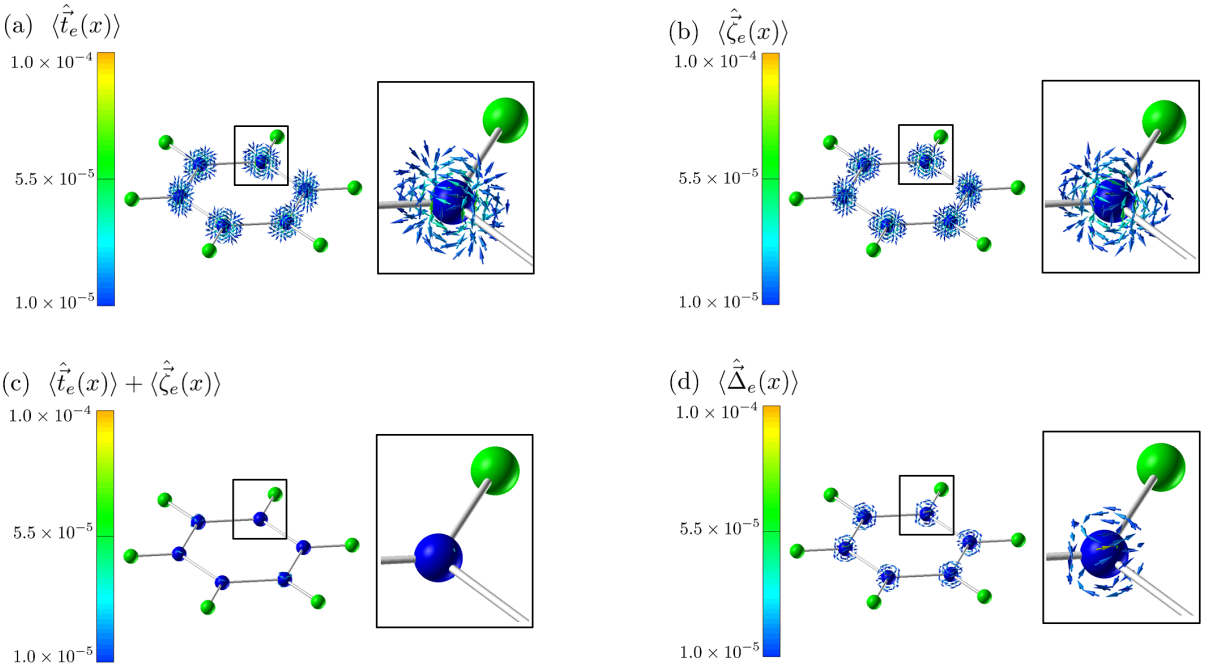

Figure 1.3: The distribution of (a) the spin torque density, (b) the zeta force density, (c) the sum of them and (d) $\langle \hat{\vec{\Delta}}_e(x) \rangle$ in C_6H_6.

to originate from the inaccuracy of our wave function. From the result of the distribution of the $\langle \hat{\vec{t}}_e \rangle - \langle \hat{\vec{\Delta}}_e \rangle$ shown in FIG. 1.2(b), it is confirmed that the inaccuracy of the spin torque density is caused by $\langle \hat{\vec{\Delta}}_e \rangle$. In other words, the accuracy of a wave function can be estimated by $\langle \hat{\vec{\Delta}}_e \rangle$ if the relativistic interaction is small enough to satisfy Eq. (1.35).

Next, we discuss local physical quantities in the ground state of C_6H_6. The numerical results of the spin torque density and the zeta force density by our four-component CI calculation are shown in FIG. 1.3. Unlike the Li atom, C_6H_6 has finite spin torque density and zeta force density. Their distributions concentrate on the carbon nuclei, where the relativistic interaction is a little larger than around the hydrogen nuclei. The cancellation between the spin torque density and the zeta force density shown in FIG. 1.3(c) indicates the accuracy of the results is sufficient. Furthermore, since the value of $\langle \hat{\vec{\Delta}}_e \rangle$ in C_6H_6 (FIG. 1.3(d)) is sufficiently smaller than that of the spin torque density, it is confirmed that these numerical results are appropriate.

The zeta potential in C_6H_6 by each method is shown in FIG. 1.4. When the Dyall's spin-free Hamiltonian is employed, the zeta potential is zero over the whole region, since the

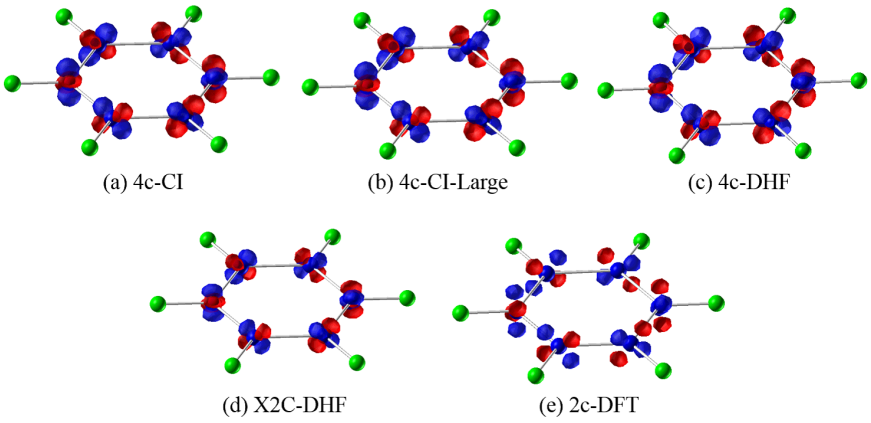

Figure 1.4: The distribution of the zeta potential in each method. Red and blue envelopes represent positive and negative zeta potential iso-surfaces, respectively. The threshold value of isosurfaces of the zeta potential is taken as 2.5×10^{-6} [a.u.]. "4c-CI-Large" means the method by use of substitution of ψ^L to Eq. (1.37). Only 2c-DFT method uses the effective core potential scheme.

Hamiltonian has no spin-orbit interactions. The distribution of the zeta potential obeys the symmetry derived from the molecular symmetry as discussed in Sec. 1.2.2. It is found that the zeta potential in the singlet state of C_6H_6 has nonzero values around carbon nuclei, even though the spin angular momentum density is zero over the whole region. This reason is as follows. Since the electrons in a closed shell are degenerate, the spin angular momentum density of an orbital χ is exactly canceled out by that of its Kramers partner $\chi_{\rm KP} = -i\Sigma^2\chi^*$ (i.e. $\chi^\dagger \frac{\hbar}{2}\vec{\Sigma}\chi = -\chi_{\rm KP}^\dagger \frac{\hbar}{2}\vec{\Sigma}\chi_{\rm KP}$). However, as for the zeta potential, such cancellation does not occur because $\chi^\dagger\gamma_5\chi = \chi_{\rm KP}^\dagger\gamma_5\chi_{\rm KP}$. Therefore, the contribution of the electrons in a closed shell to the zeta potential can be nonzero values. From FIG. 1.4, the zeta potential near carbon nuclei by the 2c-DFT method is different from that by the other methods due to the effective core potential scheme. The zeta potential with the direction of the zeta force on a plane $x = 2.6$[bohr] near the carbon nucleus by the 4c-CI method is shown in FIG. 1.5(a). The calculation results of the zeta potential on lines $y = 0.2$[bohr] and $y = 0.4$[bohr] by 4c-CI, 4c-DHF, X2C-DHF and 2c-DFT are also shown in FIG. 1.5(b) and (c). Their results indicate that the zeta potential near the nucleus is quite large because of stronger relativistic interaction. Even in such regions, the zeta potential given by the X2C-DHF method is in good agreement with that by the four-component methods. Although the accuracy of the

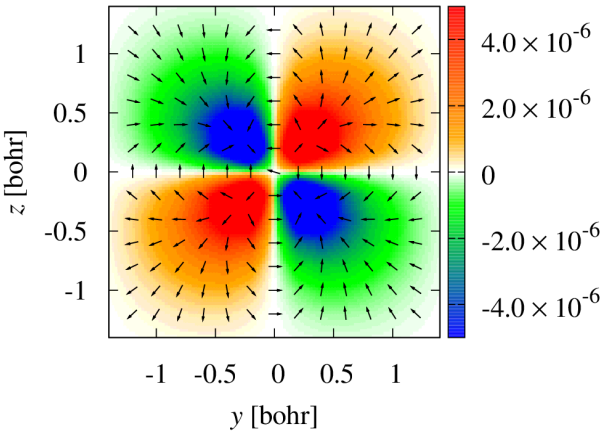

(a) The distribution of the zeta potential on the plane $x = 2.6$[bohr] and the direction of the zeta force density.

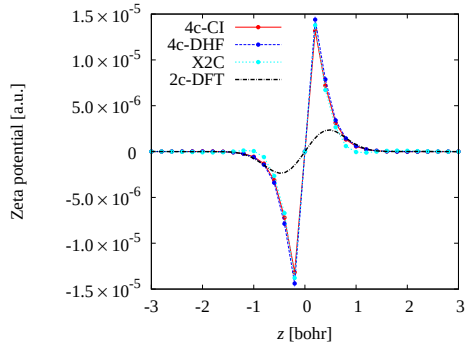

(b) Comparison of the zeta potential on the line $(x, y) = (2.6, 0.2)$[bohr] by 4c-CI, 4c-DHF, X2C-DHF and 2c-DFT.

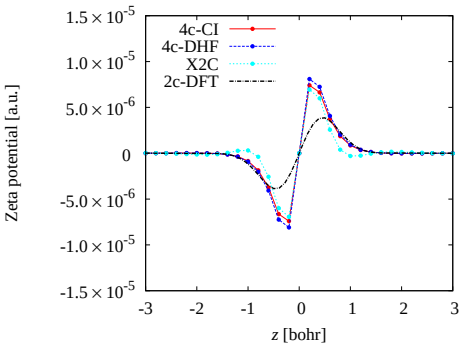

(c) Comparison of the zeta potential on the line $(x, y) = (2.6, 0.4)$[bohr] by 4c-CI, 4c-DHF, X2C-DHF and 2c-DFT.

Figure 1.5: The distribution of the zeta potential on a plane and a line in C_6H_6.

zeta potential given by the 2c-DFT method is not good in the immediate vicinity of the carbon nucleus (see FIG. 1.5(b)) due to the effective core potential, the accuracy is seen to be reasonable at a point where the effect of the core potential is negligible (see FIG. 1.5(c)).

Let us now discuss local physical quantities of each orbital. The orbital energies by Spin-Free (without the spin-orbit interaction) and 4c-DHF methods are shown in TABLE 1.1. Some orbital energies calculated by 4c-DHF are splitting due to the spin-orbit interaction, while they are degenerate when the Spin-Free Hamiltonian is used. Similarly, some large orbital angular momentums of each orbital can be found in the result of the 4c-DHF method in TABLE 1.1. This means large kinetic momentum density of each orbital exists in a local region. The distribution of the kinetic momentum density, half of the spin vorticity and

the electronic momentum density of each orbital by the 4c-DHF are shown in FIGs. 1.6, 1.7 and 1.8, respectively. The kinetic momentum density of each orbital depends on neither the orbital angular momentum nor the spin-orbit interaction energy. Local physical quantities cannot be necessarily discussed by integrated values. However, it is of course true that the orbital angular momentum depends on the distribution of the kinetic momentum density of each orbital. The orbitals which have a similar orbital angular momentum have the similar distribution pattern of the kinetic momentum density. The same thing can be said of half of the vorticity of spin. On the other hand, as shown in FIG. 1.8, each orbital has a different distribution of the total electronic momentum density, which is the sum of the kinetic momentum density and half of the spin vorticity. This is a good example that the relativistic interaction has a great influence on the local physical quantities though it has little effect on the orbital energies for a molecule made of light atoms. Furthermore, considering a photon absorption or emission process, the distribution of the total electronic momentum density of the highest occupied molecular orbital affects that of the momentum density of the interacting photon.

The distributions of the zeta potential of each orbital by the 4c-DHF are shown in FIG. 1.9. The orbitals which have a similar orbital angular momentum have the similar distribution pattern of the zeta potential as well as the kinetic momentum density. The norms of the zeta potentials of some orbitals are larger by two digits than that of the sum of all orbitals. The zeta potentials of almost degenerate orbitals cancel out well with each other (see FIG 1.10). However, the zeta potential in C_6H_6 exists because their orbital are not completely degenerate due to the relativistic interaction. Since the zeta potential of the highest occupied molecular orbital is also large, it is predicted that the norm of the zeta potential of the excited state is much larger than the ground state one. This prediction will be investigated in our future work.

Table 1.1: Orbital energies and orbital angular momentums of C_6H_6

orbital number	orbital energy (Hartree)			orbital angular momentum $\|l_z\|$		$\|l_z + s_z\|$
	Spin-Free	DHF	DHF−Spin-Free	Spin-Free	DHF	DHF
1	-11.24442898	-11.24442871	2.70×10^{-7}	2.84×10^{-4}	2.85×10^{-4}	0.500
2	-11.24386232	-11.24386205	2.70×10^{-7}	2.84×10^{-4}	5.65×10^{-3}	0.505
3	-11.24386232	-11.24386204	2.80×10^{-7}	2.84×10^{-4}	5.08×10^{-3}	0.495
4	-11.24263284	-11.24263258	2.60×10^{-7}	2.85×10^{-4}	5.83×10^{-3}	0.506
5	-11.24263284	-11.24263255	2.90×10^{-7}	2.85×10^{-4}	5.27×10^{-3}	0.494
6	-11.24203161	-11.24203134	2.70×10^{-7}	2.85×10^{-4}	2.84×10^{-4}	0.500
7	-1.15113864	-1.15113857	7.00×10^{-8}	2.40×10^{-5}	7.24×10^{-5}	0.500
8	-1.01529335	-1.01529973	-6.38×10^{-6}	2.71×10^{-5}	6.50×10^{-1}	1.150
9	-1.01529335	-1.01528684	6.51×10^{-6}	2.71×10^{-5}	6.50×10^{-1}	0.150
10	-0.82427334	-0.82429852	-2.52×10^{-5}	2.64×10^{-5}	1.31	0.814
11	-0.82427334	-0.82424811	2.52×10^{-5}	2.64×10^{-5}	1.31	1.814
12	-0.70969488	-0.70969490	-2.00×10^{-8}	1.80×10^{-5}	1.38×10^{-4}	0.500
13	-0.64367539	-0.64367558	-1.90×10^{-7}	2.36×10^{-5}	1.02×10^{-2}	0.490
14	-0.61981504	-0.61981488	1.60×10^{-7}	3.07×10^{-5}	1.06×10^{-2}	0.511
15	-0.58812832	-0.58817821	-4.99×10^{-5}	2.41×10^{-5}	2.08×10^{-1}	0.708
16	-0.58812832	-0.58807852	4.98×10^{-5}	2.41×10^{-5}	2.08×10^{-1}	0.292
17	-0.50130873	-0.50130868	5.00×10^{-8}	6.63×10^{-6}	7.26×10^{-6}	0.500
18	-0.49479202	-0.49490532	-1.13×10^{-4}	2.89×10^{-5}	1.17	0.672
19	-0.49479202	-0.49467876	1.13×10^{-4}	2.89×10^{-5}	1.17	1.672
20	-0.33639392	-0.33639417	-2.50×10^{-7}	1.00×10^{-5}	9.13×10^{-1}	0.413
21	-0.33639392	-0.33639369	2.30×10^{-7}	1.00×10^{-5}	9.13×10^{-1}	1.413

† Each orbital has degenerate α and β strings as Kramers pairs.

†† $l_z = \int \langle x(\vec{\Pi}_e(\vec{r}))_y - y(\vec{\Pi}_e(\vec{r}))_x \rangle d^3\vec{r}, \quad s_z = \int \langle (\vec{s}_e(\vec{r}))_z \rangle d^3\vec{r}$, The atomic units are used.

1.5 Conclusions

In this study, we investigate the local physical quantities for spin based on the relativistic quantum theory. We have reviewed the spin vorticity theory and explained the feature of local physical quantities for spin. In order to investigate the feature of the zeta potential in a molecular system, the relation between the zeta potential and the molecular symmetry has been discussed. After pointing out the difficulty of the rigorous formulation of local physical quantities based on the two-component relativistic quantum theory, we have proposed a simple approximation method. Numerical calculations of the zeta potential, the zeta force density and the spin torque density in Li and C_6H_6 have been performed by using the four- and two-component wave functions of the relativistic quantum mechanics as approximations of state vectors of the quantum field theory. The cancellation between the nonzero zeta force and spin torque densities is seen clearly in the ground state of C_6H_6, even though the spin angular momentum density is zero over the whole region. Moreover, the accuracy of the approximation method has been discussed by comparing some different types of relativistic numerical calculations of the zeta potential. From these results, we have found the zeta potential by the two-component relativistic quantum theory is good agreement with that by the four-component one. In our results, since we used the effective core potential, it cannot be checked whether the zeta potential by the two-component relativistic quantum theory is well consistent with full relativistic results around the vicinity of nuclei. Calculations of the local physical quantities of each orbital in C_6H_6 have been carried out by using 4c-DHF wave functions. We have found the relativistic interaction can have a great influence on the local physical quantities, even if it has little effect on the orbital energies for a molecule. In our future work, we will investigate the local physical quantities for spin in the excited state, the chiral molecules, crystal structure and high spin materials.

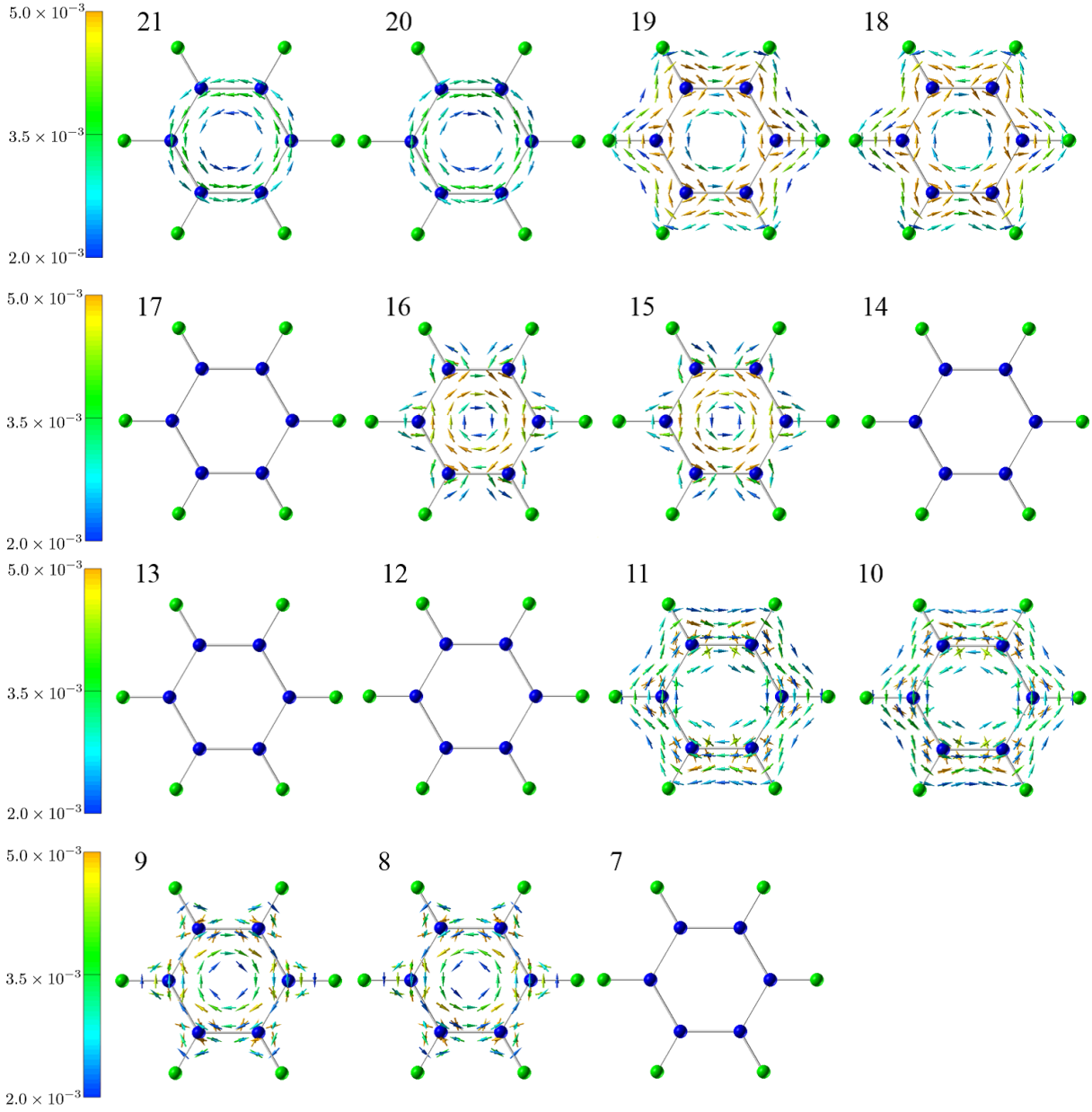

Figure 1.6: The distributions of the kinetic momentum density $\langle \hat{\vec{\Pi}}_e(\vec{r}) \rangle$ of each orbital in C_6H_6.

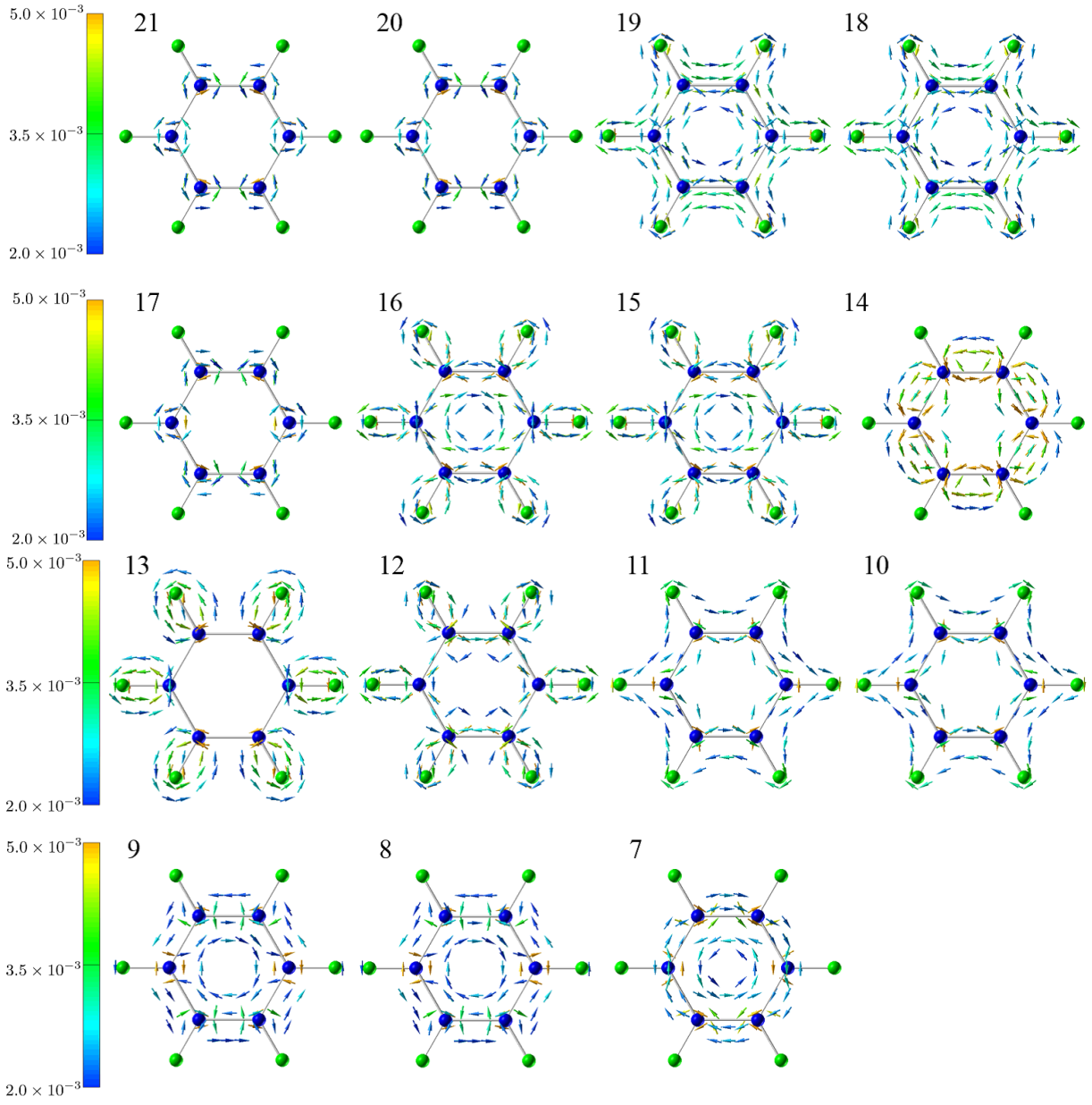

Figure 1.7: The distributions of half of the spin vorticity $\langle \frac{1}{2}\mathrm{rot}\hat{\vec{s}}_e(\vec{r})\rangle$ of each orbital in C_6H_6.

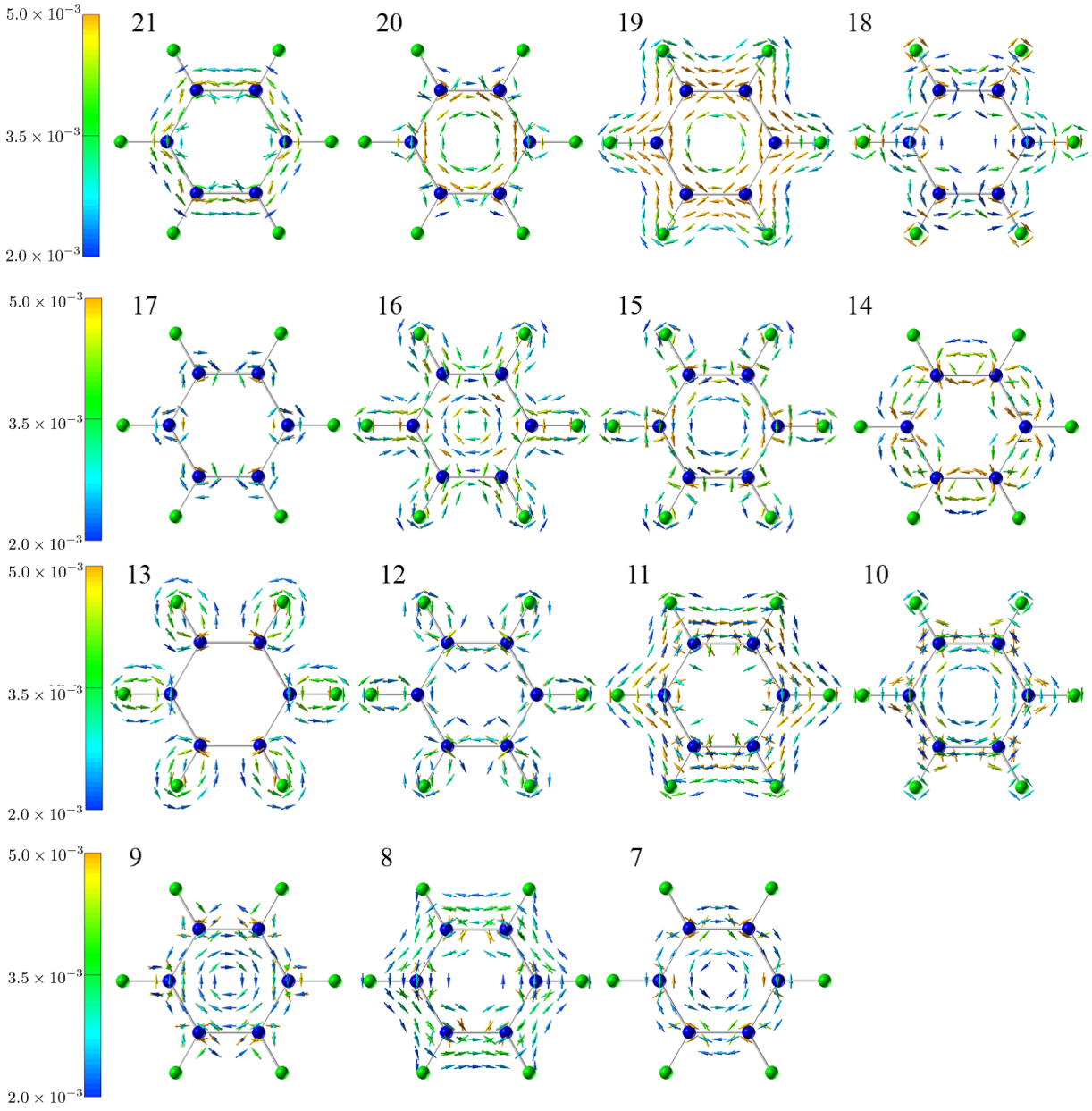

Figure 1.8: The distributions of the electronic momentum density $\langle \hat{\vec{P}}_e(\vec{r}) \rangle$ of each orbital in C_6H_6.

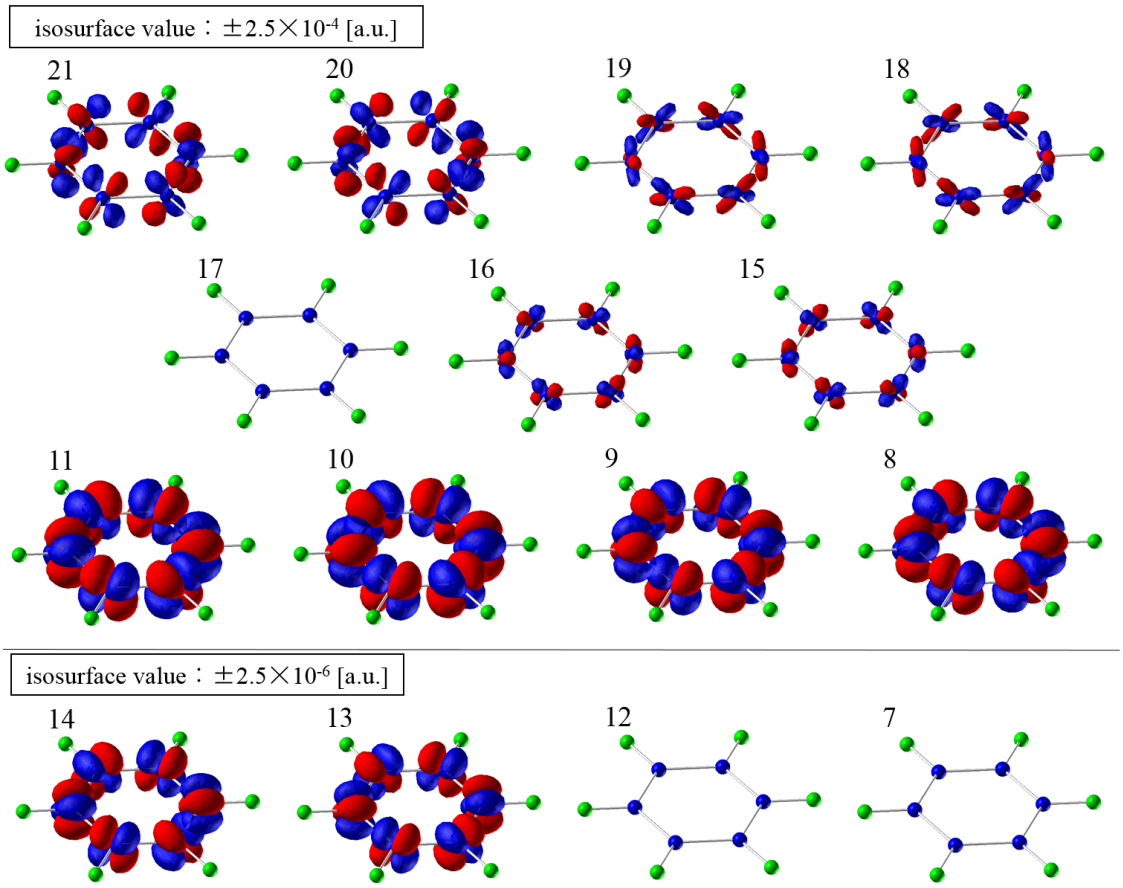

Figure 1.9: The distribution of the zeta potential of each orbital in C_6H_6. Red and blue envelopes represent positive and negative zeta potential iso-surfaces, respectively. The threshold value of isosurfaces of the zeta potential is taken as 2.5×10^{-4} [a.u.] and 2.5×10^{-6} [a.u.].

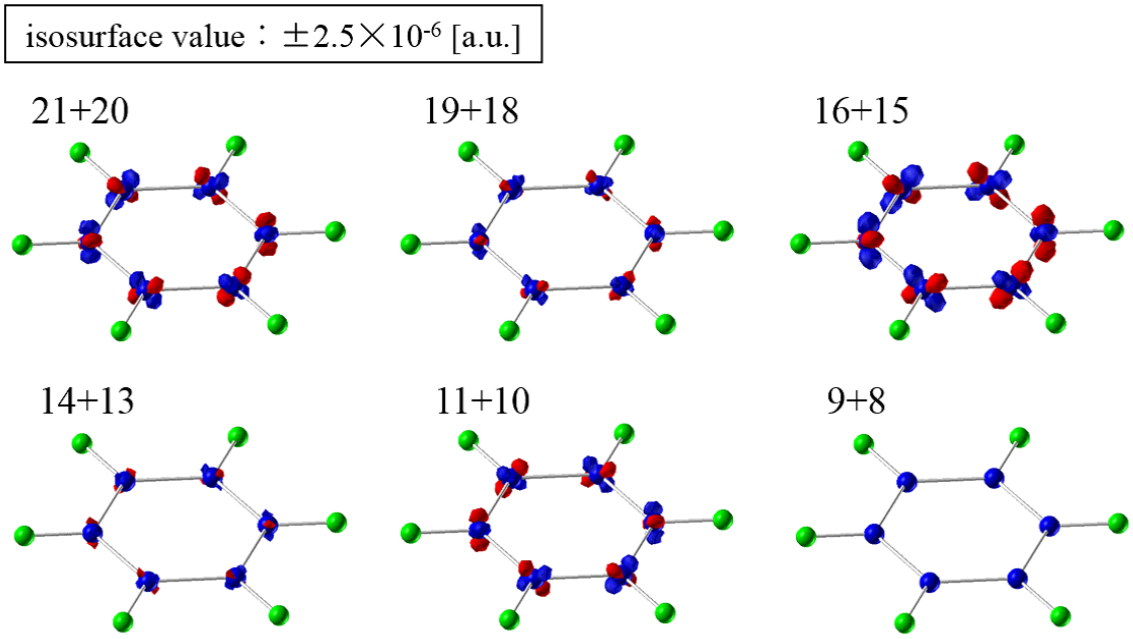

Figure 1.10: The distribution of the sum of the zeta potentials of each orbital in C_6H_6. Red and blue envelopes represent positive and negative zeta potential iso-surfaces, respectively. The threshold value of isosurfaces of the zeta potential is taken as 2.5×10^{-6} [a.u.].

Reference

[1] T. L. Gilbert, IEEE Trans. Mag., **40**, 3443 (2004).

[2] V. B. Berestetskii, E. M. Lifshitz, L. P. Pitaevskii, Quantum Electrodynamics, vol. 4 (2nd ed.) Pergamon Press, Oxford (1982).

[3] For example, see J. J. Sakurai, Advanced Quantum Mechanics (Addison-Wesley, Reading, Mass., 1976).

[4] A. Tachibana, J. Mol. Model, **11**, 301 (2005).

[5] A. Tachibana, J. Mol. Struct. (THEOCHEM) **943**, 138 (2010).

[6] M. Senami, J. Nishikawa, T. Hara, A. Tachibana, J. Phys. Soc. Jpn **79**, 084302 (2010).

[7] T. Hara, M. Senami, A. Tachibana, Phys. Lett. A. **376**, 1434 (2012).

[8] M. Fukuda, M. Senami, A. Tachibana, Advances in Quantum Methods and Applications in Chemistry, Physics, and Biology Progress in Theoretical Chemistry and Physics, Vol. 27; Eds. M. Hotokka, E. J. Brändas, J. Maruani, G. Delgado-Barrio; Springer, New York, Chapter 7, pp 131-139 (2013).

[9] A. Tachibana, J. Math. Chem. **50**, 669 (2012).

[10] A. Tachibana, Electronic Stress with Spin Vorticity. In *Concepts and Methods in Modern Theoretical Chemistry*, S. K. Ghosh and P. K. Chattaraj Eds., CRC Press, Florida (2013), pp. 235-251.

[11] A. Tachibana, J. Comput. Chem. Jpn. **13**, 18 (2014).

[12] A. Tachibana, Indian J. Chem. A, **53**, 1031 (2014).

[13] S. Weinberg, *Gravitation and Cosmology: Principles and Applications of the General Theory of Relativity* (Wiley, New York, 1972).

[14] S. Weinberg, *Quantum Theory of Fields I-III* (Cambridge University, Cambridge, 1995).

[15] L. L. Foldy, and S. A. Wouthuysen, Phys. Rev., **78**, 29 (1950); S. Tani, Prog. Theor. Phys., **6**, 267 (1951).

[16] V. Kellö, and A. Sadlej Int J Quantum Chem **68**, 159 (1998).

[17] W. Kutzelnigg and W. Liu, J. Chem. Phys., **123**, 241102 (2005).

[18] W. Liu and D. Peng, J. Chem. Phys., **125**, 044102 (2006).

[19] D. Peng, W. Liu, Y. Xiao, L. Cheng, J. Chem. Phys., **127**, 104106 (2007).

[20] M. Ilias and T. Saue, J. Chem. Phys. **126**, 064102 (2007).

[21] W. Liu and D. Peng, J. Chem. Phys. **131**, 031104 (2009).

[22] T. Saue, ChemPhysChem, **12**, 3077 (2011).

[23] W. Liu, Mol. Phys. **108**, 1679 (2010).

[24] W. Liu, Phys. Rep. **537**, 59 (2014).

[25] W. Liu, Int. J. Quantum Chem. **114**, 983 (2014).

[26] W. Liu, Int. J. Quantum Chem. **115**, 631 (2015).

[27] K. G. Dyall, J. Chem. Phys. **100**, 2118 (1994).

[28] DIRAC, a relativistic ab initio electronic structure program, Release DIRAC13 (2013), written by L. Visscher, H. J. Aa. Jensen, R. Bast, and T. Saue, with contributions from V. Bakken, K. G. Dyall, S. Dubillard, U. Ekström, E. Eliav, T. Enevoldsen, E. Faßhauer, T. Fleig, O. Fossgaard, A. S. P. Gomes, T. Helgaker, J. K. Lærdahl, Y. S. Lee, J. Henriksson, M. Iliaš, Ch. R. Jacob, S. Knecht, S. Komorovský, O. Kullie, C. V. Larsen, H. S. Nataraj, P. Norman, G. Olejniczak, J. Olsen, Y. C. Park, J. K. Pedersen, M. Pernpointner, K. Ruud, P. Sałek, B. Schimmelpfennig, J. Sikkema, A. J. Thorvaldsen, J. Thyssen, J. van Stralen, S. Villaume, O. Visser, T. Winther, and S. Yamamoto (see http://www.diracprogram.org)

[29] Available from the web site, http://dirac.chem.sdu.dk.

[30] *QEDynamics*, M. Senami, K. Ichikawa, A. Tachibana
http://www.tachibana.kues.kyoto-u.ac.jp/qed

[31] D. M. Ceperley and B. J. Alder, Phys. Rev. Lett. **45**, 566 (1980); J. P. Perdew and A. Zunger, Phys. Rev. B **23**, 5048 (1981).

[32] P. Hohenberg and W. Kohn, Phys. Rev. **136**, B864 (1964); W. Kohn and L. J. Sham, Phys. Rev. **140**, A1133 (1965).

[33] T. Ozaki, H. Kino, J. Yu, M.J. Han, M. Ohfuchi, F. Ishii, K. Sawada, Y. Kubota, T. Ohwaki, H. Weng, M. Toyoda, Y. Okuno, R. Perez, P.P. Bell, T.V.T. Duy, Yang Xiao, A.M. Ito, and K. Terakura, OpenMX package, http://www.openmx-square.org/.

[34] T. Ozaki, Phys. Rev. B **67**,155108 (2003).

Chapter 2

Local Spin Dynamics with the Electron Electric Dipole Moment

2.1 Introduction

The permanent electric dipole moment (EDM) of the electron is a significant key to reveal a violation of the time reversal ($\mathcal{T}$) symmetry. With the $\mathcal{CPT}$ invariance, this means the violation of the product of the associated charge ($\mathcal{C}$) and the spatial parity ($\mathcal{P}$), and this $\mathcal{CP}$ violation may be a hint of the mystery of the dominance of matter over antimatter in our universe. The value of the electron EDM (d_e) predicted by the standard model of particle physics ($d_e \sim 10^{-40}$e cm) is too small to be observed by present experiments. However, some extensions of the standard model, such as low-energy supersymmetric models [1], predict much larger d_e, for example $d_e \sim 10^{-27} - 10^{-29}$e cm in a supersymmetric model [2]. Therefore, the existence of a nonzero electron EDM provides the evidence of the $\mathcal{T}$-violation and judges some extension theories. In the present experiments, the upper bound of the EDM derived by using ThO and YbF molecules is reported as $d_e < 8.7 \times 10^{-29}$ [3] and $d_e < 1.05 \times 10^{-27}$ e cm [4], respectively. Hence these constraints are already in ranges predicted by supersymmetric models and experiments in the near future will find or rule out extension models of the standard model.

Experiments for searching the EDM rely on observations of spin precession induced by an electric field. Hence a larger electric field is more efficient to determine the upper bound of the electron EDM. Recently, heavy polar diatomic molecules are chosen for experimental

searches for the electron EDM, since an internal electric field in polar molecules is much larger than an external electric field in the laboratory (∼100 kV/cm). Actually, the effective electric field is reported to be 1–100 GV/cm for many polar molecules, for example YbF, BaF, and ThO by numerical computations [5–8]. In this work, we focus on the value of the effective electric field by using these diatomic molecules. In order to determine the upper bound of d_e, both the interaction energy of the EDM (E_{EDM}) and the effective electric field ($\mathcal{E}_{\mathrm{eff}} = E_{\mathrm{EDM}}/d_e$) are needed. The former can be experimentally measured by observations of spin precession, while the latter needs to be predicted by using *ab initio* calculations based on the relativistic quantum theory because relativistic effects and correlation effects are essentially important for the computation of heavy atoms. For the relativistic effects, the four-component Dirac equation should be solved to include relativistic interactions such as the spin-orbit interaction. For the correlation effects, post Hartree-Fock computations, such as configuration interaction (CI), are required. These two treatments result in a very large computational cost to calculate the effective electric field. Although some works have already been reported on the values of the effective electric field in diatomic molecules [5–8] by *ab initio* calculations with some approximations, the improvement of the precision of $\mathcal{E}_{\mathrm{eff}}$ is important for the accurate estimate of the experimental bound of the EDM. Another key point is a treatment of spin precession. The quantum mechanical approaches for spin dynamics are widely used; however, these approaches cannot explain local spin dynamics since a physical quantity in the quantum mechanics is defined by the inner product, which is derived by the integration over the whole region. In the quantum field theory, local distributions of physical quantities such as the spin angular momentum density and torque density for the spin can be predicted. The equation of motion of the spin based on the quantum field theory was proposed in Ref. [9], and our group has already discussed the local contribution of the spin torque by using numerical calculations particularly for a spin stationary state of the diatomic system of alkali atoms [10], transition element atoms [11], and allene-type molecules with chiral and achiral structures [12].

In this work, we investigate the relation between the electron EDM and the spin in the quantum field theory. The relation between the interaction energy of the electron EDM and the spin precession is explained by an approximate description of time evolution originated from the existence of the EDM. Using two approximation methods to evaluate the effective

electric field, we calculate the effective electric field in YbF, BaF, ThO, and HF^+ molecules by *ab initio* calculations based on the relativistic quantum mechanics. We reconsider the spin precession from the viewpoint of the local spin torque dynamics described by the equation of motion of the spin angular momentum density in the quantum field theory. The equation of motion of the spin is modified by the nonzero electron EDM, and then the torque density contribution is revealed. After a discussion of the calculation results of the effective electric field, the local distribution of physical quantities, the spin angular momentum density, and the EDM torque density induced by external fields, are calculated and discussed. The reason that the effective electric field in YbF is much larger than that in HF^+ is discussed from the viewpoint of the local physical quantities. This local distribution analysis indicates that even light atomic molecules could have the large effective electric field.

2.2 Theory

2.2.1 Hamiltonian density with EDM

The Dirac Lagrangian density for the electron is written as

$$\hat{\mathcal{L}}_e = c\hat{\bar{\psi}}\left(i\hbar\gamma^\mu \hat{D}_{e\mu} - m_e c\right)\hat{\psi}, \tag{2.1}$$

where $\hat{\psi}$ denotes the Dirac spinor of the electron, $\hat{\bar{\psi}} = \hat{\psi}^\dagger\gamma^0$, γ^μ are gamma matrices, m_e is the electron mass, and c is the speed of light in vacuum. Here, Greek indices run over 0 to 3. We adopt the Einstein summation convention. The gauge covariant derivative is written as $\hat{D}_{e\mu} = \partial_\mu + i\frac{Z_e e}{\hbar c}\hat{A}_\mu$, where $\hat{A}_\mu$ is the gauge field, e is the electron charge ($e > 0$), and $Z_e = -1$. By using the Euler-Lagrange equation, the equation of motion is given as

$$i\hbar c\gamma^0\gamma^\mu \hat{D}_{e\mu}\hat{\psi} - m_e c^2\gamma^0\hat{\psi} = 0. \tag{2.2}$$

The Hamiltonian density is derived by the ordinary Legendre transformation,

$$\hat{\mathcal{H}}_e(x) = c\hat{\bar{\psi}}\left(-i\hbar\gamma^k \cdot \hat{D}_{ek} + m_e c\right)\hat{\psi} + Z_e e\hat{A}_0\hat{\psi}^\dagger\hat{\psi}, \tag{2.3}$$

where Latin indices run over 1 to 3. To describe the interaction of the relativistic electron EDM, we employ the gauge- and Lorentz-invariant effective Lagrangian density for the electron EDM,

$$\hat{\mathcal{L}}_{\mathrm{EDM}} = -d_e\frac{i}{2}\hat{\bar{\psi}}\sigma^{\mu\nu}\gamma_5\hat{F}_{\mu\nu}\hat{\psi}, \tag{2.4}$$

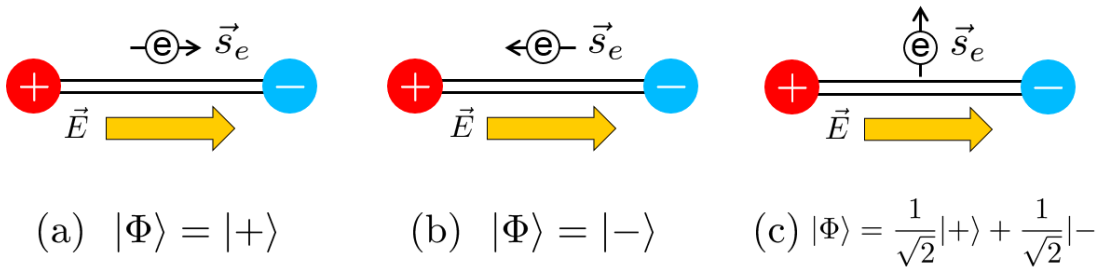

(a) $|\Phi\rangle = |+\rangle$ (b) $|\Phi\rangle = |-\rangle$ (c) $|\Phi\rangle = \frac{1}{\sqrt{2}}|+\rangle + \frac{1}{\sqrt{2}}|-\rangle$

Figure 2.1: Schematic pictures of ket states.

where d_e is the electron EDM, $\sigma^{\mu\nu} = \frac{i}{2}[\gamma^\mu, \gamma^\nu]$, $\gamma_5 = i\gamma^0\gamma^1\gamma^2\gamma^3$, and the electromagnetic field strength tensor is $\hat{F}_{\mu\nu} = \partial_\mu \hat{A}_\nu - \partial_\nu \hat{A}_\mu$. This additional term in the Lagrangian extends the Dirac equation [Eq. (2.2)] as follows:

$$i\hbar c\gamma^0\gamma^\mu \hat{D}_{e\mu}\hat{\psi} - m_e c^2\gamma^0\hat{\psi} - d_e\frac{i}{2}\gamma^0\sigma^{\mu\nu}\gamma_5\hat{F}_{\mu\nu}\hat{\psi} = 0. \tag{2.5}$$

The EDM Lagrangian density yields the EDM Hamiltonian density,

$$\hat{\mathcal{H}}_{\rm EDM}(x) = d_e\frac{i}{2}\hat{\bar{\psi}}\sigma^{\mu\nu}\gamma_5\hat{F}_{\mu\nu}\hat{\psi} \tag{2.6}$$

$$= -d_e\left(\hat{\bar{\psi}}\vec{\Sigma}\cdot\hat{\vec{E}}\hat{\psi} + i\hat{\bar{\psi}}\gamma^0\vec{\gamma}\cdot\hat{\vec{B}}\hat{\psi}\right), \tag{2.7}$$

where $\hat{\vec{E}}$ and $\hat{\vec{B}}$ are the electric and magnetic fields, respectively, and $\vec{\Sigma}$ is the 4×4 Pauli matrix.

2.2.2 Spin precession with EDM

Next, we describe a relation between the interaction energy of the EDM and spin precession. At first, neglecting the vector potential term in Eq. (2.3), we begin with the Dirac-Coulomb Hamiltonian density,

$$\hat{\mathcal{H}}_{\rm DC} = c\hat{\bar{\psi}}\left(-i\hbar\gamma^k\partial_k + m_e c\right)\hat{\psi} + Z_e e\hat{A}_0\hat{\psi}^\dagger\hat{\psi}, \tag{2.8}$$

for the system Hamiltonian. Namely, we treat other contributions, i.e., the effect of the internal vector potential and the EDM interaction, in a perturbative manner. Then, we assume that two time-independent degenerate state vectors, $|+\rangle \equiv \hat{c}_+^\dagger(t_0)|0\rangle$ and $|-\rangle \equiv \hat{c}_-^\dagger(t_0)|0\rangle$ (see FIG. 2.1), are the Heisenberg ground state of the system satisfying

$$\int \langle\pm| : \hat{\mathcal{H}}_{\rm DC}(\vec{r}, t = t_0) : |\pm\rangle d^3\vec{r} = E_0, \tag{2.9}$$

$$\int \langle\pm| : \hat{J}_{ez}(\vec{r}, t = t_0) : |\pm\rangle d^3\vec{r} = \pm|\Omega|, \tag{2.10}$$

where $\hat{J}_{ez}(x)$ is the total angular momentum density. Here, we represent normal ordering with colons. By the interaction of the EDM, these degenerate states are split into two energy levels,

$$\int \langle \pm | : \hat{\mathcal{H}}_{\mathrm{DC+EDM}}(\vec{r}, t = t_0) : |\pm\rangle d^3\vec{r} = E_0 \pm E_{\mathrm{EDM}}, \tag{2.11}$$

where $\hat{\mathcal{H}}_{\mathrm{DC+EDM}} = \hat{\mathcal{H}}_{\mathrm{DC}} + \hat{\mathcal{H}}_{\mathrm{EDM}}$. Suppose the Hamiltonian density does not depend on the time; then the electron field can be expanded approximately as the following equation:

$$\hat{\psi}(x) = \sum_{\alpha=\pm} \hat{c}_\alpha(t)\phi_\alpha(\vec{r}), \quad \hat{c}_\alpha(t) = e^{-i\omega_\alpha(t-t_0)}\hat{c}_\alpha(t_0), \tag{2.12}$$

where $\omega_\pm = (E_0 \pm E_{\mathrm{EDM}})/\hbar$. In this two-state system, a general Heisenberg state vector can be written as $|\Phi\rangle = \lambda_+|+\rangle + \lambda_-|-\rangle$, where λ_α is the normalization constant which obeys $|\lambda_+|^2 + |\lambda_-|^2 = 1$. The arbitrary operator of physical quantities $\hat{\vec{\mathcal{O}}}(x)$ such as the total angular momentum density can be written as

$$\begin{aligned}\hat{\vec{\mathcal{O}}}(x) &= \sum_{\alpha,\beta=\pm} \vec{\mathcal{O}}_{\alpha\beta}(\vec{r})\, \hat{c}^\dagger_\alpha(t)\hat{c}_\beta(t), \\ &= \sum_{\alpha,\beta=\pm} \vec{\mathcal{O}}_{\alpha\beta}(\vec{r})\, \hat{c}^\dagger_\alpha(t_0)\hat{c}_\beta(t_0) e^{+i\left(\omega_\alpha - \omega_\beta\right)(t-t_0)},\end{aligned} \tag{2.13}$$

Therefore, the time evolution of the expectation value $\langle\Phi| : \hat{\vec{\mathcal{O}}}(x) : |\Phi\rangle$ depends on the $|\omega_+ - \omega_-| = 2E_{\mathrm{EDM}}/\hbar$ approximately. This is why the interaction energy of the EDM can be determined by the observation of the spin precession.

2.2.3 The effective electric field for the electron EDM

While the observation of spin precession enables us to determine the interaction energy of the electron EDM E_{EDM}, we must still evaluate the effective electric field for the electron EDM $\mathcal{E}_{\mathrm{eff}} = E_{\mathrm{EDM}}/d_e$ to determine the value of d_e. In heavy polar diatomic molecules, which were recently chosen for experimental searches for the electron EDM, it is known that the magnetic term of the interaction energy of the electron EDM, E^B_{EDM} [contribution from the second term of Eq. (2.7)], is much smaller than the electric term, E^E_{EDM} [contribution from the first term of Eq. (2.7)]. Hence, we can write $\mathcal{E}_{\mathrm{eff}} \approx E^E_{\mathrm{EDM}}/d_e$, and this is represented as

the following form:

$$\begin{aligned}\mathcal{E}_{\text{eff}} \approx & \frac{1}{d_e}\int \left\langle \Phi \right| : \hat{\mathcal{H}}^{E}_{\text{EDM}}(\vec{r}) : \left| \Phi \right\rangle d^3\vec{r}, \\ \approx & \int \left\langle \Phi \right| : -\hat{\vec{\psi}}\vec{\Sigma}\cdot\hat{\vec{E}}\hat{\psi} : \left| \Phi \right\rangle d^3\vec{r}, \\ \approx & \int \left\langle \Phi \right| : -\hat{\vec{\psi}}\vec{\Sigma}\cdot\left(\hat{\vec{E}}^{\,\text{ele}} + \hat{\vec{E}}^{\,\text{nuc}}\right)\hat{\psi} : \left| \Phi \right\rangle d^3\vec{r}, \end{aligned} \tag{2.14}$$

where $\hat{\vec{E}}^{\,\text{ele}}(\vec{r})$ $[\hat{\vec{E}}^{\,\text{nuc}}(\vec{r})]$ is the electric field contributed by electrons (nuclei). To avoid time-consuming calculations about the first term of Eq. (2.14), some approximations are used for the internal electric field in a molecule. Two types of approximations are often used. One is the approximation that the internal electric field is replaced only with $\hat{\vec{E}}^{\,\text{nuc}}(\vec{r})$ as follows:

$$\begin{aligned}\mathcal{E}_{\text{eff}} \approx & \int \left\langle \Phi \right| : -\hat{\psi}^\dagger\left(\gamma^0 - 1\right)\vec{\Sigma}\cdot\hat{\vec{E}}\hat{\psi} : \left| \Phi \right\rangle d^3\vec{r}, \\ \approx & \int \left\langle \Phi \right| : 2\hat{\psi}_S^\dagger\vec{\sigma}\cdot\hat{\vec{E}}\hat{\psi}_S : \left| \Phi \right\rangle d^3\vec{r}, \\ \approx & \int \left\langle \Phi \right| : 2\hat{\psi}_S^\dagger\vec{\sigma}\cdot\hat{\vec{E}}^{\text{nuc}}\hat{\psi}_S : \left| \Phi \right\rangle d^3\vec{r}, \end{aligned} \tag{2.15}$$

where $\hat{\psi}_S$ is the small component of the four-component dirac spinor $\hat{\psi}$. At the first line, we use the Schiff's theorem [13]. The deviation by the approximation in the last line is reported to be within 3% for the computation of the effective electric field in YbF [5]. This is because the small component of the spin angular momentum density is concentrated on the Yb nucleus.

The other approximation is a method which uses the so-called effective one-body EDM operator [14] as follows:

$$\mathcal{E}_{\text{eff}} \approx \int \left\langle \Phi \right| : \frac{2i\hbar c}{Z_e e}\hat{\psi}^\dagger\gamma^0\gamma_5\Delta\hat{\psi} : \left| \Phi \right\rangle d^3\vec{r}, \tag{2.16}$$

where the equation is satisfied only if $|\Phi\rangle$ is exactly an eigenstate of $\int \mathcal{H}_{\text{DC}} d^3\vec{r}$ due to the Schiff's theorem [13].

In later arguments, we discuss the parallel magnetic hyperfine interaction constant defined as

$$A_\parallel = \frac{\mu_K}{I\Omega}\int \left\langle \Phi \right| : \left(Z_e e\hat{\vec{\psi}}\frac{\vec{\gamma}\times\vec{r}}{|\vec{r}|^3}\hat{\psi}\right)_z : \left| \Phi \right\rangle d^3\vec{r}, \tag{2.17}$$

where μ_K is the nuclear magnetic dipole moment, I is the nuclear spin quantum number, and Ω is the quantum number of the total electronic angular momentum projection onto

the internuclear axis. In addition, the molecular electric dipole moment (DM) is introduced as

$$\vec{\mu} = \int \langle \Phi \,|: \vec{r}\hat{\rho}\,(\vec{r}) :| \,\Phi\rangle \, d^3\vec{r}, \tag{2.18}$$

$$\hat{\rho}\,(\vec{r}) = Z_e e\hat{\psi}^\dagger\hat{\psi} + \sum_{a=1}^{N_A} Z_a e\delta\left(\vec{r} - \vec{R}_a\right), \tag{2.19}$$

where N_A is the number of nuclei, Z_a and $\vec{R}_a$ are the charge and the position of each nucleus, respectively. The DM as well as $A_\parallel$ is useful to estimate the accuracy of the electronic structure.

2.2.4 Local spin torque dynamics with EDM

We reconsider the spin precession from the viewpoint of the local spin torque dynamics. In the quantum field theory without the interaction of the electron EDM, the spin angular momentum density and its time derivative are given by [9, 15]

$$\hat{\vec{s}}_e(x) = \hat{\psi}^\dagger(x)\frac{\hbar}{2}\vec{\Sigma}\hat{\psi}(x), \tag{2.20}$$

$$\frac{\partial}{\partial t}\hat{\vec{s}}_e(x) = \hat{\vec{t}}_e(x) + \hat{\vec{\zeta}}_e(x), \tag{2.21}$$

where Eq. (2.21) is derived by using Eq. (2.2). The first term of the right-hand side of Eq. (2.21) is called the spin torque density, which gives, by the integration over the whole region, the spin torque in the Heisenberg equation of the spin in the relativistic quantum mechanics [16]. The spin torque density can be written as

$$\hat{t}^i_e(x) = \hat{t}^i_{eN}(x) + \hat{t}^i_{eA}(x), \tag{2.22}$$

$$\hat{t}^i_{eN}(x) = -\frac{i\hbar c}{2}\epsilon_{ijk}\hat{\psi}^\dagger(x)\gamma^0\gamma^k\partial_j\hat{\psi}(x) + h.c., \tag{2.23}$$

$$\hat{t}^i_{eA}(x) = -Z_e e\epsilon_{ijk}\hat{\psi}^\dagger(x)\gamma^0\gamma^k\hat{A}^j(x)\hat{\psi}(x), \tag{2.24}$$

where ϵ_{ijk} is the Levi-Civita tensor. We note that $\hat{\vec{t}}_{eA}$ is the torque by the contribution proportional to $\hat{\vec{A}}$. The second term of the right-hand side of Eq. (2.21), which is named as the zeta force density, is given as

$$\hat{\zeta}^i_e(x) = -\partial_i\hat{\phi}_5(x), \tag{2.25}$$

$$\hat{\phi}_5(x) = \frac{\hbar c}{2}\hat{\psi}^\dagger(x)\gamma_5\hat{\psi}(x). \tag{2.26}$$

The zeta force density $\hat{\vec{\zeta}}_e$ is represented as the gradient of the zeta potential $\hat{\phi}_5$, which can be rewritten as $\hat{\phi}_5 = \frac{\hbar c}{2}\left(\hat{\psi}_R^\dagger\hat{\psi}_R - \hat{\psi}_L^\dagger\hat{\psi}_L\right)$ by using the right-handed and left-handed spinors: $\hat{\psi}_R = [(1+\gamma_5)/2]\hat{\psi}$ and $\hat{\psi}_L = [(1-\gamma_5)/2]\hat{\psi}$. The zeta force density integrated over the whole region is zero, as seen from Eq. (2.25). Hence when we consider the equation of motion of the spin after the integration, the local contribution of the zeta force density is lost and Eq. (2.21) can be identified with the ordinary Heisenberg equation of the spin in the relativistic quantum mechanics [16]. Note that Eq. (2.21) is known to be derived naturally by the "quantum spin vorticity principle" [17–21].

The contribution of the electron EDM to the torque for the spin is considered. The EDM Lagrangian [Eq. (2.4)] gives the additional local spin torque density $\hat{\vec{t}}_{\rm EDM}(x)$,

$$\hat{\vec{t}}_{\rm EDM}(x) = \hat{\vec{t}}^{E}_{\rm EDM}(x) + \hat{\vec{t}}^{B}_{\rm EDM}(x), \tag{2.27}$$

$$\hat{\vec{t}}^{E}_{\rm EDM}(x) = d_e\hat{\bar{\psi}}(x)\left(\vec{\Sigma}\times\hat{\vec{E}}(x)\right)\hat{\psi}(x), \tag{2.28}$$

$$\hat{\vec{t}}^{B}_{\rm EDM}(x) = d_e i\hat{\bar{\psi}}(x)\gamma^0\left(\vec{\gamma}\times\hat{\vec{B}}(x)\right)\hat{\psi}(x), \tag{2.29}$$

where we separate the EDM torque density $\hat{\vec{t}}_{\rm EDM}$ into the electric term $\hat{\vec{t}}^{E}_{\rm EDM}$ and the magnetic term $\hat{\vec{t}}^{B}_{\rm EDM}$. We note that the EDM torque has a component perpendicular to both the electric and magnetic fields. Finally, the equation of motion of the spin angular momentum density with the contribution of the electron EDM is summarized as

$$\frac{\partial}{\partial t}\hat{\vec{s}}_e(x) = \hat{\vec{t}}_e(x) + \hat{\vec{\zeta}}_e(x) + \hat{\vec{t}}_{\rm EDM}(x). \tag{2.30}$$

For example, in recent experiments for the electron EDM, using heavy polar diatomic molecules, the spin precession of the state $|\Phi\rangle = (|+\rangle + |-\rangle)/\sqrt{2}$ (see FIG. 2.1) is observed. The torque accelerating spin by the EDM effective electric field corresponds to $\int\langle\Phi|\hat{\vec{t}}_{\rm EDM}(x)|\Phi\rangle d^3\vec{r}$. However, our Eq. (2.30) can explain even local distributions of the physical quantities in a molecule. If one could estimate the spin angular momentum density and the local torque densities in a local region, it would present a different way to observe the electron EDM. In a later section, we calculate the local distribution of such quantities as a demonstration.

2.3 Computational details

We calculate the effective electric fields for the purpose of checking the accuracy of the electronic state by comparing the other groups' results of the effective electric field in order to prepare the electronic states for calculations of the local physical quantities. All of the effective electric fields are consistently calculated at the configuration interaction with all single and double excitations (CISD) level to serve as useful references. We calculate the effective electric fields in YbF ($^2\Sigma_{1/2}$), BaF ($^2\Sigma_{1/2}$), and ThO ($^3\Delta_1$) under the two types of approximations, Eqs. (2.15) and (2.16). In order to investigate the origin of large effective electric fields, we also calculate the effective electric field in HF^+ ($^2\Pi_{1/2}$), which also has a large molecular electric dipole moment. We use four-component wave functions of these molecules in the relativistic quantum mechanics as a substitution of those in the quantum field theory. The four-component wave functions are derived by using DIRAC13 program package [22]. We use the uncontracted Dyall's four-component double zeta (DZ), triple zeta (TZ), and quadruple zeta (QZ) basis sets which have correlating functions for all shells [23]. After Dirac-Hartree-Fock computations with the Dirac-Coulomb Hamiltonian, CI computations are performed in the restricted active space (RAS) method by using the DIRRCI module. We carry out various CISD calculations to investigate the effect of a basis set and the importance of core correlation effects. We refer to the name of CI wave-function models as ne-CISD or ne-MR$_K$-CISD, where n represents the number of active electrons. Models of ne-MR$_K$-CISD are used only for calculation of the ThO molecule, and MR is the multireference CI. The reference states are generated by average-of-configuration open-shell calculations for averaging with two electrons in the Th($7s, 6d\delta$) Kramers pairs. The subscript K represents the number of active valence spinor spaces. When $K = 3$, only the Th($7s, 6d\delta$) spinors are used in the RAS2 space. In another case, $K = 10$, the Th($7s, 6d, 7p, 8s$) spinors are used in the RAS2 space. For YbF and ThO, we performed only a single geometry calculation with the bond length shown in TABLE 2.1, whose values are reported in Refs. [24] and [8] for YbF and ThO, respectively. For BaF and HF^+, their bond lengths are determined by geometrical optimization computations at the Hartree-Fock level.

The nuclear-spin quantum numbers I and the nuclear magnetic dipole moments μ_K used in the calculations of the nuclear magnetic hyperfine coupling constant are listed in

Table 2.1: Bond length for each molecule.

Species (state)	Bond length (Å)
YbF ($^2\Sigma_{1/2}$)	2.073
ThO ($^3\Delta_1$)	1.840
BaF ($^2\Sigma_{1/2}$)	2.253 (DZ)
	2.189 (TZ)
	2.182 (QZ)
HF^+ ($^2\Pi_{1/2}$)	0.991 (DZ)
	0.987 (TZ)
	0.986 (QZ)

TABLE 2.2. Although the experimental value $\mu_{\rm Th}$ does not have even two significant digits, we adopt the center value $\mu_{\rm Th} = 0.46$ as the face value for calculations of $|A_{\parallel}^{\rm Th}|$, by neglecting its accuracy. In addition, we investigate the distributions of the electron density and the local spin angular momentum density in these molecules to investigate the origin of large effective electric fields.

We also investigate the distributions of the local spin torque density and the local EDM torque density of YbF as a demonstration. For the demonstration, we use the normalized external electric field and magnetic field to make the demonstration simple. Namely, we consider a situation that the external static electric field $\vec{E}_{\rm ext} = (1, 0, 0)$ and magnetic field $\vec{B}_{\rm ext} = (1, 0, 0)$ (in atomic units) are applied at $t = 0$ on YbF. Then, the external vector potential is set to $\vec{A}_{\rm ext} = \frac{1}{2}\vec{B}_{\rm ext} \times \vec{r}$. Even if the external fields are multiplied by a constant

Table 2.2: Nuclear magnetic dipole moment for each atom in Ref. [25]. The uncertainty in the experimental result is given in parentheses.

Species	I	μ_K[a] (nm)
$^{171}_{70}$Yb	1/2	0.4937
$^{229}_{90}$Th	5/2	0.46(4)
$^{137}_{56}$Ba	3/2	0.9374

[a] μ_K is the K's nuclear magnetic dipole moment in units of the nuclear magneton μ_N (nm).

Table 2.3: Effective electric field in YbF. The uncertainty in the experimental result is given in parentheses.

YbF($^2\Sigma_{1/2}$) Method/Basis	Active orbitals	virt. orb. cutoff (hartree)	$\mathcal{E}_{\rm eff}^{\rm ob}$ ($\frac{\rm GV}{\rm cm}$)	$\mathcal{E}_{\rm eff}^{\rm nuc}$ ($\frac{\rm GV}{\rm cm}$)	$\lvert A_\parallel^{\rm Yb}\rvert$ (MHz)	DM (D)
31e-CISD/DZ	$25-80$	1.82	21.0	21.7	6207	3.49
31e-CISD/TZ	$25-80$	0.92	19.7	20.1	5674	3.59
31e-CISD/QZ	$25-80$	0.60	19.8	20.2	5727	3.59
31e-CISD/QZ	$25-109$	1.30	20.8	21.2	5992	3.45
31e-CISD/QZ	$25-127$	2.00	20.3	20.7	5885	3.38
79e-CISD/QZ	$1-109$	1.30	20.8	21.2	6002	3.44
Experiment					7822(5)[a]	3.91(4)[b]
GRECP/RASSCF/EO[c]				24.9	7842	
31e-RASCI[d]				24.06		
79e-CCSD/QZ[e]			23.1			3.60

[a]Ref. [27], [b]Ref. [28], [c]Ref. [29], [d]Ref. [30], [e]Ref. [6]

number, the distribution pattern of the torque density does not change. If we investigate the spin precession used in present EDM experiments, the state $|\Phi\rangle = (|+\rangle + |-\rangle)/\sqrt{2}$ (see FIG. (2.1)) should be used. However, it is hard to calculate the EDM torque term induced by the internal electric field for its state. Therefore, we choose the state $|\Phi\rangle = |-\rangle$, which is the same one used for the calculation of the effective electric field. The electric field induced by the internal particle is not included in our computations of local torque density for this state, since the direction of the integration of the internal electric field over a molecule is the same as that of the spin and the contribution to the EDM torque is considered to be small, as seen from Eq. (2.28). The computations of the effective electric field and local physical quantities are performed by the QEDynamics program package [26] developed in our group.

2.4 Results and Discussion

The calculation results of the effective electric field with two approximations are shown in TABLEs 2.3(YbF), 2.4(BaF), 2.5(ThO), and 2.6(HF^+). In these tables, $\mathcal{E}_{\rm eff}^{\rm nuc}$ is the approximation using only the nuclear electric field [Eq. (2.15)] and $\mathcal{E}_{\rm eff}^{\rm ob}$ is the approximation using the effective one-body operator [Eq. (2.16)]. In our results, the difference between the two approximations is not large and is within a few percents, except for HF^+ which is

Table 2.4: Effective electric field in BaF. The uncertainty in the experimental result is given in parentheses.

BaF($^2\Sigma_{1/2}$) Method/Basis	Active orbitals	virt. orb. cutoff (hartree)	$\mathcal{E}_{\rm eff}^{\rm ob}$ ($\frac{\rm GV}{\rm cm}$)	$\mathcal{E}_{\rm eff}^{\rm nuc}$ ($\frac{\rm GV}{\rm cm}$)	$\lvert A_\parallel^{\rm Ba}\rvert$ (MHz)	DM (D)
17e-CISD/DZ	$25-92$	8.00	4.62	4.87	1647	3.08
17e-CISD/TZ	$25-92$	2.20	4.58	4.67	1580	2.20
17e-CISD/QZ	$25-92$	0.80	4.51	4.58	1552	2.36
65e-CISD/DZ	$1-92$	8.00	4.32	4.56	1589	3.11
Experiment					2453(9)[a]	3.1702(15)[b]
RASSCF/EO[c]			7.51		2224	
17e-RASCI[d]				7.28		3.203

[a]Ref. [31], [b]Ref. [32], [c]Ref. [33], [d]Ref. [7]

computed only for a comparison with heavy polar diatomic molecules. This confirms that the large contribution to $\mathcal{E}_{\rm eff}$ arises from electrons near a nucleus, and hence the difference between the two approximations may become large for lighter molecules. For this reason, we also show the parallel magnetic hyperfine interaction constant $A_\parallel$, which is sensitive to the electronic structure near the nucleus.

It is known that a post Hartree-Fock computation is efficient for large basis sets, i.e., triple zeta or larger. Actually, the dependence on basis sets can be clarified from the results of YbF in TABLE 2.3. The effect of the change from DZ to TZ on calculation results is much larger than that of the change from TZ to QZ. The same feature can be seen in the results of BaF (TABLE 2.4). Focusing on the number of active orbitals in TABLE 2.3, we can find that the number of virtual orbitals included in the CISD calculation is a more influential one than the number of core orbitals in the active space. Although our best result of YbF, 79e-CISD/QZ, is not in sufficient agreement with the experimental data $A_\parallel$, it would be improved by including more virtual orbitals in the CI active space. Nevertheless, the value of the effective electric field is consistent with other theoretical works, though our result is slightly smaller.

Our best result of the dipole moment in BaF (3.11 Debye) is very close to the experimental value (3.1702(15) Debye [32]), whereas the parallel magnetic hyperfine interaction constant (1589 MHz) is far from the experimental value (2453(9) MHz [31]). In addition, our result $\mathcal{E}_{\rm eff}^{\rm nuc} = 4.56$ GV/cm is much smaller than Nayak's result 7.28 GV/cm [7] and

Table 2.5: Effective electric field in ThO. The uncertainty in the experimental result is given in parentheses.

ThO($^3\Delta_1$) Method/Basis	Active orbitals	virt. orb. cutoff (hartree)	$\mathcal{E}_{\rm eff}^{\rm ob}$ ($\frac{\rm GV}{\rm cm}$)	$\mathcal{E}_{\rm eff}^{\rm nuc}$ ($\frac{\rm GV}{\rm cm}$)	$\lvert A_\parallel^{\rm Th}\rvert$ (MHz)	DM (D)
18e-MR_3-CISD/DZ	$41-109$	2.00	68.8	71.1	1154	3.47
18e-MR_3-CISD/TZ	$41-134$	2.00	67.2	69.4	1330	3.53
18e-MR_3-CISD/TZ	$41-185$	5.50	66.5	68.6	1151	3.66
18e-MR_{10}-CISD/DZ	$41-109$	2.00	75.6	78.1	1280	3.86
18e-MR_{10}-CISD/TZ	$41-134$	2.00	71.3	73.6	1156	3.86
Experiment						4.098(3)[a]
18e-MR_{12}-CISD/TZ[b]			75.2		1369	
38e-2c-CCSD(T)[c]			81.5		1357	4.23

[a]Ref. [34], [b]Ref. [8], [c]Ref. [35]

Table 2.6: Effective electric field in HF^+.

$HF^+(^2\Pi_{1/2})$ Method/Basis	Active orbitals[†]	$\mathcal{E}_{\rm eff}^{\rm ob}$ ($\frac{\rm GV}{\rm cm}$)	$\mathcal{E}_{\rm eff}^{\rm nuc}$ ($\frac{\rm GV}{\rm cm}$)	DM (D)
9e-CISD/DZ	$1-42$	2.16×10^{-3}	3.65×10^{-3}	2.66
9e-CISD/TZ	$1-80$	2.53×10^{-3}	3.16×10^{-3}	2.60
9e-CISD/QZ	$1-140$	2.64×10^{-3}	3.04×10^{-3}	2.59

[†] All the virtual orbitals are included into the active space.

Table 2.7: Summary of $\mathcal{E}_{\rm eff}$ for each molecule.

Species (state)	Method/Basis	$\mathcal{E}_{\rm eff}^{\rm ob}$ (GV/cm)	$\mathcal{E}_{\rm eff}^{\rm nuc}$ (GV/cm)
YbF ($^2\Sigma_{1/2}$)	79e-CISD/QZ	20.8	21.2
BaF ($^2\Sigma_{1/2}$)	65e-CISD/DZ	4.32	4.56
ThO ($^3\Delta_1$)	18e-MR_{10}-CISD/TZ	71.3	73.6
HF^+ ($^2\Pi_{1/2}$)	9e-CISD/QZ	2.64×10^{-3}	3.04×10^{-3}

Kozlov's result 7.51 GV/cm [33]. The reason seems to be the differences of the number of orbitals in the active space and reference states.

From the results of ThO shown in TABLE 2.5, the improvement from MR_3-CISD to MR_{10}-CISD brings a notable increase of $\mathcal{E}_{\rm eff}$. Detailed discussions about correlation models of ThO have already been reported in the work of Fleig and Nayak [8]. They mentioned that the addition of σ-type spinors to the active space brings a significant change of the electronic structure of ThO. Our best result $\mathcal{E}_{\rm eff}^{\rm ob} = 71.3$ GV/cm is close enough to the result of Fleig and Nayak, 75.2 GV/cm [8].

As shown in TABLE 2.6, the effective electric field in HF^+ is quite small compared to the other molecules, though HF^+ has a large molecular electric dipole moment. The reason is discussed later from a viewpoint of local distribution of physical quantities. Our best results of each molecule are summarized in TABLE 2.7. The electronic states of these correlation models are used for the later discussion about local physical quantities.

Let us now investigate the distribution of local physical quantities defined by the quantum field theory. The distributions of local physical quantities on a plane including the internuclear axis in YbF, BaF, ThO and HF^+ are shown in FIGs. 2.2–2.5, respectively. Panels (a) – (c) show the results of the electron density, the norm of the spin angular momentum density, and the norm of the small component of the spin angular momentum density $|\langle\hat{\psi}_S^\dagger \frac{\hbar}{2}\vec{\sigma}\hat{\psi}_S\rangle|$, all in atomic units. The electron density distributions of YbF, BaF, and ThO have a very similar pattern. The distribution patterns of the spin angular momentum density are quite different from those of the electron density. The distribution patterns of the spin angular momentum density and its small component contribution of YbF are similar to those of BaF, since both of them are in the same state $^2\Sigma_{1/2}$. A remarkable feature of the spin angular momentum density distribution in YbF is that its distribution is not symmetric for both sides of internuclear axis around nuclei and is concentrated at a little distance away from nuclei. This feature is common with that of YbF, BaF, and ThO, which have the large $\mathcal{E}_{\rm eff}$, while it is not seen in HF^+. In FIGs. 2.6(a) and 2.7(a), we compare the distribution patterns of the spin angular momentum density in YbF and HF^+, respectively. This feature is highlighted in these figures. However, for the effective electric field, $\langle\hat{\psi}_S^\dagger \frac{\hbar}{2}\vec{\sigma}\hat{\psi}_S\rangle$ is more important than the spin angular momentum density itself. The norm value of $\langle\hat{\psi}_S^\dagger \frac{\hbar}{2}\vec{\sigma}\hat{\psi}_S\rangle$ in HF^+ is as large as that in YbF. Since Eq. (2.15) indicates that the

value of the effective electric field depends on the scalar product of $\hat{\psi}_S^\dagger \frac{\hbar}{2}\vec{\sigma}\hat{\psi}_S$ and $\hat{\vec{E}}^{\rm nuc}$, one may presume that the effective electric field in HF^+ is as large as that of YbF; however, this presumption is seen to be wrong from TABLE 2.7. As shown in FIGs. 2.5(c) and 2.7(b), the distribution pattern of $\langle\hat{\psi}_S^\dagger \frac{\hbar}{2}\vec{\sigma}\hat{\psi}_S\rangle$ in HF^+ is nearly antisymmetric to a plane which intersects orthogonally with the internuclear axis on the F nucleus, while the electric field of a nucleus is distributed almost spherically and the direction is radial from the F nucleus. On the other hand, the distribution pattern in YbF shown in Fig. 2.6(b) is asymmetric, though its magnitude of symmetry breaking is smaller than the spin angular momentum density itself. These features can be seen more clearly from the distributions of $\langle 2\hat{\psi}_S^\dagger \vec{\sigma}\hat{\psi}_S \cdot \hat{\vec{E}}^{\rm nuc}\rangle$ in YbF and HF^+ shown in FIG. 2.8. This means that not only the large nucleus charge but also the asymmetric pattern of $|\langle\hat{\psi}_S^\dagger \frac{\hbar}{2}\vec{\sigma}\hat{\psi}_S\rangle|$ are important features of the large effective electric field. As a result, although $|\langle\hat{\psi}_S^\dagger \frac{\hbar}{2}\vec{\sigma}\hat{\psi}_S\rangle|$ in HF^+ is as large as that in YbF, the integration of the inner product of $\hat{\psi}_S^\dagger \vec{\sigma}\hat{\psi}_S$ and $\hat{\vec{E}}^{\rm nuc}$ over the whole region is much smaller than that in YbF. In other words, it can be predicted that even light atomic molecules could have the large effective electric field if the small component of the spin angular momentum density has an asymmetric distribution pattern.

Next, the vector potential term of the spin torque density $\langle\hat{\vec{t}}_{eA}\rangle$ and the EDM torque densities in YbF are shown in FIG. 2.9. In this article, we adopt atomic units for torque. Among three heavy molecules, we choose YbF for a demonstration, since this molecule is very consistent with other works and is a familiar one due to many works reported by many groups, while the other two molecules have the same features discussed below. The magnetic term of the EDM torque density $\langle\hat{\vec{t}}^B_{\rm EDM}\rangle$ is perpendicular to the magnetic field as seen from Eq. (2.29), and its distribution is concentrated around the nuclei. On the other hand, the electric term of the EDM torque density $\langle\hat{\vec{t}}^E_{\rm EDM}\rangle$ is also perpendicular to the electric field and its distribution pattern is almost the same as that of the spin angular momentum density, where both features are seen from Eq. (2.28). We also calculate the integration of each torque contribution over the whole region. The value of the vector potential term of the spin torque is $\int\langle\hat{\vec{t}}_{eA}\rangle d^3\vec{r} \approx (0.0, -1.8\times10^{-3}, 0.0)$, which is perpendicular to both magnetic field and spin angular momentum. The integrated value of the electric term of EDM torque density is $(0.0, 1.0\times d_e, 0.0)$, which is much larger than that of the magnetic term, $(0.0, 7.3\times10^{-6}\times d_e, 0.0)$. This difference between their integrated values can be

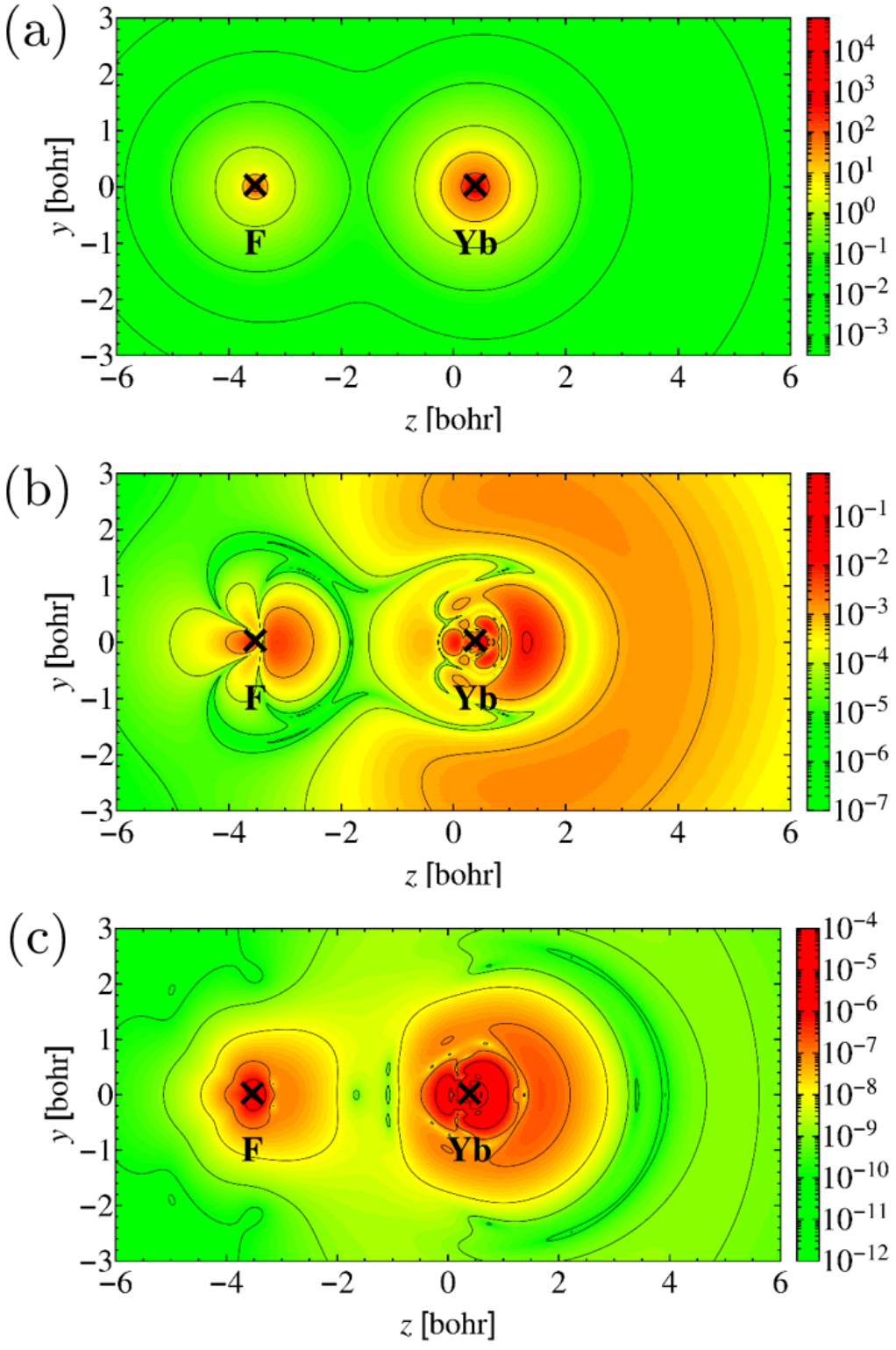

Figure 2.2: The distributions of (a) the electron density, (b) the norm of the spin angular momentum density, and (c) the norm of the small component of the spin angular momentum density on a plane including the internuclear axis in YbF. All values are shown in atomic units.

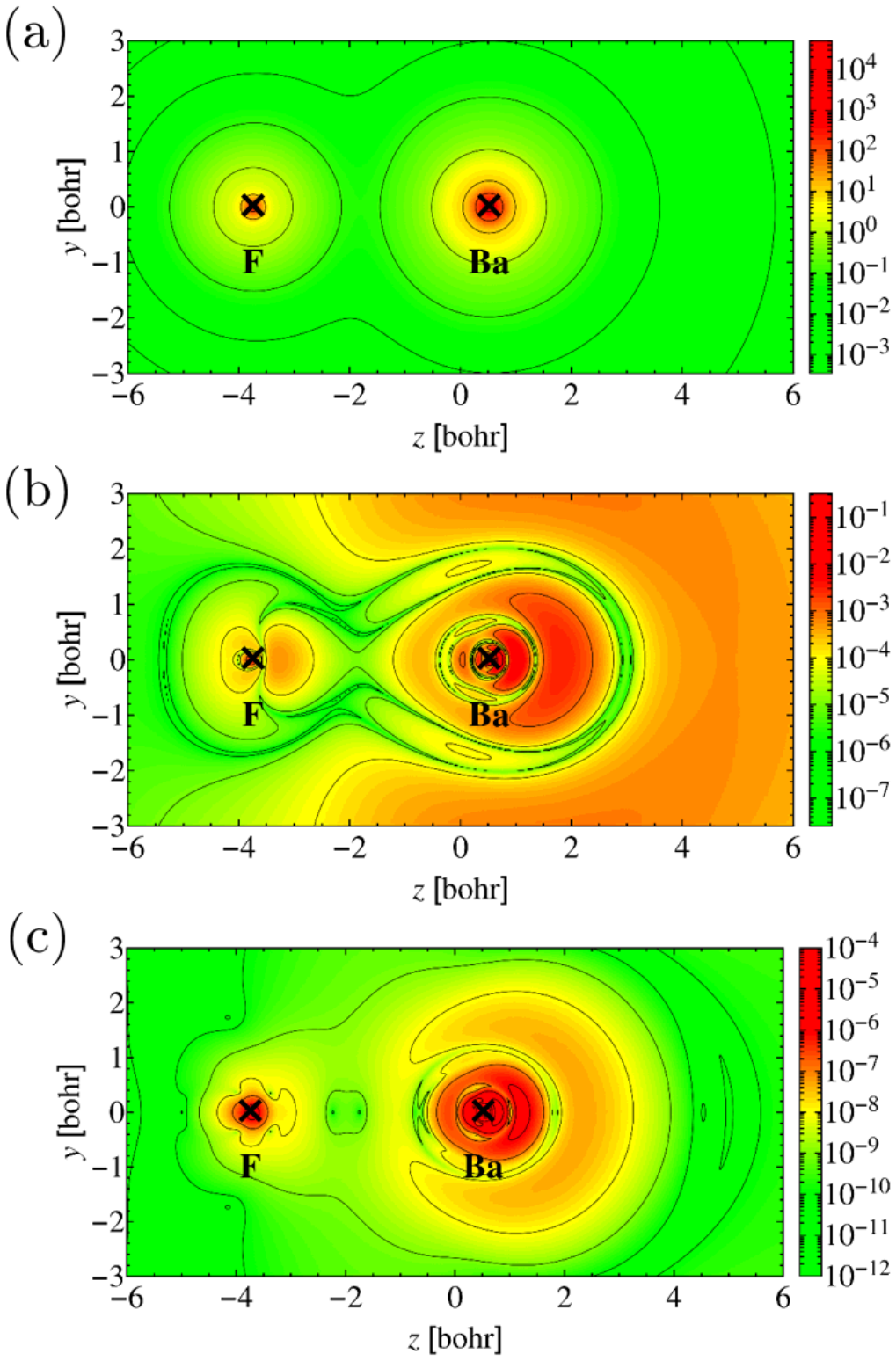

Figure 2.3: The distributions of (a) the electron density, (b) the norm of the spin angular momentum density, and (c) the norm of the small component of the spin angular momentum density on a plane including the internuclear axis in BaF. All values are shown in atomic units.

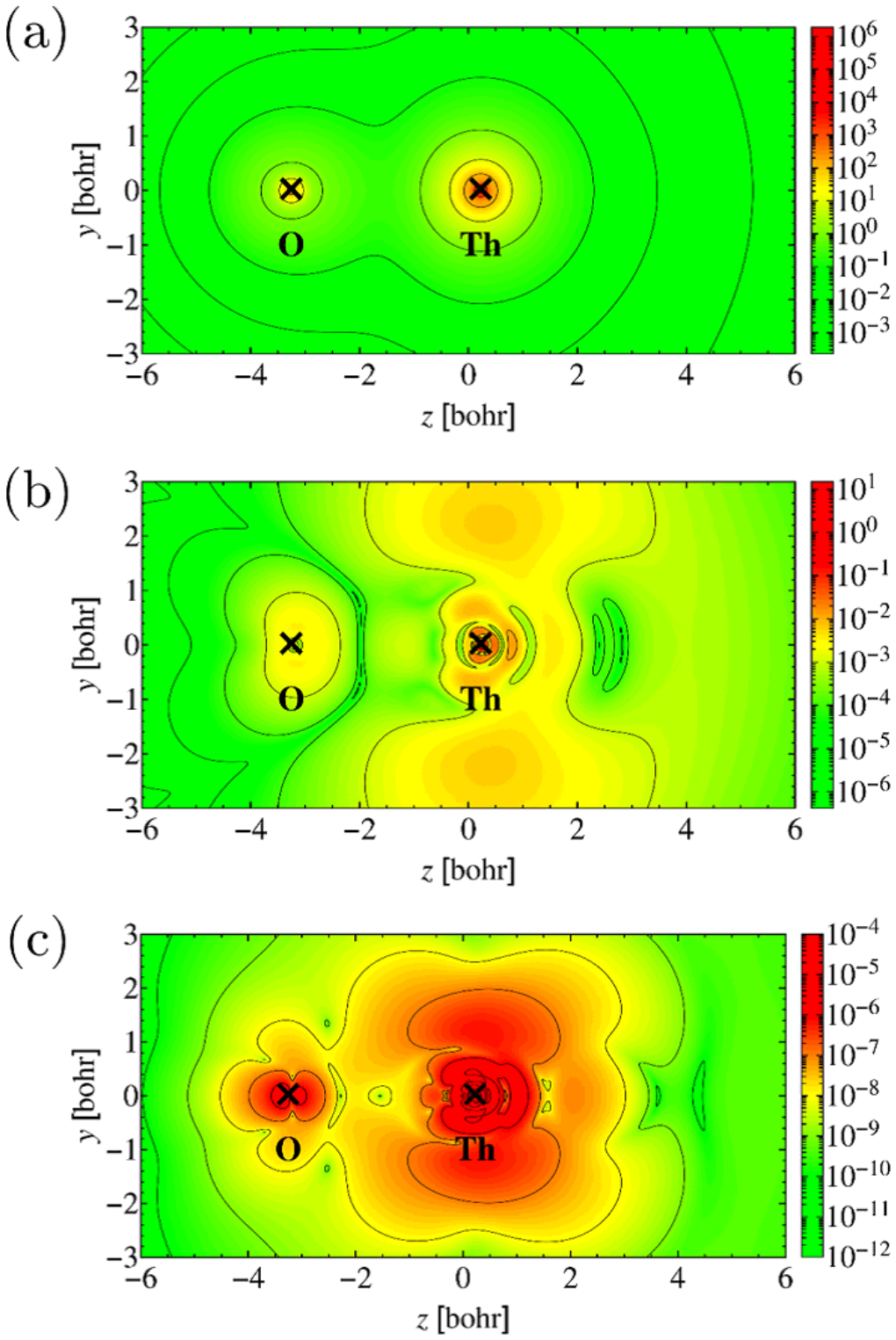

Figure 2.4: The distributions of (a) the electron density, (b) the norm of the spin angular momentum density, and (c) the norm of the small component of the spin angular momentum density on a plane including the internuclear axis in ThO. All values are shown in atomic units.

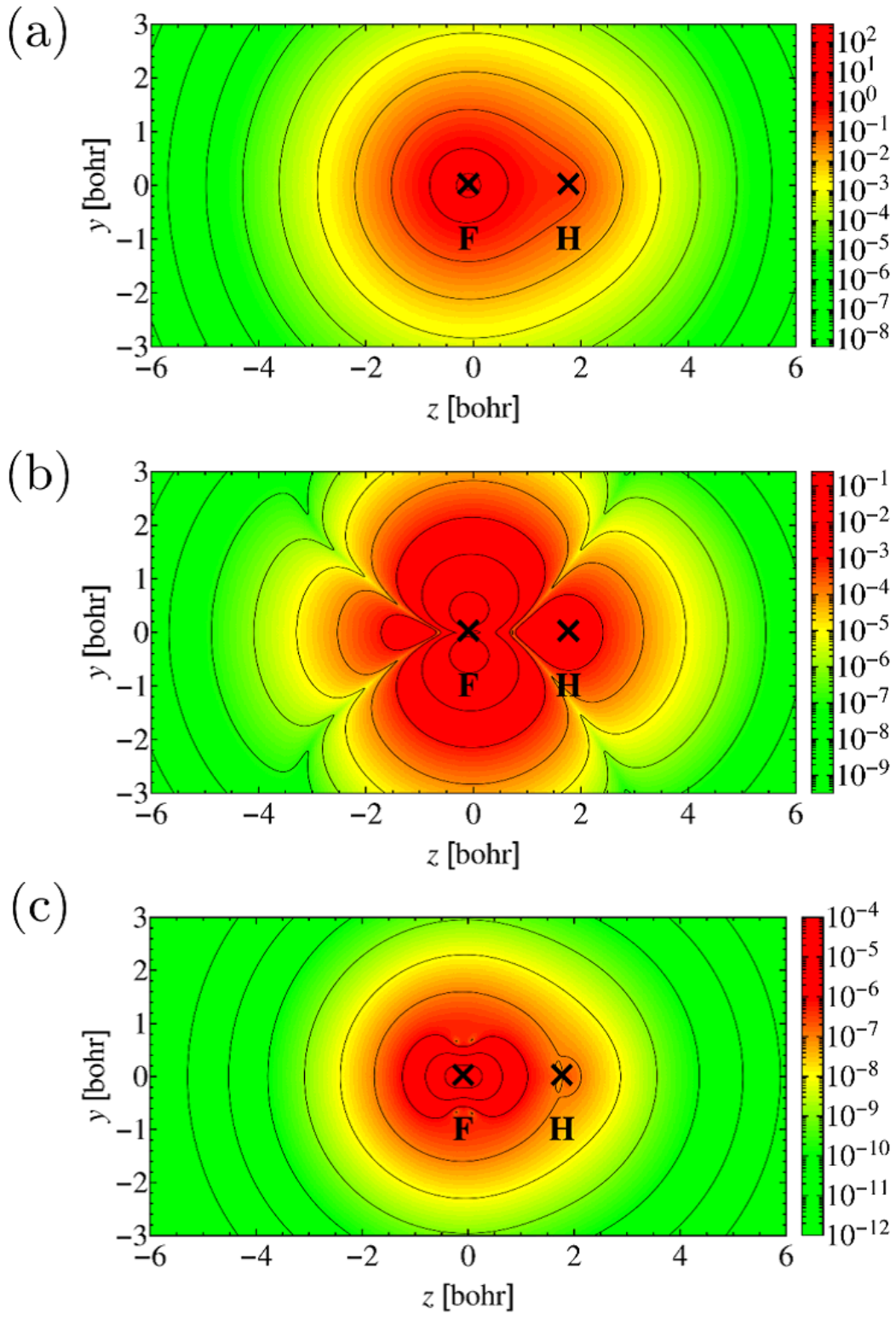

Figure 2.5: The distributions of (a) the electron density, (b) the norm of the spin angular momentum density, and (c) the norm of the small component of the spin angular momentum density on a plane including the internuclear axis in HF^+. All values are shown in atomic units.

explained by the difference of their distribution patterns. Since the distribution of $\langle \hat{\vec{t}}^B_{\rm EDM} \rangle$ forms vortices around the nuclei, $\int \langle \hat{\vec{t}}^B_{\rm EDM} \rangle d^3\vec{r}$ is averaged out drastically.

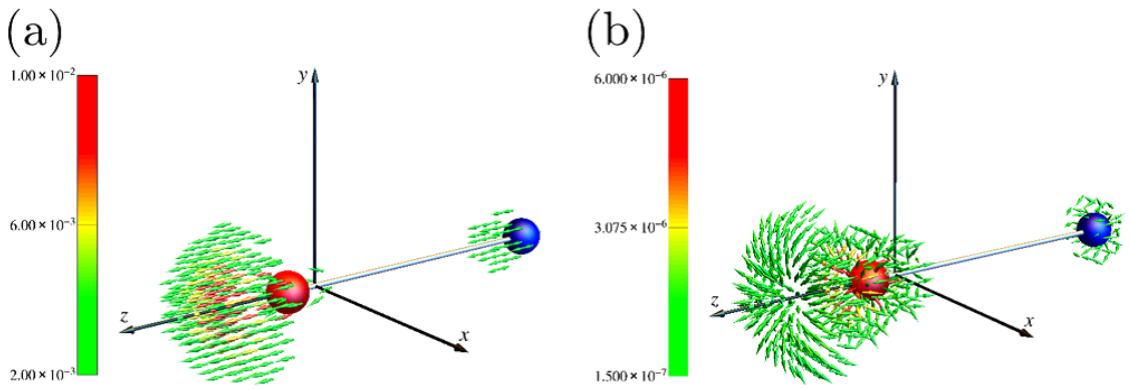

Figure 2.6: Distributions of (a) the spin angular momentum density $\langle \hat{\vec{s}}_e \rangle$ and (b) the small component of the spin angular momentum density $\langle \hat{\psi}^\dagger_S \frac{\hbar}{2} \vec{\sigma} \hat{\psi}_S \rangle$ in YbF. The red sphere represents the Yb nucleus and the blue one represents the F nucleus. The color means the value of densities in atomic units.

These results confirm that the equation of motion of spin [Eq. (2.30)] based on the quantum field theory enables us to estimate the integrated value and even to visualize the local pictures of spin torque dynamics, which give us a different perspective of local spin dynamics.

2.5 Conclusions

In this paper, we have studied the spin dynamics of the electron from the viewpoint of the electron EDM in the framework of the quantum field theory. The relation between the interaction energy of the electron EDM and the spin precession is described approximately by time evolution originated from the existence of the EDM. We have calculated $\mathcal{E}_{\rm eff}$ for YbF ($^2\Sigma_{1/2}$), BaF ($^2\Sigma_{1/2}$), ThO ($^3\Delta_1$), and HF^+ ($^2\Pi_{1/2}$) by CI computations based on RASCI. From the viewpoint of the local spin torque dynamics, the modification of the equation of motion of the spin angular momentum density has been discussed and we have shown the spin angular momentum density and the EDM torque density for the above molecules. We have demonstrated that the local pictures of the spin and torque help us to understand some of the physical origin of spin phenomena. We have predicted that even light atomic

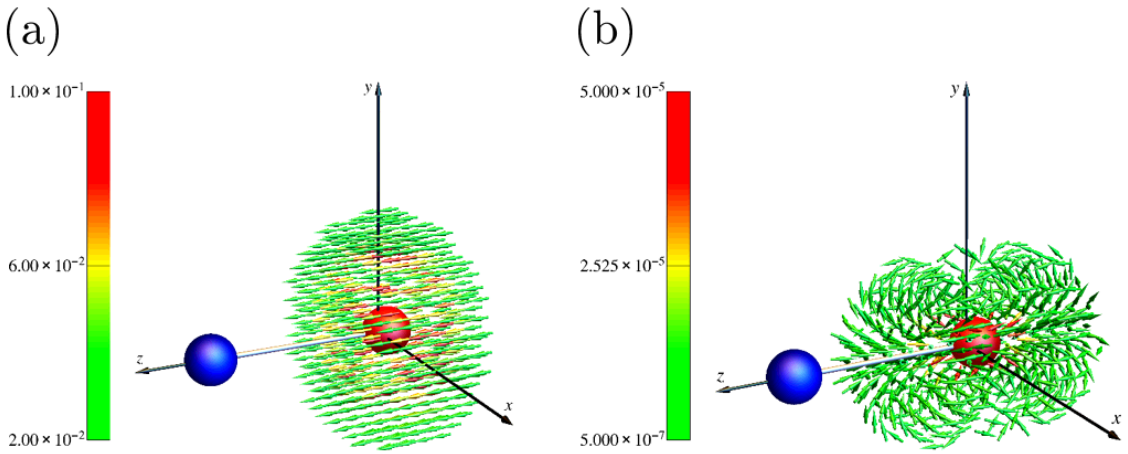

Figure 2.7: Distributions of (a) the spin angular momentum density $\langle \hat{\vec{s}}_e \rangle$ and (b) the small component of the spin angular momentum density $\langle \hat{\psi}_S^\dagger \frac{\hbar}{2} \vec{\sigma} \hat{\psi}_S \rangle$ in HF^+. The red sphere represents the F nucleus and the blue one represents the H nucleus. The color shows the value of densities in atomic units.

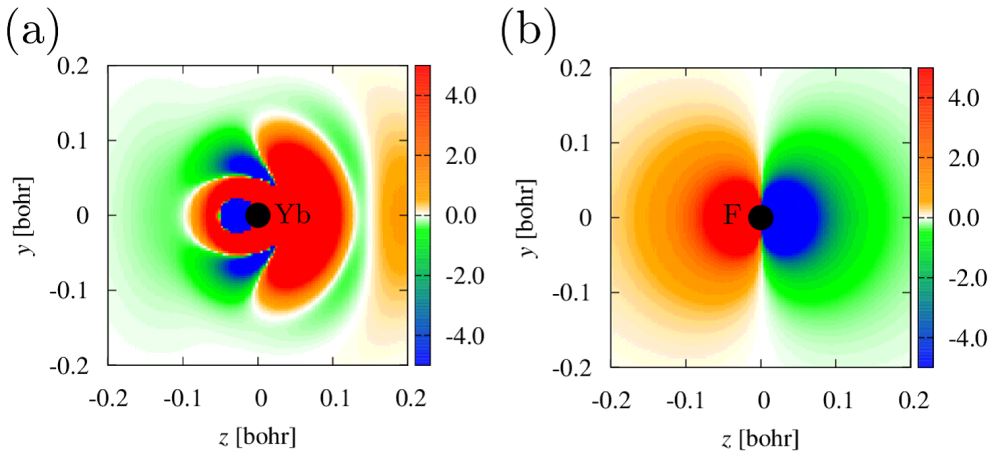

Figure 2.8: The distributions of $\langle 2\hat{\psi}_S^\dagger \vec{\sigma} \hat{\psi}_S \cdot \hat{\vec{E}}^{\mathrm{nuc}} \rangle$ in (a) YbF around the Yb nucleus and (b) HF^+ around the F nucleus (in atomic units).

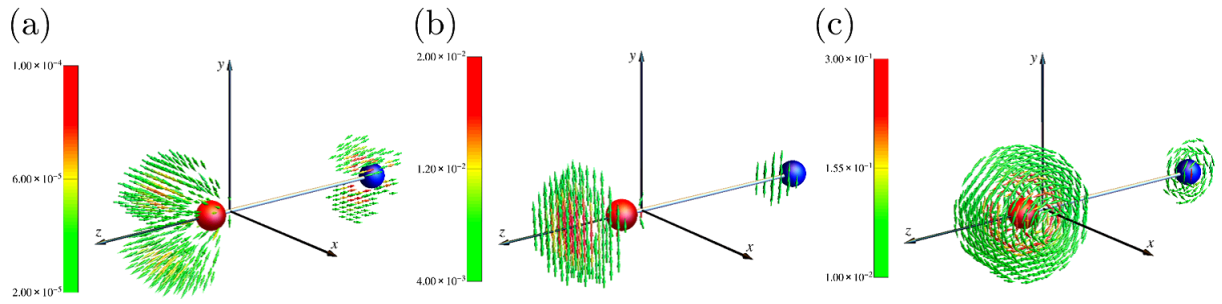

Figure 2.9: Distributions of (a) the vector potential term of the spin torque density $\langle \hat{\vec{t}}_{eA} \rangle$, (b) the electric term of the EDM torque density $\langle \hat{\vec{t}}^{E}_{\mathrm{EDM}} \rangle$, and (c) the magnetic term of the EDM torque density $\langle \hat{\vec{t}}^{B}_{\mathrm{EDM}} \rangle$ in YbF. The red sphere represents the Yb nucleus and the blue one represents the F nucleus. The color shows the value of the torque in atomic units.

molecules could have the large effective electric field if the small component of the spin angular momentum density has an asymmetric distribution pattern. In a future work, we will investigate the distribution of the local physical quantities for other molecules and explore new prediction methods of the spin precession. We also study the relation between the local distributions of the torque for the spin and the internal electric field, which is used for experiments in the search for the electron EDM.

Reference

[1] For example see, M. Drees, R. M. Godbole and P. Roy, Theory and Phenomenology of Particles, (World Scientific, Singapore, 2004).

[2] J. Hisano, M. Nagai, T. Naganawa, M. Senami, Phys. Lett. B **644**, 256 (2007).

[3] The ACME Collaboration *et al.*, Science **343**, 269 (2014).

[4] J. J. Hudson *et al.*, Nature (London) **473**, 493 (2011); D. M. Kara *et al.*, New J. Phys. **14**, 103051 (2012).

[5] H. M. Quiney et al, J. Phys. B. **31**, L85 (1998).

[6] M. Abe, G. Gopakumar, M. Hada, B. P. Das, H. Tatewaki, D. Mukherjee, Phys. Rev. A **90**, 022501 (2014).

[7] M. K. Nayak and R. K. Chaudhuri, J. Phys. B: At. Mol. Opt. Phys. **39**, 1231 (2006).

[8] T. Fleig, M. K. Nayak, J. Mol. Spectroscopy, **300**, 16 (2014).

[9] A. Tachibana, J. Mol. Model, **11**, 301 (2005).

[10] M. Senami, J. Nishikawa, T. Hara, A. Tachibana, J. Phys. Soc. Jpn **79**, 084302 (2010).

[11] T. Hara, M. Senami, A. Tachibana, Phys. Lett. A. **376**, 1434 (2012).

[12] M. Fukuda, M. Senami, A. Tachibana, Advances in Quantum Methods and Applications in Chemistry, Physics, and Biology Progress in Theoretical Chemistry and Physics, Vol. 27, edited by M. Hotokka, E. J. Brändas, J. Maruani, and G. Delgado-Barrio (Springer, New York, 2013) Chap. 7, pp. 131–139.

[13] L. Schiff, Phys. Rev. **132**, 2194, (1963).

[14] B. P. Das, in *Aspects of Many-Body Effects in Molecules and Extended Systems*, edited by D. Mukherjee (Springer, Berlin, 1989), p. 411.

[15] A. Tachibana, J. Mol. Struct. (THEOCHEM) **943**, 138 (2010).

[16] For example, see A. Messiah, Quantum Mechanics (North-Holland, New York, 1961).

[17] A. Tachibana, J. Math. Chem. **50**, 669 (2012).

[18] A. Tachibana, in *Concepts and Methods in Modern Theoretical Chemistry*, edited by S. K. Ghosh and P. K. Chattaraj , (CRC, Boca Raton, FL, 2013), pp. 235–251.

[19] A. Tachibana, J. Comput. Chem. Jpn. **13**, 18 (2014).

[20] A. Tachibana, Indian J. Chem. A, **53**, 1031 (2014).

[21] A. Tachibana, J. Math. Chem. **53**, 1943 (2015).

[22] DIRAC, a relativistic ab initio electronic structure program, Release DIRAC13 (2013), written by L. Visscher, H. J. Aa. Jensen, R. Bast, and T. Saue, with contributions from V. Bakken, K. G. Dyall, S. Dubillard, U. Ekström, E. Eliav, T. Enevoldsen, E. Faßhauer, T. Fleig, O. Fossgaard, A. S. P. Gomes, T. Helgaker, J. K. Lærdahl, Y. S. Lee, J. Henriksson, M. Iliaš, Ch. R. Jacob, S. Knecht, S. Komorovský, O. Kullie, C. V. Larsen, H. S. Nataraj, P. Norman, G. Olejniczak, J. Olsen, Y. C. Park, J. K. Pedersen, M. Pernpointner, K. Ruud, P. Sałek, B. Schimmelpfennig, J. Sikkema, A. J. Thorvaldsen, J. Thyssen, J. van Stralen, S. Villaume, O. Visser, T. Winther, and S. Yamamoto (see http://www.diracprogram.org)

[23] K. G. Dyall, Theor. Chem. Acc., **117**, 491 (2007); K. G. Dyall, J. Phys. Chem. A., **113**, 12638 (2009); A. S. P. Gomes, K. G. Dyall and L. Visscher, Theor. Chem. Acc., **127**, 369 (2010); K. G. Dyall, *ibid.* **131**, 1217 (2012).

[24] J. Phys. B: At. Mol. Opt. Phys., **31**, 1409 (1998).

[25] N. J. Stone, At. Data Nucl. Data Tables, **90**, 75 (2005).

[26] *QEDynamics*, M. Senami, K. Ichikawa, A. Tachibana
http://www.tachibana.kues.kyoto-u.ac.jp/qed/

[27] R. J. Van Zee, M. L. Seely, T. C. DeVore, and W. Weltner, Jr., J. Phys. Chem., **82**, 1192 (1978).

[28] B. E. Sauer, J. Wang, and E. A. Hinds, J. Chem. Phys., bf 105, 7412 (1996).

[29] N. S. Mosyagin, M. G. Kozlov and A. V. Titov, J. Phys. B: At. Mol. Opt. Phys. **31** L763 (1998).

[30] M. K. Nayak and R. K. Chaudhuri, Pramana **73**, 581 (2009).

[31] W. E. Ernst, J. Kändler, and T. Törring, J. Chem. Phys., **80**, 2283 (1984).

[32] L. B. Knight Jr., W. C. Easley, W. Weltner Jr., and M. Wilson, J. Chem. Phys., **41**, 2836 (1964).

[33] M. G. Kozlov, A. V. Titov, N. S. Mosyagin, and P. V. Souchko, Phys. Rev. A **56**, R3326(R) (1997).

[34] P. Hess, Ph.D. thesis, Harvard University, 2014; see http://laserstorm.harvard.edu/edm//publications.html.

[35] L. V. Skripnikov and A. V. Titov, J. Chem. Phys. **142**, 024301 (2015).

Chapter 3

Dynamical Picture of Spin Hall Effect Based on Quantum Spin Vorticity Theory

3.1 Introduction

The spin Hall effect (SHE), which refers to a conversion of an electric current into a transverse flow of spin, is one of the most important phenomena in the field of spintronics. Historically, the SHE was predicted theoretically first [1], and later experimental observations were performed in various types of materials by novel technology. The SHE was proposed theoretically as an analogue of the anomalous Hall effect [2]. Early proposed theories for the SHE are the so-called extrinsic mechanisms, which are based on the spin dependent scattering of electrons by impurities [1, 3]. Later, the intrinsic mechanism of the SHE in a semiconductor system was proposed on the basis of the concept of dissipationless quantum spin currents [4, 5]. Although theoretical discussion about the origin of the SHE still continues, many experiments show the SHE is an observable physical phenomenon. The first experimental observation of the SHE in a semiconductor was performed by Kato *et al.* [6] They detected electrically induced spin accumulation near the edges of the semiconductor by using Kerr rotation microscopy. Subsequently, Wunderlich *et al.* demonstrated the SHE by detecting circularly polarized light emitted from a light-emitting diode structure [7]. Furthermore, observations of the SHE in a metallic conductor [8, 9], and the inverse SHE

(ISHE) [10, 11], have been already reported. As for the theoretical side, an effective theory for spin-Hall effect not only in insulating but on equal footing also in conducting state by using a fully relativistic but model Hamiltonian has been discussed [12].

So far, the SHE has been treated by using the concept of the spin current. Even if the idea of the spin current is suitable to analyze application devices, it is insufficient to understand spin dynamical phenomena from the viewpoint of fundamental physics. Namely, it is significant to understand such phenomena by dynamical pictures depicted with quantities derived from the symmetric energy-momentum tensor. From this point of view, in this study, we discuss theoretical aspects of the SHE and ISHE on the basis of a more fundamental theory called the "quantum spin vorticity theory" [13–17], which can give physical dynamical quantities as local quantities. While quantum mechanics cannot explain local contribution due to the definition of the inner product, which is derived by the integration over the whole region, quantum field theory can give the definition of local physical quantities without losing local contributions. Therefore, the quantum spin vorticity theory gives the equation of motion of local spin and the equation for the vorticity of the spin without losing local contributions. In particular, the "spin vorticity", which is a local quantity defined as the rotation of the spin angular momentum density, is neglected in the framework of quantum mechanics. On the other hand, the quantum spin vorticity theory reveals that the spin vorticity is crucial for investigating spin dynamics as a component of the local momentum density. The spin vorticity helps us to understand spin phenomena in molecular systems and even in condensed matter systems from a unified viewpoint.

In this paper, firstly we review the quantum spin vorticity theory. After we explain the local physical quantities, which are defined in quantum field theory, we show numerical calculation results of the local physical quantities in a simple carbon chain under a bias voltage as a demonstration. For these calculations of the local physical quantities defined by quantum field theory, we use a quantum mechanical wave packet by the non-equilibrium Green's function method as an approximation to a quantum field theoretical one. Finally, we show the SHE and ISHE can be explained by a local dynamical picture without introducing the spin current but with the spin vorticity.

3.2 Quantum Spin Vorticity Theory

First of all, we review the quantum spin vorticity theory. In this paper, we discuss this theory in the framework of general relativity, though it can be applied even in the framework of supergravity [16]. In general relativity, the energy-momentum tensor obtained from the variational principle with a Lagrangian which is invariant under the general coordinate transformation must be a symmetric tensor. This requirement leads to the equation of spin dynamics, which reveals an important role of the spin vorticity for spin dynamics in the limit to the Minkowski space-time. We begin by introducing the Lagrangian density $\hat{L}$ for the quantum electrodynamics system with an electromagnetic field under external gravity. The Lagrangian density $\hat{L}$ is written as the sum of the Lagrangian density of the electron $\hat{L}_e$ and that of the electromagnetic field $\hat{L}_{\rm EM}$,

$$\hat{L}_e = \frac{c}{2}\left(\hat{\bar{\psi}}(i\hbar\gamma^a e_a{}^\mu \hat{D}_{e\mu}(g) - m_e c)\hat{\psi} + h.c.\right), \quad \hat{L}_{EM} = -\frac{1}{16\pi}\hat{F}_{\mu\nu}\hat{F}_{\rho\sigma}g^{\mu\rho}g^{\nu\sigma}, \tag{3.1}$$

where $\hat{\psi}$ denotes the Dirac spinor of the electron, $\hat{\bar{\psi}} = \hat{\psi}^\dagger\gamma^0$, γ^a are Dirac gamma matrices, $e_a{}^\mu$ is the tetrad field, m_e is the electron mass, c is the speed of light in vacuum, and $g^{\mu\nu}$ is the metric tensor. The electromagnetic field strength tensor is $\hat{F}_{\mu\nu} = \partial_\mu\hat{A}_\nu - \partial_\nu\hat{A}_\mu$, where $\hat{A}_\mu$ is the gauge field. Here, Greek indices and Latin indices from a to d run over 0 to 3. The former refers to the general coordinate indices, while the latter refers to the local Lorentz frame indices. We adopt the Einstein summation convention. The gravitational covariant derivative is written as

$$\hat{D}_{e\mu}(g) = \hat{D}_{e\mu} + i\frac{1}{2\hbar}\gamma_{ab\mu}J^{ab}, \quad \hat{D}_{e\mu} = \partial_\mu + i\frac{Z_e e}{\hbar c}\hat{A}_\mu, \tag{3.2}$$

where $\hat{D}_{e\mu}$ is the gauge covariant derivative, $J^{ab} = \frac{i\hbar}{4}\left[\gamma^a, \gamma^b\right]$, $\gamma_{ab\mu}$ is the spin connection [18], e is the electron charge ($e > 0$) and $Z_e = -1$. The variational principle for the system action with respect to the tetrad field leads to the symmetric energy-momentum tensor $T_{\mu\nu}$ as follows [19]:

$$\hat{T}_{\mu\nu} = \frac{1}{\sqrt{-g}}\eta_{ab}e^b{}_\nu\frac{\delta\left(\hat{L}\sqrt{-g}\right)}{\delta e_a{}^\mu} = \hat{T}_{e\mu\nu} + \hat{T}_{{\rm EM}\mu\nu}. \tag{3.3}$$

Writing the right-hand side explicitly,

$$\hat{T}_{e\mu\nu} = -\hat{\varepsilon}^{\Pi}_{\mu\nu} - \hat{\tau}^{\Pi}_{e\mu\nu}(g) - g_{\mu\nu}\hat{L}_e = \hat{T}_{e\nu\mu}, \tag{3.4}$$

$$\hat{\varepsilon}^{\Pi}_{\mu\nu} = -\frac{1}{\sqrt{-g}}\eta_{ab}e^{b}{}_{\nu}\left[\frac{\partial\left(\hat{L}_e\sqrt{-g}\right)}{\partial\gamma^{cd}{}_{\rho}}\frac{\partial\gamma^{cd}{}_{\rho}}{\partial e_a{}^{\mu}} - \partial_\sigma\left(\frac{\partial\left(\hat{L}_e\sqrt{-g}\right)}{\partial\gamma^{cd}{}_{\rho}}\frac{\partial\gamma^{cd}{}_{\rho}}{\partial\left(\partial_\sigma e_a{}^{\mu}\right)}\right)\right], \tag{3.5}$$

$$\hat{\tau}^{\Pi}_{e\mu\nu}(g) = -\frac{1}{\sqrt{-g}}\eta_{ab}e^{b}{}_{\nu}\frac{\partial\left(\hat{L}_e\sqrt{-g}\right)}{\partial e_a{}^{\mu}} = \frac{c}{2}\left(\hat{\psi}^\dagger\gamma^0\gamma_\nu\left(-i\hbar\hat{D}_\mu(g)\right)\hat{\psi} + h.c.\right), \tag{3.6}$$

$$\hat{T}_{\mathrm{EM}\mu\nu} = -\frac{1}{4\pi}g^{\rho\sigma}\hat{F}_{\mu\rho}\hat{F}_{\nu\sigma} - g_{\mu\nu}\hat{L}_{\mathrm{EM}} = \hat{T}_{\mathrm{EM}\nu\mu}, \tag{3.7}$$

where $g = \det g_{\mu\nu}$ and $\eta_{\mu\nu} = \mathrm{diag}(1,-1,-1,-1) = \eta^{\mu\nu}$. The concrete expression of Eq. (3.5) is written in Ref. [13]. Note that $\hat{\varepsilon}^{\Pi}_{\mu\nu}$ and $\hat{\tau}^{\Pi}_{e\mu\nu}(g)$ are not necessarily symmetric tensors. To emphasize this, we put the superscript Π and call them symmetry-polarized geometrical tensor and symmetry-polarized electronic stress tensor, respectively [13]. These tensors can be decomposed into a symmetric part and an anti-symmetric part as $\hat{\varepsilon}^{\Pi\mu\nu} = \hat{\varepsilon}^{S\mu\nu} + \hat{\varepsilon}^{A\mu\nu}$ and $\hat{\tau}^{\Pi\mu\nu}_{e}(g) = \hat{\tau}^{S\mu\nu}_{e}(g) + \hat{\tau}^{A\mu\nu}_{e}(g)$.

Since the energy-momentum tensor is symmetric, the anti-symmetric parts $\hat{\varepsilon}^{A}_{\mu\nu}$ and $\hat{\tau}^{A}_{e\mu\nu}$ cancel with each other:

$$\hat{\varepsilon}^{A\mu\nu} + \hat{\tau}^{A\mu\nu}_{e}(g) = 0. \tag{3.8}$$

Eq. (3.8) is called the quantum spin vorticity principle. In the limit to the Minkowski spacetime, it is revealed that Eq. (3.8) describes spin dynamics. In the limit of $e^{a}{}_{\mu} \to \delta^{a}{}_{\mu}$ and $g_{\mu\nu} \to \eta_{\mu\nu}$, the symmetric energy-momentum tensors $\hat{T}^{\mu\nu}_{e}$ and $\hat{T}^{\mu\nu}_{\mathrm{EM}}$ are reduced to

$$\hat{T}^{\mu\nu}_{e} = -\hat{\varepsilon}^{\Pi\mu\nu} - \hat{\tau}^{\Pi\mu\nu}_{e} - \eta^{\mu\nu}\hat{L}_e, \quad \hat{T}^{\mu\nu}_{\mathrm{EM}} = -\frac{1}{4\pi}\eta^{\rho\sigma}\hat{F}^{\mu}{}_{\rho}\hat{F}^{\nu}{}_{\sigma} - \eta^{\mu\nu}\hat{L}_{EM}, \tag{3.9}$$

$$\hat{\varepsilon}^{\Pi\mu\nu} = -\frac{\hbar}{4Z_e e}\epsilon^{\mu\nu\lambda\sigma}\partial_\lambda\hat{j}_{5\sigma}, \quad \hat{\tau}^{\Pi\mu\nu}_{e} = \frac{c}{2}\left(\hat{\psi}^\dagger\gamma^0\gamma^\nu\left(-i\hbar\hat{D}^{\mu}_{e}\right)\hat{\psi} + h.c.\right), \tag{3.10}$$

where $\epsilon^{\mu\nu\lambda\sigma}$ is the Levi-Civita tensor, $\hat{j}^{\mu}_{5} = Z_e ec\hat{\bar{\psi}}\gamma^\mu\gamma_5\hat{\psi}$ is the chiral current and $\gamma_5 = i\gamma^0\gamma^1\gamma^2\gamma^3$. Then, Eq. (3.8) is also reduced to the following equations:

$$\frac{\partial}{\partial t}\hat{\vec{s}}_e = \hat{\vec{t}}_e + \hat{\vec{\zeta}}_e, \tag{3.11}$$

$$\mathrm{rot}\hat{\vec{s}}_e = \frac{1}{2}\left(\hat{\bar{\psi}}\vec{\gamma}\left(i\hbar\hat{D}_{e0}\right)\hat{\psi} + h.c.\right) - \hat{\vec{\Pi}}_e, \tag{3.12}$$

where the spin angular momentum density $\hat{\vec{s}}_e$, the spin torque density $\hat{\vec{t}}_e$, the zeta force

density $\hat{\vec{\zeta}}_e$, and the kinetic momentum density $\hat{\vec{\Pi}}_e$ are defined as

$$\hat{s}_e^i = \hat{\psi}^\dagger \frac{\hbar}{2}\Sigma^i \hat{\psi} = \frac{\hbar}{2Z_e ec}\hat{j}_5^i, \quad \hat{t}_e^i = -\epsilon_{ijk}\hat{\tau}_e^{Ajk}, \tag{3.13}$$

$$\hat{\zeta}_e^i = -\partial_i \hat{\phi}_5, \quad \hat{\phi}_5 = \frac{\hbar}{2Z_e e}\hat{j}_5^0, \quad \hat{\Pi}_e^i = \frac{1}{2}\left(\hat{\bar{\psi}}\gamma^0\left(i\hbar\hat{D}_e^i\right)\hat{\psi} + h.c.\right). \tag{3.14}$$

In the equations above, Σ^i is the 4×4 Pauli matrix, and ϵ_{ijk} is the Levi-Civita tensor. Hereafter, Latin letters run from 1 to 3. As are clear from the above definitions, these operators are expressed by using the field operators of the electron $\hat{\psi}$ and the photon $\hat{A}^\mu$. The physical quantities are given as expectation values for a time-independent state vector in the Heisenberg picture such as $\mathcal{O} = \langle\Phi|\hat{\mathcal{O}}|\Phi\rangle - \langle 0|\hat{\mathcal{O}}|0\rangle$. Actual effects of condensed matter, which may break some symmetry, are included in the state vector.

Apparently, Eq. (3.11) and Eq. (3.12) are the equation of motion of the spin angular momentum density and the equation for the vorticity of spin, respectively. We note that Eqs. (3.11) and (3.12) are related to the angular momentum and momentum, respectively. The equation of motion of spin angular momentum density shown in Eq. (3.11) is derived in the framework of quantum field theory, and hence it does not average out the local contribution, while the Heisenberg equation in relativistic quantum mechanics [20] cannot describe local spin dynamics since a physical quantity in quantum mechanics is defined by the inner product, which is derived by the integration over the whole region. The zeta force density does not appear in the equation of motion of spin in the framework of relativistic quantum mechanics. In present experimental apparatuses, the local effect of the zeta force density is integrated into a small surface effect, so that it has not been observed experimentally yet. For example, the details of the spin torque and the zeta force for atomic and molecular systems were discussed in Ref. [21-23].

Let us now focus on Eq. (3.12). It implies that the vorticity of the electronic spin contributes to the momentum of the electron. We can see the fact clearly from the expression of the electronic momentum density $\hat{P}_e^i = \frac{1}{c}\hat{T}_e^{i0}$, which includes half of the spin vorticity as follows [14]:

$$\hat{\vec{P}}_e = \hat{\vec{\Pi}}_e + \frac{1}{2}\mathrm{rot}\hat{\vec{s}}_e. \tag{3.15}$$

Although the second term, which is the contribution from spin, as well as the zeta force density disappears after integration over the whole of space, its contribution cannot be neglected in a local region as well as the zeta force density. In other words, the electronic

momentum density, which is derived by the covariant symmetry of the general coordinate transformation, includes the local contribution of half of the spin vorticity unlike the definition of the momentum in quantum mechanics. Furthermore, the time derivative of the electronic momentum density is given as

$$\frac{\partial}{\partial t}\hat{\vec{P}}_e = \hat{\vec{L}}_e + \hat{\vec{\tau}}_e{}^S, \tag{3.16}$$

where $\hat{\vec{L}}_e = \hat{\vec{E}}\hat{j}_e^0 + \frac{1}{c}\hat{\vec{j}}_e \times \hat{\vec{B}}$ is the Lorentz force density, $\hat{j}_e^\mu = Z_e ec\hat{\bar{\psi}}\gamma^\mu\hat{\psi}$ is the electronic charge current density, $\hat{\vec{E}} = -\mathrm{grad}\hat{A}_0 - \frac{1}{c}\frac{\partial \hat{\vec{A}}}{\partial t}$ is the electric field and $\hat{\vec{B}} = \mathrm{rot}\hat{\vec{A}}$ is the magnetic field. The second term on the right-hand side, $\hat{\vec{\tau}}_e{}^S = \mathrm{div}\hat{\overleftrightarrow{\tau}}_e{}^S$, is the tension density [24, 25], which is defined as the divergence of the symmetric parts of the electronic stress tensor $\hat{\overleftrightarrow{\tau}}_e{}^S$. Since the tension density as well as the spin vorticity disappears after integrating over the whole region, the above equation is reduced to $\frac{\partial}{\partial t}\int \hat{\vec{\Pi}}_e d^3\vec{r} = \int \hat{\vec{L}}_e d^3\vec{r}$, which is a well known equation of motion in the framework of relativistic quantum mechanics [20]. By using Eq. (3.11), the time derivative of half of the spin vorticity is given easily as follows:

$$\frac{\partial}{\partial t}\left(\frac{1}{2}\mathrm{rot}\,\hat{\vec{s}}_e\right) = \frac{1}{2}\mathrm{rot}\,\hat{\vec{t}}_e = -\,\mathrm{div}\hat{\overleftrightarrow{\tau}}_e{}^A. \tag{3.17}$$

This means that the divergence of the anti-symmetric part of the stress tensor $\hat{\overleftrightarrow{\tau}}_e{}^A$ generates spin vorticity. By using Eq. (3.17), Eq. (3.16) can be rewritten as

$$\frac{\partial}{\partial t}\hat{\vec{\Pi}}_e = \hat{\vec{L}}_e + \hat{\vec{\tau}}_e{}^S - \frac{1}{2}\mathrm{rot}\,\hat{\vec{t}}_e. \tag{3.18}$$

Equations (3.17) and (3.18) express that the rotation of the spin torque density $\hat{\vec{t}}_e$ as driving force generates the kinetic momentum density $\hat{\vec{\Pi}}_e$ accompanying the generation of half of the spin vorticity, $\frac{1}{2}\mathrm{rot}\hat{\vec{s}}_e$. This interpretation is a consequence of the quantum spin vorticity theory.

Thus, in the spin vorticity theory, the equations regarding operators of the physical quantities derived from the energy-momentum tensor are discussed. When we calculate a physical quantity, we need both the operator of the physical quantity and the state vector of quantum field theory. The equations of operators discussed in the spin vorticity theory can be applied to QED systems universally, though the validity of the result of the physical quantity depends on how the state vector of the system is calculated.

3.3 Numerical calculations of spin vorticity

As an application example of the quantum spin vorticity theory, we demonstrate the generation of the spin vorticity in a local region by using a simple carbon chain, attaching both edges to electrodes in the presence of a finite bias voltage. The carbon chain is one of the ideal model systems for studying the electronic structure under a bias voltage and is also applicable in molecular device design as one of the nano carbon systems (such as rings, fullerenes, and graphenes). Therefore, the carbon chain is suitable for our first demonstration to understand spin phenomena in condensed matter and molecular systems from a unified viewpoint. Although, rigorously speaking, the electronic bound state of quantum field theory is required for calculations of the local physical quantities, such a calculation method is not established for our purpose at this moment. (Incidentally, we are trying to develop a program code *QEDynamics* [28] to calculate the electronic state described by quantum field theory, but this is still work in progress.) Therefore, we use a relativistic quantum mechanical wave packet as an approximation to the state vector of quantum field theory in order to calculate the local physical quantities, which are given as the expectation values of the density operators defined by quantum field theory. Nevertheless, it is sufficient to grasp some aspects of the spin vorticity. This wave packet in the steady state of the system is given by an *ab initio* calculation based on density-functional theory (DFT). Although this system is not dynamical, the local picture in the nonequilibrium state can be demonstrated. The electronic structure is calculated by means of a non-equilibrium Green's function method [29, 30] coupled with a local spin density approximation [31] in density-functional theory [32]. Since this method is widely used for calculations of spin densities induced by a bias voltage [33], it is suitable to demonstrate the distribution calculation of the local physical quantities such as the spin vorticity. The electronic state calculation is performed by an *ab initio* DFT code, OPENMX [33, 34]. We use *QEDynamics* [28] to calculate local physical quantities, which are calculated by using the 2-component relativistic wave function as a substitute for the large component of the 4-component relativistic wave function. The electronic structure of a straight carbon chain with bond length of 1.5 Å under a finite bias voltage of 0.1 V is self-consistently determined under an electronic temperature of 300 K. Pseudoatomic orbitals centered on atomic sites are used as the basis function set [35]. We use the pseudoatomic orbitals specified by C5.0-$s2p2d1$, where C stands for the atomic symbol, 5.0 represents the

cutoff radius (bohr), and $s2p2d1$ means the employment of two, two, and one orbitals for the s, p, and d component, respectively. The cutoff energy is set to 180 Ryd. The system we use consists of left and right electrodes and a central region. The electrodes are made of semi-infinite carbon chains and the central region contains eighteen carbon atoms.

The results are shown in FIG. 3.1. The kinetic momentum density, the spin angular momentum density and the spin vorticity of the system without bias voltage are smaller by two digits than those with the bias voltage 0.1 V. Hence, we only show the local physical quantities in the presence of the bias voltage 0.1 V in FIG. 3.1. Local physical quantities around six atoms in the center of the system, where the attaching electrodes have little direct effect, are shown in FIGs. 3.1 (a), (c) and (e). FIGs. 3.1 (b) and (d) show local physical quantities around a nucleus on a plane perpendicular to the carbon chain. The kinetic momentum density $\vec{\Pi}_e(\vec{r})$ is distributed along the π-bondings (FIG. 3.1 (a)). On the other hand, we can see the spin angular momentum density $\vec{s}_e(\vec{r})$ is distributed circularly around the nuclei (FIGs. 3.1 (c) and (d)), and therefore, the spin vorticity $\mathrm{rot}\vec{s}_e(\vec{r})$ is concentrated around a nucleus (FIG. 3.1 (e)). The distribution of the spin angular momentum density on the cross section shown in FIG. 3.1 (c) is similar to spin accumulation on a flat device which is observed experimentally as the SHE. However, in case of the carbon chain, the spin angular momentum density forms clear vortices because of the rotational symmetry of the system.

3.4 Application to the Spin Hall Effect

Finally, we propose a new dynamical picture of the SHE based on the spin vorticity theory. The conventional SHE refers to the conversion of a charge current into a transverse spin current due to the spin-orbit interaction [see Fig. 3.2(a)]. Although definitions of the spin current are discussed in Ref. [26], it is actually almost impossible to observe the spin current directly by electromagnetic detection. Furthermore, the relation between spin currents and observable physical quantities such as spin accumulation is unclear. This is because total spin is not conserved in general due to for example spin damping by spin-orbit interactions [27]. However, in the quantum spin vorticity theory, the dynamical picture of the SHE is not dependent on the concept of the spin current. Alternatively, the spin

transfer can be explained by the time evolution of the spin vorticity without invoking the spin current. Half of the spin vorticity is introduced naturally as a component of the electron momentum density on the basis of the quantum spin vorticity theory as mentioned above. In addition, the spin vorticity is an observable local physical quantity in principle and actually can be measured experimentally by the distribution of the spin angular momentum density for a system with large scale spin distribution such as the SHE, since the spin vorticity is defined as the rotation of the spin angular momentum density.

After all, the SHE is described by using the spin vorticity as follows. When the electric field is given in a conductor, the Lorentz force density $\vec{L}_e$ is generated. The Lorentz force density increases the total electronic momentum density $\vec{P}_e$, which consists of the kinetic momentum density $\vec{\Pi}_e$ and half of the spin vorticity $\frac{1}{2}\mathrm{rot}\vec{s}_e$ (see Eqs. (3.15) and (3.16)). The degree of the assignment of $\vec{P}_e$ to $\vec{\Pi}_e$ and $\frac{1}{2}\mathrm{rot}\vec{s}_e$ depends on the divergence of the anti-symmetric stress tensor $\overleftrightarrow{\tau}_e^A$ at each point in the space-time (see Eqs. (3.17) and (3.18)). Since the anti-symmetric stress tensor is zero in the non-relativistic limit, the relativistic interaction is necessary for the generation of the spin vorticity. Therefore, the spin vorticity is generated mainly around nuclei (or impurities), where the relativistic interaction is strong in the conductor. In addition, the superposition of the spin vorticity causes accumulation of spin at both edges of the conductor [see Fig. 3.3(a)]. Similarly, although the conventional ISHE refers to the conversion of an injected spin current into a transverse charge current or voltage [see Fig. 3.2(b)], this phenomenon is described by using the electron spin vorticity theory as follows. When the rotation of the spin torque density is given in a conductor, the distribution of the spin angular momentum density become non-uniform, and it generates the spin vorticity (see Eq. (3.17)). According to Eq. (3.18), the rotation of the spin torque also accelerates the electron, and it generates the kinetic momentum density [see Fig. 3.3(b)]. The degree of the generation of half of the spin vorticity and the kinetic momentum density depends on the divergence of the anti-symmetric stress tensor $\overleftrightarrow{\tau}_e^A$ at each point in the space-time (see Eqs. (3.17) and (3.18)). Of course, the value and direction of the spin vorticity induced by a bias voltage depend on the species of nuclei and structures. Therefore, we will try to evaluate local physical quantities of more complex structures which are used in the fields of spintronics and multiferroics in our near future work.

3.5 Conclusions

In this paper, we have proposed the dynamical local picture of the spin Hall effect based on the quantum spin vorticity principle. In the quantum spin vorticity principle, half of the spin vorticity is introduced naturally as a component of the electron momentum density. We have performed numerical calculations of the local distributions of the kinetic momentum density and the spin vorticity induced by a finite bias voltage by using a relativistic quantum mechanical wave packet as an approximation to the state vector of the quantum field theory. We also proposed new dynamical pictures of the SHE and ISHE based on the quantum spin vorticity theory. The SHE is described as *the generation of the spin vorticity by the applied electric field in a conductor.* The ISHE is described as *the acceleration of the electron by the rotation of the spin torque density as driving force accompanying the generation of the spin vorticity in a conductor.* The spin vorticity will be a key to give unified understanding of physical phenomena related to spin in condensed matter and molecular systems beyond the field of spintronics.

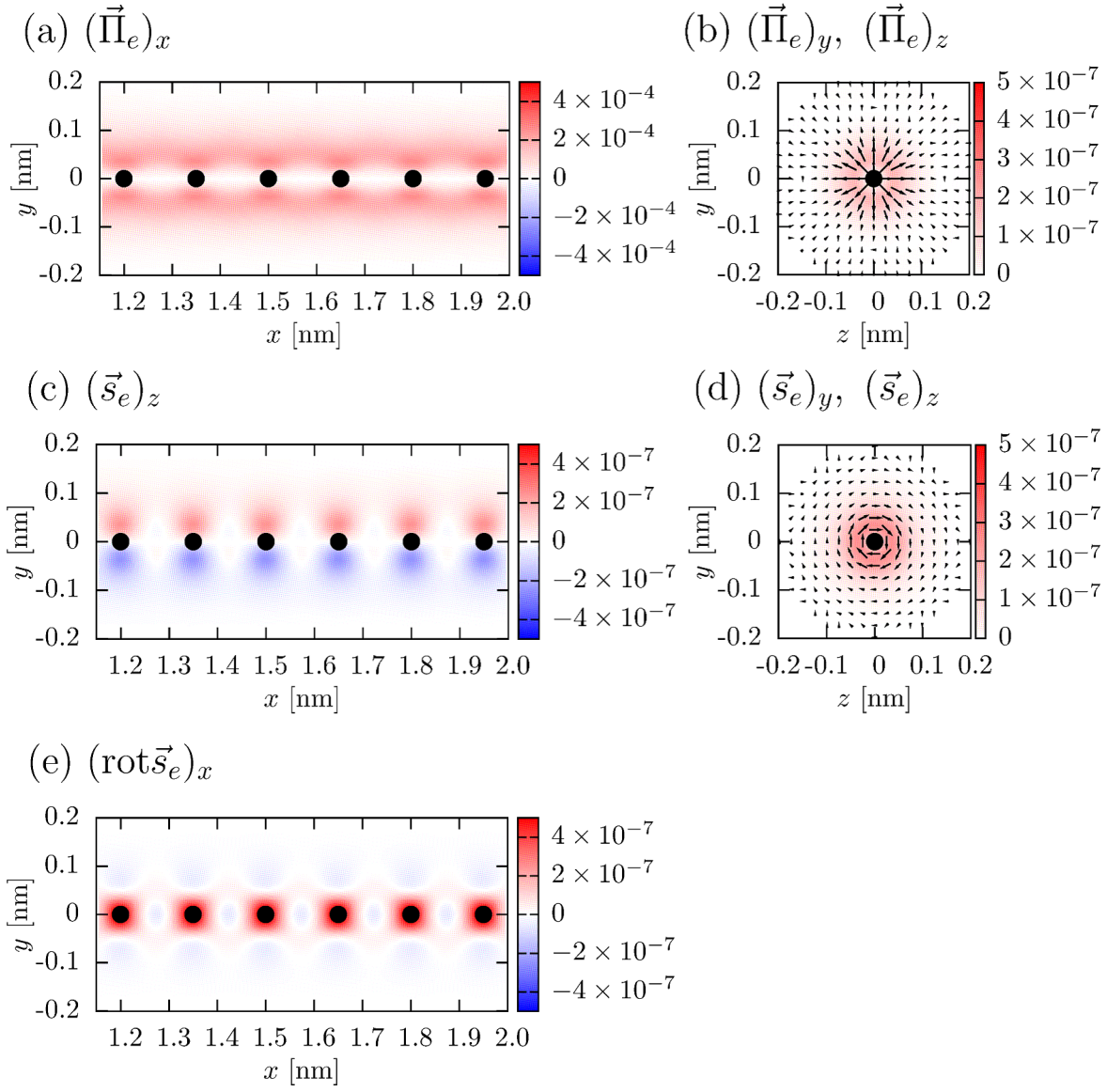

Figure 3.1: (a) The distributions of the x component of the kinetic momentum density on the plane $z = 0\,[\mathrm{nm}]$, and (b) y and z components on the plane $x = 1.65\,[\mathrm{nm}]$. (c) The distributions of the z component of the spin angular momentum density on the plane $z = 0\,[\mathrm{nm}]$, and (d) y and z components on the plane $x = 1.65\,[\mathrm{nm}]$. (e) The distribution of the x component of the spin vorticity on the plane $z = 0\,[\mathrm{nm}]$. The y and z components of the spin vorticity on the plane $z = 0\,[\mathrm{nm}]$ are negligibly small. In panels (b) and (d), the vectors consist of y and z components, and the color maps represent the norm of the vectors.

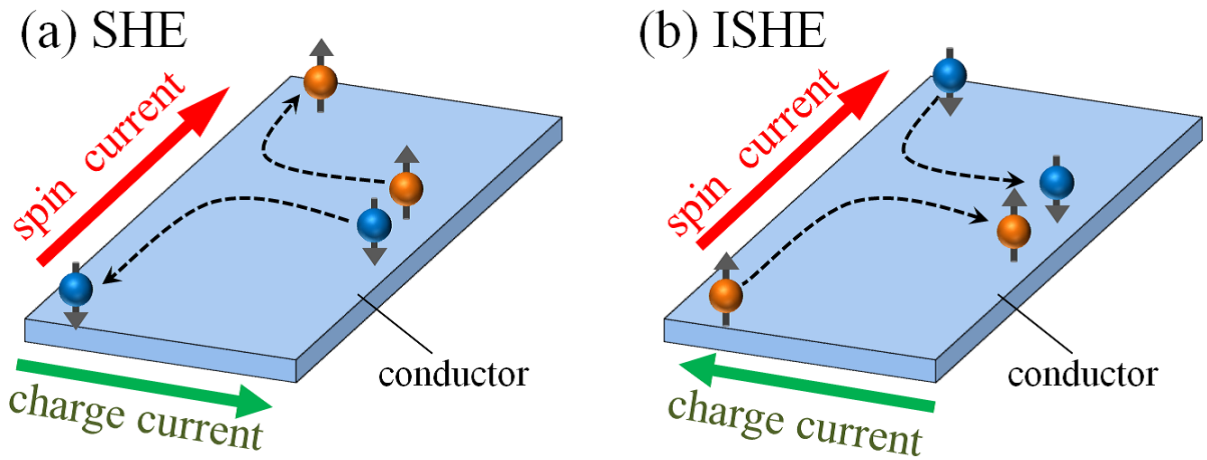

Figure 3.2: Conventional concepts of SHE and ISHE. (a) The SHE is understood as a conversion of a charge current into a transverse spin current. (b) The ISHE is understood as a conversion of an injected spin current into a transverse charge current.

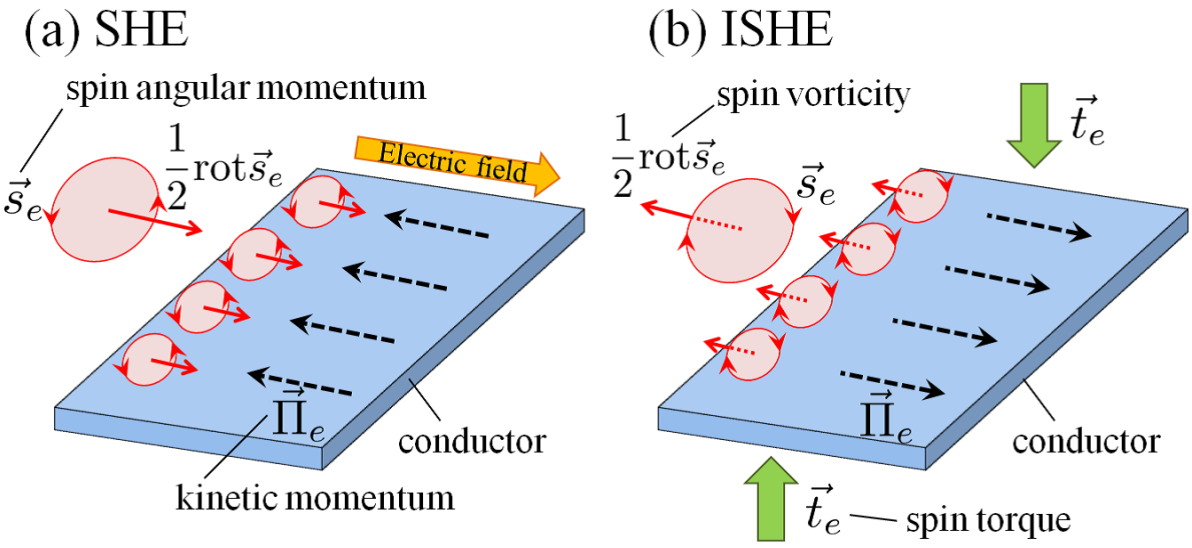

Figure 3.3: Concept based on the quantum spin vorticity theory. (a) The SHE is understood as the generation of the spin vorticity by the applied electric field. (b) The ISHE is understood as the acceleration of the electron by the rotation of the spin torque density as driving force accompanying the generation of half of the spin vorticity.

Reference

[1] M. I. Dyakonov and V. I. Perel, JETP Lett. **13**, 467 (1971); Phys. Lett. **A35**, 459 (1971).

[2] N. Nagaosa, J. Sinova, S. Onoda, A. H. MacDonald, and N. P. Ong, Rev. Mod. Phys. **82**, 1539 (2010).

[3] J. E. Hirsch, Phys. Rev. Lett. **83**, 1834 (1999).

[4] S. Murakami, N. Nagaosa and S.-C. Zhang, Science **301**, 1348 (2003).

[5] J. Sinova, D. Culcer, Q. Niu, N. A. Sinitsyn, T. Jungwirth, and A. H. MacDonald, Phys. Rev. Lett. **92**, 126603 (2004).

[6] Y. K. Kato, R. C. Myers, A. C. Gossard, and D. D. Awschalom, Science **306**, 1910 (2004).

[7] J. Wunderlich, B. Kaestner, J. Sinova, and T. Jungwirth, Phys. Rev. Lett. **94**, 047204 (2005).

[8] S. O. Valenzuela and M. Tinkham, Nature **442**, 176-179 (2007).

[9] T. Kimura, Y. Otani, T. Sato, S. Takahashi, and S. Maekawa, Phys. Rev. Lett. **98**, 156601 (2007).

[10] E. Saitoh, M. Ueda, H. Miyajima, and G. Tatara, Appl. Phys. Lett. **88**, 182509 (2006).

[11] K. Ando and E. Saitoh, Nat. Commun. **3**, 629 (2012).

[12] Y. Fuseya, M. Ogata, and H. Fukuyama, J. Phys. Soc. Jpn. **81**, 093704 (2012).

[13] A. Tachibana, J. Math. Chem. **50**, 669 (2012).

[14] A. Tachibana, Electronic Stress with Spin Vorticity. In *Concepts and Methods in Modern Theoretical Chemistry*, S. K. Ghosh and P. K. Chattaraj Eds., CRC Press, Florida (2013), pp. 235-251.

[15] A. Tachibana, J. Comput. Chem. Jpn. **13**, 18 (2014).

[16] A. Tachibana, Indian J. Chem. A, **53**, 1031 (2014).

[17] A. Tachibana, J. Math. Chem. **53**, 1943 (2015).

[18] S. Weinberg, *Quantum Theory of Fields III* (Cambridge University, Cambridge, 1995)

[19] S. Weinberg, *Gravitation and Cosmology: Principles and Applications of the General Theory of Relativity* (Wiley, New York, 1972)

[20] For example, see A. Messiah, *Quantum Mechanics* (North-Holland, New York, 1961).

[21] M. Senami, J. Nishikawa, T. Hara, A. Tachibana, J. Phys. Soc. Jpn **79**, 084302 (2010).

[22] T. Hara, M. Senami, A. Tachibana, Phys. Lett. A. **376**, 1434 (2012).

[23] M. Fukuda, M. Senami, A. Tachibana, *Progress in Theoretical Chemistry and Physics*, Vol. 27; Eds. M. Hotokka, E. J. Brandas, J. Maruani, G. Delgado-Barrio; Springer, Chapter 7, pp. 131-139 (2013).

[24] A. Tachibana, J. Chem. Phys. **115**, 3497 (2001).

[25] A. Tachibana, J. Mol. Struct. :(THEOCHEM) **943**, 138 (2010).

[26] "Spin Current", Oxford University Press, Eds. S. Maekawa, S. O. Valenzuela, E. Saitoh, and T. Kimura (2012).

[27] A. Takeuchi, K. Hosono and G. Tatara, Phys. Rev. B **81**, 144405 (2010).

[28] *QEDynamics*, M. Senami, K. Ichikawa, A. Tachibana
http://www.tachibana.kues.kyoto-u.ac.jp/qed/

[29] L. V. Keldysh, Sov. Phys. JETP **20**, 1018 (1965); C. Caroli, R. Combescot, P. Nozieres, and D. Saint-James, J. Phys. C **4**, 916 (1971).

[30] H. Kondo, H. Kino, J. Nara, T. Ozaki, and T. Ohno, Phys. Rev. B **73**, 235323 (2006).

[31] D. M. Ceperley and B. J. Alder, Phys. Rev. Lett. **45**, 566 (1980); J. P. Perdew and A. Zunger, Phys. Rev. B **23**, 5048 (1981).

[32] P. Hohenberg and W. Kohn, Phys. Rev. **136**, B864 (1964); W. Kohn and L. J. Sham, Phys. Rev. **140**, A1133 (1965).

[33] T. Ozaki, K. Nishio, and H. Kino, Phys. Rev. B **81**, 035116 (2010).

[34] T. Ozaki *et al.*, OpenMX package, http://www.openmx-square.org/.

[35] T. Ozaki, Phys. Rev. B **67**,155108 (2003).

Part II

Studies of Time-evolution Simulation Method of Operators in Quantum Electrodynamics

Chapter 4

Study of Simulation Method of Time Evolution in Rigged QED

4.1 Introduction

Recently, the technology for observation and manipulation of quantum systems involving the interaction between light and matter is developed with increasing speed and new experimental tools are becoming available. Remarkable features of such developments include real-time observation [1, 2], single-photon generation [3–6] and so on. Then, as for the theoretical side, it would be desirable to develop a formalism to simulate dynamical phenomena observed by such experiments treating light and matter and the interaction between them as accurately as possible. That is, by Quantum Electrodynamics (QED).

QED is probably the most successful fundamental physical theory we have. It is the theory of electrically charged particles and photons and interactions between them, taking the form of quantum theory of fields. Its accurate predictions include the Lamb shift of the energy levels of the hydrogen atom and the anomalous magnetic moment of the electron. In addition to such stationary properties, it can also predict dynamical properties like the cross section for the electron-positron scattering (Bhabha scattering) to a great accuracy. The successes are due to the development of the method to compute the QED interaction as a perturbation. The success of the perturbative approach, in turn, owes much to the capability of preparing the asymptotic states as the unperturbed states (and of course to the renormalizability). It has been long since such formalism was established [7, 8].

However, use of the asymptotic states and subsequently the S-matrix formulation has shortcomings when we would like to know the step-by-step time evolution of the quantum system employing QED. This is because it just describes the transition between infinite past ("in-state") and infinite future ("out-state"). Although it works fine for calculations of cross sections of scattering processes or energy shifts of bound states, it cannot be used for simulating the time evolution of the quantum system.

Hence, so far, simulations of time evolution of the quantum system involving light and matter are performed using the time-dependent Schrödinger or Dirac equation with classical electromagnetic fields (*i.e.* semi-classical treatment) [9–11] or using a quantized photon field with the very much simplified matter part (so that the interaction between the photon and matter is introduced somewhat in an *ad hoc* manner) [12–14]. It is true that these approximations are appropriate for a wide range of systems. For example, the former treatment is reasonable for a photon field produced by laser and the latter treatment for a system in cavity QED. We consider, however, it is of great importance to develop a simulation method based on QED in the form of quantum field theory, and without recourse to the perturbative approach.[1]

Besides the non-perturbative time evolution scheme, what we wish to add to the standard QED framework is the atomic nucleus. This is because, contrary to the high-energy physics application, the existence of the atomic nuclei is essential for atomic and molecular science in which we are interested. We would like to have a field theoretic QED formalism which is applicable to low energy phenomena such as chemical reactions and photoionization process. In this paper, as has been proposed in Ref. [17, 18], we include the atomic nucleus degree of freedom in the framework of the Rigged QED.

The Rigged QED [17–19] is a theory which has been proposed to treat dynamics of charged particles and photons in atomic and molecular systems in a quantum field theoretic way. In addition to the ordinary QED which is Lorentz invariant with Dirac (electron) field and U(1) gauge (photon) field, Schrödinger fields which represent atomic nuclei are added. In this way, dynamics of nuclei and their interaction with photons can be treated in a unified manner. Incidentally, we here note on semantics of the word "rigged". It has a

[1] In Refs. [15, 16], a formalism to simulate the dynamics of the quantum Dirac field has been developed but in the absence of the photon field.

nautical connotation as in the phrase "fully rigged ship" and means "equipped".[2] Namely, the Rigged QED is "QED equipped with Schrödinger fields" as we just described above.

Including the atomic nucleus degrees of freedom as quantum fields is crucial. Since we would like to treat the interaction between an electron and an atomic nuclei or between two nuclei as the one which is mediated by the quantized photon field (not by the classical electromagnetic field), we need to express the atomic nuclei as quantum fields. Then, it is necessary to compute the interaction non-perturbatively due to the existence of the bound states. Although this is a difficult task to achieve, in this way, we can go beyond the quantum mechanical treatment with perturbative QED corrections. We believe such a theoretical technique opens up a way to study and predict new phenomena.

To solve the dynamics of the Rigged QED in a non-perturbative manner, we need different techniques from those developed for the standard QED. In this paper, as a first step toward this issue, we propose a procedure to expand the Dirac field operator by solutions of the Dirac equation for electrons in nuclear potential and derive time evolution equations for the electron annihilation and creation operators. Similarly, the Schrödinger field operators are expanded by nucleus annihilation and creation operators. Then we derive time evolution equations for these annihilation and creation operators and discuss how time evolution of the operators for physical quantities can be calculated. In the end, we propose a method to approximate the operator equations by c-number equations and show some numerical results.

Before ending this section, we note on our notations and conventions which will be used in this paper. They mostly follow those of Refs. [17–19]. We use the Gaussian system of units. c denotes the speed of light in vacuum, $\hbar$ the reduced Planck constant and e the electron charge magnitude (so that e is positive). We put a hat to indicate a quantum operator to distinguish it from a c-number. A dagger as a superscript is used to express Hermite conjugate. A commutator is denoted by square brackets as $[A, B] \equiv AB - BA$ and an anti-commutator by curly brackets as $\{A, B\} \equiv AB + BA$. We denote the spacetime coordinate as $x = (x^\mu) = (x^0, x^i) = (ct, \vec{r})$ where the Greek letter runs from 0 to 3 and the Latin letter from 1 to 3. We adopt the convention that repeated Greek indices implies a summation over

[2]Similar use of the word "rigged" is found in a quantum mechanical context as "rigged Hilbert space" which means Hilbert space equipped with distribution theory [20]. But it should be noted that the concept of the rigged Hilbert space is not used in the rigged QED.

0 to 3. Other summations are explicitly written. The transformation between contravariant and covariant vectors are done by the metric tensor $g_{\mu\nu} = \mathrm{diag}(1, -1, -1, -1) = g^{\mu\nu}$. The gamma matrices are denoted by γ^μ.

This paper is organized as follows. In the next section, the framework of the Rigged QED which is relevant to the present study is reviewed briefly. In Sec. 4.3, we introduce annihilation and creation operators for each field operator and describe how we expand the field operators. In particular, Sec. 4.3.3 discusses how we treat the photon field operator in a non-perturbative manner following Ref. [18]. In Sec. 4.4, we derive time evolution equations for these annihilation and creation operators and discuss how time evolution of the operators for physical quantities can be calculated. In Sec. 4.5, we propose a method to approximate the evolution equations of the operators by the evolution equations for the density matrices of electrons and atomic nuclei. Under this approximation, we carry out numerical simulation of the time evolution of electron charge density of a hydrogen atom. The last section is devoted to our conclusion.

4.2 Rigged QED

In this section, we briefly review the general setting of Rigged QED [17–19] by showing its Lagrangian and equations of motion for the field operators.

4.2.1 Lagrangian

First, we describe Rigged QED in terms of the Lagrangian. A part of the Rigged QED Lagrangian is the ordinary QED Lagrangian. The Lagrangian density operator of QED can be written as

$$\hat{L}_{\mathrm{QED}}(x) = -\frac{1}{16\pi}\hat{F}_{\mu\nu}(x)\hat{F}^{\mu\nu}(x) + \hat{L}_e\left(\left\{\hat{\psi}, \hat{D}_{e\mu}\hat{\psi}\right\}; x\right), \tag{4.1}$$

where $\hat{F}_{\mu\nu}(x)$ is the electromagnetic field strength tensor which can be expressed by the photon field $\hat{A}_\mu(x)$ as

$$\hat{F}_{\mu\nu}(x) \;=\; \partial_\mu \hat{A}_\nu(x) - \partial_\nu \hat{A}_\mu(x). \tag{4.2}$$

We note here that we adopt the Coulomb gauge $\vec{\nabla} \cdot \hat{\vec{A}}(x) = 0$ in this work. $\hat{L}_e$ is the Lagrangian density operator for the electron

$$\hat{L}_e \left(\left\{ \hat{\psi}, \hat{D}_{e\mu} \hat{\psi} \right\}; x \right) = c \hat{\bar{\psi}}(x) \left(i\hbar \gamma^\mu \hat{D}_{e\mu}(x) - m_e c \right) \hat{\psi}(x), \tag{4.3}$$

where m_e is the electron mass and the Dirac field operator $\hat{\psi}(x)$ represents the electron (and positron). The operator with a bar on top is defined by $\hat{\bar{\psi}}(x) \equiv \hat{\psi}^\dagger(x)\gamma^0$. We denote the gauge covariant derivative for the electron as

$$\hat{D}_{e\mu}(x) = \partial_\mu + i \frac{Z_e e}{\hbar c} \hat{A}_\mu(x), \quad Z_e = -1. \tag{4.4}$$

The Rigged QED Lagrangian is this QED Lagrangian "rigged" with the Lagrangian of the atomic nuclei which are represented by Schrödinger fields. We denote the Schrödinger field operator for the nucleus a by $\hat{\chi}_a(x)$. This satisfies commutation relations if a is boson and anticommutation relations if a is fermion (which in turn is determined by the nuclear spin of a). The Lagrangian density operator for the atomic nucleus a can be written as

$$\hat{L}_a \left(\left\{ \hat{\chi}_a, \hat{D}_{a0} \hat{\chi}_a, \hat{\vec{D}}_a^2 \hat{\chi}_a \right\}; x \right) = \hat{\chi}_a^\dagger(x) \left(i\hbar c \hat{D}_{a0}(x) + \frac{\hbar^2}{2m_a} \hat{\vec{D}}_a^2(x) \right) \hat{\chi}_a(x), \tag{4.5}$$

where m_a is the mass of the nucleus a and the gauge covariant derivative of a is

$$\hat{D}_{a\mu}(x) = \partial_\mu + i \frac{Z_a e}{\hbar c} \hat{A}_\mu(x), \tag{4.6}$$

where Z_a is the a's atomic number. Thus, when we have N_n types of atomic nuclei in the system,

$$\begin{aligned} \hat{L}_{\text{RiggedQED}}(x) &= -\frac{1}{16\pi} \hat{F}_{\mu\nu}(x) \hat{F}^{\mu\nu}(x) + \hat{L}_e \left(\left\{ \hat{\psi}, \hat{D}_{e\mu} \hat{\psi} \right\}; x \right) \\ &\quad + \sum_{a=1}^{N_n} \hat{L}_a \left(\left\{ \hat{\chi}_a, \hat{D}_{a0} \hat{\chi}_a, \hat{\vec{D}}_a^2 \hat{\chi}_a \right\}; x \right), \end{aligned} \tag{4.7}$$

is the Rigged QED Lagrangian density operator. We note that this Lagrangian has $U(1)$ gauge symmetry but the Lorentz symmetry is broken by $\hat{L}_a$. This, however, will not be a problem since we are not going to solve the dynamics in a Lorentz covariant way.

4.2.2 Equation of motion

Here, we show the equations of motion for field operators, $\hat{\psi}(x)$, $\hat{\chi}_a(x)$ and $\hat{A}_\mu(x)$, in Rigged QED. They are given by the principle of least action from the Lagrangian density

operators introduced above. We also define the charge density operator $\hat{\rho}(x)$ and the charge current density operator $\hat{\vec{j}}(x)$.

We begin with the Dirac field operator $\hat{\psi}(x)$. Since the "rigged" part of the Lagrangian $\hat{L}_a$ does not explicitly depend on $\hat{\psi}(x)$, the equation of motion of $\hat{\psi}(x)$ is same as one in the ordinary QED. That is

$$i\hbar\gamma^\mu \hat{D}_{e\mu}(x)\hat{\psi}(x) = m_e c\hat{\psi}(x), \tag{4.8}$$

if written covariantly, and it can be also expressed in a form

$$i\hbar\frac{\partial\hat{\psi}(x)}{\partial t} = \left\{(Z_e e)\hat{A}_0(x) + \vec{\alpha}\cdot\left(-i\hbar c\vec{\nabla} - (Z_e e)\hat{\vec{A}}(x)\right) + m_e c^2\beta\right\}\hat{\psi}(x), \tag{4.9}$$

which has the same form as a Hamiltonian form of the Dirac equation. In our notation of the gamma matrices, $\beta = \gamma^0$ and $\vec{\alpha} = \gamma^0\vec{\gamma}$.

As for the Schrödinger field operator $\hat{\chi}_a(x)$, we obtain the equation of motion in the same form as the Schrödinger equation of the non-relativistic quantum mechanics as

$$i\hbar\frac{\partial}{\partial t}\hat{\chi}_a(x) = -\frac{\hbar^2}{2m_a}\hat{\vec{D}}_a^2(x)\hat{\chi}_a(x) + Z_a e\hat{A}_0(x)\hat{\chi}_a(x). \tag{4.10}$$

This can also be written as

$$\begin{aligned} i\hbar\frac{\partial}{\partial t}\hat{\chi}_a(x) &= -\frac{\hbar^2}{2m_a}\left\{\vec{\nabla}^2 - 2i\frac{Z_a e}{\hbar c}\hat{\vec{A}}(x)\cdot\vec{\nabla} - \left(\frac{Z_a e}{\hbar c}\right)^2\hat{\vec{A}}(x)\cdot\hat{\vec{A}}(x)\right\}\hat{\chi}_a(x) \\ &\quad + Z_a e\hat{A}_0(x)\hat{\chi}_a(x), \end{aligned} \tag{4.11}$$

where we use the Coulomb gauge condition $\vec{\nabla}\cdot\hat{\vec{A}}(x) = 0$.

Finally, the equations of motion for the photon field $\hat{A}_\mu(x)$ have the same form as the inhomogeneous Maxwell equations of the classical electrodynamics. In the Coulomb gauge, we have

$$-\nabla^2\hat{A}_0(x) = 4\pi\hat{\rho}(x), \tag{4.12}$$

$$\frac{1}{c}\frac{\partial}{\partial t}\vec{\nabla}\hat{A}_0(x) + \left(\frac{1}{c^2}\frac{\partial^2}{\partial t^2} - \nabla^2\right)\hat{\vec{A}}(x) = \frac{4\pi}{c}\hat{\vec{j}}(x), \tag{4.13}$$

where $\hat{\rho}(x)$ is the charge density operator, $\hat{\vec{j}}(x)$ is the charge current density operator. Note that in the case of Rigged QED, $\hat{\rho}(x)$ and $\hat{\vec{j}}(x)$ include the contribution from atomic nuclei in addition to that of electrons. These "rigged" charge and current are described below.

The charge density operator $\hat{\rho}(x)$ is the sum of electron charge density operator $\hat{\rho}_e(x)$ and atomic nuclear charge density operator $\hat{\rho}_a(x)$:

$$\hat{\rho}(x) = \hat{\rho}_e(x) + \sum_{a=1}^{N_n} \hat{\rho}_a(x), \tag{4.14}$$

where

$$\begin{aligned} \hat{\rho}_e(x) &= Z_e e \hat{\bar{\psi}}(x)\gamma^0\hat{\psi}(x), & (4.15)\\ \hat{\rho}_a(x) &= Z_a e \hat{\chi}_a^\dagger(x)\hat{\chi}_a(x). & (4.16) \end{aligned}$$

Similarly, the charge current density operator $\hat{\vec{j}}(x)$ is the sum of electron charge current density operator $\hat{\vec{j}}_e(x)$ and atomic nuclear charge current density operator $\hat{\vec{j}}_a(x)$:

$$\hat{\vec{j}}(x) = \hat{\vec{j}}_e(x) + \sum_{a=1}^{N_n} \hat{\vec{j}}_a(x), \tag{4.17}$$

where

$$\begin{aligned} \hat{\vec{j}}_e(x) &= Z_e e c \hat{\bar{\psi}}(x)\vec{\gamma}\hat{\psi}(x), & (4.18)\\ \hat{\vec{j}}_a(x) &= \frac{Z_a e}{2m_a}\left(i\hbar\hat{\chi}_a^\dagger(x)\hat{\vec{D}}_a(x)\hat{\chi}_a(x) - i\hbar\left(\hat{\vec{D}}_a(x)\hat{\chi}_a(x)\right)^\dagger \cdot \hat{\chi}_a(x)\right). & (4.19) \end{aligned}$$

Here, in passing, some notes are in order. First, the equations of continuity hold for each species, namely,

$$\frac{\partial}{\partial t}\hat{\rho}_\alpha(x) + \mathrm{div}\hat{\vec{j}}_\alpha(x) = 0, \tag{4.20}$$

where $\alpha = e$ or a. Second, $\hat{\rho}_\alpha(x)$ ($\alpha = e$ or a) is connected to position probability density operator $\hat{N}_\alpha(x)$ as $\hat{\rho}_\alpha(x) = Z_\alpha e \hat{N}_\alpha(x)$ and $\hat{\vec{j}}_\alpha(x)$ is connected to velocity density operator $\hat{\vec{v}}_\alpha(x)$ as $\hat{\vec{j}}_\alpha(x) = Z_\alpha e \hat{\vec{v}}_\alpha(x)$.

In summary, the rigged charge and the rigged current are

$$\begin{aligned} \hat{\rho}(x) &= Z_e e \hat{\bar{\psi}}(x)\gamma^0\hat{\psi}(x) + \sum_a^{N_n} Z_a e \hat{\chi}_a^\dagger(x)\hat{\chi}_a(x), & (4.21)\\ \hat{\vec{j}}(x) &= Z_e e c \hat{\bar{\psi}}(x)\vec{\gamma}\hat{\psi}(x) \\ &\quad + \sum_a^{N_n} \frac{Z_a e}{2m_a}\left(i\hbar\hat{\chi}_a^\dagger(x)\hat{\vec{D}}_a(x)\hat{\chi}_a(x) - i\hbar\left(\hat{\vec{D}}_a(x)\hat{\chi}_a(x)\right)^\dagger \cdot \hat{\chi}_a(x)\right). & (4.22) \end{aligned}$$

Now, we have a closed set of time evolution equations for field operators $\hat{\psi}(x)$, $\hat{\chi}_a(x)$ and $\hat{A}_\mu(x)$: Eqs. (4.9), (4.11), (4.12), (4.13), (4.21) and (4.22). To solve them, we rewrite them

using annihilation and creation operators as is done in ordinary QED (or other quantum field theories). In the next section, we describe how we expand the field operators by the annihilation and creation operators and derive time evolution equations for them.

4.3 Expansion of field operators by annihilation and creation operators

In this section, we introduce annihilation and creation operators for each field operator and describe our expansion method. As is explained in the following, definitions for annihilation and creation operators are different from those used in the conventional QED treatment. This reflects our aim to treat dynamics of electrons, photons and atomic nuclei in atomic and molecular systems, which are bound states, in a non-perturbative manner.

4.3.1 Electron field

In QED, the electron is expressed by the Dirac field operator $\hat{\psi}(x)$ and it is usually expanded by plane waves, which are solutions for the free Dirac equation. As is well-established, this works extremely fine for the mostly considered QED processes which are represented by scattering cross sections. This is because those processes are described by a perturbation series to non-interacting system with the interaction mediated by photons treated as the perturbation.

In our case, however, since molecular systems are highly non-perturbative and electrons are bounded, the same method is not likely to work. In addition, what we want to know is not the cross section, which just describes the transition between infinite past ("in-state") and infinite future ("out-state"), but time step-by-step evolution of the systems. To this end, we propose an alternative way to expand $\hat{\psi}(x)$ as

$$\hat{\psi}(ct,\vec{r}) = \sum_{n=1}^{N_D} \left[\hat{e}_n(t)\psi_n^{(+)}(\vec{r}) + \hat{f}_n^\dagger(t)\psi_n^{(-)}(\vec{r}) \right], \tag{4.23}$$

$$\hat{\psi}^\dagger(ct,\vec{r}) = \sum_{n=1}^{N_D} \left[\hat{e}_n^\dagger(t)\psi_n^{\dagger(+)}(\vec{r}) + \hat{f}_n(t)\psi_n^{\dagger(-)}(\vec{r}) \right], \tag{4.24}$$

where $\hat{e}_n(t)/\hat{e}_n^\dagger(t)$ is the electron annihilation/creation operator, $\hat{f}_n(t)/\hat{f}_n^\dagger(t)$ is the positron annihilation/creation operator and $\psi_n^{(+)}(\vec{r})$ ($\psi_n^{(-)}(\vec{r})$) are the four-component wave functions

of the electron (the positron), which are solutions of the time-independent Dirac equation for a particle in a nucleus field. Concretely, $\psi_n^{(\pm)}(\vec{r})$ can be considered as the n-th molecular orbitals which are obtained by solving the four-component Dirac Hartree-Fock equation for the system and N_D is the number of the basis set.

We note that this expansion of the field operator is similar to the Furry representation (picture) of ordinary QED [21, 22] in a sense that it uses the solutions of the Dirac equation in an external field. However, the annihilation/creation operators in the Furry representation do not depend on time (so it can be considered as a variant of the interaction picture) whereas those in our expansion carry all the time-dependence of the field operator. In other words, we adopt to work in Heisenberg picture. Since we wish to solve the dynamics of the system in a non-perturbative manner, the use of interaction picture does not make our problem easier.

Before proceeding further, to make equations below less cluttered, we introduce our notation for the annihilation/creation operators and the electron/positron wavefunctions. We define

$$\hat{e}_{n^+} \equiv \hat{e}_n, \tag{4.25}$$

$$\hat{e}_{n^-} \equiv \hat{f}_n^\dagger, \tag{4.26}$$

and

$$\psi_{n^+}(\vec{r}) \equiv \psi_n^{(+)}(\vec{r}), \tag{4.27}$$

$$\psi_{n^-}(\vec{r}) \equiv \psi_n^{(-)}(\vec{r}). \tag{4.28}$$

Note that the positron creation operator does not have a dagger as superscript in our notation. Then the field operator expansion eq. (4.23) can be written as

$$\hat{\psi}(ct, \vec{r}) = \sum_{n=1}^{N_D} \sum_{a=\pm} \hat{e}_{n^a}(t) \psi_{n^a}(\vec{r}), \tag{4.29}$$

and orthonormality of the wavefunctions can be expressed as

$$\int d^3\vec{r}\, \psi_{n^a}^\dagger(\vec{r}) \psi_{m^b}(\vec{r}) = \delta_{nm}\delta_{ab}. \tag{4.30}$$

The anti-commutation relation can be written by

$$\left\{ \hat{e}_{n^a}, \hat{e}_{m^b}^\dagger \right\} = \delta_{nm}\delta_{ab}, \tag{4.31}$$

and anti-commutators of other combinations are zero. Also, for later use, we define the electron excitation operator

$$\hat{\mathcal{E}}_{n^a m^b} \equiv \hat{e}^\dagger_{n^a} \hat{e}_{m^b}. \tag{4.32}$$

4.3.2 Nucleus field

We expand the Schrödinger field operator $\hat{\chi}_a(x)$ for the atomic nucleus a by the nucleus annihilation operator $\hat{c}_{ai}$ and creation operator $\hat{c}^\dagger_{ai}$ as

$$\hat{\chi}_a(ct, \vec{r}) = \sum_{i=1}^{N_S} \hat{c}_{ai}(t) \chi_{ai}(\vec{r}), \tag{4.33}$$

$$\hat{\chi}^\dagger_a(ct, \vec{r}) = \sum_{i=1}^{N_S} \hat{c}^\dagger_{ai}(t) \chi^*_{ai}(\vec{r}), \tag{4.34}$$

where $\chi_{ai}(\vec{r})$ is a set of orthonormal functions

$$\int d^3\vec{r}\, \chi^*_{ai}(\vec{r}) \chi_{aj}(\vec{r}) = \delta_{ij}. \tag{4.35}$$

The commutation relation for $\hat{c}_{ai}$ and $\hat{c}^\dagger_{ai}$ is $\left[\hat{c}_{ai}, \hat{c}^\dagger_{aj}\right] = \delta_{ij}$ and the anti-commutation relation is $\left\{\hat{c}_{ai}, \hat{c}^\dagger_{aj}\right\} = \delta_{ij}$. For the other combinations, (anti-)commutators are zero. Which of them is imposed depends on the a's nuclear spin. If a has (half-)integer spin, the (anti-)commutation relation is imposed.

As is done for the electron case, we define the nucleus excitation operator

$$\hat{\mathcal{C}}_{aij} \equiv \hat{c}^\dagger_{ai} \hat{c}_{aj}, \tag{4.36}$$

for the later convenience.

4.3.3 Photon field

In QED, the photon is expressed by a vector field operator $\hat{A}_\mu(x)$ with $U(1)$ gauge symmetry. In the standard QED treatment, the quantization is performed to free electromagnetic field and the interaction with the electron is taken into account as a perturbation. Although this is not the way we try to solve the dynamics of the system as mentioned previously, since we are going to use the expression of the quantized free field as a part of $\hat{A}_\mu(x)$, we begin by showing its expression. We call this $\hat{A}_{\mathrm{rad},\mu}(x)$ to distinguish from the total

$\hat{A}_\mu(x)$. In the Coulomb gauge, as is commonly done when quantizing the electromagnetic field (e.g. Ref. [7, 8, 12]), we have

$$\hat{A}^0_{\rm rad}(ct,\vec{r}) = 0, \tag{4.37}$$

$$\hat{A}^k_{\rm rad}(ct,\vec{r}) = \frac{\sqrt{4\pi\hbar^2 c}}{\sqrt{(2\pi\hbar)^3}}\sum_{\sigma=\pm1}\int\frac{d^3\vec{p}}{\sqrt{2p^0}}\Big[\hat{a}(\vec{p},\sigma)e^k(\vec{p},\sigma)e^{-icp^0t/\hbar}e^{i\vec{p}\cdot\vec{r}/\hbar} + \hat{a}^\dagger(\vec{p},\sigma)e^{*k}(\vec{p},\sigma)e^{icp^0t/\hbar}e^{-i\vec{p}\cdot\vec{r}/\hbar}\Big], \tag{4.38}$$

where $\hat{a}(\vec{p},\sigma)$ is the annihilation operator of the photon with momentum $\vec{p}$ and helicity σ and $\vec{e}$ is the polarization vector. The photon annihilation/creation operators satisfy the commutation relation

$$[\hat{a}(\vec{p},\sigma),\hat{a}^\dagger(\vec{p}\,',\sigma')] = \delta(\vec{p}-\vec{p}\,')\delta_{\sigma\sigma'}, \tag{4.39}$$

and commutators of the other combinations are zero. As for the polarization vector, when we take the photon momentum in the polar coordinate as

$$\vec{p} = \begin{pmatrix} p^0\sin\theta\cos\phi \\ p^0\sin\theta\sin\phi \\ p^0\cos\theta \end{pmatrix}, \tag{4.40}$$

($0\le\theta\le\pi$, $0\le\phi<2\pi$, $|\vec{p}|=p^0$), we have

$$\vec{e}(\vec{p},\sigma) = \frac{1}{\sqrt{2}}\begin{pmatrix} \cos\phi\cos\theta\mp i\sin\phi \\ \sin\phi\cos\theta\pm i\cos\phi \\ -\sin\theta \end{pmatrix}, \tag{4.41}$$

where the double sign corresponds to $\sigma=\pm1$. We note that $\hat{A}^0_{\rm rad}(ct,\vec{r})$ and $\hat{\vec{A}}_{\rm rad}(ct,\vec{r})$ by construction satisfy Maxwell equations (4.12) and (4.13) with the right-hand-sides being zero (*i.e.* equations for free fields).

To solve the dynamics of the system non-perturbatively, we take advantage of the fact that the formal solutions of the inhomogeneous Maxwell equations (4.12) and (4.13) are known from the classical electrodynamics [23]. We shall employ the strategy to express $\hat{A}_\mu(x)$ by such solutions [18].

As for the first inhomogeneous Maxwell equation (4.12), since it only contains the scalar potential $\hat{A}^0(ct,\vec{r})$, its solution is readily written by the sum of the solution of Eq. (4.12)

with the right-hand-side being zero and the particular solution of Eq. (4.12). The former is $\hat{A}^0_{\rm rad}(ct,\vec{r})$ which is zero (Eq. (4.37)) and the latter is known as the solution of the Poisson equation. Thus,

$$\hat{A}_0(ct,\vec{r}) = \int d^3\vec{s}\,\frac{\hat{\rho}(ct,\vec{s})}{|\vec{r}-\vec{s}|}. \tag{4.42}$$

As for the second inhomogeneous Maxwell equation (4.13), we can make it simpler by decomposing the current $\hat{\vec{j}}(x)$ into the transversal component $\hat{\vec{j}}_T(x)$ and the longitudinal component $\hat{\vec{j}}_L(x)$ as

$$\hat{\vec{j}}(x) \;=\; \hat{\vec{j}}_T(x) + \hat{\vec{j}}_L(x), \tag{4.43}$$

where $\vec{\nabla}\cdot\hat{\vec{j}}_T(x) = 0$ and $\vec{\nabla}\times\hat{\vec{j}}_L(x) = 0$. This transforms Eq. (4.13) into two equations each involving only $\hat{A}^0(ct,\vec{r})$ or $\hat{\vec{A}}(ct,\vec{r})$

$$\left(\frac{1}{c^2}\frac{\partial^2}{\partial t^2} - \nabla^2\right)\hat{\vec{A}}(x) = \frac{4\pi}{c}\hat{\vec{j}}_T(x), \tag{4.44}$$

$$\frac{\partial}{\partial t}\vec{\nabla}\hat{A}_0(x) = 4\pi\hat{\vec{j}}_L(x). \tag{4.45}$$

Since we have already found $\hat{A}_0(x)$ as Eq. (4.42), Eq. (4.45) tells us $\hat{\vec{j}}_L(x)$, which in turn gives the right-hand-side of Eq. (4.44) by $\hat{\vec{j}}(\vec{r}) - \hat{\vec{j}}_L(\vec{r})$. Then we can obtain the solution of Eq. (4.44) by the sum of the solution of Eq. (4.44) with the right-hand-side being zero and the particular solution of Eq. (4.44). The former is $\hat{\vec{A}}_{\rm rad}(ct,\vec{r})$ (Eq. (4.38)) which is written by the annihilation/creation operators and the latter is known from the classical electromagnetism, which we shall call $\hat{\vec{A}}_A(ct,\vec{r})$. Written explicitly,

$$\hat{\vec{A}}_A(ct,\vec{r}) = \frac{1}{c}\int d^3\vec{s}\,\frac{\hat{\vec{j}}_T(cu,\vec{s})}{|\vec{r}-\vec{s}|}, \tag{4.46}$$

where

$$u = t - \frac{|\vec{r}-\vec{s}|}{c}. \tag{4.47}$$

In summary, the vector potential $\hat{\vec{A}}(ct,\vec{r})$ is

$$\hat{\vec{A}}(ct,\vec{r}) = \hat{\vec{A}}_{\rm rad}(ct,\vec{r}) + \hat{\vec{A}}_A(ct,\vec{r}), \tag{4.48}$$

which are given by Eqs. (4.38), (4.46) and (4.47).

4.3.4 Charge density and charge current density

In this subsection we express the charge density operator $\hat{\rho}(x)$ (Eq. (4.21)) and the charge current density operator $\hat{\vec{j}}(x)$ (Eq. (4.22)) in terms of annihilation and creation operators (or excitation operators) which are defined in previous subsections.

The expression for the electronic charge density operator can be derived by substituting Eq. (4.29) into Eq. (4.15), and the atomic nucleus charge density operator by Eq. (4.33) into Eq. (4.16). They give

$$\hat{\rho}_e(x) = \sum_{p,q=1}^{N_D} \sum_{c,d=\pm} \rho_{p^c q^d}(\vec{r}) \hat{\mathcal{E}}_{p^c q^d}, \tag{4.49}$$

$$\hat{\rho}_a(x) = \sum_{i,j=1}^{N_S} \rho_{aij}(\vec{r}) \hat{\mathcal{C}}_{aij}, \tag{4.50}$$

where

$$\rho_{p^c q^d}(\vec{r}) \equiv (Z_e e) \psi^\dagger_{p^c}(\vec{r}) \psi_{q^d}(\vec{r}), \tag{4.51}$$

$$\rho_{aij}(\vec{r}) \equiv (Z_a e) \chi^*_{ai}(\vec{r}) \chi_{aj}(\vec{r}). \tag{4.52}$$

The expression for the charge current density operator can be derived in a similar manner. From Eq. (4.18), the electronic charge current density operator is

$$\hat{j}^k_e(x) = \sum_{p,q=1}^{N_D} \sum_{c,d=\pm} j^k_{p^c q^d}(\vec{r}) \hat{\mathcal{E}}_{p^c q^d}, \tag{4.53}$$

where

$$j^k_{p^c q^d}(\vec{r}) \equiv Z_e \, e \, c \left[\psi^\dagger_{p^c}(\vec{r}) \gamma^0 \gamma^k \psi_{q^d}(\vec{r}) \right]. \tag{4.54}$$

From Eq. (4.19), the atomic nucleus charge current density operator is

$$\hat{j}^k_a(x) = \sum_{i,j=1}^{N_S} \left\{ j^k_{aij}(\vec{r}) \hat{\mathcal{C}}_{aij} - \frac{(Z_a e)}{m_a c} \rho_{aij}(\vec{r}) \left(\hat{A}^k_{\rm rad} \hat{\mathcal{C}}_{aij} + \hat{c}^\dagger_{ai} \hat{A}^k_A \hat{c}_{aj} \right) \right\}, \tag{4.55}$$

where

$$j^k_{aij}(\vec{r}) \equiv -(Z_a e) \frac{i\hbar}{2m_a} \left\{ \chi^*_{ai}(\vec{r}) \nabla^k \chi_{aj}(\vec{r}) - \left(\nabla^k \chi^*_{ai}(\vec{r}) \right) \chi_{aj}(\vec{r}) \right\}. \tag{4.56}$$

Note that in our notation the spatial components of the covariant derivative are $\vec{D}(x) = -\vec{\nabla} + i \frac{q}{\hbar c} \vec{A}(x)$. Also, we have used the fact that $\hat{c}_{aj}$ commutes with $\hat{A}^k_{\rm rad}$ but not with $\hat{A}^k_A$.

Therefore, the total charge density operator $\hat{\rho}(x)$ and the charge current density operator $\hat{\vec{j}}(x)$ are

$$\hat{\rho}(x) = \sum_{p,q=1}^{N_D} \sum_{c,d=\pm} \rho_{p^c q^d}(\vec{r}) \hat{\mathcal{E}}_{p^c q^d} + \sum_{a=1}^{N_n} \sum_{i,j=1}^{N_S} \rho_{aij}(\vec{r}) \hat{\mathcal{C}}_{aij}, \tag{4.57}$$

$$\begin{aligned} \hat{j}^k(x) &= \sum_{p,q=1}^{N_D} \sum_{c,d=\pm} j^k_{p^c q^d}(\vec{r}) \hat{\mathcal{E}}_{p^c q^d} \\ &\quad + \sum_{a=1}^{N_n} \sum_{i,j=1}^{N_S} \left\{ j^k_{aij}(\vec{r}) \hat{\mathcal{C}}_{aij} - \frac{(Z_a e)}{m_a c} \rho_{aij}(\vec{r}) \left(\hat{A}^k_{\text{rad}} \hat{\mathcal{C}}_{aij} + \hat{c}^\dagger_{ai} \hat{A}^k_A \hat{c}_{aj} \right) \right\}. \end{aligned} \tag{4.58}$$

Now, we can rewrite the scalar potential $\hat{A}^0(ct, \vec{r})$ using the excitation operators. Substituting Eq. (4.57) into Eq. (4.42) gives

$$\hat{A}_0(ct, \vec{r}) = \sum_{p,q=1}^{N_D} \sum_{c,d=\pm} V_{p^c q^d}(\vec{r}) \hat{\mathcal{E}}_{p^c q^d} + \sum_{a=1}^{N_n} \sum_{i,j=1}^{N_S} V_{aij}(\vec{r}) \hat{\mathcal{C}}_{aij}, \tag{4.59}$$

where we define integrals

$$V_{p^c q^d}(\vec{R}) \equiv \int d^3\vec{s} \frac{\rho_{p^c q^d}(\vec{s})}{|\vec{s} - \vec{R}|}, \tag{4.60}$$

$$V_{aij}(\vec{R}) \equiv \int d^3\vec{s} \frac{\rho_{aij}(\vec{s})}{|\vec{s} - \vec{R}|}. \tag{4.61}$$

Then, we can express $\hat{\vec{j}}_L(x)$ using the excitation operators via Eq. (4.45). Substituting Eq. (4.59) into Eq. (4.45) gives

$$\hat{j}^k_L(x) = -\sum_{p,q=1}^{N_D} \sum_{c,d=\pm} E^k_{p^c q^d}(\vec{r}) \frac{d\hat{\mathcal{E}}_{p^c q^d}}{dt} - \sum_{a=1}^{N_n} \sum_{i,j=1}^{N_S} E^k_{aij}(\vec{r}) \frac{d\hat{\mathcal{C}}_{aij}}{dt}, \tag{4.62}$$

where we define integrals

$$E^k_{p^c q^d}(\vec{R}) \equiv -\frac{1}{4\pi} \frac{\partial}{\partial R^k} V_{p^c q^d}(\vec{R}) = -\frac{Z_e e}{4\pi} \int d^3\vec{s}\, \psi^\dagger_{p^c}(\vec{s}) \psi_{q^d}(\vec{s}) \frac{(\vec{s} - \vec{R})^k}{|\vec{s} - \vec{R}|^3}, \tag{4.63}$$

$$E^k_{aij}(\vec{R}) \equiv -\frac{1}{4\pi} \frac{\partial}{\partial R^k} V_{aij}(\vec{R}) = -\frac{Z_a e}{4\pi} \int d^3\vec{s}\, \chi^*_{ai}(\vec{s}) \chi_{aj}(\vec{s}) \frac{(\vec{s} - \vec{R})^k}{|\vec{s} - \vec{R}|^3}. \tag{4.64}$$

Finally, we can obtain $\hat{\vec{j}}_T(x)$ from Eqs. (4.58) and (4.62), and in turn $\hat{\vec{A}}_A(ct, \vec{r})$ using Eq. (4.46). However, the existence of retardation (Eq. (4.47)) in the right-hand-side of Eq. (4.46) prevent us from making the expression of $\hat{\vec{A}}_A(ct, \vec{r})$ simpler. In other words, $\hat{\vec{A}}_A(ct, \vec{r})$ is determined by $\hat{\vec{j}}_T$ at earlier times than t, whose expression contains $\hat{\vec{A}}_A$ at these times. Thus, $\hat{\vec{A}}_A(ct, \vec{r})$ is computed step-by-step in time using all the information of itself at earlier times.

4.4 Time evolution of annihilation and creation operators

In this section, we derive time evolution equations for annihilation operators of the electron $\hat{e}_{p^c}$ and the nucleus $\hat{c}_{ai}$. Those for the creation operators can be obtained by taking Hermite conjugate. We note that in our formalism, the photon annihilation operator $\hat{a}(\vec{p},\sigma)$ does not depend on time as is in the standard QED treatment. We also discuss the time evolution of the excitation operators and physical quantities.

4.4.1 Electron annihilation operator

We first derive the time derivative of the electron annihilation operator $\hat{e}_{p^c}$. This is obtained by substituting the expansion (4.29) into (4.9), multiplying by $\psi^\dagger_{p^c}(\vec{r})$ and integrating over $\vec{r}$. Then, the orthonormality of the wavefunctions (Eq. (4.30)) yields

$$i\hbar\frac{\partial\hat{e}_{p^c}}{\partial t} = \sum_{q=1}^{N_D}\sum_{d=\pm}\left(\hat{I}_{1p^cq^d}+\hat{I}_{2p^cq^d}+\hat{I}_{3p^cq^d}+\hat{I}_{4p^cq^d}\right)\hat{e}_{q^d}, \tag{4.65}$$

where

$$\hat{I}_{1p^cq^d} = \int d^3\vec{r}\,\psi^\dagger_{p^c}(\vec{r})\vec{\alpha}\cdot\left(-i\hbar c\vec{\nabla}\right)\psi_{q^d}(\vec{r}), \tag{4.66}$$

$$\hat{I}_{2p^cq^d} = \int d^3\vec{r}\,\psi^\dagger_{p^c}(\vec{r})\vec{\alpha}\cdot\left(-(Z_ee)\hat{\vec{A}}(x)\right)\psi_{q^d}(\vec{r}), \tag{4.67}$$

$$\hat{I}_{3p^cq^d} = \int d^3\vec{r}\,\psi^\dagger_{p^c}(\vec{r})(m_ec^2)\beta\psi_{q^d}(\vec{r}), \tag{4.68}$$

$$\hat{I}_{4p^cq^d} = \int d^3\vec{r}\,\psi^\dagger_{p^c}(\vec{r})(Z_ee)\hat{A}_0(x)\psi_{q^d}(\vec{r}). \tag{4.69}$$

$\hat{I}_{1p^cq^d}$ and $\hat{I}_{3p^cq^d}$ are contributions from kinetic energy and mass energy respectively. We define the electron kinetic energy integral

$$T_{p^cq^d} \equiv -i\hbar c\int d^3\vec{r}\,\psi^\dagger_{p^c}(\vec{r})\gamma^0\vec{\gamma}\cdot\vec{\nabla}\psi_{q^d}(\vec{r}), \tag{4.70}$$

and the electron mass energy integral

$$M_{p^cq^d} \equiv m_ec^2\int d^3\vec{r}\,\psi^\dagger_{p^c}(\vec{r})\gamma^0\psi_{q^d}(\vec{r}). \tag{4.71}$$

Then, we have $\hat{I}_{1p^cq^d} = T_{p^cq^d}$ and $\hat{I}_{3p^cq^d} = M_{p^cq^d}$.

$\hat{I}_{4p^cq^d}$ can be rewritten using Eq. (4.59) as

$$\hat{I}_{4p^cq^d} = \int d^3\vec{r}\,\rho_{p^cq^d}(\vec{r})\hat{A}_0(x) \tag{4.72}$$

$$= \sum_{r,s=1}^{N_D}\sum_{e,f=\pm}(p^cq^d|r^es^f)\hat{\mathcal{E}}_{r^es^f} + \sum_{a=1}^{N_n}\sum_{i,j=1}^{N_S}(p^cq^d|i_aj_a)\hat{\mathcal{C}}_{aij}, \tag{4.73}$$

where we define two types of four-center integral as

$$(p^cq^d|r^es^f) \equiv (Z_ee)^2\int d^3\vec{r}\,d^3\vec{s}\,\psi^\dagger_{p^c}(\vec{r})\psi_{q^d}(\vec{r})\frac{1}{|\vec{r}-\vec{s}|}\psi^\dagger_{r^e}(\vec{s})\psi_{s^f}(\vec{s}), \tag{4.74}$$

$$(p^cq^d|i_aj_a) \equiv (Z_ee)(Z_ae)\int d^3\vec{r}\,d^3\vec{s}\,\psi^\dagger_{p^c}(\vec{r})\psi_{q^d}(\vec{r})\frac{1}{|\vec{r}-\vec{s}|}\chi^*_{ai}(\vec{s})\chi_{aj}(\vec{s}). \tag{4.75}$$

We can write $\hat{I}_{2p^cq^d}$ using Eq. (4.54) as

$$\hat{I}_{2p^cq^d} = -\frac{1}{c}\int d^3\vec{r}\,\vec{j}_{p^cq^d}(\vec{r})\cdot\left(\hat{\vec{A}}_{\rm rad}(x)+\hat{\vec{A}}_A(x)\right). \tag{4.76}$$

Here, the term including $\hat{\vec{A}}_{\rm rad}(x)$ can be written, by substituting Eq. (4.38), as

$$\begin{aligned}
&-\frac{1}{c}\int d^3\vec{r}\,\vec{j}_{p^cq^d}(\vec{r})\cdot\hat{\vec{A}}_{\rm rad}(x)\\
&= -\frac{1}{c}\frac{\sqrt{4\pi\hbar^2c}}{\sqrt{(2\pi\hbar)^3}}\sum_{\sigma=\pm1}\int\frac{d^3\vec{p}}{\sqrt{2p^0}}\times\\
&\quad\left[\vec{F}_{p^cq^d}(\vec{p})\cdot\vec{e}(\vec{p},\sigma)e^{-icp^0t/\hbar}\hat{a}(\vec{p},\sigma)+\vec{F}_{p^cq^d}(-\vec{p})\cdot\vec{e^*}(\vec{p},\sigma)e^{icp^0t/\hbar}\hat{a}^\dagger(\vec{p},\sigma)\right],
\end{aligned} \tag{4.77}$$

where we define the integral which is the Fourier transformation of the function for the electron charge current density (Eq. (4.54))

$$F^k_{p^cq^d}(\vec{p}) \equiv \int d^3\vec{r}\,j^k_{p^cq^d}(\vec{r})e^{i\vec{p}\cdot\vec{r}/\hbar}. \tag{4.78}$$

The term including $\hat{\vec{A}}_A(x)$ can be written, by substituting Eq. (4.46), as

$$-\frac{1}{c}\int d^3\vec{r}\,\vec{j}_{p^cq^d}(\vec{r})\cdot\hat{\vec{A}}_A(x) = -\frac{1}{c^2}\int d^3\vec{r}\,d^3\vec{s}\,\frac{\vec{j}_{p^cq^d}(\vec{r})\cdot\hat{\vec{j}}_T(cu,\vec{s})}{|\vec{r}-\vec{s}|}. \tag{4.79}$$

Further simplification is not possible due to the retardation $u = t - \frac{|\vec{r}-\vec{s}|}{c}$ in $\hat{\vec{j}}_T$.

Putting these all together, we obtain

$$
\begin{aligned}
i\hbar\frac{\partial \hat{e}_{p^c}}{\partial t} &= \sum_{q=1}^{N_D}\sum_{d=\pm}(T_{p^cq^d}+M_{p^cq^d})\hat{e}_{q^d} + \sum_{q,r,s=1}^{N_D}\sum_{d,e,f=\pm}(p^cq^d|r^es^f)\hat{\mathcal{E}}_{r^es^f}\hat{e}_{q^d} \\
&+ \sum_{q=1}^{N_D}\sum_{d=\pm}\sum_{a=1}^{N_n}\sum_{i,j=1}^{N_S}(p^cq^d|i_aj_a)\hat{\mathcal{C}}_{aij}\hat{e}_{q^d} \\
&- \frac{1}{c^2}\sum_{q=1}^{N_D}\sum_{d=\pm}\int d^3\vec{r}\,d^3\vec{s}\,\frac{\vec{j}_{p^cq^d}(\vec{r})\cdot\hat{\vec{j}}_T(cu,\vec{s})}{|\vec{r}-\vec{s}|}\hat{e}_{q^d} \\
&- \frac{1}{c}\frac{\sqrt{4\pi\hbar^2c}}{\sqrt{(2\pi\hbar)^3}}\sum_{q=1}^{N_D}\sum_{d=\pm}\sum_{\sigma=\pm1}\int\frac{d^3\vec{p}}{\sqrt{2p^0}}\times \\
&\left[\vec{F}_{p^cq^d}(\vec{p})\cdot\vec{e}(\vec{p},\sigma)e^{-icp^0t/\hbar}\hat{a}(\vec{p},\sigma)\hat{e}_{q^d} + \vec{F}_{p^cq^d}(-\vec{p})\cdot\vec{e^*}(\vec{p},\sigma)e^{icp^0t/\hbar}\hat{a}^\dagger(\vec{p},\sigma)\hat{e}_{q^d}\right] \quad (4.80)
\end{aligned}
$$

The Born-Oppenheimer approximation version of this equation is derived in the Appendix 4.6.

4.4.2 Nucleus annihilation operator

We next derive the time derivative of the nucleus annihilation operator $\hat{c}_{ai}$. Similarly to the electron case, this is obtained by substituting the expansion (4.33) into (4.11), multiplying by $\chi^*_{ai}(\vec{r})$ and integrating over $\vec{r}$. Then, the orthonormality of the expansion functions (Eq. (4.35)) yields

$$
i\hbar\frac{\partial \hat{c}_{ai}}{\partial t} = \sum_{j=1}^{N_S}\left(\hat{I}_{1aij}+\hat{I}_{2aij}+\hat{I}_{3aij}+\hat{I}_{4aij}\right)\hat{c}_{aj}, \quad (4.81)
$$

where

$$
\begin{aligned}
\hat{I}_{1aij} &= -\frac{\hbar^2}{2m_a}\int d^3\vec{r}\,\chi^*_{ai}(\vec{r})\vec{\nabla}^2\chi_{aj}(\vec{r}), & (4.82)\\
\hat{I}_{2aij} &= \frac{i\hbar Z_ae}{m_ac}\int d^3\vec{r}\,\hat{\vec{A}}(x)\cdot\left(\chi^*_{ai}(\vec{r})\vec{\nabla}\chi_{aj}(\vec{r})\right), & (4.83)\\
\hat{I}_{3aij} &= \frac{(Z_ae)^2}{2m_ac^2}\int d^3\vec{r}\,\hat{\vec{A}}(x)\cdot\hat{\vec{A}}(x)\chi^*_{ai}(\vec{r})\chi_{aj}(\vec{r}), & (4.84)\\
\hat{I}_{4aij} &= (Z_ae)\int d^3\vec{r}\,\hat{A}_0(x)\chi^*_{ai}(\vec{r})\chi_{aj}(\vec{r}). & (4.85)
\end{aligned}
$$

$\hat{I}_{1aij}$ is the contribution from nucleus kinetic energy. Defining the nucleus kinetic energy integral by

$$
T_{aij} = -\frac{\hbar^2}{2m_a}\int d^3\vec{r}\,\chi^*_{ai}(\vec{r})\vec{\nabla}^2\chi_{aj}(\vec{r}), \quad (4.86)
$$

we have $\hat{I}_{1aij} = T_{aij}$.

$\hat{I}_{4aij}$ can be rewritten using Eq. (4.59).

$$\hat{I}_{4aij} = \int d^3\vec{r}\,\rho_{aij}(\vec{r})\hat{A}_0(x) \tag{4.87}$$

$$= \sum_{p,q=1}^{N_D}\sum_{c,d=\pm}(p^c q^d|i_a j_a)\hat{\mathcal{E}}_{p^c q^d} + \sum_{b=1}^{N_n}\sum_{k,l=1}^{N_S}(i_a j_a|k_b l_b)\hat{\mathcal{C}}_{bkl}, \tag{4.88}$$

where we use Eq. (4.75) and define another four-center integral

$$(i_a j_a|k_b l_b) \equiv (Z_a e)(Z_b e)\int d^3\vec{r}\,d^3\vec{s}\,\chi^*_{ai}(\vec{r})\chi_{aj}(\vec{r})\frac{1}{|\vec{r}-\vec{s}|}\chi^*_{bk}(\vec{s})\chi_{bl}(\vec{s}). \tag{4.89}$$

$\hat{I}_{2aij}$ can be written as

$$\hat{I}_{2aij} = -\frac{1}{c}\int d^3\vec{r}\,\vec{j}_{aij}(\vec{r})\cdot\left(\hat{\vec{A}}_{\rm rad}(x) + \hat{\vec{A}}_A(x)\right), \tag{4.90}$$

where we integrate by parts, use the Coulomb gauge condition and Eq. (4.56). We note that this has the same form as Eq. (4.76) but $\vec{j}_{p^c q^d}(\vec{r})$ replaced by $\vec{j}_{aij}(\vec{r})$. Then the term including $\hat{\vec{A}}_{\rm rad}(x)$ should have the right-hand-side of Eq. (4.77) but $\vec{F}_{p^c q^d}(\vec{p})$ (Eq. (4.78)) replaced by $\vec{F}_{aij}(\vec{p})$ where

$$F^k_{aij}(\vec{p}) \equiv \int d^3\vec{r}\,j^k_{aij}(\vec{r})e^{i\vec{p}\cdot\vec{r}/\hbar}, \tag{4.91}$$

is the Fourier transformation of the function for the nucleus charge current density (Eq. (4.56)). Also, the term including $\hat{\vec{A}}_A(x)$ is Eq. (4.79) but $\vec{j}_{p^c q^d}(\vec{r})$ replaced by $\vec{j}_{aij}(\vec{r})$.

$\hat{I}_{3aij}$ can be decomposed into four terms because $\hat{\vec{A}}_{\rm rad}(x)$ and $\hat{\vec{A}}_A(x)$ do not commute. Namely,

$$\hat{I}_{3aij} = \frac{Z_a e}{2m_a c^2}\int d^3\vec{r}\,\left(\hat{\vec{A}}_{\rm rad}\cdot\hat{\vec{A}}_{\rm rad} + \hat{\vec{A}}_{\rm rad}\cdot\hat{\vec{A}}_A + \hat{\vec{A}}_A\cdot\hat{\vec{A}}_{\rm rad} + \hat{\vec{A}}_A\cdot\hat{\vec{A}}_A\right)\rho_{aij}(\vec{r}). \tag{4.92}$$

Since the last three terms involve $\hat{\vec{A}}_A(x)$ which includes the retarded potential, we cannot make their expression simpler. The first term can be rewritten using the Fourier transformation of the function for the nucleus charge density (Eq. (4.52)),

$$F_{aij}(\vec{p}) \equiv \int d^3\vec{r}\,\rho_{aij}(\vec{r})e^{i\vec{p}\cdot\vec{r}/\hbar}, \tag{4.93}$$

and subsequently defining

$$G_{aij}(\vec{p},\sigma,\vec{q},\tau) \equiv \vec{e}(\vec{p},\sigma)\cdot\vec{e}(\vec{q},\tau)\,F_{aij}(\vec{p}+\vec{q}), \tag{4.94}$$

as

$$\frac{Z_a e}{2m_a c^2}\int d^3\vec{r}\left(\hat{\vec{A}}_{\rm rad}\cdot\hat{\vec{A}}_{\rm rad}\right)\rho_{aij}(\vec{r}) = \frac{Z_a e}{4\pi^2 m_a \hbar c}\sum_{\sigma,\tau=\pm1}\int\frac{d^3\vec{p}}{\sqrt{2p^0}}\frac{d^3\vec{q}}{\sqrt{2q^0}}\times$$

$$\Big[G_{aij}(\vec{p},\sigma,\vec{q},\tau)e^{-ic(p^0+q^0)t/\hbar}\hat{a}(\vec{p},\sigma)\hat{a}(\vec{q},\tau)+G_{aij}(\vec{p},\sigma,-\vec{q},\tau)e^{-ic(p^0-q^0)t/\hbar}\hat{a}(\vec{p},\sigma)\hat{a}^\dagger(\vec{q},\tau)+$$

$$G_{aij}(-\vec{p},\sigma,\vec{q},\tau)e^{ic(p^0-q^0)t/\hbar}\hat{a}^\dagger(\vec{p},\sigma)\hat{a}(\vec{q},\tau)+G_{aij}(-\vec{p},\sigma,-\vec{q},\tau)e^{ic(p^0+q^0)t/\hbar}\hat{a}^\dagger(\vec{p},\sigma)\hat{a}^\dagger(\vec{q},\tau)\Big] \quad (4.95)$$

where we used $e^\mu(-\vec{p},\sigma)=e^{*\mu}(\vec{p},\sigma)$.

4.4.3 Excitation operators and physical quantities

As is shown in Eqs. (4.49) and (4.50), operators for physical quantities are expressed by the excitation operators $\hat{\mathcal{E}}_{p^cq^d}$ (Eq. (4.32)) and $\hat{\mathcal{C}}_{aij}$ (Eq. (4.36)). (For the field operator expression of other physical quantities of our interests, we refer Refs. [17, 19].) Thus, we here show the time derivative of $\hat{\mathcal{E}}_{p^cq^d}$ and $\hat{\mathcal{C}}_{aij}$.

As for $\hat{\mathcal{E}}_{p^cq^d}$, Eqs. (4.32) and (4.65) (and its Hermite conjugate) give

$$i\hbar\frac{d\hat{\mathcal{E}}_{p^cq^d}}{dt} = \sum_{r=1}^{N_D}\sum_{e=\pm}\left(-\hat{e}^\dagger_{r^e}\hat{I}_{r^ep^c}\hat{e}_{q^d}+\hat{e}^\dagger_{p^c}\hat{I}_{q^dr^e}\hat{e}_{r^e}\right), \quad (4.96)$$

where we define $\hat{I}_{p^cq^d}\equiv\hat{I}_{1p^cq^d}+\hat{I}_{2p^cq^d}+\hat{I}_{3p^cq^d}+\hat{I}_{4p^cq^d}$ and use $\hat{I}^\dagger_{p^cq^d}=\hat{I}_{q^dp^c}$. Similarly, Eqs. (4.36) and (4.81) (and its Hermite conjugate) give

$$i\hbar\frac{d\hat{\mathcal{C}}_{aij}}{dt} = \sum_{k=1}^{N_S}\left(-\hat{c}^\dagger_{ak}\hat{I}_{aki}\hat{c}_{aj}+\hat{c}^\dagger_{ai}\hat{I}_{ajk}\hat{c}_{ak}\right) \quad (4.97)$$

where we define $\hat{I}_{aij}\equiv\hat{I}_{1aij}+\hat{I}_{2aij}+\hat{I}_{3aij}+\hat{I}_{4aij}$ and use $\hat{I}^\dagger_{aij}=\hat{I}_{aji}$.

Finally, we describe how we can calculate physical quantities from these equations taking the electronic charge density for example. The electronic charge density operator is shown in Eq. (4.49). To make the operator observable, we have to take its expectation value. Since we work in the Heisenberg picture as we have mentioned in Sec. 4.3, the operator is sandwiched by time-independent initial bra and ket. Let $|\Phi\rangle$ be such a ket vector which is constructed by multiplying the vacuum $|0\rangle$ by the creation operators at the initial time in an appropriate manner for a desired initial condition. Then the electronic charge density $\rho_e(ct,\vec{r})$ is

$$\rho_e(ct,\vec{r})=\langle\Phi|:\hat{\rho}_e(ct,\vec{r}):|\Phi\rangle=\sum_{p,q=1}^{N_D}\sum_{c,d=\pm}\rho_{p^cq^d}(\vec{r})\langle\Phi|:\hat{\mathcal{E}}_{p^cq^d}(t):|\Phi\rangle, \quad (4.98)$$

where :: denotes the operator in between should be normal ordered. Alternatively, we can also say the physical quantity should be defined to have zero vacuum expectation value: $\langle\Phi| : \hat{\mathcal{E}}_{p^c q^d}(t) : |\Phi\rangle = \langle\Phi|\hat{\mathcal{E}}_{p^c q^d}(t)|\Phi\rangle - \langle 0|\hat{\mathcal{E}}_{p^c q^d}(t)|0\rangle$. This expectation value can be computed using the (anti-)commutation relations after $\hat{\mathcal{E}}_{p^c q^d}(t)$ is expressed by the operators at the initial time via the evolution equation Eq. (4.96). To express $\hat{\mathcal{E}}_{p^c q^d}(t)$ in terms of the annihilation/creation operators at the initial time, we may discretize the time variable and solve Eqs. (4.96) and (4.97) step by step in time direction. Although this procedure and subsequent computation of the expectation value can in principle be carried out, since we are dealing with the differential equations of operators, which are not commutative, the algebraic manipulation required is hugely demanding. The difficulty would increase very rapidly as the time steps grow. We consider such brute force computation is important to obtain as exact results as possible and it may not be impossible to do so employing recent developments in the field of computer algebra [24, 25]. At this stage, however, it is more important to look for a method to truck the time evolution of the physical quantities based on Eqs. (4.96) and (4.97) with suitable approximations. We will discuss such a method in next section.

4.5 Approximation by density matrix equations

At the end of the previous section, we have pointed out that the excitation operator equations of the Rigged QED, Eqs. (4.96) and (4.97), are practically impossible to solve by the present computational technology. We therefore propose an approximation method, which is described in this section. We also show a result of numerical calculation based on that approximation for a hydrogen atom.

4.5.1 Density matrix equations

We begin by introducing density matrices for electrons and atomic nuclei. They are defined by the expectation values (Sec. 4.4.3) of the corresponding excitation operators and we denote them as $\mathcal{E}_{p^c q^d}$ and $\mathcal{C}_{aij}$ respectively. Namely, the electron density matrix $\mathcal{E}_{p^c q^d}$ is

$$\mathcal{E}_{p^c q^d}(t) \equiv \langle\Phi| : \hat{\mathcal{E}}_{p^c q^d}(t) : |\Phi\rangle, \tag{4.99}$$

and the atomic nucleus density matrix $\mathcal{C}_{aij}$ is

$$\mathcal{C}_{aij}(t) \equiv \langle\Phi| : \hat{\mathcal{C}}_{aij}(t) : |\Phi\rangle. \tag{4.100}$$

The first step of our approximation is to replace $\hat{\vec{A}}_A$ and $\hat{\vec{j}}_T$ by their expectation values, which are denoted by

$$\vec{\mathcal{A}}_A \equiv \langle\Phi| : \hat{\vec{A}}_A : |\Phi\rangle, \tag{4.101}$$

$$\vec{\mathcal{J}}_T \equiv \langle\Phi| : \hat{\vec{j}}_T : |\Phi\rangle. \tag{4.102}$$

Using the density matrices, they are expressed as

$$\mathcal{J}^k_T(x) = \mathcal{J}^k(x) - \mathcal{J}^k_L(x), \tag{4.103}$$

$$\begin{aligned}\mathcal{J}^k(x) &= \sum_{p,q=1}^{N_D}\sum_{c,d=\pm} j^k_{p^c q^d}(\vec{r})\mathcal{E}_{p^c q^d} \\ &\quad + \sum_{a=1}^{N_n}\sum_{i,j=1}^{N_S}\left\{ j^k_{aij}(\vec{r})\mathcal{C}_{aij} - \frac{(Z_a e)}{m_a c}\rho_{aij}(\vec{r})\left(\langle\hat{A}^k_{\rm rad}\rangle\mathcal{C}_{aij} + \mathcal{A}^k_A\mathcal{C}_{aij}\right)\right\},\end{aligned} \tag{4.104}$$

$$\mathcal{J}^k_L(x) = -\sum_{p,q=1}^{N_D}\sum_{c,d=\pm} E^k_{p^c q^d}(\vec{r})\frac{d\mathcal{E}_{p^c q^d}}{dt} - \sum_{a=1}^{N_n}\sum_{i,j=1}^{N_S} E^k_{aij}(\vec{r})\frac{d\mathcal{C}_{aij}}{dt}, \tag{4.105}$$

where $\langle\hat{A}^k_{\rm rad}\rangle = \langle\Phi|\hat{A}^k_{\rm rad}|\Phi\rangle$, and

$$\vec{\mathcal{A}}_A(ct,\vec{r}) = \frac{1}{c}\int d^3\vec{s}\,\frac{\vec{\mathcal{J}}_T(cu,\vec{s})}{|\vec{r}-\vec{s}|}, \qquad u = t - \frac{|\vec{r}-\vec{s}|}{c}. \tag{4.106}$$

The second step is to replace $\hat{A}_0$ by its expectation value. This leads to replacement of the excitation operators in $\hat{I}_{4p^c q^d}$ and $\hat{I}_{4aij}$ (Eqs. (4.73) and (4.88)) by corresponding density matrices.

The final step is taking the expectation values of the time evolution equations of the excitation operators, Eqs. (4.96) and (4.97), to obtain those of the density matrices. Then, the evolution equation of electron density matrix is derived from Eq. (4.96) as

$$i\hbar\frac{d\mathcal{E}_{p^c q^d}}{dt} = \sum_{r=1}^{N_D}\sum_{e=\pm}\left(-\mathcal{I}_{r^e p^c}\mathcal{E}_{r^e q^d} + \mathcal{I}_{q^d r^e}\mathcal{E}_{p^c r^e}\right), \tag{4.107}$$

where $\mathcal{I}_{p^c q^d} \equiv \mathcal{I}_{1p^c q^d} + \mathcal{I}_{2p^c q^d} + \mathcal{I}_{3p^c q^d} + \mathcal{I}_{4p^c q^d}$ and

$$\mathcal{I}_{1p^c q^d} = T_{p^c q^d}, \tag{4.108}$$

$$\mathcal{I}_{2p^c q^d} = -\frac{1}{c}\int d^3\vec{r}\,\vec{j}_{p^c q^d}(\vec{r}) \cdot \left(\langle \hat{\vec{A}}_{\rm rad}(x)\rangle + \vec{\mathcal{A}}_A(x)\right), \tag{4.109}$$

$$\mathcal{I}_{3p^c q^d} = M_{p^c q^d}, \tag{4.110}$$

$$\mathcal{I}_{4p^c q^d} = \sum_{r,s=1}^{N_D}\sum_{e,f=\pm}(p^c q^d|r^e s^f)\mathcal{E}_{r^e s^f} + \sum_{a=1}^{N_n}\sum_{i,j=1}^{N_S}(p^c q^d|i_a j_a)\mathcal{C}_{aij}. \tag{4.111}$$

Similarly, the evolution equation of atomic nucleus density matrix is derived from Eq. (4.97) as

$$i\hbar\frac{d\mathcal{C}_{aij}}{dt} = \sum_{k=1}^{N_S}(-\mathcal{I}_{aki}\mathcal{C}_{akj} + \mathcal{I}_{ajk}\mathcal{C}_{aik}) \tag{4.112}$$

where we define $\mathcal{I}_{aij} \equiv \mathcal{I}_{1aij} + \mathcal{I}_{2aij} + \mathcal{I}_{3aij} + \mathcal{I}_{4aij}$ and

$$\mathcal{I}_{1aij} = T_{aij}, \tag{4.113}$$

$$\mathcal{I}_{2aij} = -\frac{1}{c}\int d^3\vec{r}\,\vec{j}_{aij}(\vec{r}) \cdot \left(\langle \hat{\vec{A}}_{\rm rad}(x)\rangle + \vec{\mathcal{A}}_A(x)\right), \tag{4.114}$$

$$\mathcal{I}_{3aij} = \frac{Z_a e}{2m_a c^2}\int d^3\vec{r}\,\left(\langle \hat{\vec{A}}_{\rm rad}\cdot\hat{\vec{A}}_{\rm rad}\rangle + 2\langle\hat{\vec{A}}_{\rm rad}\rangle\cdot\vec{\mathcal{A}}_A + \vec{\mathcal{A}}_A\cdot\vec{\mathcal{A}}_A\right)\rho_{aij}(\vec{r}), \tag{4.115}$$

$$\mathcal{I}_{4aij} = \sum_{p,q=1}^{N_D}\sum_{c,d=\pm}(p^c q^d|i_a j_a)\mathcal{E}_{p^c q^d} + \sum_{b=1}^{N_n}\sum_{k,l=1}^{N_S}(i_a j_a|k_b l_b)\mathcal{C}_{bkl}. \tag{4.116}$$

Eqs. (4.107) and (4.112), together with Eqs. (4.103)-(4.106), form a closed set of time evolution equations of the density matrices. Since they are c-number quantities, they can be solved by a straightforward manner.

4.5.2 Numerical calculation

We here show the result of numerical computation of solving the equations derived in Sec. 4.5.1. We adopt to make the equations simpler by employing further approximations. One is neglecting $\vec{\mathcal{A}}_A$ contribution from the vector potential to avoid heavy numerical integration involving the retarded potential. Another is the Born-Oppenheimer approximation (Sec. 4.6) to eliminate the degree of freedom of the atomic nucleus density matrix. Then, we need to only solve the equation for the electron density matrix Eq. (4.107) with $\mathcal{I}_{p^c q^d}$ being

$$\mathcal{I}_{p^c q^d} = h_{p^c q^d} + \sum_{r,s=1}^{N_D}\sum_{e,f=\pm}(p^c q^d|r^e s^f)\mathcal{E}_{r^e s^f} - \frac{1}{c}\int d^3\vec{r}\,\vec{j}_{p^c q^d}(\vec{r})\cdot\langle\hat{\vec{A}}_{\rm rad}(x)\rangle, \tag{4.117}$$

where the first term on the right-hand side is defined by Eq. (4.126) and the third term can be written as Eq. (4.77) with $\hat{a}$ and $\hat{a}^\dagger$ replaced by $\langle\hat{a}\rangle$ and $\langle\hat{a}^\dagger\rangle$ respectively.

Now, we describe our computational setups for solving time evolution of electron charge density of a hydrogen atom. The orbital functions which are used to expand the electron field operator (Sec. 4.3.1) are obtained by the publicly available DIRAC 10 code [26]. The Dirac-Coulomb Hamiltonian and the STO-3G basis set are used. Note that in this basis set, the electron density matrix is 4×4 matrix whose components denote electron (1^+), its Kramers partner ($\bar{1}^+$), positron (1^-) and its Kramers partner ($\bar{1}^-$). The initial state for the electron is taken to be the ground state. In terms of the electron density matrix, at the initial time, $\mathcal{E}_{1^+1^+} = 1$ and the other components are set to be zero. As for the initial state for the photon, we perform calculation with and without initial photon field. When we include initial photon, we assume coherent state for the initial state so that $\langle\hat{a}\rangle$ and $\langle\hat{a}^\dagger\rangle$ have non-zero values. We take the coherent state to be that of a single mode with the eigenvalue equals to 1. The mode is chosen to be in the x-direction ($\theta = \pi/2$ and $\phi = 0$) and the polarization to be $\sigma = +1$ (see Sec. 4.3.3). The momentum p^0 is taken to be 1, 10 and 20. We work in the atomic units so that $m_e = e = \hbar = 1$ and $c = 137.035999679$. The 1 a.u. of time corresponds to 2.419×10^{-17} s or 24.19 as.

As is described in Sec. 4.4.3, the electronic charge density $\rho_e(ct, \vec{r})$ is calculated as Eq. (4.98). In our approximation by the density matrix,

$$\rho_e(ct, \vec{r}) = \sum_{p,q=1}^{N_D} \sum_{c,d=\pm} \rho_{p^c q^d}(\vec{r}) \mathcal{E}_{p^c q^d}(t). \tag{4.118}$$

We compute this quantity at $(x, y, z) = (1, 0, 0)$ and plot the time evolution in Figs. 4.1-4.4. Fig. 4.1 shows the result with no photon in the initial bra and ket. Figs. 4.2, 4.3 and 4.4 show the result with the initial photon bra and ket taken as a coherent state (as describe above in detail) with $p^0 = 1$, 10 and 20 respectively.

The common feature of these results is the oscillatory behavior. From the visual inspection of the figures, there are two types of oscillations. First, we see very rapid oscillations with the period of about 1.7×10^{-4} a.u. in all of Figs. 4.1-4.4. Second, as is seen in Figs. 4.3 and 4.4, there are oscillations with longer period which modulate the rapid oscillations. They have the period of roughly 4.6×10^{-3} a.u and 2.3×10^{-3} a.u in Figs. 4.3 and 4.4 respectively. These numbers suggest the origins of the oscillations. The period of rapid ones

is very close to the period which is determined from mass scales of electron and positron, that is, $2\pi/(2m_e c^2) = 1.67 \times 10^{-4}$. The longer periods seen in Figs. 4.3 and 4.4 are very close to the period which is determined from the initial photon momentum, $2\pi/(p^0 c)$, giving 4.59×10^{-3} and 2.29×10^{-3} for $p^0 = 10$ and 20 respectively. The interpretation of the latter oscillations is that they are caused by the initial photon state which operates as the external oscillating electromagnetic field. Technically, they originate from the third term of Eq. (4.117) and the time scale of the oscillations is easily read off from Eq. (4.77). As for the former rapid oscillations, since it has the period of twice the mass of electron (or positron), it can be interpreted as the fluctuations originated from virtual electron-positron pair creations. The numerical origin is of course the mass term, Eq. (4.71), in the first term of Eq. (4.117). To see this electron-positron oscillations more explicitly, in Fig. 4.5, we plot the time evolution of $(1^+, 1^-)$-component of the electron density matrix in the case of no photon in the initial state. (Note that 1^+ denotes electron and 1^- positron as explained earlier.) We see the oscillations with the period same as those in Fig. 4.1. Although some of the other components exhibit similar oscillatory behavior, their amplitudes are much smaller and almost all of the contribution to the oscillations come from the $(1^+, 1^-)$-component.

4.6 Conclusion

In this paper, we have discussed how we formulate time evolution of physical quantities in the framework of the Rigged QED treating non-perturbatively the interactions among electrons, atomic nuclei and photons. We have defined the time-dependent annihilation/creation operators for the electron and the atomic nucleus from corresponding field operators by expanding them by appropriate functions of spatial coordinates. The photon fields have been shown to expressed by the photon annihilation/creation operators of the free photon field and those of the electron and the atomic nucleus. This enabled us to include the interactions mediated by the photon field in a non-perturbative manner. We then have derived the time evolution equations for the excitation operators of the electron and the atomic nucleus and sketched how physical quantities can be computed from them.

We have pointed out that the last parts of the procedure are very computationally demanding. Solving the coupled evolution equations for the electron and nucleus excitation

operators by a finite difference method in time requires sophisticated coding technique due to non-commutativity of the operators. The existence of the retarded potential makes the time evolution method more difficult. Also, since the coefficients of the equations involve spatial integration of up to six dimensions, their computation is very time-consuming. After that, similar difficulty of non-commutative algebra lies in computing expectation values of the time-evolved excitation operators to obtain time-evolved physical quantities. This is somewhat alleviated by the use of the Wick's theorem but it still requires large computational resource even with small number of time steps. It is true that such brute force evaluation can be carried out for a few time steps for a small system and would be feasible in future for longer time scale and larger systems considering the recent development in computer science and technology. Also, it is certainly meaningful to obtain accurate results in such a way. However, at this beginning stage, we consider it is more important to look for approximation methods to truck the time evolution of the physical quantities without too much computational time.

Therefore, we have proposed a method to approximate the time evolution equations of the operators by replacing some operators with their expectation value in the evolution equations. In other words, in an exact sense, we have to compute expectation value after the operators are evolved, but, in our approximation, some operators are replaced by their expectation values and expectation values are evolved. Although this method has room for improvement, we consider this is a good point to start. In fact, the numerical result of the time evolution of charge density of a hydrogen atom exhibits the oscillatory feature which is considered to originate from the electron-positron pair creations. This shows that our simplified way of computation can reproduce one of the most notable features of QED. Even within the framework of this approximation, there are a lot more works to be done. In our near future work, we will remove the Born-Oppenheimer approximation and will include the full effect of vector potential.

Reference

[1] M. Drescher, M. Hentschel, R. Kienberger, M. Uiberacker, V. Yakovlev, A. Scrinzi, Th. Westerwalbesloh, U. Kleineberg, U. Heinzmann, and F. Krausz, Nature **419**, 803 (2002).

[2] F. Krausz and M. Ivanov, Rev. Mod. Phys. **81**, 163 (2009).

[3] H. J. Kimble, Physica Scripta, **T76**, 127 (1998).

[4] J. Claudon et al., Nature Photon. **4**, 174 (2010).

[5] G. S. Buller and R. J. Collins, Meas. Sci. Technol. **21**, 012002 (2010).

[6] I. Aharonovich, S. Castelletto, D. A. Simpson, C. H. Su, A. D. Greentree and S. Prawer, Rep. Prog. Phys. **74**, 076501 (2011).

[7] M. E. Peskin and D. V. Schroeder, *An Introduction to Quantum Field Theory* (Westview Press, Boulder, 1995).

[8] S. Weinberg, *The Quantum Theory of Fields: Volume I Foundations* (Cambridge University Press, Cambridge, 1995).

[9] D. Bauer and P. Kobal, Comput. Phys. Commun. **174**, 396 (2006).

[10] G. R. Mocken and C. H. Keitel, Comput. Phys. Commun. **178**, 868 (2008).

[11] T. Iwasa and K. Nobusada, Phys. Rev. A **80**, 043409 (2009).

[12] R. Loudon, *The Quantum Theory of Light* (Oxford University Press, New York, 2000).

[13] P. Meystre, *Atom Optics* (Springer-Verlag, New York, 2001).

[14] S. Haroche and J. M. Raimond, *Exploring the Quantum Atoms, Cavities and Photons* (Oxford University Press, New York, 2006).

[15] P. Krekora, K. Cooley, Q. Su, and R. Grobe, Phys. Rev. Lett. **95**, 070403 (2005).

[16] P. Krekora, Q. Su, and R. Grobe, Phys. Rev. A **73**, 022114 (2006).

[17] A. Tachibana, J. Chem. Phys. **115**, 3497 (2001).

[18] A. Tachibana, in *Fundamental World of Quantum Chemistry, A Tribute to the Memory of Per-Olov Löwdin*, ed. by E. J. Brändas and E. S. Kryachko, (Kluwer Academic, Dordrecht, 2003), Vol. 2, p. 211.

[19] A. Tachibana, J. Mol. Struct. (THEOCHEM), **943**, 138 (2010).

[20] I. M. Gelfand and N. Y. Vilenkin, *Generalized Functions*, Vol. IV (Academic Press, New York, 1964).

[21] E. M. Lifshitz and L. P. Pitaevskiĭ, *Relativistic Quantum Theory Part 2* (Pergamon Press, Oxford, 1974).

[22] W. H. Furry, Phys. Rev. **81**, 115 (1951).

[23] L. D. Landau and E. M. Lifshitz, *The Classical Theory of Fields* (Butterworth-Heinemann, Oxford, 1987).

[24] Wolfram Research, Inc., Mathematica, Version 8.0, Champaign, IL (2010).

[25] Y. Hardy, K. S. Tan and W. Steeb, *Computer Algebra with Symbolic C++* (World Scientific Publishing, Singapore, 2008).

[26] DIRAC, a relativistic ab initio electronic structure program, Release DIRAC10 (2010), written by T. Saue, L. Visscher and H. J. Aa. Jensen, with contributions from R. Bast, K. G. Dyall, U. Ekström, E. Eliav, T. Enevoldsen, T. Fleig, A. S. P. Gomes, J. Henriksson, M. Iliaš, Ch. R. Jacob, S. Knecht, H. S. Nataraj, P. Norman, J. Olsen, M. Pernpointner, K. Ruud, B. Schimmelpfennig, J. Sikkema, A. Thorvaldsen, J. Thyssen, S. Villaume, and S. Yamamoto (see http://dirac.chem.vu.nl)

APPENDIX A: Born-Oppenheimer approximation

In this section, we show the time evolution equation of the operators for the electron under the Born-Oppenheimer (BO) approximation. Namely, we fix positions of the nuclei. Since the Rigged QED is proposed to include nucleus motion, this approximation is somewhat contradictory. However, there are many phenomena which can be described under the BO approximation. Moreover, since it eliminates the nucleus degree of freedom, the equations become extremely simpler and more accurate results can be obtained with less difficulty compared with the non-BO case. Thus, we consider it would be useful to present here the BO approximated version of the evolution equations.

Under the BO approximation, the atomic nuclear charge density operator $\hat{\rho}_a(x)$ (Eq. (4.16)) is given by

$$\hat{\rho}_a(x) = Z_a e\, \delta(\vec{r} - \vec{R}_a), \tag{4.119}$$

where $\vec{R}_a$ is the position for the nucleus a, $\vec{R}_a = \vec{R}_{a_1} \oplus \vec{R}_{a_2} \oplus \cdots \oplus \vec{R}_{a_{n_a}}$ specified by the generic direct sum of c-numbered n_a vectors that are clamped in space if any, with which mandatory manipulation for a function f of $\vec{R}_a$ should read $f(\vec{R}_a) = \sum_{k=1}^{n_a} f(\vec{R}_{a_k})$ as made obvious, and the atomic nuclear charge current density operator $\hat{\vec{j}}_a(x) = \vec{0}$.

This approximates the operators shown in 4.3.4 as follows. Eq. (4.59) is simplified as

$$\hat{A}_0(ct, \vec{r}) = \sum_{p,q=1}^{N_D} \sum_{c,d=\pm} V_{p^c q^d}(\vec{r}) \hat{\mathcal{E}}_{p^c q^d} + \sum_{a=1}^{N_n} \frac{Z_a e}{|\vec{r} - \vec{R}_a|}, \tag{4.120}$$

Eq. (4.58) as

$$\hat{j}^k(x) \;=\; \sum_{p,q=1}^{N_D} \sum_{c,d=\pm} j^k_{p^c q^d}(\vec{r}) \hat{\mathcal{E}}_{p^c q^d}, \tag{4.121}$$

and Eq. (4.62) as

$$\hat{j}^k_L(x) \;=\; -\sum_{p,q=1}^{N_D} \sum_{c,d=\pm} E^k_{p^c q^d}(\vec{r}) \frac{d\hat{\mathcal{E}}_{p^c q^d}}{dt}. \tag{4.122}$$

Then $\hat{\vec{A}}_A(ct, \vec{r})$ can be written as

$$\hat{\vec{A}}_A(ct, \vec{r}) \;=\; \frac{1}{c} \sum_{p,q=1}^{N_D} \sum_{c,d=\pm} \int d^3\vec{s} \left\{ \frac{\vec{j}_{p^c q^d}(\vec{s})}{|\vec{r} - \vec{s}|} \hat{\mathcal{E}}_{p^c q^d}(u) + \frac{\vec{E}_{p^c q^d}(\vec{s})}{|\vec{r} - \vec{s}|} \frac{d\hat{\mathcal{E}}_{p^c q^d}}{dt}(u) \right\}, \tag{4.123}$$

where $u = t - \frac{|\vec{r}-\vec{s}|}{c}$.

In addition, $\hat{I}_{4p^c q^d}$ (Eq. (4.73)) is simplified as

$$\hat{I}_{4p^c q^d} = \sum_{r,s=1}^{N_D} \sum_{e,f=\pm} (p^c q^d | r^e s^f) \hat{\mathcal{E}}_{r^e s^f} + \sum_{a=1}^{N_n} (Z_a e) V_{p^c q^d}(\vec{R}_a). \tag{4.124}$$

Therefore, the BO approximation version of Eq. (4.80) can be written as

$$\begin{aligned} i\hbar \frac{\partial \hat{e}_{p^c}}{\partial t} &= \sum_{q=1}^{N_D} \sum_{d=\pm} h_{p^c q^d} \hat{e}_{q^d} + \sum_{q,r,s=1}^{N_D} \sum_{d,e,f=\pm} (p^c q^d | r^e s^f) \hat{\mathcal{E}}_{r^e s^f} \hat{e}_{q^d} \\ &\quad - \frac{1}{c^2} \sum_{q,r,s=1}^{N_D} \sum_{d,e,f=\pm} \int d^3\vec{r}\, d^3\vec{s} \left\{ \frac{\vec{j}_{p^c q^d}(\vec{r}) \cdot \vec{j}_{r^e s^f}(\vec{s})}{|\vec{r}-\vec{s}|} \hat{\mathcal{E}}_{r^e s^f}(u) + \frac{\vec{j}_{p^c q^d}(\vec{r}) \cdot \vec{E}_{r^e s^f}(\vec{s})}{|\vec{r}-\vec{s}|} \frac{d\hat{\mathcal{E}}_{r^e s^f}}{dt}(u) \right\} \hat{e}_{q^d} \\ &\quad - \frac{1}{c} \frac{\sqrt{4\pi\hbar^2 c}}{\sqrt{(2\pi\hbar)^3}} \sum_{q=1}^{N_D} \sum_{d=\pm} \sum_{\sigma=\pm 1} \int \frac{d^3\vec{p}}{\sqrt{2p^0}} \times \\ &\qquad \left[\vec{F}_{p^c q^d}(\vec{p}) \cdot \vec{e}(\vec{p},\sigma) e^{-icp^0 t/\hbar} \hat{a}(\vec{p},\sigma) \hat{e}_{q^d} + \vec{F}_{p^c q^d}(-\vec{p}) \cdot \vec{e}^*(\vec{p},\sigma) e^{icp^0 t/\hbar} \hat{a}^\dagger(\vec{p},\sigma) \hat{e}_{q^d} \right], \end{aligned} \tag{4.125}$$

where we define

$$h_{p^c q^d} \equiv T_{p^c q^d} + M_{p^c q^d} + \sum_{a=1}^{N_n} (Z_a e) V_{p^c q^d}(\vec{R}_a). \tag{4.126}$$

Under the BO approximation, this is the only equation which governs the time evolution of the system.

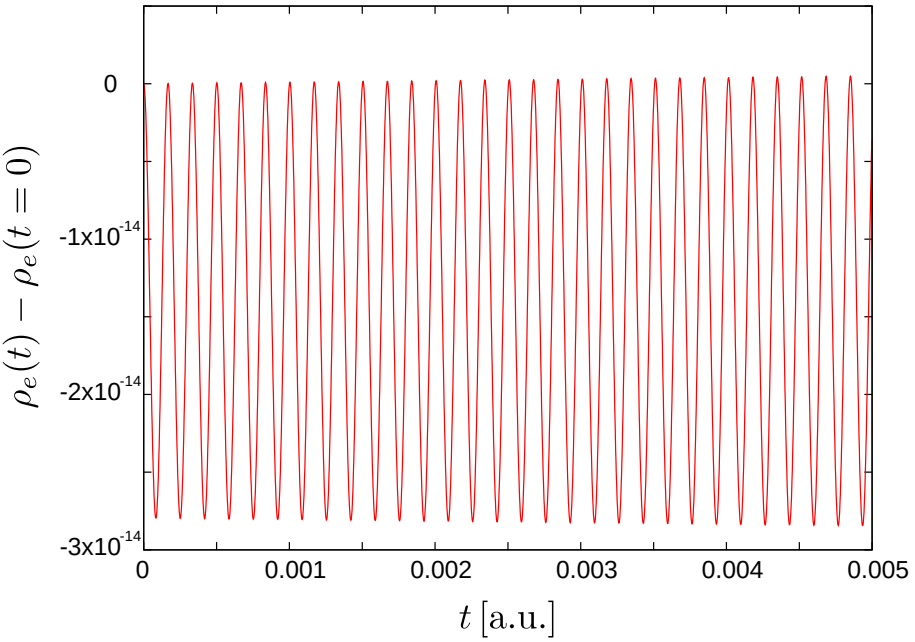

Figure 4.1: The time evolution of charge density of the hydrogen atom at $(x, y, z) = (1, 0, 0)$. The variation from the initial value is plotted. The atomic units are used. There is no photon in the initial state.

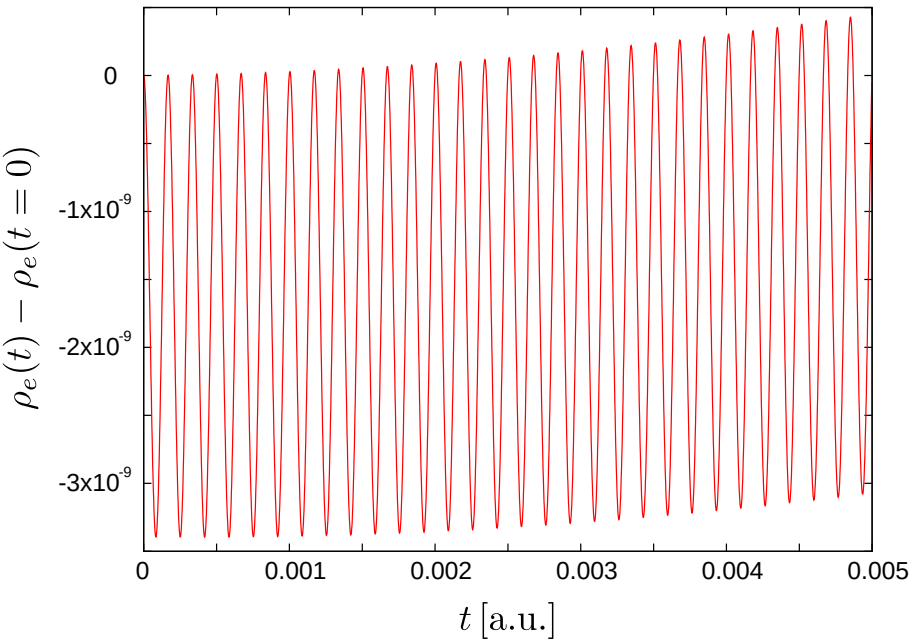

Figure 4.2: Similar to Fig. 4.1 but the initial photon state with $p^0 = 1$.

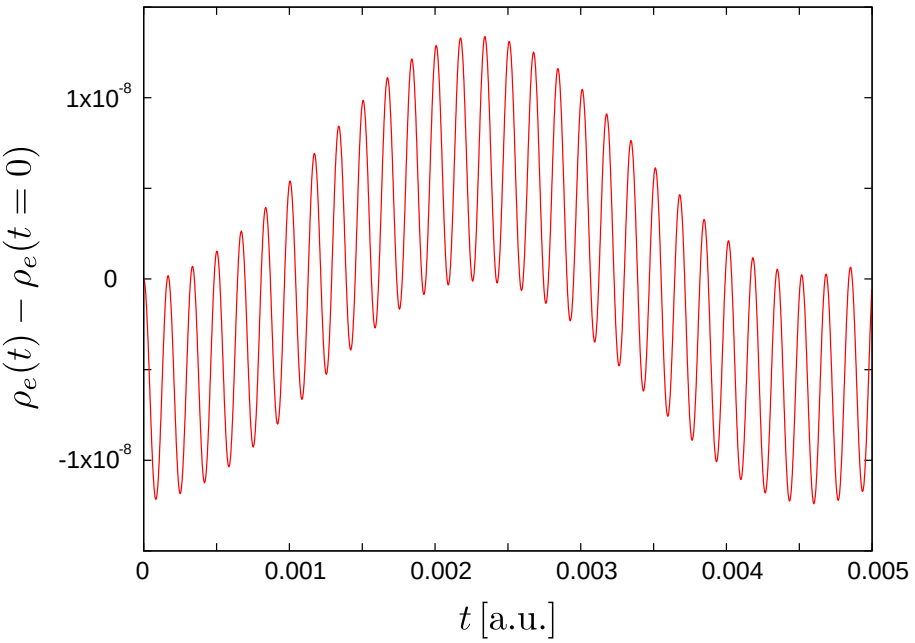

Figure 4.3: Similar to Fig. 4.1 but the initial photon state with $p^0 = 10$.

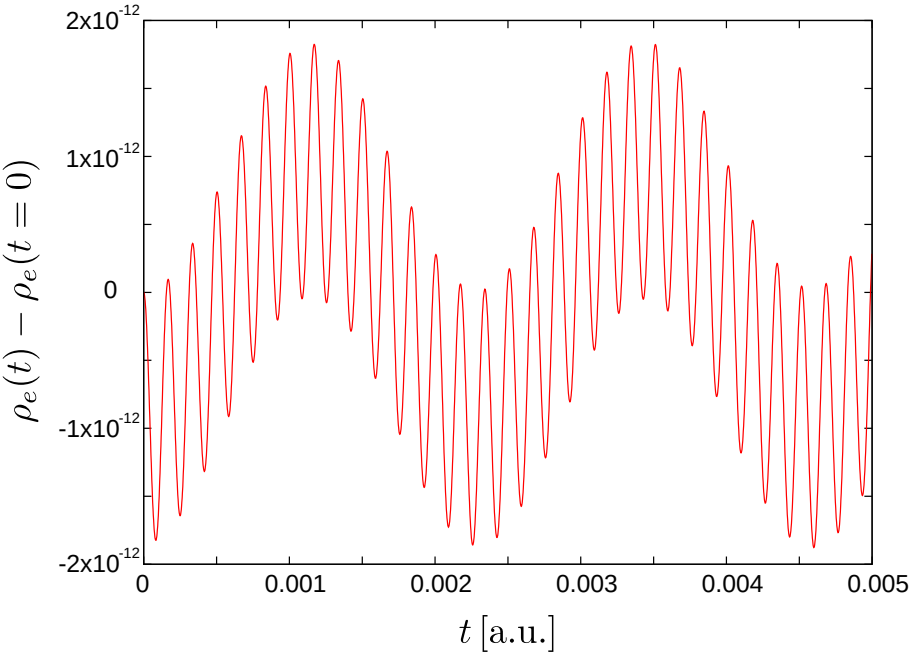

Figure 4.4: Similar to Fig. 4.1 but the initial photon state with $p^0 = 20$.

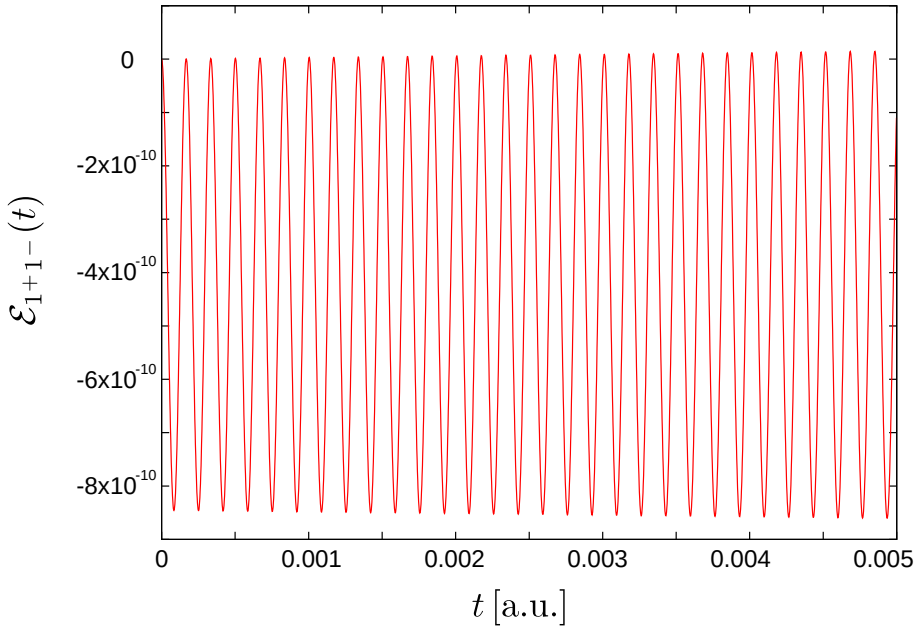

Figure 4.5: The time evolution of the $(1^+, 1^-)$-component of the electron density matrix for no photon in the initial state.

Chapter 5

Study of Simulation Method of Time Evolution of Atomic and Molecular Systems by Quantum Electrodynamics

5.1 Introduction

The elementary processes of almost every phenomenon in condensed matter physics and chemistry can be regarded as time evolution of a system which consists of interacting charged particles and photons. The physical theories which describe such a system are electromagnetism and quantum mechanics, and their unified theory has already been constructed before the middle of last century as the quantum electrodynamics (QED), taking the form of quantum field theory. The QED is the most stringently tested theory of physics and its precision is confirmed by many types of experiments of elementary particle physics. It can be considered as the most successful fundamental physical theory we have.

However, there has been only limited use of QED in the fields such as condensed matter physics and quantum chemistry. There are a lot of works to simulate the time evolution of the quantum systems involving light and matter by using the time-dependent Schrödinger, Dirac, or DFT (density functional theory) equation with classical electromagnetic fields (*i.e.* semi-classical approximation) [1–4], but both matter and light are not treated as quantized

fields. In some simulations, the quantum photon field is used but the matter part and its interaction with the photon are much more simplified than QED [5–7], or the quantum Dirac field is used for electrons but the interaction is not given by the photon field [8, 9]. In atomic physics and quantum chemistry, QED is only regarded as a small correction to the Coulomb potential which appears in the time-independent Dirac equation [10–12], and not considered in dynamical situations.

It is true that the approximations above are valid for a broad range of systems so far, but the atomic, molecular, and optical physics experiments are in rapid progress recently. It is now possible to measure, fabricate, and control structures on the atomic and molecular scale with the advances in nanotechnology. A single photon and a single electron spin can be measured and manipulated by the current technology of photonics and spintronics [13–16]. Moreover, developments in the laser science have made it possible to observe a phenomenon at the time scale of femtosecond to attosecond time scales [17, 18]. Considering such progress in the experiments of smaller space-time scales and the most fundamental particle properties, it is important for the theoretical side to develop a simulation method based on as an elementary theory as possible. This is the reason why we try to formulate a time evolution simulation method for atomic and molecular systems, which consist of electrons, atomic nuclei and photons, closely following QED in the form of quantum field theory.

To achieve our goal to develop a method to simulate time evolution of atomic and molecular systems by QED, we have to overcome some issues which do not appear in the ordinary QED. When we say the ordinary QED, we mean that it is a relativistic (Lorentz invariant) quantum field theory and the calculation method of the scattering amplitude is performed by the covariant perturbation theory [19, 20]. It implies that the only transition between infinite past ("in-state") and infinite future ("out-state") is concerned and the quantum fields in those states ("asymptotic states") can be treated like non-interacting fields. This in turn makes it possible to apply the perturbative approach by taking the asymptotic states (where fields are described by non-interacting Hamiltonian) as the unperturbed states and interaction as the perturbation. Also, the perturbative method is established in a quite systematic way, owing to the Lorentz invariance of the theory. Although such a method yields physical quantities which can be precisely compared with experiments of particle physics in particular, it is not sufficient for our interests. For simulating time evolution of atomic and

molecular systems, there are mainly three issues we have to face which are not simultaneously concerned in the ordinary QED: (i) there are atomic nuclei, which are non-relativistic and not elementary particles, (ii) the matter particles in those systems are in bound states, (iii) we would like to follow the finite time evolution of the systems step by step.

In fact, there have already been methods which can partly treat these three points within the framework of quantum field theory. First, as for (i), there are effective field theories in which nucleons are treated as quantized fields [21, 22], but the computation is within the scattering theory, so they are not suited to our needs of (ii) and (iii). In principle, since the nucleons consist of quarks and gluons which are described by quantum chromodynamics (QCD), they can be treated in a quantum field theoretic way, and the method of lattice field theory has been well developed to perform non-perturbative calculation of QCD, known as lattice QCD calculation. However, it takes too much computational time even to describe a nucleon as a bound state of quarks, and adding QED to study atoms is much more unpractical. Other shortcomings include that the current lattice field theory is developed only to describes an equilibrium state and time evolution cannot be treated. Also, in contrast to lattice QCD, lattice QED has a problem that, being $U(1)$ gauge theory which does not exhibit asymptotic freedom, the continuum limit of lattice spacing cannot be taken. Second, as for (ii), a well-known technique is the Bethe-Salpeter equation [23]. In Ref. [24], the Bethe-Salpeter equation and various other techniques to describe bound states in QED are reviewed, but those incorporating (i) or (iii) are not found. Finally, as for (iii), some formalisms are known to describe a non-equilibrium state by quantum field theory, such as closed time path (CTP) formalism [25, 26] and thermo field dynamics [27]. In particular, CTP formalism is applied to gauge theory including QED and QCD, but currently not for bound state problems. This is because the CTP formalism uses systematic perturbative expansion based on the interaction picture, but we cannot divide the QED hamiltonian into unperturbed and interaction parts when we consider bound states.

Therefore, to simulate time evolution of atomic and molecular systems based on QED, we cannot just use preexisting formalisms as mentioned above. We briefly explain our proposals [28, 29] to cope with these issues in the following. First of all, as for (i), we add the atomic nuclei degree of freedom as Schrödinger fields, and the interaction with the photon field is determined from $U(1)$ gauge symmetry as usual [28]. Although this deprives

the theory of the Lorentz invariance, since we try to follow the finite time evolution of the system, this would not be a crucial problem. Next, as for (ii), in order to describe the bound state, we expand the matter field operators by localized wavepackets, not by the usual plane waves, and define the creation and annihilation operators [29]. In the case of the Dirac field operator for electrons, for example, we may adopt the stationary solutions of the Dirac equation under the existence of external electrostatic field, as the expansion functions. This is similar to the Furry picture [30, 31], but, as described below, we do not assume the time-dependence of the operators which is determined by the energy eigenvalues. Finally, as for (iii), we follow the time evolution using the equations of motion of the field operator in the Heisenberg picture [29]. As is mentioned earlier, since we do not have well-defined division between unperturbed and interaction parts of the QED hamiltonian for the bound state, we cannot work in the interaction picture.

The setups described above determine the evolution equations of field operators, and those of creation and annihilation operators, but we have to make further approximations and assumptions to obtain the evolution equations for the expectation value of physical quantities. In Ref. [29], we have studied the time evolution of one of the most basic physical quantity operators, the electronic charge density operator, and have discussed approximation methods to obtain the time evolution of its expectation value. The charge density operator is expressed by the product of two creation or annihilation operators, which is called an excitation operator, but since the time derivative of creation and annihilation operators contains more than one of these operators, the time differential equation of the excitation operator is not closed. In other words, differentiating the excitation operator yields operators which cannot be expressed by the excitation operator. Such a problem is generic for interacting quantum field theories [25], and not special to our approach. In Ref. [29], we have introduced several approximations to obtain the time evolution equation for the expectation value of the excitation operator, which is called a density matrix, and numerically solved the time evolution of the density matrix. The time evolution of the expectation value of the charge density operator has been obtained by multiplying the density matrix by the expansion functions of the field operator. Then, we have found that the time evolution of the charge density of a hydrogen atom exhibits very rapid oscillations of the period $\approx 1.7\times10^{-4}$ a.u. (4.1×10^{-21} s), which corresponds to the inverse of twice the electron

mass. This is interpreted as the fluctuations originated from the virtual electron-positron pair creations and annihilations, showing the effect of QED, and we have designated the phenomenon as "electron-positron oscillations".

In the present paper, we improve one of the approximations employed in Ref. [29] with respect to the terms which include the photon creation and annihilation operators. In our formalism, the time derivative of the electron excitation operator has the terms which consist of two creation or annihilation operators sandwiching a photon creation or annihilation operator (we call this type of operator by "$\hat{e}^\dagger\hat{a}\hat{e}$-type operator" for short). In Ref. [29], when we take the expectation value of these terms, we have factorized the terms into the expectation value of the excitation operator and that of the photon creation or annihilation operator. After this approximation, these terms give finite contribution only when an initial photon state is a coherent state, which is an eigenstate of the photon annihilation operator. In particular, they vanish for the photon vacuum state. To go one step further, we, in this paper, do not perform the above factorization, and solve the time evolution equation of the $\hat{e}^\dagger\hat{a}\hat{e}$-type operators simultaneously with that of the excitation operator. As we show in a later section, this procedure corresponds to counting the self-energy process of the electron (the electron emits a photon and then absorbs it again), and, consistently, it gives non-zero contribution even when the initial state is the photon vacuum state.

This paper is organized as follows. In Sec. 5.2, we derive the time evolution equations of the quantum operators. After we describe how we expand field operators and define creation and annihilation operators, we show time derivative of the creation and annihilation operators from the equations of motion of the quantum fields. Then, we derive the time evolution equation of the excitation operator and $\hat{e}^\dagger\hat{a}\hat{e}$-type operator. In Sec. 5.3, we derive time evolution equations of the density matrix by taking the expectation value of the time derivative of the excitation operator. We explain our approximation methods to derive closed sets of time evolution equations. In Sec. 5.4, we show the results of numerical computation of these equations for a hydrogen atom and molecule. Finally, Sec. 5.5 is devoted to our conclusion. The notations and conventions follow those in Refs. [28, 29, 32, 33].

5.2 Evolution equations for quantum operators

We would like to describe atoms and molecules as systems which consist of electrons, atomic nuclei and photons. In this paper, we work in the Born-Oppenheimer (BO) approximation, in which positions of the atomic nuclei are fixed. Then, only electrons and photons are described as quantum field operators, and atomic nuclei contribute to the charge density as delta functions. The source of the photon field can be both electrons and atomic nuclei. The quantum field operators which appear in this paper are the four-component Dirac field operator $\hat{\psi}(x)$ for the electron, and the $U(1)$ gauge field $\hat{A}_\mu(x)$ for the photon. (Incidentally, the approach to treat the electron as the two-component Schrödinger field [34] is also developed in our group. See Refs. [35–37] for details.) Although there are some overlaps in this section with the contents in Ref. [29], we reproduce them in the reorganized form for the convenience of the readers.

5.2.1 Definitions of creation and annihilation operators

Our expansion of the Dirac field operator is

$$\hat{\psi}(ct, \vec{r}) = \sum_{n=1}^{N_D} \sum_{a=\pm} \hat{e}_{n^a}(t) \psi_{n^a}(\vec{r}), \tag{5.1}$$

where $\psi_{n^+}(\vec{r})$ and $\psi_{n^-}(\vec{r})$ are respectively the n-th electron and positron solutions of the four-component Dirac-Hartree-Fock equation under the existence of external electrostatic field, and they form an orthonormal basis set as $\int d^3\vec{r}\, \psi^\dagger_{n^a}(\vec{r}) \psi_{m^b}(\vec{r}) = \delta_{nm}\delta_{ab}$. In Eq. (5.1), N_D is the number of the electron expansion functions, which is same as one of the positron expansion functions. Considering the Kramers pair, N_D usually equals to twice the number of basis functions used to solve the Dirac equation. We note that N_D has to be infinite to make the expansion function set complete, but this is not available in numerical calculation. In practice, we use a finite set which only spans a certain region of the complete space. We should interpret thus obtained results as phenomena within the subspace spanned by the finite set of expansion functions. We may use any localized wavepackets for the expansion functions, but the above choice is convenient because we can obtain such functions easily by the publicly available code like DIRAC [38]. The creation and annihilation operators are defined as the coefficients of the expansion functions and carry the time dependence.

In our notation, $\hat{e}_{n^+}$ is the electron annihilation operator and $\hat{e}_{n^-}$ is the positron creation operator. Accordingly, $\hat{e}^\dagger_{n^+}$ is the electron creation operator and $\hat{e}^\dagger_{n^-}$ is the positron annihilation operator. In the literature, a creation operator is usually expressed by an operator with a dagger as superscript, but, note that, in our notation, the positron creation operator does not carry a dagger whereas the positron annihilation operator does. We adopt this notation to make compact the expression of the expansion of Eq. (5.1) and equations below. The equal-time anti-commutation relation can be written as $\left\{\hat{e}_{n^a}(t), \hat{e}^\dagger_{m^b}(t)\right\} = \delta_{nm}\delta_{ab}$, and anti-commutators of other combinations are zero.

For later convenience, we here define the electronic excitation operator, which is formed from two creation or annihilation operators as

$$\hat{\mathcal{E}}_{n^a m^b} \equiv \hat{e}^\dagger_{n^a}\hat{e}_{m^b}. \tag{5.2}$$

Then, the electronic charge density operator and current density operators are written by the excitation operator as

$$\hat{\rho}_e(x) = \sum_{n,m=1}^{N_D}\sum_{a,b=\pm}\rho_{n^a m^b}(\vec{r})\hat{\mathcal{E}}_{n^a m^b}(t), \tag{5.3}$$

$$\hat{j}^k_e(x) = \sum_{n,m=1}^{N_D}\sum_{a,b=\pm} j^k_{n^a m^b}(\vec{r})\hat{\mathcal{E}}_{n^a m^b}(t), \tag{5.4}$$

where we define

$$\rho_{n^a m^b}(\vec{r}) \equiv (Z_e e)\psi^\dagger_{n^a}(\vec{r})\psi_{m^b}(\vec{r}), \tag{5.5}$$

$$j^k_{n^a m^b}(\vec{r}) \equiv Z_e\, e\, c\left[\psi^\dagger_{n^a}(\vec{r})\gamma^0\gamma^k\psi_{m^b}(\vec{r})\right], \tag{5.6}$$

and $Z_e = -1$. The total charge density operator have contribution from both electrons and atomic nuclei, $\hat{\rho}(x) = \hat{\rho}_e(x) + \sum_{a=1}^{N_n}\hat{\rho}_a(x)$, where $\hat{\rho}_a(x)$ is the atomic nuclear charge density operator, a denotes the type of atomic nucleus and we assume N_n types of atomic nuclei in the system. Under the BO approximation, $\hat{\rho}_a(x) = Z_a e\,\delta^{(3)}(\vec{r} - \vec{R}_a)$, where Z_a is the nucleus a's atomic number, and $\vec{R}_a$ should be understood as the direct sum of the position of each nucleus of type a (see Appendix of Ref. [29] for details). As for the total charge current density operator, since there is no contribution from the atomic nuclei under the BO approximation, we have $\hat{\vec{j}}(x) = \hat{\vec{j}}_e(x)$. Although we do not compute the energy of the system in this paper, it may be instructive to show the QED Hamiltonian operator. This is shown in Appendix 5.5.

As for the photon field operator, we use the integral equation form of the equation of motion. Namely, we use the fact that the formal solutions of the inhomogeneous Maxwell equations are known from the classical electrodynamics [5, 39, 40], and express $\hat{A}_\mu(x)$ by such solutions [28, 29]. Similar technique is used to derive the so-called Yang-Feldman equation, which is originally introduced to discuss the S-matrix of QED in Heisenberg picture [41]. We adopt the Coulomb gauge, $\vec{\nabla}\cdot\hat{\vec{A}}(x)=0$. Then, the scalar potential is given by

$$\hat{A}_0(ct,\vec{r}) = \int d^3\vec{s}\,\frac{\hat{\rho}(ct,\vec{s})}{|\vec{r}-\vec{s}|}, \tag{5.7}$$

and the vector potential by

$$\hat{\vec{A}}(ct,\vec{r}) = \hat{\vec{A}}_{\rm rad}(ct,\vec{r}) + \hat{\vec{A}}_A(ct,\vec{r}), \tag{5.8}$$

where the first term is the quantized free radiation field in the Coulomb gauge [5, 42] and the second term is the retarded potential. $\hat{\vec{A}}_{\rm rad}(ct,\vec{r})$ is expressed as

$$\begin{aligned}\hat{A}^k_{\rm rad}(ct,\vec{r}) &= \frac{\sqrt{4\pi\hbar^2 c}}{\sqrt{(2\pi\hbar)^3}}\sum_{\sigma=\pm1}\int\frac{d^3\vec{p}}{\sqrt{2p^0}}\Big[\hat{a}_{\vec{p}\sigma}e^k(\vec{p},\sigma)e^{-icp^0t/\hbar}e^{i\vec{p}\cdot\vec{r}/\hbar}\\ &\quad +\hat{a}^\dagger_{\vec{p}\sigma}e^{*k}(\vec{p},\sigma)e^{icp^0t/\hbar}e^{-i\vec{p}\cdot\vec{r}/\hbar}\Big],\end{aligned} \tag{5.9}$$

where $\hat{a}_{\vec{p}\sigma}$ ($\hat{a}^\dagger_{\vec{p}\sigma}$) are the annihilation (creation) operator of the photon with momentum $\vec{p}$ and helicity σ, and $\vec{e}$ is the polarization vector. They satisfy the commutation relation $[\hat{a}_{\vec{p}\sigma},\hat{a}^\dagger_{\vec{q}\tau}]=\delta(\vec{p}-\vec{q})\delta_{\sigma\tau}$, and commutators of the other combinations are zero. Our convention for $\vec{e}(\vec{p},\sigma)$ is found in Ref. [29]. $\hat{\vec{A}}_A(ct,\vec{r})$ is expressed as

$$\hat{\vec{A}}_A(ct,\vec{r}) = \frac{1}{c}\int d^3\vec{s}\,\frac{\hat{\vec{j}}_T(cu,\vec{s})}{|\vec{r}-\vec{s}|}, \tag{5.10}$$

where we define the retarded time $u=t-|\vec{r}-\vec{s}|/c$, and $\hat{\vec{j}}_T(x)$ is the transversal component of the current. Writing explicitly,

$$\hat{j}^k_T(cu,\vec{s}) = \sum_{p,q=1}^{N_D}\sum_{c,d=\pm}\left\{j^k_{p^cq^d}(\vec{s})\hat{\mathcal{E}}_{p^cq^d}(u)+E^k_{p^cq^d}(\vec{s})\frac{d\hat{\mathcal{E}}_{p^cq^d}}{dt}(u)\right\}, \tag{5.11}$$

where

$$E^k_{n^am^b}(\vec{R}) = -\frac{Z_e e}{4\pi}\int d^3\vec{s}\,\psi^\dagger_{n^a}(\vec{s})\psi_{m^b}(\vec{s})\frac{(\vec{s}-\vec{R})^k}{|\vec{s}-\vec{R}|^3}. \tag{5.12}$$

As we mentioned in Sec. 5.1, we do not consider the usual asymptotic states of the field operator, in which the state becomes non-interacting as $t\to-\infty$ asymptotically. We assume

that the interaction is absent for $t < 0$ and the free part expressed above by $\hat{A}_{\mathrm{rad},\mu}(x)$ is considered to realize at $t = 0$. This, in particular, implies the initial condition

$$\hat{j}^{\mu}(cu, \vec{s}) = 0, \quad u < 0, \tag{5.13}$$

and enables us to rewrite the retarded potential as [34]

$$\hat{\vec{A}}_A(ct, \vec{r}) = \frac{1}{c^2\pi} \int_0^t du \int_{-\infty}^{\infty} d\alpha \exp\left(i\alpha(t-u)^2\right) \int d^3\vec{s}\, \hat{\vec{j}}_T(cu, \vec{s}) \exp\left(-i\alpha \frac{(\vec{r}-\vec{s})^2}{c^2}\right) \tag{5.14}$$

To derive this, we use the following formulae for the delta function $\delta(x^2-a^2) = \{\delta(x-a) + \delta(x+a)\}/(2a)$ with $a > 0$, and $\delta((t-u)^2 - (\vec{r}-\vec{s})^2/c^2) = \frac{1}{2\pi}\int_{-\infty}^{\infty} d\alpha \exp[i\alpha\{(t-u)^2 - (\vec{r}-\vec{s})^2/c^2\}]$. This form may be convenient for the numerical calculation since the retarded time is eliminated, but at the cost of increasing the dimension of integration.

In passing, some comments on our assumption at the initial time ($t = 0$) may be in order. Following Ref. [43], we assume that the parameters and fields which appear in the equations of motion have been renormalized at $t = 0$. Specifically, the renormalization has been performed in a standard manner as $m_e = m_{eB} + \delta m_e$, $e = \sqrt{Z_3} e_B$, $\hat{\psi}(x) = \hat{\psi}_B(x)/\sqrt{Z_2}$ and $\hat{A}^{\mu}(x) = \hat{A}^{\mu}_B(x)/\sqrt{Z_3}$, where "B" in the subscripts denotes a bare parameter or a bare field, and δm_e, Z_2 and Z_3 are the renormalization constants. However, it does not mean that we do not need renormalization at $t > 0$. In fact, as is discussed later in this paper, the electron mass is shown to be increased by including the self-energy process in our time evolution simulation.

5.2.2 Time evolution of annihilation and creation operators

The time derivative of $\hat{e}_{n^a}$ is given by substituting the expansion Eq. (5.1) into the Dirac field equation, multiplying by $\psi^{\dagger}_{n^a}(\vec{r})$, integrating over $\vec{r}$, and using the orthonormality condition [29]. This leads to

$$\begin{aligned}
i\hbar \frac{\partial \hat{e}_{n^a}}{\partial t} &= \sum_{m=1}^{N_D} \sum_{b=\pm} h_{n^a m^b} \hat{e}_{m^b} + \sum_{m,p,q=1}^{N_D} \sum_{b,c,d=\pm} (n^a m^b | p^c q^d) \hat{e}^{\dagger}_{p^c} \hat{e}_{q^d} \hat{e}_{m^b} \\
&- \frac{1}{c^2} \sum_{m=1}^{N_D} \sum_{b=\pm} \sum_{k=1}^{3} \int d^3\vec{r}\, d^3\vec{s}\, j^k_{n^a m^b}(\vec{r}) \frac{\hat{j}^k_T(cu, \vec{s})}{|\vec{r}-\vec{s}|} \hat{e}_{m^b} \\
&- \frac{\sqrt{4\pi\hbar^2}}{\sqrt{c(2\pi\hbar)^3}} \sum_{m=1}^{N_D} \sum_{b=\pm} \sum_{k=1}^{3} \sum_{\sigma=\pm 1} \int \frac{d^3\vec{p}}{\sqrt{2p^0}} \Big[F^k_{n^a m^b}(\vec{p}) e^k(\vec{p}, \sigma) e^{-icp^0 t/\hbar}\, \hat{a}_{\vec{p}\sigma} \hat{e}_{m^b} \\
&\quad + F^k_{n^a m^b}(-\vec{p}) e^{*k}(\vec{p}, \sigma) e^{icp^0 t/\hbar}\, \hat{a}^{\dagger}_{\vec{p}\sigma} \hat{e}_{m^b} \Big],
\end{aligned} \tag{5.15}$$

where the various coefficient matrices are defined as follows. In the first term, we define

$$h_{n^a m^b} = T_{n^a m^b} + M_{n^a m^b} + \sum_{a=1}^{N_n} (Z_a e) V_{n^a m^b}(\vec{R}_a), \tag{5.16}$$

where $T_{n^a m^b}$ is the electronic kinetic energy integral, $M_{n^a m^b}$ is the electronic mass energy integral, and $V_{n^a m^b}(\vec{R})$ is the nuclear attraction integral, respectively defined as

$$T_{n^a m^b} \equiv -i\hbar c \int d^3\vec{r}\, \psi^\dagger_{n^a}(\vec{r}) \gamma^0 \vec{\gamma} \cdot \vec{\nabla} \psi_{m^b}(\vec{r}), \tag{5.17}$$

$$M_{n^a m^b} \equiv m_e c^2 \int d^3\vec{r}\, \psi^\dagger_{n^a}(\vec{r}) \gamma^0 \psi_{m^b}(\vec{r}), \tag{5.18}$$

$$V_{n^a m^b}(\vec{R}) \equiv (Z_e e) \int d^3\vec{s}\, \frac{\psi^\dagger_{n^a}(\vec{s}) \psi_{m^b}(\vec{s})}{|\vec{s} - \vec{R}|}. \tag{5.19}$$

They originate respectively in the kinetic term, mass term, and the nuclear charge contribution to the scalar potential term.

In the second term of Eq. (5.15), we define the electronic repulsion integral

$$(n^a m^b | p^c q^d) \equiv (Z_e e)^2 \int d^3\vec{r}\, d^3\vec{s}\, \psi^\dagger_{n^a}(\vec{r}) \psi_{m^b}(\vec{r}) \frac{1}{|\vec{r} - \vec{s}|} \psi^\dagger_{p^c}(\vec{s}) \psi_{q^d}(\vec{s}). \tag{5.20}$$

This term originates in the electronic charge contribution to the scalar potential term. The third and forth terms of Eq. (5.15) originate in the vector potential term. The former comes from the retarded part $\hat{\vec{A}}_A$ (5.10) and the latter from the free radiation part $\hat{\vec{A}}_{\rm rad}$ (5.9). Finally, in the forth term of Eq. (5.15), we define

$$F^k_{n^a m^b}(\vec{p}) \equiv \int d^3\vec{r}\, j^k_{n^a m^b}(\vec{r}) e^{i\vec{p}\cdot\vec{r}/\hbar}. \tag{5.21}$$

5.2.3 Time evolution of excitation and $\hat{e}^\dagger \hat{a} \hat{e}$-type operators

In this paper, we are interested in the time evolution of electronic charge density, and its operator $\hat{\rho}_e(x)$ is expressed by the excitation operator as Eq. (5.3). Since the excitation operator carries every time dependence of $\hat{\rho}_e(x)$, what we need to know is the time evolution equation of the excitation operator.

The time derivative of the excitation operator $\hat{\mathcal{E}}_{n^a m^b}$ (5.2) can be written as

$$\frac{\partial \hat{\mathcal{E}}_{n^a m^b}}{\partial t} = (\hat{O}_{m^b n^a})^\dagger + \hat{O}_{n^a m^b}, \tag{5.22}$$

where we define

$$\hat{O}_{n^a m^b} \equiv \hat{e}^\dagger_{n^a} \frac{\partial \hat{e}_{m^b}}{\partial t}. \tag{5.23}$$

Using Eq. (5.15), this can be readily obtained as

$$
\begin{aligned}
i\hbar\hat{O}_{n^a m^b} &= \sum_{r=1}^{N_D}\sum_{e=\pm} h_{m^b r^e}\hat{e}^\dagger_{n^a}\hat{e}_{r^e} + \sum_{r,p,q=1}^{N_D}\sum_{e,c,d=\pm}(m^b r^e|p^c q^d)\hat{e}^\dagger_{n^a}\hat{e}^\dagger_{p^c}\hat{e}_{q^d}\hat{e}_{r^e} \\
&- \frac{1}{c^2}\sum_{r=1}^{N_D}\sum_{e=\pm}\sum_{k=1}^{3}\int d^3\vec{r}\, d^3\vec{s}\, j^k_{m^b r^e}(\vec{r})\hat{e}^\dagger_{n^a}\frac{\hat{j}^k_T(cu,\vec{s})}{|\vec{r}-\vec{s}|}\hat{e}_{r^e} \\
&- \frac{1}{\sqrt{2\pi^2\hbar c}}\sum_{r=1}^{N_D}\sum_{e=\pm}\sum_{\sigma=\pm 1}\int\frac{d^3\vec{p}}{\sqrt{2p^0}}\left[\mathcal{F}_{m^b r^e\vec{p}_\sigma}(t)\hat{e}^\dagger_{n^a}\hat{a}_{\vec{p}_\sigma}\hat{e}_{r^e} + \mathcal{F}^*_{r^e m^b\vec{p}_\sigma}(t)\hat{e}^\dagger_{n^a}\hat{a}^\dagger_{\vec{p}_\sigma}\hat{e}_{r^e}\right],
\end{aligned}
\tag{5.24}
$$

where we have defined

$$
\mathcal{F}_{n^a m^b\vec{p}_\sigma}(t) \equiv \sum_{k=1}^{3} F^k_{n^a m^b}(\vec{p})e^k(\vec{p},\sigma)e^{-icp^0 t/\hbar},
\tag{5.25}
$$

to make the expression shorter. For later convenience, we call the second term of Eq. (5.24) "four-electron term", the third term "retarded potential term", and the forth term "radiation term".

Next, we consider the time derivative of the $\hat{e}^\dagger\hat{a}\hat{e}$-type operators. Since the time derivative of $\hat{e}^\dagger_{m^b}\hat{a}^\dagger_{\vec{p}_\sigma}\hat{e}_{n^a}$ is known by taking the Hermite conjugate of that of $\hat{e}^\dagger_{n^a}\hat{a}_{\vec{p}_\sigma}\hat{e}_{m^b}$, we only show the latter below. This can be expressed as

$$
\frac{\partial}{\partial t}\left\{\hat{e}^\dagger_{n^a}\hat{a}_{\vec{p}_\sigma}\hat{e}_{m^b}\right\} = (\hat{Q}_{m^b\vec{p}_\sigma n^a})^\dagger + \hat{P}_{n^a\vec{p}_\sigma m^b},
\tag{5.26}
$$

where we define

$$
\hat{P}_{n^a\vec{p}_\sigma m^b} \equiv \hat{e}^\dagger_{n^a}\hat{a}_{\vec{p}_\sigma}\frac{\partial\hat{e}_{m^b}}{\partial t},
\tag{5.27}
$$

$$
\hat{Q}_{n^a\vec{p}_\sigma m^b} \equiv \hat{e}^\dagger_{n^a}\hat{a}^\dagger_{\vec{p}_\sigma}\frac{\partial\hat{e}_{m^b}}{\partial t}.
\tag{5.28}
$$

Using Eq. (5.15), we obtain

$$
\begin{aligned}
i\hbar\hat{P}_{n^a\vec{p}_\sigma m^b} &= \sum_{r=1}^{N_D}\sum_{e=\pm} h_{m^b r^e}\hat{e}^\dagger_{n^a}\hat{a}_{\vec{p}_\sigma}\hat{e}_{r^e} + \sum_{r,p,q=1}^{N_D}\sum_{e,c,d=\pm}(m^b r^e|p^c q^d)\hat{e}^\dagger_{n^a}\hat{a}_{\vec{p}_\sigma}\hat{e}^\dagger_{p^c}\hat{e}_{q^d}\hat{e}_{r^e} \\
&- \frac{1}{c^2}\sum_{r=1}^{N_D}\sum_{e=\pm}\sum_{k=1}^{3}\int d^3\vec{r}\, d^3\vec{s}\, j^k_{m^b r^e}(\vec{r})\hat{e}^\dagger_{n^a}\hat{a}_{\vec{p}_\sigma}\frac{\hat{j}^k_T(cu,\vec{s})}{|\vec{r}-\vec{s}|}\hat{e}_{r^e} \\
&- \frac{1}{\sqrt{2\pi^2\hbar c}}\sum_{r=1}^{N_D}\sum_{e=\pm}\sum_{\tau=\pm 1}\int\frac{d^3\vec{q}}{\sqrt{2q^0}} \\
&\quad\times\left[\mathcal{F}_{m^b r^e\vec{q}_\tau}(t)\hat{e}^\dagger_{n^a}\hat{a}_{\vec{p}_\sigma}\hat{a}_{\vec{q}_\tau}\hat{e}_{r^e} + \mathcal{F}^*_{r^e m^b\vec{q}_\tau}(t)\hat{e}^\dagger_{n^a}\hat{a}_{\vec{p}_\sigma}\hat{a}^\dagger_{\vec{q}_\tau}\hat{e}_{r^e}\right],
\end{aligned}
\tag{5.29}
$$

and

$$
\begin{aligned}
i\hbar\hat{Q}_{n^a\vec{p}_\sigma m^b} &= \sum_{r=1}^{N_D}\sum_{e=\pm} h_{m^b r^e}\hat{e}^\dagger_{n^a}\hat{a}^\dagger_{\vec{p}_\sigma}\hat{e}_{r^e} + \sum_{r,p,q=1}^{N_D}\sum_{e,c,d=\pm}(m^b r^e|p^c q^d)\hat{e}^\dagger_{n^a}\hat{a}^\dagger_{\vec{p}_\sigma}\hat{e}^\dagger_{p^c}\hat{e}_{q^d}\hat{e}_{r^e} \\
&- \frac{1}{c^2}\sum_{r=1}^{N_D}\sum_{e=\pm}\sum_{k=1}^{3}\int d^3\vec{r}\,d^3\vec{s}\,j^k_{m^b r^e}(\vec{r})\hat{e}^\dagger_{n^a}\hat{a}^\dagger_{\vec{p}_\sigma}\frac{\hat{j}^k_T(cu,\vec{s})}{|\vec{r}-\vec{s}|}\hat{e}_{r^e} \\
&- \frac{1}{\sqrt{2\pi^2\hbar c}}\sum_{r=1}^{N_D}\sum_{e=\pm}\sum_{\tau=\pm1}\int\frac{d^3\vec{q}}{\sqrt{2q^0}} \\
&\quad\times\left[\mathcal{F}_{m^b r^e\vec{q}_\tau}(t)\hat{e}^\dagger_{n^a}\hat{a}^\dagger_{\vec{p}_\sigma}\hat{a}_{\vec{q}_\tau}\hat{e}_{r^e} + \mathcal{F}^*_{r^e m^b\vec{q}_\tau}(t)\hat{e}^\dagger_{n^a}\hat{a}^\dagger_{\vec{p}_\sigma}\hat{a}^\dagger_{\vec{q}_\tau}\hat{e}_{r^e}\right].
\end{aligned}
\tag{5.30}
$$

We note that the last term of $\hat{P}_{n^a\vec{p}_\sigma m^b}$ includes the operator product of the form $\hat{e}^\dagger_{n^a}\hat{a}_{\vec{p}_\sigma}\hat{a}^\dagger_{\vec{q}_\tau}\hat{e}_{r^e}$. This combination of the operators could express a self-energy process, in which the electron emits a photon and then absorbs it again. The effect of the self-energy process will be discussed and numerically demonstrated in Sec. 5.4.3.

5.3 Evolution equations for density matrix

5.3.1 Definition of density matrix

We begin by introducing notations regarding expectation values. We denote the expectation value of the excitation operator with respect to the Heisenberg initial ket $|\Phi\rangle$ by

$$
\mathcal{E}_{n^a m^b} \equiv \langle\Phi|\hat{\mathcal{E}}_{n^a m^b}|\Phi\rangle, \tag{5.31}
$$

and call this quantity the density matrix. Below, we sometimes write just brackets around the operator to denote the expectation value with respect to $|\Phi\rangle$, namely, $\langle\cdots\rangle \equiv \langle\Phi|\cdots|\Phi\rangle$ where $\cdots$ stands for some operators. Since $(\hat{\mathcal{E}}_{n^a m^b})^\dagger = \hat{e}^\dagger_{m^b}\hat{e}_{n^a} = \hat{\mathcal{E}}_{m^b n^a}$, taking the expectation value yields $(\mathcal{E}_{n^a m^b})^* = \mathcal{E}_{m^b n^a}$, showing that the density matrix is a Hermite matrix. Similarly, we define the expectation value of Eq. (5.23) as $\mathcal{O}_{n^a m^b} \equiv \langle\Phi|\hat{O}_{n^a m^b}|\Phi\rangle$. Then, since $\langle(\hat{O}_{n^a m^b})^\dagger\rangle = (\mathcal{O}_{n^a m^b})^* = \mathcal{O}^\dagger_{m^b n^a}$, taking the expectation value of Eq. (5.22) leads to

$$
\frac{\partial\mathcal{E}_{n^a m^b}}{\partial t} = \mathcal{O}^\dagger_{n^a m^b} + \mathcal{O}_{n^a m^b}, \tag{5.32}
$$

which is the time evolution equation for the density matrix.

Using the density matrix, the expectation value of the electronic charge density operator, Eq. (5.3), can be written as

$$\langle\Phi|\hat{\rho}_e(x)|\Phi\rangle = \sum_{n,m=1}^{N_D}\sum_{a,b=\pm}\rho_{n^a m^b}(\vec{r})\mathcal{E}_{n^a m^b}(t). \tag{5.33}$$

However, this quantity has a non-zero value when the Heisenberg initial ket is the vacuum, $|\Phi\rangle = |0\rangle$, at $t = 0$. (Remember that $\hat{e}_{n^-}$ is the positron creation operator.) As is done in the ordinary QED, this can be remedied by computing the expectation value of the normal-ordered product of the operators at $t = 0$. In the case of $\hat{\rho}_e(x)$, this can be accomplished by subtracting the vacuum expectation value of $\hat{\rho}_e(x)$ at $t = 0$. Then, we shall define the electronic charge density $\rho_e(x)$ as the expectation value of the electronic charge density operator after this subtraction. Writing explicitly,

$$\rho_e(x) = \sum_{n,m=1}^{N_D}\sum_{a,b=\pm}\rho_{n^a m^b}(\vec{r})\left\{\mathcal{E}_{n^a m^b}(t) - \mathcal{E}^0_{n^a m^b}(t=0)\right\}, \tag{5.34}$$

where we define $\mathcal{E}^0_{n^a m^b} \equiv \langle 0|\hat{\mathcal{E}}_{n^a m^b}|0\rangle$.

5.3.2 Four-electron term and retarded potential term

The four-electron term consists of four electron creation or annihilation operators. We approximate this term by

$$\begin{aligned}\langle\hat{e}^\dagger_{n^a}\hat{e}^\dagger_{p^c}\hat{e}_{q^d}\hat{e}_{r^e}\rangle &\approx \langle\hat{e}^\dagger_{n^a}\hat{e}_{r^e}\rangle\langle\hat{e}^\dagger_{p^c}\hat{e}_{q^d}\rangle - \langle\hat{e}^\dagger_{n^a}\hat{e}_{q^d}\rangle\langle\hat{e}^\dagger_{p^c}\hat{e}_{r^e}\rangle \\ &= \mathcal{E}_{n^a r^e}\mathcal{E}_{p^c q^d} - \mathcal{E}_{n^a q^d}\mathcal{E}_{p^c r^e}.\end{aligned} \tag{5.35}$$

This decomposition holds exactly for $t = 0$ and the approximation is motivated by this fact. In our previous paper Ref. [29], we have only used the first term, and the second term, which describes the exchange effect, has been omitted.

As for the retarded potential term, since $\hat{j}^k_T$ is expressed as Eq. (5.11), it seems to have the same structure as the four-electron term. However, since $\hat{j}^k_T$ is computed at the retarded time and contains a time derivative of the excitation operator, the approximation like Eq. (5.35) is not applicable. Thus, we approximate this term by just replacing $\hat{j}^k_T$ by its expectation value as

$$\langle\hat{e}^\dagger_{n^a}(t)\hat{j}^k_T(cu,\vec{s})\hat{e}_{r^e}(t)\rangle \approx \langle\hat{j}^k_T(cu,\vec{s})\rangle\langle\hat{e}^\dagger_{n^a}(t)\hat{e}_{r^e}(t)\rangle = \mathcal{J}^k_T(cu,\vec{s})\mathcal{E}_{n^a r^e}(t), \tag{5.36}$$

where we define $\mathcal{J}_T^k \equiv \langle\Phi|\hat{j}_T^k|\Phi\rangle$. With this approximation, the two space integrations over $\vec{r}$ and $\vec{s}$ in the expectation value of the retarded term becomes that of c-number. In this six-dimensional integration, the retarded time u depends both on $\vec{r}$ and $\vec{s}$, so the integration has to be done numerically, which is not practical. To avoid the six-dimensional numerical integration, we rewrite the expression into the form in which the retarded time is eliminated. This is done by the same process as the one used to derive Eq. (5.14). Then, for the expectation value of the retarded term, we have

$$-\frac{1}{c^2}\sum_{r=1}^{N_D}\sum_{e=\pm}\sum_{k=1}^{3}\int d^3\vec{r}\,d^3\vec{s}\,j^k_{m^br^e}(\vec{r})\frac{\mathcal{J}_T^k(cu,\vec{s})}{|\vec{r}-\vec{s}|}\mathcal{E}_{n^ar^e}(t) = \sum_{r=1}^{N_D}\sum_{e=\pm} I_{j_T}[\mathcal{E},\dot{\mathcal{E}}]_{m^br^e}(t)\mathcal{E}_{n^ar^e}(t), \quad (5.37)$$

where we define

$$\begin{aligned} I_{j_T}[\mathcal{E},\dot{\mathcal{E}}]_{m^br^e}(t) &\equiv -\frac{1}{c^3\pi}\sum_{p,q=1}^{N_D}\sum_{c,d=\pm}\int_0^t du\int_{-\infty}^{\infty} d\alpha \exp\left(i\alpha(t-u)^2\right) \\ &\quad\times\left\{I_{jj,m^br^ep^cq^d}(\alpha)\mathcal{E}_{p^cq^d}(u) + I_{jE,m^br^ep^cq^d}(\alpha)\frac{d\mathcal{E}_{p^cq^d}}{dt}(u)\right\}, \quad (5.38) \end{aligned}$$

with

$$I_{jj,m^br^ep^cq^d}(\alpha) \equiv \sum_{k=1}^{3}\int d^3\vec{r}\,d^3\vec{s}\,j^k_{m^br^e}(\vec{r})j^k_{p^cq^d}(\vec{s})\exp\left(-i\alpha\frac{(\vec{r}-\vec{s})^2}{c^2}\right), \quad (5.39)$$

$$I_{jE,m^br^ep^cq^d}(\alpha) \equiv \sum_{k=1}^{3}\int d^3\vec{r}\,d^3\vec{s}\,j^k_{m^br^e}(\vec{r})E^k_{p^cq^d}(\vec{s})\exp\left(-i\alpha\frac{(\vec{r}-\vec{s})^2}{c^2}\right). \quad (5.40)$$

Here, we put $[\mathcal{E},\dot{\mathcal{E}}]$ after I_{j_T} for the notation of the integral (5.38) in order to emphasize that it depends on the density matrix and its time derivative at times earlier than t. Since the functions appearing in Eqs. (5.39) and (5.40) are defined by Eqs. (5.6) and (5.12), I_{jj} and I_{jE} are four-center integrals and analytic formulae can be obtained when the expansion functions of the Dirac field operator are gaussian functions. We show the integral formulae in the Appendix 5.5.

5.3.3 Radiation term

In this section, we describe two approximation methods for the expectation value of the radiation term. We first describe the simplest approximation method, which is same as the one adopted in Ref. [29]. In this approximation, we use

$$\langle\hat{e}^\dagger_{n^a}\hat{a}_{\vec{p}_\sigma}\hat{e}_{r^e}\rangle \approx \langle\hat{a}_{\vec{p}_\sigma}\rangle\langle\hat{e}^\dagger_{n^a}\hat{e}_{r^e}\rangle = \langle\hat{a}_{\vec{p}_\sigma}\rangle\mathcal{E}_{n^ar^e}, \quad (5.41)$$

and, similarly, $\langle \hat{e}^\dagger_{n^a} \hat{a}^\dagger_{\vec{p}_\sigma} \hat{e}_{r^e} \rangle \approx \langle \hat{a}_{\vec{p}_\sigma} \rangle^* \mathcal{E}_{n^a r^e}$. This factorization holds exactly for $t = 0$, when $\hat{e}_{n^a}$ and $\hat{a}_{\vec{p}_\sigma}$ commutes, and the approximation is motivated by this fact. We note that this term may give finite contribution only when the initial photon state is a coherent state, which is an eigenstate of the photon annihilation operator. Then, combined with the approximations described in the previous subsection, we obtain

$$\begin{aligned} i\hbar \mathcal{O}_{n^a m^b} &= \sum_{r=1}^{N_D} \sum_{e=\pm} h_{m^b r^e} \mathcal{E}_{n^a r^e} + \sum_{r,p,q=1}^{N_D} \sum_{e,c,d=\pm} (m^b r^e | p^c q^d) \left(\mathcal{E}_{n^a r^e} \mathcal{E}_{p^c q^d} - \mathcal{E}_{n^a q^d} \mathcal{E}_{p^c r^e} \right) \\ &+ \sum_{r=1}^{N_D} \sum_{e=\pm} I_{j_T}[\mathcal{E}, \dot{\mathcal{E}}]_{m^b r^e}(t) \mathcal{E}_{n^a r^e} \\ &- \frac{1}{\sqrt{2\pi^2 \hbar c}} \sum_{r=1}^{N_D} \sum_{e=\pm} \sum_{\sigma=\pm 1} \int \frac{d^3\vec{p}}{\sqrt{2p^0}} \left[\mathcal{F}_{m^b r^e \vec{p}_\sigma}(t) \langle \hat{a}_{\vec{p}_\sigma} \rangle \mathcal{E}_{n^a r^e} + \mathcal{F}^*_{r^e m^b \vec{p}_\sigma}(t) \langle \hat{a}_{\vec{p}_\sigma} \rangle^* \mathcal{E}_{n^a r^e} \right]. \end{aligned} \tag{5.42}$$

This gives us a closed differential equation for the density matrix.

In the second approximation method, we do not use the above factorization. We use evolution equation for the expectation value of the $\hat{e}^\dagger \hat{a} \hat{e}$-type operators simultaneously with one for the density matrix. We first define

$$\mathcal{E}_{n^a \vec{p}_\sigma m^b} \equiv \langle \Phi | \hat{e}^\dagger_{n^a} \hat{a}_{\vec{p}_\sigma} \hat{e}_{m^b} | \Phi \rangle. \tag{5.43}$$

Note that $\langle \Phi | \hat{e}^\dagger_{n^a} \hat{a}^\dagger_{\vec{p}_\sigma} \hat{e}_{m^b} | \Phi \rangle = \mathcal{E}^*_{m^b \vec{p}_\sigma n^a}$. We next define the expectation value of the operator $\hat{P}_{n^a \vec{p}_\sigma m^b}$, Eq. (5.27), as $\mathcal{P}_{n^a \vec{p}_\sigma m^b} \equiv \langle \Phi | \hat{P}_{n^a \vec{p}_\sigma m^b} | \Phi \rangle$. Similarly for the operator $\hat{Q}_{n^a \vec{p}_\sigma m^b}$, Eq. (5.28), we define $\mathcal{Q}_{n^a \vec{p}_\sigma m^b} \equiv \langle \Phi | \hat{Q}_{n^a \vec{p}_\sigma m^b} | \Phi \rangle$. Then, the expectation value of Eq. (5.24) can be written as

$$\begin{aligned} i\hbar \mathcal{O}_{n^a m^b} &= \sum_{r=1}^{N_D} \sum_{e=\pm} h_{m^b r^e} \mathcal{E}_{n^a r^e} + \sum_{r,p,q=1}^{N_D} \sum_{e,c,d=\pm} (m^b r^e | p^c q^d) \left(\mathcal{E}_{n^a r^e} \mathcal{E}_{p^c q^d} - \mathcal{E}_{n^a q^d} \mathcal{E}_{p^c r^e} \right) \\ &+ \sum_{r=1}^{N_D} \sum_{e=\pm} I_{j_T}[\mathcal{E}, \dot{\mathcal{E}}]_{m^b r^e}(t) \mathcal{E}_{n^a r^e} \\ &- \frac{1}{\sqrt{2\pi^2 \hbar c}} \sum_{r=1}^{N_D} \sum_{e=\pm} \sum_{\sigma=\pm 1} \int \frac{d^3\vec{p}}{\sqrt{2p^0}} \left[\mathcal{F}_{m^b r^e \vec{p}_\sigma}(t) \mathcal{E}_{n^a \vec{p}_\sigma r^e} + \mathcal{F}^*_{r^e m^b \vec{p}_\sigma}(t) \mathcal{E}^*_{r^e \vec{p}_\sigma n^a} \right], \end{aligned} \tag{5.44}$$

and the time evolution of $\mathcal{E}_{n^a \vec{p}_\sigma m^b}$ can be expressed as

$$\frac{\partial \mathcal{E}_{n^a \vec{p}_\sigma m^b}}{\partial t} = \mathcal{Q}^*_{m^b \vec{p}_\sigma n^a} + \mathcal{P}_{n^a \vec{p}_\sigma m^b}, \tag{5.45}$$

which is obtained by taking the expectation value of Eq. (5.26).

As for $\mathcal{P}_{n^a\vec{p}_\sigma m^b}$, the expectation value of the operator product in the second term of Eq. (5.29) is approximated to be

$$\langle \hat{e}^\dagger_{n^a}\hat{a}_{\vec{p}_\sigma}\hat{e}^\dagger_{p^c}\hat{e}_{q^d}\hat{e}_{r^e}\rangle \approx \langle \hat{a}_{\vec{p}_\sigma}\rangle \left\{ \langle \hat{e}^\dagger_{n^a}\hat{e}_{r^e}\rangle\langle \hat{e}^\dagger_{p^c}\hat{e}_{q^d}\rangle - \langle \hat{e}^\dagger_{n^a}\hat{e}_{q^d}\rangle\langle \hat{e}^\dagger_{p^c}\hat{e}_{r^e}\rangle \right\}. \tag{5.46}$$

In this approximation, we assume that the initial photon state is a number state and not a coherent state. Then, since $\langle \hat{a}_{\vec{p}_\sigma}\rangle = 0$, the contribution of this term vanishes. The third term of Eq. (5.29) includes the retarded time and its expectation value would be approximated in the same way as the retarded potential term of Eq. (5.24). Following the procedure described below Eq. (5.36), we have the expression of the form of Eq. (5.37) with $\mathcal{E}_{n^a r^e}(t)$ replaced by $\mathcal{E}_{n^a\vec{p}_\sigma r^e}(t)$. The forth term of Eq. (5.29) includes two four-operator terms, which are approximated to be

$$\langle \hat{e}^\dagger_{n^a}\hat{a}_{\vec{p}_\sigma}\hat{a}_{\vec{q}_\tau}\hat{e}_{r^e}\rangle \approx \langle \hat{a}_{\vec{p}_\sigma}\hat{a}_{\vec{q}_\tau}\rangle\langle \hat{e}^\dagger_{n^a}\hat{e}_{r^e}\rangle, \tag{5.47}$$

$$\langle \hat{e}^\dagger_{n^a}\hat{a}_{\vec{p}_\sigma}\hat{a}^\dagger_{\vec{q}_\tau}\hat{e}_{r^e}\rangle \approx \langle \hat{a}_{\vec{p}_\sigma}\hat{a}^\dagger_{\vec{q}_\tau}\rangle\langle \hat{e}^\dagger_{n^a}\hat{e}_{r^e}\rangle. \tag{5.48}$$

Since we do not consider a coherent state for the initial photon state as mentioned above, $\langle \hat{a}_{\vec{p}_\sigma}\hat{a}_{\vec{q}_\tau}\rangle = 0$ in the first equation and its contribution vanishes. In the second equation, since $\langle \hat{a}_{\vec{p}_\sigma}\hat{a}^\dagger_{\vec{q}_\tau}\rangle = (n_{\vec{p}_\sigma}+1)\delta^{(3)}(\vec{p}-\vec{q})\delta_{\sigma\tau}$, where $n_{\vec{p}_\sigma}$ is the occupation number of the photon mode $(\vec{p},\sigma)$ in the initial state, it may give a non-zero contribution. Putting these approximations together, we have

$$\begin{aligned} i\hbar\mathcal{P}_{n^a\vec{p}_\sigma m^b} &= \sum_{r=1}^{N_D}\sum_{e=\pm} h_{m^b r^e}\mathcal{E}_{n^a\vec{p}_\sigma r^e} + \sum_{r=1}^{N_D}\sum_{e=\pm} I_{j_T}[\mathcal{E},\dot{\mathcal{E}}]_{m^b r^e}(t)\mathcal{E}_{n^a\vec{p}_\sigma r^e} \\ &- \frac{1}{\sqrt{2\pi^2\hbar c}}\sum_{r=1}^{N_D}\sum_{e=\pm}\frac{1}{\sqrt{2p^0}}\mathcal{F}^*_{r^e m^b\vec{p}_\sigma}(t)(n_{\vec{p}_\sigma}+1)\mathcal{E}_{n^a r^e}, \end{aligned} \tag{5.49}$$

when we assume a number state for the photon initial state. The expectation value of Eq. (5.30) can be approximated in a similar manner to be

$$\begin{aligned} i\hbar\mathcal{Q}_{n^a\vec{p}_\sigma m^b} &= \sum_{r=1}^{N_D}\sum_{e=\pm} h_{m^b r^e}\mathcal{E}^*_{r^e\vec{p}_\sigma n^a} + \sum_{r=1}^{N_D}\sum_{e=\pm} I_{j_T}[\mathcal{E},\dot{\mathcal{E}}]_{m^b r^e}(t)\mathcal{E}^*_{r^e\vec{p}_\sigma n^a} \\ &- \frac{1}{\sqrt{2\pi^2\hbar c}}\sum_{r=1}^{N_D}\sum_{e=\pm}\frac{1}{\sqrt{2p^0}}\mathcal{F}_{m^b r^e\vec{p}_\sigma}(t)n_{\vec{p}_\sigma}\mathcal{E}_{n^a r^e}, \end{aligned} \tag{5.50}$$

where we have used $\langle \hat{a}^\dagger_{\vec{p}_\sigma}\hat{a}_{\vec{q}_\tau}\rangle = n_{\vec{p}_\sigma}\delta^{(3)}(\vec{p}-\vec{q})\delta_{\sigma\tau}$.

5.4 Results

In this section, we show the results of numerical solution of the time evolution equations which have been derived in the previous section. The computation is performed for a hydrogen atom and molecule using the QEDynamics code [44] developed in our group. In Sec. 5.4.1, we describe our setups for numerical calculation including the initial condition for the density matrix. The results of two approximation methods discussed in Sec. 5.3.3 are respectively presented in Sec. 5.4.2 and Sec. 5.4.3.

5.4.1 Setups for numerical calculation

To perform numerical calculation, we first need to determine an orthonormal set of expansion functions to define the electron creation and annihilation operators, as explained in Sec. 5.2.1. We generate the set by solving the Dirac equation with the four-component Dirac-Coulomb hamiltonian. They are computed by the publicly available program package DIRAC [38], using the Hartree-Fock method with the STO-3G basis set. Note that, for the hydrogen atom in this basis set, we have two ($= N_D$) orbitals for electron and positron respectively taking into account the Kramers partners. The density matrix is 4×4 matrix whose components denote electron (1^+), its Kramers partner ($\bar{1}^+$), positron (1^-), and its Kramers partner ($\bar{1}^-$). As shown here, we put a bar on the orbital number to denote the Kramers partner. Similarly, the size of the density matrix for the hydrogen molecule in this basis set is 8 ($N_D = 4$).

We next explain the initial condition for the density matrix. We choose the initial Heisenberg ket $|\Phi\rangle$ to be the ground states of the hydrogen atom and molecule, which are obtained by the above explained computation method. Namely, expressing $|\Phi\rangle = |\Phi_e\rangle \otimes |\Phi_{ph}\rangle$, where $|\Phi_e\rangle$ is the electron part and $|\Phi_{ph}\rangle$ is the photon part, we use $|\Phi_e\rangle = \hat{e}^\dagger_{1^+}|0\rangle$ for the hydrogen atom, and $|\Phi_e\rangle = \hat{e}^\dagger_{\bar{1}^+}\hat{e}^\dagger_{1^+}|0\rangle$ for the hydrogen molecule. In general, the ground state of a N_e-electron system in the Hartree-Fock method is expressed as $|\Phi_e\rangle = \prod_{i=1}^{N_e/2} \hat{e}^\dagger_{\bar{i}^+}\hat{e}^\dagger_{i^+}|0\rangle$ when N_e is even, and $|\Phi_e\rangle = \hat{e}^\dagger_{((N_e+1)/2)^+}\prod_{i=1}^{(N_e-1)/2} \hat{e}^\dagger_{\bar{i}^+}\hat{e}^\dagger_{i^+}|0\rangle$ when N_e is odd. For later use, we here introduce the terminology "occupied" orbitals. If $|\Phi_e\rangle$ contains $\hat{e}^\dagger_{i^+}$, the i-th electron orbital is called "occupied" (i can be with or without bar), and we can write $|\Phi_e\rangle = \prod_{i=\text{occupied}} \hat{e}^\dagger_{i^+}|0\rangle$. Then, using the anti-commutation relation, the initial condition

for the density matrix is

$$\mathcal{E}_{n^a m^b}(t=0) = \begin{cases} \delta_{nm} & (a=b=+,\ n:\text{occupied}) \\ \delta_{nm} & (a=b=-) \\ 0 & (\text{otherwise}) \end{cases} . \tag{5.51}$$

In particular, the vacuum expectation value at $t = 0$, which is needed to compute Eq. (5.34), is

$$\mathcal{E}^0_{n^a m^b}(t=0) = \begin{cases} \delta_{nm} & (a=b=-) \\ 0 & (\text{otherwise}) \end{cases} . \tag{5.52}$$

Other numerical details are as follows. We work in the atomic units so that $m_e = e = \hbar = 1$, and $c = 137.035999679$. The 1 a.u. of time corresponds to 2.419×10^{-17} s or 24.19 as. As for the positions of the atomic nuclei, we locate them at the origin in the case of the hydrogen atom, and at $(x, y, z) = (0, 0, \pm 0.7)$ in the case of the hydrogen molecule. For both hydrogen atom and molecule, we report the electronic charge density at $(x, y, z) = (0, 0, 1)$. To solve the differential equations, we use the Euler method with the time step 10^{-9} a.u. In this paper, we omit the contribution from the retarded potential by setting the integral $I_{j_T}[\mathcal{E}, \dot{\mathcal{E}}]$, Eq. (5.38), to be zero. This integral, including numerical integration, has to be computed at every time step, and performing this straightforwardly takes too much computational time. We shall study an effective approximation method in our future work, and just neglect it in the present work.

5.4.2 Effect of photon coherent state

In this section, we show the results when the first approximation method explained in Sec. 5.3.3 is adopted. Namely, we solve the time differential equation (5.32) using Eq. (5.42). As mentioned in the end of Sec. 5.4.1, the third term of Eq. (5.42), expressing the retarded potential, is neglected. As for the photon initial Heisenberg ket, when there is no radiation field, $|\Phi_{ph}\rangle = |0\rangle$, since $\langle \hat{a}_{\vec{p}\sigma} \rangle = 0$, the forth term of Eq. (5.42) is dropped. In fact, $\langle \hat{a}_{\vec{p}\sigma} \rangle = 0$ holds when $|\Phi_{ph}\rangle$ is any photon number state. We may have $\langle \hat{a}_{\vec{p}\sigma} \rangle \neq 0$ when $|\Phi_{ph}\rangle$ is a coherent state, and we study its effect in this section. Since we quantize the radiation field in the whole space, we consider the continuous-mode coherent state. Following the notation of Ref. [5], we denote it as $|\{\alpha\}\rangle$. This is characterized by the eigenvalues of the photon

annihilation operator of each mode $(\vec{p},\sigma)$ as

$$\hat{a}_{\vec{p}\sigma}|\{\alpha\}\rangle = \alpha(\vec{p},\sigma)|\{\alpha\}\rangle, \tag{5.53}$$

where $\alpha(\vec{p},\sigma)$ is called spectral amplitude [5]. In this paper, we use the delta-function type spectral amplitude and its center is chosen to be a mode $(\vec{p}_j,\sigma_j)$, as

$$\alpha(\vec{p},\sigma) = \alpha_j \delta^{(3)}(\vec{p}-\vec{p}_j)\delta_{\sigma\sigma_j}. \tag{5.54}$$

Such photon state corresponds to a classical oscillating electromagnetic field whose propagating direction is $\vec{p}_j$, direction of circularly polarization is σ_j, and amplitude is proportional to α_j. The period of the oscillations is determined by $p^0 = |\vec{p}_j|$ as $2\pi/(p^0 c)$.

We first show the results when there is no initial radiation field. The case of the hydrogen atom is shown in the upper panel of Fig. 5.1 and the case of the hydrogen molecule is in the upper panel of Fig. 5.2. In these figures, the variation of the electronic charge density from its initial value is plotted. The common feature is the oscillations with very short period of about 1.7×10^{-4} a.u. As has been argued in Ref. [29], since this is very close to the period which is determined from twice the mass of electron, $2\pi/(2m_e c^2) = 1.67 \times 10^{-4}$, it can be interpreted as the fluctuations originated from virtual electron-positron pair creations and annihilations. Hence, we call this phenomenon the "electron-positron oscillations" [29]. In Ref. [29], we show this using the hydrogen atom. In this paper, we show that the electron-positron oscillations occur similarly for the hydrogen molecule, and expect that we find them universally for any atomic and molecular systems.

We next show the results when the initial photon state is a coherent state. We choose its spectral amplitude to be the form expressed by Eq. (5.54) with $\vec{p}_j/|\vec{p}_j| = (1,0,0)$ and $\sigma_j = +1$. We compute the cases with $p^0 = 10$ and 20 for each hydrogen atom and molecule. The case of $p^0 = 10$ (20) is shown in the middle (lower) panel in Figs. 5.1 and 5.2. In these panels, we can see that the electron-positron oscillations with the short period are modulated by the longer period oscillations which are caused by the external oscillating electromagnetic field. In fact, the periods of the modulating oscillations seen in the panels for $p^0 = 10$ in both hydrogen atom and molecule are close to $2\pi/(p^0 c) = 4.59 \times 10^{-3}$ a.u. Similarly, in the panels for $p^0 = 20$, we see the periods of the modulating oscillations are close to $2\pi/(p^0 c) = 2.29 \times 10^{-3}$ a.u. We note that we have tuned the value of α_j for each case, in order to make these effects visible clearly. We have chosen $\alpha_j = 10^3$ (10^4) when

$p^0 = 10$ (20) for the hydrogen atom and $\alpha_j = 2 \times 10^4$ (10^5) when $p^0 = 10$ (20) for the hydrogen molecule.

We note that whether this "electron-positron oscillations" is a real physical phenomenon or an artifact of our model is an open question. We can say with certainty that the electron-positron oscillations are caused by including the positron solutions in our expansion functions for the Dirac field operator (so they do not take place if we model the electron by the Schrödinger field), and, in fact, $(1^+, 1^-)$-component of the density matrix oscillates in the case of the hydrogen atom simulation. However, it is also true that the results are obtained with several approximations and some ingredients of QED are missing. In particular, including the retarded potential may affect the electron-positron oscillations.

5.4.3 Effect of electron self-energy

In this section, we show the results when the second approximation method explained in Sec. 5.3.3 is adopted. Namely, we solve time differential equations (5.32) and (5.45) using Eqs. (5.44), (5.49) and (5.50). As in Sec. 5.4.2, the terms which originate from the retarded potential are neglected. As for the photon initial Heisenberg ket, we assume that there is no radiation field, $|\Phi_{ph}\rangle = |0\rangle$, in this section. Therefore, the occupation number is zero for every photon mode $(\vec{p}, \sigma)$, $n_{\vec{p}\sigma} = 0$. However, even in such a case, as is expressed by the factor $(n_{\vec{p}\sigma} + 1)$ in the third term of Eq. (5.49), every photon mode contributes to the radiation term. This is reasonable because, as is mentioned in the end of Sec. 5.2.3, this term comes from a self-energy process of the electron, in which the electron emits a virtual photon and then absorbs it again. This virtual photon could have any momentum.

Before showing our results, we explain here the numerical details regarding the discretization of the photon modes. We have to discretize the index $\vec{p}_\sigma$ in $\mathcal{E}_{n^a \vec{p}_\sigma m^b}$ to perform numerical calculation. We adopt the spherical coordinate system (p^0, θ, ϕ) to express $\vec{p}$ and use equally spaced grid points for each coordinate whose numbers are denoted by N_{p^0}, N_θ and N_ϕ respectively. One more parameter we need to specify is the maximum of p^0, denoted by $p^0_{\max}$. We first set $N_\theta = 5$ and $N_\phi = 4$, and compare the case with $(p^0_{\max}, N_{p^0}) = (10, 10)$ and the case with $(p^0_{\max}, N_{p^0}) = (20, 20)$. Since the results do not change, we adopt $(p^0_{\max}, N_{p^0}) = (10, 10)$ in the following. As for the choice of (N_θ, N_ϕ), the result with $(N_\theta, N_\phi) = (7, 8)$ is slightly different from the case with $(N_\theta, N_\phi) = (5, 4)$, but it is almost same as the result with

$(N_\theta, N_\phi) = (11, 10)$. Therefore, in summary, we adopt $(p^0_{\max}, N_{p^0}, N_\theta, N_\phi) = (10, 10, 11, 10)$ as the photon-mode discretization parameters.

The results are shown in Fig. 5.3, the upper panel for the hydrogen atom and the lower panel for the hydrogen molecule. As in Sec. 5.4.2, the variation of the electronic charge density from its initial value is plotted. In each panel, the solid red line shows the result without the self-energy process and the green dashed line shows one including the self-energy process. Note that computation for the case without the self-energy process is same as the one described in Sec. 5.4.2. However, in Fig. 5.3, the results are multiplied by 10^4 for the hydrogen atom and by 10^2 for the hydrogen molecule in order to make easy the comparison with the case including the self-energy process. In the figure, we see the electron-positron oscillations still take place when we include the self-energy process for both hydrogen atom and molecule. However, the period of the oscillations is slightly shorter than the case without the self-energy process. We have mentioned earlier that this rapid oscillations are originated from virtual electron-positron pair creations and annihilations and their period is inversely proportional to the electron mass. Therefore, decrease in the period implies increase in the electron mass. This is reasonable because the electron mass should be increased by including the self-energy process.

We note that this "increase" in the electron mass is not the physical reality. The self-energy of the electron is the interaction energy between the electron and the electromagnetic field which is originated from the electron itself [40, 42]. (It exists for either classical or quantum electrodynamics.) Since this is something we cannot remove from the electron, the total energy including the self-energy is considered to give the observed electron mass. This is the idea of the (mass) renormalization. Although the method of the renormalization is well-established for the ordinary perturbative QED, since it is based on the notion of the asymptotic states, which exist in the infinite past and future, it is not straightforwardly applicable to our QED simulation in which finite time evolution is followed. We have succeeded in extracting the self-energy of the electron in our simulation. Our next task is how to renormalize the "increase" in the electron mass, and this will be studied in our future work.

In the end of this section, we shall make comments on the self-energy effect. Although the change in the period of the electron-positron oscillations can be interpreted as the electron

mass shift due to the self-energy effect, one may wonder why the shift is not infinite as in the ordinary QED. One reason is that we have truncated the infinitely many hierarchy of time evolution equations of operators at the level of $\hat{e}^\dagger\hat{a}\hat{e}$-type operator. We would have a greater self-energy effect by considering the time evolution equation of higher order operators such as the $\hat{e}^\dagger\hat{a}\hat{a}^\dagger\hat{e}$-type operator, which appears in the last term of Eq. (5.29). Another reason is that we have only included localized wavepackets for the expansion functions in Eq. (5.1). During the self-energy process, when the electron emits the virtual photon, the electron could be in an unbounded state as a virtual particle, but such a state cannot be expressed by our present expansion functions. In order to improve this point, we may add plane wave functions to the expansion functions to express continuum modes.

5.5 Conclusion

In this paper, we have discussed a method to follow the step-by-step time evolution of atomic and molecular systems based on QED. Our strategy includes expanding the electron field operator by localized wavepackets to define creation and annihilation operators and following the time evolution using the equations of motion of the field operator in the Heisenberg picture. Under the BO approximation, we have first derived a time evolution equation for the excitation operator, which is the product of two creation or annihilation operators. We need this operator to construct operators of physical quantities such as the electronic charge density operator. We have then described our approximation methods to obtain time differential equations of the electronic density matrix, which is defined as the expectation value of the excitation operator.

In particular, we have presented two approximation methods for the expectation value of the radiation term, which includes the $\hat{e}^\dagger\hat{a}\hat{e}$-type operators. One is to factorize their expectation values into the expectation value of the excitation operator and that of the photon creation or annihilation operator, and has been used to study the effect of external oscillating electromagnetic field by setting the initial photon state as a coherent state. Another is to solve the time evolution equation of the $\hat{e}^\dagger\hat{a}\hat{e}$-type operators simultaneously with that of the excitation operator, which enables us to include the self-energy effect of the electron. By solving these equations numerically, we have shown the electron-positron

oscillations appear in the charge density of a hydrogen atom and molecule, for the cases both with and without including the self-energy process. We have also shown that the period of the electron-positron oscillations becomes shorter by including the self-energy process, and it can be interpreted as the increase in the electron mass due to the self-energy.

Although the results obtained in this paper can be reasonably interpreted so far, there are many things to incorporate for establishing the time evolution simulation method of atomic and molecular systems based on QED. Two important points which are not included in the present work are computation of the retarded potential and renormalization of the electron mass. As for the retarded potential, its computation is likely to be achieved by using the gaussian integral formulae which have been derived in the Appendix, although we need efficient approximation and storage methods. As for the electron mass renormalization, we shall develop a different method from that of the ordinary QED, because our renormalization should also be performed step-by-step in time. Specifically, we may need a time-dependent renormalization factor. These issues will be addressed in our future works and incorporated in our computation code.

Reference

[1] D. Bauer and P. Kobal, Comput. Phys. Commun. **174**, 396 (2006).

[2] G. R. Mocken and C. H. Keitel, Comput. Phys. Commun. **178**, 868 (2008).

[3] T. Iwasa and K. Nobusada, Phys. Rev. A **80**, 043409 (2009).

[4] C. J. Joachain, N. J. Kylstra, and R. M. Potvliege, *Atoms in Intense Laser Fields*, Cambridge University Press, New York, 2012.

[5] R. Loudon, *The Quantum Theory of Light*, Oxford University Press, New York, 2000.

[6] P. Meystre, *Atom Optics*, Springer-Verlag, New York, 2001.

[7] S. Haroche and J. M. Raimond, *Exploring the Quantum Atoms, Cavities and Photons*, Oxford University Press, New York, 2006.

[8] P. Krekora, K. Cooley, Q. Su, and R. Grobe, Phys. Rev. Lett. **95**, 070403 (2005).

[9] P. Krekora, Q. Su, and R. Grobe, Phys. Rev. A **73**, 022114 (2006).

[10] K. G. Dyall and K. Fægri, Jr., *Introduction to Relativistic Quantum Chemistry*, Oxford University Press, New York, 2007.

[11] M. Reiher and A. Wolf, *Relativistic Quantum Chemistry*, Wiley-VCH, Weinheim, 2009.

[12] I. Lindgren, *Relativistic Many-Body Theory*, Springer, New York, 2011.

[13] H. J. Kimble, Physica Scripta, **T76**, 127 (1998).

[14] J. Claudon et al., Nature Photon. **4**, 174 (2010).

[15] G. S. Buller and R. J. Collins, Meas. Sci. Technol. **21**, 012002 (2010).

[16] I. Aharonovich, S. Castelletto, D. A. Simpson, C. H. Su, A. D. Greentree and S. Prawer, Rep. Prog. Phys. **74**, 076501 (2011).

[17] M. Drescher, M. Hentschel, R. Kienberger, M. Uiberacker, V. Yakovlev, A. Scrinzi, Th. Westerwalbesloh, U. Kleineberg, U. Heinzmann, and F. Krausz, Nature **419**, 803 (2002).

[18] F. Krausz and M. Ivanov, Rev. Mod. Phys. **81**, 163 (2009).

[19] M. E. Peskin and D. V. Schroeder, *An Introduction to Quantum Field Theory*, Westview Press, Boulder, 1995.

[20] S. Weinberg, *The Quantum Theory of Fields: Volume I Foundations*, Cambridge University Press, Cambridge, 1995.

[21] S. Weinberg, *The Quantum Theory of Fields: Volume II Modern Applications*, Cambridge University Press, Cambridge, 1996.

[22] S. Weinberg, Phys. Lett. **B251**, 288 (1990).

[23] E. E. Salpeter and H. A. Bethe, Phys. Rev. **84**, 1232 (1951).

[24] H. Grotch and D. A. Owen, Foundations of Physics **32**, 1419 (2002).

[25] J. Rammer, *Quantum Field Theory of Non-equilibrium States*, Cambridge University Press, New York, 2007.

[26] E. A. Calzetta and B. B. Hu, *Nonequilibrium Quantum Field Theory*, Cambridge University Press, New York, 2008.

[27] H. Umezawa, *Advanced Field Theory*, AIP Press, New York, 1993

[28] A. Tachibana, Field Energy Density In Chemical Reaction Systems. In *Fundamental World of Quantum Chemistry, A Tribute to the Memory of Per-Olov Löwdin*, E. J. Brändas and E. S. Kryachko Eds., Kluwer Academic Publishers, Dordrecht (2003), Vol. II, pp 211-239.

[29] K. Ichikawa, M. Fukuda and A. Tachibana, Int. J. Quant. Chem. **113**, 190 (2013)

[30] W. H. Furry, Phys. Rev. **81**, 115 (1951).

[31] E. M. Lifshitz and L. P. Pitaevskiĭ, *Relativistic Quantum Theory Part 2*, Pergamon Press, Oxford, 1974.

[32] A. Tachibana, J. Chem. Phys. **115**, 3497 (2001).

[33] A. Tachibana, J. Mol. Struct. (THEOCHEM), **943**, 138 (2010).

[34] A. Tachibana, Electronic Stress with Spin Vorticity. In *Concepts and Methods in Modern Theoretical Chemistry*, S. K. Ghosh and P. K. Chattaraj Eds., CRC Press, Florida (2013), pp 235-251

[35] M. Senami, T. Miyazato, S. Takada, Y. Ikeda, and A. Tachibana, J. Phys.: Conf. Ser. **454**, 012052 (2013).

[36] M. Senami, Y. Ogiso, T. Miyazato, F. Yoshino, Y. Ikeda, and A. Tachibana, Trans. Mat. Res. Soc. Japan **38**, 535 (2013).

[37] M. Senami, S. Takada, and A. Tachibana, JPS Conf. Proc. **1**, 016014 (2014).

[38] DIRAC, a relativistic ab initio electronic structure program, Release DIRAC12 (2012), written by H. J. Aa. Jensen, R. Bast, T. Saue, and L. Visscher, with contributions from V. Bakken, K. G. Dyall, S. Dubillard, U. Ekström, E. Eliav, T. Enevoldsen, T. Fleig, O. Fossgaard, A. S. P. Gomes, T. Helgaker, J. K. Lærdahl, Y. S. Lee, J. Henriksson, M. Iliaš, Ch. R. Jacob, S. Knecht, S. Komorovský, O. Kullie, C. V. Larsen, H. S. Nataraj, P. Norman, G. Olejniczak, J. Olsen, Y. C. Park, J. K. Pedersen, M. Pernpointner, K. Ruud, P. Sałek, B. Schimmelpfennig, J. Sikkema, A. J. Thorvaldsen, J. Thyssen, J. van Stralen, S. Villaume, O. Visser, T. Winther, and S. Yamamoto (see http://www.diracprogram.org)

[39] L. D. Landau and E. M. Lifshitz, *The Classical Theory of Fields*, Butterworth-Heinemann, Oxford, 1987.

[40] J. D. Jackson, *Classical electrodynamics*, Wiley, New York, 1998.

[41] C. N. Yang and D. Feldman, Phys. Rev. **79**, 972 (1950).

[42] J. J. Sakurai, *Advanced Quantum Mechanics*, Addison-Wesley, New York, 1967.

[43] A. Tachibana, J. Mol. Model. **11**, 301 (2005).

[44] QEDynamics, M. Senami, K. Ichikawa and A. Tachibana
http://www.tachibana.kues.kyoto-u.ac.jp/qed/index.html

[45] L. E. McMurchie and E. R. Davidson, J. Comput. Phys. **26**, 218 (1978)

APPENDIX A: QED Hamiltonian operator and energy

The QED Hamiltonian density operator $\hat{H}_{\rm QED}(\vec{r})$ [28, 33] can be expressed by a sum of the electromagnetic field energy density operator $\hat{H}_{\gamma}(\vec{r})$ and the energy density operator of electron $\hat{H}_{e}(\vec{r})$ (Ref. [33], Eqs. (3.4) and (3.5)). The QED Hamiltonian operator can be written as

$$\begin{aligned}\int d^3\vec{r}\hat{H}_{\rm QED}(\vec{r}) &= \int d^3\vec{r}\left[\frac{1}{2}\hat{A}_0\hat{\rho}+\frac{1}{8\pi}\left(\frac{1}{c}\frac{\partial\hat{\vec{A}}}{\partial t}\right)^2-\frac{1}{8\pi}\hat{\vec{A}}\cdot\nabla^2\hat{\vec{A}}\right.\\ &\left.+c\hat{\bar{\psi}}\left\{-i\hbar\vec{\gamma}\cdot\left(\vec{\nabla}-i\frac{Z_e e}{\hbar c}\hat{\vec{A}}\right)+m_e c\right\}\hat{\psi}\right], \qquad (5.55)\end{aligned}$$

in the Coulomb gauge. This can be expressed using the creation and annihilation operators by substituting Eqs. (5.1), (5.7), (5.8), (5.9), and (5.10). Since the terms involving $\hat{\vec{A}}$ cannot be put in a simpler form due to the existence of the retarded time, we show the Hamiltonian operator expressed by the creation and annihilation operators under the electrostatic limit, namely $\hat{\vec{A}}=0$,

$$\begin{aligned}&\int d^3\vec{r}\hat{H}_{\rm QED,electrostatic}(\vec{r})\\ &=\sum_{n,m=1}^{N_D}\sum_{a,b=\pm}h_{n^a m^b}\hat{\mathcal{E}}_{n^a m^b}+\frac{1}{2}\sum_{n,m,p,q=1}^{N_D}\sum_{a,b,c,d=\pm}(n^a q^d|m^b p^c)\hat{e}^{\dagger}_{n^a}\hat{e}^{\dagger}_{m^b}\hat{e}_{p^c}\hat{e}_{q^d}, \qquad (5.56)\end{aligned}$$

where the coefficient matrices are defined in Eqs. (5.16) and (5.20). Here, we have excluded some terms which are infinite constants.

By taking the expectation value of the normal-ordered product of Eq. (5.56) with respect to the Heisenberg ket, we can obtain the energy of the system under the electrostatic limit,

$E_{\mathrm{QED,electrostatic}}$. When the Heisenberg ket is assumed to be the one introduced in Sec. 5.4.1, at $t = 0$, it gives the ordinary DHF energy as

$$E_{\mathrm{QED,electrostatic}} = \sum_{n=1}^{N_D} \sum_{a=\oplus} h_{n^a n^a} + \frac{1}{2} \sum_{n,m=1}^{N_D} \sum_{a,b=\oplus} \left\{ (n^a n^a | m^b m^b) - (n^a m^b | m^b n^a) \right\}, \quad (5.57)$$

where $\oplus$ denotes the occupied electron orbitals.

APPENDIX B: Molecular integral formulae for retarded potential term

When we compute the retarded potential term as described in Sec. 5.3.2, we need two types of four-center integrals shown in Eqs. (5.39) and (5.40). To our knowledge, gaussian integral formulae which are needed to compute them are not seen in literature. In the present paper, the retarded potential term is neglected as explained in Sec. 5.4, but we shall derive the formulae in this section for convenience of future works. The formulae and derivation here are based on a method described in Ref. [45].

Let us write an unnormalized gaussian function whose center is on $\vec{A}$ and exponent is α_A as

$$\tilde{g}(\vec{r}; \vec{A}, \alpha_A, \vec{n}) \equiv (x - A_x)^{n_x} (y - A_y)^{n_y} (z - A_z)^{n_z} e^{-\alpha_A |\vec{r} - \vec{A}|^2}. \quad (5.58)$$

Then, we need the integral of the form

$$\int d^3\vec{r}\, d^3\vec{s}\, \tilde{g}(\vec{r}; \vec{R}_i, \alpha_i, \vec{n}_i) \tilde{g}(\vec{r}; \vec{R}_j, \alpha_j, \vec{n}_j) \tilde{g}(\vec{s}; \vec{R}_k, \alpha_k, \vec{n}_k) \tilde{g}(\vec{s}; \vec{R}_l, \alpha_l, \vec{n}_l) \theta(\vec{r}, \vec{s}), \quad (5.59)$$

with $\theta(\vec{r}, \vec{s})$ being

$$\theta_{jj}(\vec{r}, \vec{s}; \alpha) \equiv \exp\left(-i\alpha \frac{|\vec{r} - \vec{s}|^2}{c^2} \right), \quad (5.60)$$

for Eq. (5.39), and

$$\theta^k_{jE}(\vec{r}, \vec{s}; \alpha) \equiv \int d^3\vec{t} \left\{ \frac{\partial}{\partial t^k} \frac{1}{|\vec{s} - \vec{t}|} \right\} \exp\left(-i\alpha \frac{|\vec{r} - \vec{t}|^2}{c^2} \right), \quad (5.61)$$

for Eq. (5.40). Note that this becomes the usual electronic repulsion integral when $\theta(\vec{r}, \vec{s}) = 1/|\vec{r} - \vec{s}|$. In the method of Ref. [45], in order to compute the integral of the form Eq. (5.59), we first need to compute

$$[000|\theta|000] = \int d^3\vec{r}\, d^3\vec{s} \exp\left(-\alpha_P |\vec{r} - \vec{P}|^2 \right) \exp\left(-\alpha_Q |\vec{s} - \vec{Q}|^2 \right) \theta(\vec{r}, \vec{s}), \quad (5.62)$$

where

$$\alpha_P = \alpha_i + \alpha_j, \tag{5.63}$$

$$\vec{P} = \frac{\alpha_i \vec{R}_i + \alpha_j \vec{R}_j}{\alpha_i + \alpha_j}, \tag{5.64}$$

$$\alpha_Q = \alpha_k + \alpha_l, \tag{5.65}$$

$$\vec{Q} = \frac{\alpha_k \vec{R}_k + \alpha_l \vec{R}_l}{\alpha_k + \alpha_l}, \tag{5.66}$$

and then compute

$$[NLM|\theta|N'L'M'] = \left(\frac{\partial}{\partial P_x}\right)^N \left(\frac{\partial}{\partial P_y}\right)^L \left(\frac{\partial}{\partial P_z}\right)^M \left(\frac{\partial}{\partial Q_x}\right)^{N'} \left(\frac{\partial}{\partial Q_y}\right)^{L'} \left(\frac{\partial}{\partial Q_z}\right)^{M'} [000|\theta|000]\,. \tag{5.67}$$

Finally, Eq. (5.59) is obtained by summation over N, L, M, N', L' and M' after multiplying $[NLM|\theta|N'L'M']$ by appropriate coefficients which depend on $\vec{n}_i$, $\vec{n}_j$, $\vec{n}_k$ and $\vec{n}_l$. Thus, we show below $[000|\theta|000]$ and $[NLM|\theta|N'L'M']$ for θ_{jj} and θ^k_{jE}.

We first consider the case of $\alpha = 0$. As for θ_{jj}, since $\theta_{jj}(\vec{r}, \vec{s}; \alpha = 0) = 1$, Eq. (5.59) is the product of two overlap integrals. As for θ_{jE}, Eq. (5.59) is shown to be divergent.

In the case of $\alpha \neq 0$, we can show that

$$[000|\theta_{jj}|000] = \pi^3 B^{-3/2} \exp\left(-\alpha_T |\vec{D}|^2\right), \tag{5.68}$$

$$\left[000|\theta^k_{jE}|000\right] = -4\pi^4 B^{-3/2} F_1(\alpha_T |\vec{D}|^2) D^k, \tag{5.69}$$

where

$$\vec{D} = \vec{P} - \vec{Q}, \tag{5.70}$$

$$A = \frac{i\alpha}{c^2}, \tag{5.71}$$

$$B = A(\alpha_p + \alpha_q) + \alpha_p \alpha_q, \tag{5.72}$$

$$C = \alpha_p \alpha_q A, \tag{5.73}$$

$$\alpha_T = \left(\frac{1}{\alpha_p} + \frac{1}{\alpha_q} + \frac{1}{A}\right)^{-1} = \frac{C}{B}, \tag{5.74}$$

and

$$F_j(T) = \int_0^1 u^{2j} \exp\left(-Tu^2\right) du, \tag{5.75}$$

is a function defined in Ref. [45] and its recursion formula is also discussed there.

The differentiation to derive $[NLM|\theta|N'L'M']$ can be done in a straightforward manner. As for θ_{jj}, we can show

$$\begin{aligned}[NLM|\theta_{jj}|N'L'M'] &= \pi^3 B^{-3/2} \exp\left(-\alpha_T |\vec{D}|^2\right) \alpha_T^{\frac{N+L+M+N'+L'+M'}{2}} (-1)^{N+L+M} \\ &\times H_{N+N'}(\alpha_T^{1/2} D_x) H_{L+L'}(\alpha_T^{1/2} D_y) H_{M+M'}(\alpha_T^{1/2} D_z), \end{aligned} \tag{5.76}$$

where $H_n(x)$ is a Hermite polynomial of degree n. As for θ_{jE}, we can show

$$\begin{aligned}\left[NLM|\theta^x_{jE}|N'L'M'\right] &= -4\pi^4 B^{-3/2} (-1)^{N'+L'+M'} \\ &\times \left\{ D_x \tilde{R}_{N+N',L+L',M+M'} + (N+N') \tilde{R}_{N+N'-1,L+L',M+M'} \right\}, \end{aligned} \tag{5.77}$$

$$\begin{aligned}\left[NLM|\theta^y_{jE}|N'L'M'\right] &= -4\pi^4 B^{-3/2} (-1)^{N'+L'+M'} \\ &\times \left\{ D_y \tilde{R}_{N+N',L+L',M+M'} + (L+L') \tilde{R}_{N+N',L+L'-1,M+M'} \right\}, \end{aligned} \tag{5.78}$$

$$\begin{aligned}\left[NLM|\theta^z_{jE}|N'L'M'\right] &= -4\pi^4 B^{-3/2} (-1)^{N'+L'+M'} \\ &\times \left\{ D_z \tilde{R}_{N+N',L+L',M+M'} + (M+M') \tilde{R}_{N+N',L+L',M+M'-1} \right\}, \end{aligned} \tag{5.79}$$

Here, we have defined

$$\tilde{R}_{NLM} = \left(\frac{\partial}{\partial D_x}\right)^N \left(\frac{\partial}{\partial D_y}\right)^L \left(\frac{\partial}{\partial D_z}\right)^M F_1(T), \tag{5.80}$$

where $T = \alpha_T (D_x^2 + D_y^2 + D_z^2)$. For generating a table of all $\tilde{R}_{NLM}$ up to some maximum $N+L+M$, recursion relations discussed in Ref. [45] can be applied. In particular, we can use the recursion relation for the more general integral R_{NLMj},

$$\begin{aligned} R_{NLMj} &= (-\alpha_T^{1/2})^{N+L+M} (-2\alpha_T)^j \\ &\times \int_0^1 u^{N+L+M+2j} H_N(\alpha_T^{1/2} D_x u) H_L(\alpha_T^{1/2} D_y u) H_M(\alpha_T^{1/2} D_z u) e^{-Tu^2} du, \end{aligned} \tag{5.81}$$

through the relation

$$\tilde{R}_{NLM} = \frac{R_{NLM1}}{-2\alpha_T}. \tag{5.82}$$

The details of the recursion relations and efficient numerical techniques are found in Ref. [45].

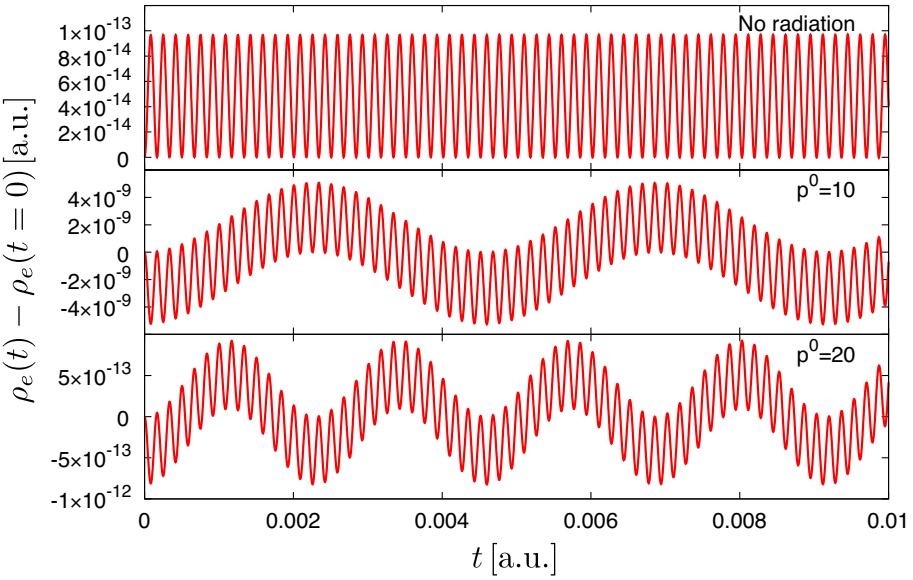

Figure 5.1: Time evolution of the charge density of the hydrogen atom at $(x, y, z) = (0, 0, 1)$. The variation from the initial value is plotted. The upper panel shows the result when there is no photon in the initial state. In the middle and lower panels, the initial photon states are chosen to be coherent states with the photon modes whose energy is $p^0 = 10$ and 20 respectively. In both cases, they are chosen to be circularly polarized in the positive direction and have momenta in the direction of x-axis positive. See the texts for other details.

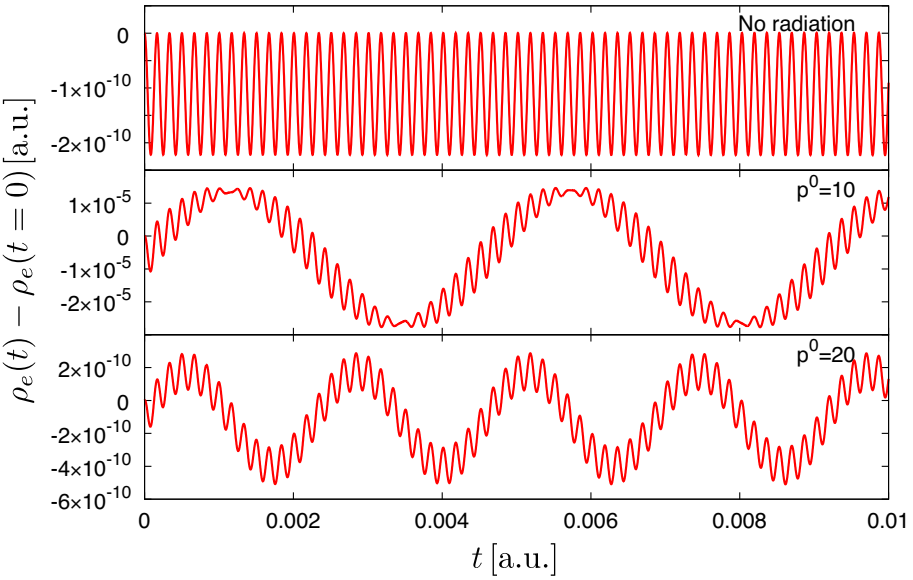

Figure 5.2: Similar to Fig. 5.1 for the hydrogen molecule.

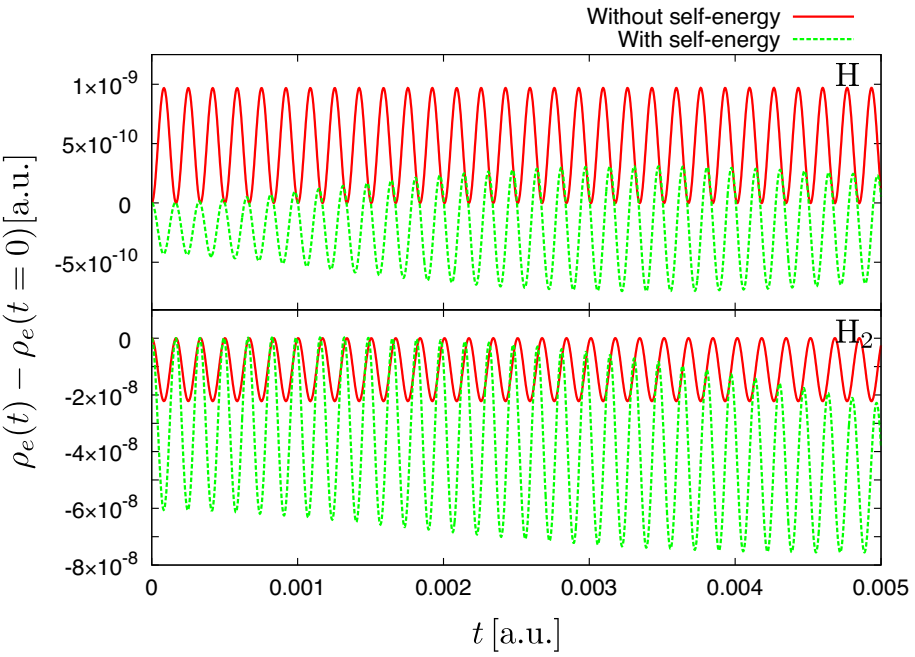

Figure 5.3: Time evolution of the charge density of the hydrogen atom (upper panel) and molecule (lower panel) at $(x, y, z) = (0, 0, 1)$. The variation from the initial value is plotted. There is no photon in the initial state. The cases without and with the self-energy process are respectively plotted by the red solid lines and green dashed lines in each panel. As for the case without the self-energy process, to make comparison easily, we plot the values which are multiplied by 10^4 for H and by 10^2 for H_2.

Chapter 6

Computational Method for the Retarded Potential in the Real-time Simulation of Quantum Electrodynamics

6.1 Introduction

Quantum electrodynamics (QED) is a quantum theory of fields which describes the interaction between photons and charged particles, such as electrons and positrons. The quantum field theory is conventionally solved using the covariant perturbation theory and this has succeeded in explaining many physical phenomena with very high accuracy. However, the perturbation theory is not suitable to follow the real-time evolution of the system. It can only compute such quantity as a cross section, which just measures difference between the infinite past and infinite future, not the time evolution step by step.

This is not so satisfactory because recent experiments can probe shorter and shorter time scale about the ultrafast electronic dynamics in matter [1]. This includes photophysical and photochemical processes, and the real-time observation of such processes as photoemission from atoms, molecules, and surfaces is now possible at the attosecond order [2]. Note that phenomena in which particle number changes, for instance photoemission, cannot be treated in a strict sense by quantum mechanics of point particles, and we need to use quantum field

theory for their rigorous treatment. This is because, while particle number is conserved in quantum mechanics of point particles, quantum field theory provides a framework in which it is allowed to change. Since photoemission involves photons, the quantum field theory we need is QED. Therefore, in order to compare theoretical prediction with these time-resolved experiments and future more precise experiments, we need a real-time simulation based on QED, and, for that purpose, a non-perturbative method has to be developed.

Some ingredients required for such a method have been discussed in Ref. [3] by one of the authors. There, it has been argued that, for the quantum field theoretic real-time simulation, it is not sufficient only to compute the time evolution of a wavefunction as is done in the quantum mechanics of point particles, but we also need to compute the time evolution of field operators (Heisenberg operators defined at each point in the spacetime) as well. These two types of time evolution are called the "dual Cauchy problem" of quantum field theory in Ref. [3], and we have to combine them to obtain time evolution of the expectation value of a quantum field operator corresponding to some physical quantity. Note that the Heisenberg ket vector is expressed by a linear combination of basis ket vectors whose coefficients are wavefunctions. The basis ket vectors in turn are constructed by operating appropriate field operators on the vacuum ket vector. The time evolutions of the wavefunctions and field operators cancel each other to make the Heisenberg ket time-independent. This paper concerns one of the issues regarding the time evolution of the field operators which appear in QED.

In the literature, a method for solving quantum field theory in Heisenberg picture has been developed by Abe and Nakanishi [4], with the special interest in the application for quantum gravity, in which the perturbation theory fails. Although the solution for QED is discussed in Ref. [5], their method is quite formal and not convenient for our numerical approach. In particular, the solution in Ref. [5] is given as the expansion in powers of the electromagnetic coupling constant (electron charge magnitude), which seems to be not truly non-perturbative. We wish to pursue a way to directly solve the quantum field equations of motion of QED by numerical means.

As for our approach, while theoretical developments are found in Refs. [6–10], we have been developing a prototype code for a real-time simulation based on QED in Refs. [11–13]. One of the important points we have dropped in Refs. [11, 12] is the retarded potential term

for the photon field. In other words, we have regarded the photon field as a free radiation field and ignored the contribution from the electric current generated by the electron dynamics. The reason why we could not have included such an important term is that we did not have a practical way to compute an oscillatory integral over the infinite interval involved in it. We shall report in this paper that there is an efficient method for such an integration [14, 15] based on so-called double exponential (DE) formula [16].

This paper is organized as follows. In Sec. 6.2, we briefly review the equations of motion of QED field operators, and the canonical commutation or anticommutation relations among them. In Sec. 6.3, we derive the evolution equation for the electron creation and annihilation operators, and describe how the integrations for the retarded potential arise. In Sec. 6.4, we show the results for the numerical integration of retarded potential terms using the DE formula. Finally, Sec. 6.5 is devoted to our conclusion.

6.2 Time evolution equations for the quantum fields

In this paper, there appear two types of quantum field operators, the four-component Dirac field operator $\hat{\psi}(x)$ for the electron and positron, and the $U(1)$ gauge field operator $\hat{A}_\mu(x)$ for the photon. (Incidentally, the approach to treat the electron as the two-component Schrödinger field [10] is also developed in our group. See Refs. [17–19] for details.) Their time evolutions are given by the Dirac equation and Maxwell equation. Since we assume the canonical quantization formalism, the quantum operators satisfy the equal-time commutation or anticommutation relations. Although these are textbook matters (*e.g.* [20]), we describe them briefly in this section to set up our notations. We work in the Gaussian systems of electromagnetic units. As for the physical constants, we use c for the speed of light in vacuum, $\hbar$ for the reduced Planck constant, e for the electron charge magnitude ($e > 0$), and m_e for the electron mass. The relativistic notations are as follows. The spacetime coordinate is expressed as $x = (x^\mu) = (x^0, x^i) = (ct, \vec{r})$, where the Greek index runs from 0 to 3 and the Latin index from 1 to 3. We adopt a convention that the repeated indices are summed, unless otherwise indicated. We use the metric tensor defined by $\eta_{\mu\nu} = \mathrm{diag}(1, -1, -1, -1) = \eta^{\mu\nu}$ for the transformation between contravariant and covariant vectors. The spacetime derivative is defined by $\partial_\mu = \frac{\partial}{\partial x^\mu} = \left(\frac{1}{c}\frac{\partial}{\partial t}, \vec{\nabla}\right)$. The gamma matrices

are denoted by γ^μ.

The Dirac equation in the covariant form is $i\hbar\gamma^\mu \hat{D}_{e\mu}(x)\hat{\psi}(x) = m_e c\hat{\psi}(x)$, where the gauge covariant derivative is defined by $\hat{D}_{e\mu}(x) = \partial_\mu + i\frac{Z_e e}{\hbar c}\hat{A}_\mu(x)$ with $Z_e = -1$, and this can be written as

$$i\hbar\frac{\partial}{\partial t}\hat{\psi}(x) = \left\{-i\hbar c\gamma^0\vec{\gamma}\cdot\vec{\nabla} - (Z_e e)\gamma^0\vec{\gamma}\cdot\hat{\vec{A}}(x) + m_e c^2\gamma^0 + (Z_e e)\hat{A}_0(x)\right\}\hat{\psi}(x). \quad (6.1)$$

As we adopt the Coulomb gauge, $\vec{\nabla}\cdot\hat{\vec{A}}(x) = 0$, the Maxwell equation is given by

$$\left(\frac{1}{c^2}\frac{\partial^2}{\partial t^2} - \nabla^2\right)\hat{\vec{A}}(x) = \frac{4\pi}{c}\hat{\vec{j}}_T(x), \quad (6.2)$$

where $\hat{\vec{j}}_T(x)$ is the transversal part of the charge current density operator $\hat{\vec{j}}(x)$:

$$\hat{\vec{j}}_T(x) = \hat{\vec{j}}(x) - \frac{1}{4\pi}\vec{\nabla}\frac{\partial}{\partial t}\hat{A}_0(x). \quad (6.3)$$

The scalar potential is given by

$$\hat{A}_0(ct,\vec{r}) = \int d^3\vec{s}\,\frac{\hat{\rho}(ct,\vec{s})}{|\vec{r}-\vec{s}|}, \quad (6.4)$$

where $\hat{\rho}(x)$ is the charge density operator, as the solution of the Poisson equation. Here, $\hat{\rho}(x)$ and $\hat{\vec{j}}(x)$ are given in terms of the Dirac field operator, respectively, by

$$\hat{\rho}(x) = Z_e e\hat{\psi}^\dagger(x)\hat{\psi}(x), \quad (6.5)$$

$$\hat{\vec{j}}(x) = Z_e\, e\, c\,\hat{\psi}^\dagger(x)\gamma^0\vec{\gamma}\hat{\psi}(x), \quad (6.6)$$

where the dagger is used to express Hermite conjugate.

The equal-time anticommutation relations for $\hat{\psi}(x)$ are

$$\left\{\hat{\psi}_\alpha(ct,\vec{r}),\hat{\psi}^\dagger_\beta(ct,\vec{s})\right\} = \delta^{(3)}(\vec{r}-\vec{s})\delta_{\alpha\beta}, \quad (6.7)$$

$$\left\{\hat{\psi}_\alpha(ct,\vec{r}),\hat{\psi}_\beta(ct,\vec{s})\right\} = 0, \quad (6.8)$$

$$\left\{\hat{\psi}^\dagger_\alpha(ct,\vec{r}),\hat{\psi}^\dagger_\beta(ct,\vec{s})\right\} = 0, \quad (6.9)$$

where $\alpha,\beta = 1,...,4$ are spinor indices and the curly brackets are the anticommutator so that $\{A,B\} = AB + BA$. The equal-time commutation relations for $\hat{\vec{A}}(x)$ consistent with the Coulomb gauge condition are

$$\left[\hat{A}^i(ct,\vec{r}),\hat{A}^j(ct,\vec{s})\right] = 0, \quad (6.10)$$

$$\left[\hat{E}^i_T(ct,\vec{r}),\hat{E}^j_T(ct,\vec{s})\right] = 0, \quad (6.11)$$

$$\frac{1}{4\pi c}\left[\hat{A}^i(ct,\vec{r}),\hat{E}^j_T(ct,\vec{s})\right] = i\hbar\eta^{ij}\delta^{(3)}(\vec{r}-\vec{s}) + i\hbar\frac{\partial}{\partial r^i}\frac{\partial}{\partial r^j}\left(-\frac{1}{4\pi}\cdot\frac{1}{|\vec{r}-\vec{s}|}\right), \quad (6.12)$$

where the square brackets are the commutator so that $[A, B] = AB - BA$, and $\hat{\vec{E}}_T(x)$ is the transversal part of the electric field operator:

$$\hat{\vec{E}}_T(x) = -\frac{1}{c}\frac{\partial \hat{\vec{A}}(x)}{\partial t}. \tag{6.13}$$

Finally, $\hat{\psi}(x)$ commutes with $\hat{\vec{A}}(x)$ at equal times:

$$\left[\hat{\psi}_\alpha(ct, \vec{r}), \hat{A}^i(ct, \vec{s})\right] = 0. \tag{6.14}$$

6.3 Time evolution of creation and annihilation operators

Time evolution equations of the quantum fields given by Eqs. (6.1) and (6.2) are very difficult to solve because not only they are nonlinear partial integro-differential equations but also they are equations for non-commutative operators which obey the commutation and anticommutation relations Eqs. (6.7)-(6.12) and (6.14). In this section, we describe our prescription to make the equations more tractable. Although there are some overlaps with the contents in Refs. [11, 12], we reproduce them in the reorganized form for the convenience of the readers.

Regarding $\hat{\psi}(x)$, we introduce creation and annihilation operators which carry the time dependence as follows [11, 12]. The field operator is expanded by a set of four-component orthonormal functions $\psi_{n^a}(\vec{r})$ as

$$\hat{\psi}(x) = \sum_{n=1}^{N_D} \sum_{a=\pm} \psi_{n^a}(\vec{r}) \hat{e}_{n^a}(t), \tag{6.15}$$

where $\int d^3\vec{r}\, \psi^\dagger_{n^a}(\vec{r}) \psi_{m^b}(\vec{r}) = \delta_{nm}\delta_{ab}$. In our notation, $a = +$ and $a = -$ represent electron and positron respectively, so that $\hat{e}_{n^+}$ is the electron annihilation operator and $\hat{e}_{n^-}$ is the positron creation operator. If the expansion functions are complete, the anticommutation relations Eqs. (6.7)-(6.9) lead to $\left\{\hat{e}_{n^a}(t), \hat{e}^\dagger_{m^b}(t)\right\} = \delta_{nm}\delta_{ab}$, $\{\hat{e}_{n^a}(t), \hat{e}_{m^b}(t)\} = 0$, $\left\{\hat{e}^\dagger_{n^a}(t), \hat{e}^\dagger_{m^b}(t)\right\} = 0$, respectively. Note that N_D, the number of the electron expansion function, has to be infinite to make the expansion function set complete. As we can only use a finite set in numerical computation, thus obtained results should be interpreted as phenomena within the finite subspace.

As for $\hat{\vec{A}}(x)$, we first consider the integrated form of the Maxwell equation (6.2) using the retarded Green function [7, 9]. The solution can be expressed by a sum of the radiation vector potential and the retarded potential as $\hat{\vec{A}}(ct,\vec{r}) = \hat{\vec{A}}_{\rm rad}(ct,\vec{r}) + \hat{\vec{A}}_A(ct,\vec{r})$, where

$$\hat{\vec{A}}_{\rm rad}(ct,\vec{r}) = \frac{\sqrt{4\pi\hbar^2 c}}{\sqrt{(2\pi\hbar)^3}} \sum_{\sigma=\pm 1} \int \frac{d^3\vec{p}}{\sqrt{2p^0}} \left[\hat{a}_{\vec{p}_\sigma} \vec{e}(\vec{p},\sigma) e^{-icp^0 t/\hbar} e^{i\vec{p}\cdot\vec{r}/\hbar} + \hat{a}^\dagger_{\vec{p}_\sigma} \vec{e}^{\,*}(\vec{p},\sigma) e^{icp^0 t/\hbar} e^{-i\vec{p}\cdot\vec{r}/\hbar} \right], \tag{6.16}$$

$$\hat{\vec{A}}_A(ct,\vec{r}) = \frac{1}{c} \int d^3\vec{s} \frac{\hat{\vec{j}}_T(cu,\vec{s})}{|\vec{r}-\vec{s}|}, \quad u = t - \frac{|\vec{r}-\vec{s}|}{c}. \tag{6.17}$$

In Eq. (6.16), $\vec{p}$ and σ denote the photon momentum and helicity respectively. The usual dispersion relation $p^0 = |\vec{p}|$ holds and the polarization vector $\vec{e}(\vec{p},\sigma)$ satisfies $\vec{p}\cdot\vec{e}(\vec{p},\sigma) = 0$, $\sum_{\sigma=\pm 1} e^i(\vec{p},\sigma) e^{*j}(\vec{p},\sigma) = -\eta^{ij} - \frac{p^i p^j}{|\vec{p}|^2}$, and $\sum_{k=1}^3 e^k(\vec{p},\sigma) e^{*k}(\vec{p},\tau) = \delta_{\sigma\tau}$. The photon annihilation operator $\hat{a}_{\vec{p}_\sigma}$ satisfies the commutation relations $[\hat{a}_{\vec{p}_\sigma}, \hat{a}_{\vec{q}_\tau}] = [\hat{a}^\dagger_{\vec{p}_\sigma}, \hat{a}^\dagger_{\vec{q}_\tau}] = 0$ and $[\hat{a}_{\vec{p}_\sigma}, \hat{a}^\dagger_{\vec{q}_\tau}] = \delta^{(3)}(\vec{p}-\vec{q})\delta_{\sigma\tau}$ to be consistent with Eqs. (6.10)-(6.12). Note that $\hat{a}_{\vec{p}_\sigma}$ is time-independent.

The integration of Eq. (6.17) contains the retarded time u, which reflects the fact that the speed of light (the maximum speed at which the information can be transmitted) is finite and we only use the information from the past. Since u depends on space variables, it is difficult to perform the integration in this form. We rewrite it using the delta function formulae with the causality ($\hat{\vec{j}}_T(cu,\vec{r}) = 0$ for $u > t$) and the initial condition ($\hat{\vec{j}}_T(cu,\vec{r}) = 0$ for $u < t_0$) as

$$\hat{\vec{A}}_A(ct,\vec{r}) = \frac{1}{c^2\pi} \int_{t_0}^{t} du' \int_{-\infty}^{\infty} d\alpha \int d^3\vec{s}\, \hat{\vec{j}}_T(cu',\vec{s}) \exp\left[i\alpha \left\{ (t-u')^2 - \frac{(\vec{r}-\vec{s})^2}{c^2} \right\} \right], \tag{6.18}$$

separating the time and space variables [3, 10]. The integration with respect to u' represents the accumulation of contributions from past data, and the integration with respect to α sweeps out the non-causal data. As for the initial condition, we note that we set the Cauchy problem of QED by assuming the synchronization of the clocks at different space points at $t = t_0$, when canonical quantization is performed with the definition of the vacuum ket vector $|0\rangle$. Hence, the vacuum and field operators are not defined for $t < t_0$.

We can express Eq. (6.18) with the creation and annihilation operators by using Eqs. (6.3), (6.4), (6.5), (6.6), and (6.15) as

$$\hat{A}^k_A(ct,\vec{r}) = \frac{1}{c^2\pi} \sum_{p,q=1}^{N_D} \sum_{c,d=\pm} \int_{t_0}^{t} du' \left\{ K^k_{j,p^c q^d}(\vec{r};t-u') \hat{\mathcal{E}}_{p^c q^d}(u') + K^k_{E,p^c q^d}(\vec{r};t-u') \frac{d\hat{\mathcal{E}}_{p^c q^d}}{dt}(u') \right\}, \tag{6.19}$$

where we define the frequently encountered combination of the operator $\hat{\mathcal{E}}_{p^c q^d}(t) = \hat{e}^\dagger_{p^c}(t)\hat{e}_{q^d}(t)$, and c-number integrals

$$K^k_{j,p^c q^d}(\vec{r};t-u') = \int_{-\infty}^{\infty} d\alpha\, I^k_{j,p^c q^d}(\vec{r};\alpha)\exp\left(i\alpha(t-u')^2\right), \tag{6.20}$$

$$K^k_{E,p^c q^d}(\vec{r};t-u') = \int_{-\infty}^{\infty} d\alpha\, I^k_{E,p^c q^d}(\vec{r};\alpha)\exp\left(i\alpha(t-u')^2\right). \tag{6.21}$$

Here, the integrals $I^k_{j,p^c q^d}(\vec{r};\alpha)$ and $I^k_{E,p^c q^d}(\vec{r};\alpha)$ are defined as

$$I^k_{j,p^c q^d}(\vec{r};\alpha) = \int d^3\vec{s}\, j^k_{p^c q^d}(\vec{s})\exp\left(-i\alpha\frac{(\vec{r}-\vec{s})^2}{c^2}\right), \tag{6.22}$$

$$I^k_{E,p^c q^d}(\vec{r};\alpha) = \int d^3\vec{s}\, E^k_{p^c q^d}(\vec{s})\exp\left(-i\alpha\frac{(\vec{r}-\vec{s})^2}{c^2}\right), \tag{6.23}$$

respectively using following functions

$$j^k_{p^c q^d}(\vec{s}) = Z_e\, e\, c\left[\psi^\dagger_{p^c}(\vec{s})\gamma^0\gamma^k\psi_{q^d}(\vec{s})\right], \tag{6.24}$$

$$E^k_{p^c q^d}(\vec{s}) = -\frac{Z_e e}{4\pi}\int d^3\vec{t}\,\psi^\dagger_{p^c}(\vec{t})\psi_{q^d}(\vec{t})\frac{(\vec{t}-\vec{s})^k}{|\vec{t}-\vec{s}|^3}. \tag{6.25}$$

Finally, we obtain the time evolution equation for the creation and annihilation operators by substituting the vector potential, (6.16) and (6.19), into the Dirac equation (6.1), and applying the expansion (6.15) as

$$\begin{aligned} i\hbar\frac{d\hat{e}_{n^a}}{dt}(t) &= \sum_{m=1}^{N_D}\sum_{b=\pm}(T_{n^a m^b} + M_{n^a m^b})\hat{e}_{m^b}(t) + \sum_{m,p,q=1}^{N_D}\sum_{b,c,d=\pm}(n^a m^b|p^c q^d)\hat{\mathcal{E}}_{p^c q^d}(t)\hat{e}_{m^b}(t) \\ &- \frac{1}{c^3\pi}\sum_{m,p,q=1}^{N_D}\sum_{b,c,d=\pm}\int_{t_0}^{t} du'\Bigg\{K_{jj,n^a m^b p^c q^d}(t-u')\hat{\mathcal{E}}_{p^c q^d}(u') \\ &\quad + K_{jE,n^a m^b p^c q^d}(t-u')\frac{d\hat{\mathcal{E}}_{p^c q^d}}{dt}(u')\Bigg\}\hat{e}_{m^b}(t) \\ &- \sqrt{\frac{1}{2\pi^2\hbar c}}\sum_{m=1}^{N_D}\sum_{b=\pm}\sum_{\sigma=\pm 1}\int\frac{d^3\vec{p}}{\sqrt{2p^0}}\left[\mathcal{F}_{n^a m^b\vec{p}_\sigma}(t)\hat{a}_{\vec{p}_\sigma} + \mathcal{F}^*_{m^b n^a\vec{p}_\sigma}(t)\hat{a}^\dagger_{\vec{p}_\sigma}\right]\hat{e}_{m^b}(t), \end{aligned} \tag{6.26}$$

where we define the kinetic energy integral $T_{n^a m^b} = -i\hbar c\int d^3\vec{r}\,\psi^\dagger_{n^a}(\vec{r})\gamma^0\gamma^k\partial_k\psi_{m^b}(\vec{r})$, the mass energy integral $M_{n^a m^b} = m_e c^2\int d^3\vec{r}\,\psi^\dagger_{n^a}(\vec{r})\gamma^0\psi_{m^b}(\vec{r})$, the two-electron-repulsion integral $(n^a m^b|p^c q^d) = (Z_e e)^2\int d^3\vec{r}\,d^3\vec{s}\,\psi^\dagger_{n^a}(\vec{r})\psi_{m^b}(\vec{r})\frac{1}{|\vec{r}-\vec{s}|}\psi^\dagger_{p^c}(\vec{s})\psi_{q^d}(\vec{s})$, and $\mathcal{F}_{n^a m^b\vec{p}_\sigma}(t) = \sum_{k=1}^{3} e^k(\vec{p},\sigma)e^{-icp^0 t/\hbar}F^k_{n^a m}$ which is defined using the Fourier transform of $j^k_{n^a m^b}(\vec{r})$, $F^k_{n^a m^b}(\vec{p}) \equiv \int d^3\vec{r}\, j^k_{n^a m^b}(\vec{r})e^{i\vec{p}\cdot\vec{r}/\hbar}$. In

Eq. (6.26), we also define integrals which originate from the interaction between the electronic current and retarded potential as

$$K_{jj,n^a m^b p^c q^d}(t-u') = \int_{-\infty}^{\infty} d\alpha\, I_{jj,n^a m^b p^c q^d}(\alpha) \exp\left(i\alpha(t-u')^2\right), \tag{6.27}$$

$$K_{jE,n^a m^b p^c q^d}(t-u') = \int_{-\infty}^{\infty} d\alpha\, I_{jE,n^a m^b p^c q^d}(\alpha) \exp\left(i\alpha(t-u')^2\right), \tag{6.28}$$

where

$$I_{jj,n^a m^b p^c q^d}(\alpha) = \sum_{k=1}^{3} \int d^3\vec{r}\, j^k_{n^a m^b}(\vec{r}) I^k_{j,p^c q^d}(\vec{r};\alpha) \tag{6.29}$$

$$= \sum_{k=1}^{3} \int d^3\vec{r}\, d^3\vec{s}\, j^k_{n^a m^b}(\vec{r}) j^k_{p^c q^d}(\vec{s}) \exp\left(-i\alpha\frac{(\vec{r}-\vec{s})^2}{c^2}\right), \tag{6.30}$$

$$I_{jE,n^a m^b p^c q^d}(\alpha) = \sum_{k=1}^{3} \int d^3\vec{r}\, j^k_{n^a m^b}(\vec{r}) I^k_{E,p^c q^d}(\vec{r};\alpha) \tag{6.31}$$

$$= \sum_{k=1}^{3} \int d^3\vec{r}\, d^3\vec{s}\, j^k_{n^a m^b}(\vec{r}) E^k_{p^c q^d}(\vec{s}) \exp\left(-i\alpha\frac{(\vec{r}-\vec{s})^2}{c^2}\right). \tag{6.32}$$

6.4 Numerical integration of retarded potential terms

As is described in the previous section, we have rewritten the coupled Maxwell-Dirac field equations into the evolution equation for the electron creation and annihilation operators, Eq. (6.26). That is, we have succeeded in converting the partial integro-differential equations for the quantum operators, which depend on space-time coordinate, into the ordinary integro-differential equation for the creation and annihilation operators, which carry only the time variable. While some of the coefficients of the evolution equation, $T_{n^a m^b}$, $M_{n^a m^b}$, $(n^a m^b|p^c q^d)$, and $F^k_{n^a m^b}(\vec{p})$, are well-known molecular integrals, $K_{jj,n^a m^b p^c q^d}$ and $K_{jE,n^a m^b p^c q^d}$ do not appear in the quantum chemistry computation using the electrostatic Hamiltonian. Below, we describe how we may practically compute them. Our computation assumes that the expansion functions $\psi_{n^a}(\vec{r})$ for the Dirac field operator to be expressed by a linear combination of Gaussian type orbitals. We use the DIRAC program package [21] to generate $\psi_{n^a}(\vec{r})$. The results are reported in the atomic units, in which the speed of light is $c = 137.035999679$ and 1 a.u. of time equals to 24.19 as.

We begin with the computation of $K_{jj,n^a m^b p^c q^d}$ defined by Eq. (6.27). As this integral depends on the parameter $t-u'$, which represents the difference between the present time

t and the past time u', if we want to perform a simulation from $t = t_0$ to $t = t_{end}$, we need $K_{jj,n^a m^b p^c q^d}$ with $t - u'$ ranging from 0 to t_{end}. Therefore, unless $t - u' = 0$, $K_{jj,n^a m^b p^c q^d}$ is an oscillatory integral over the infinite interval, which is in general difficult to make converge. In fact, although we have tried to use the Romberg integration of improper integrals such as found in Ref. [22] and the fast Fourier transform, these methods turn out to be not practical. Then, we have noticed that an efficient method for such a Fourier-type integral (the value of a Fourier transform at a particular point) has been developed in Ref. [14, 15] based on the DE formula [16], and its implementation is made publicly available by the developer [23]. We perform the integration with respect to α in Eq. (6.27) by using the Ooura's code, and the six-dimesional integration with respect to spatial coordinates in Eq. (6.30) by using the analytic formula explained in the Appendix 6.5.

The numerical results for $K_{jj,n^a m^b p^c q^d}$ as a function of $t - u'$ are shown in Fig. 6.1. The expansion functions are generated by solving the four-component Dirac equation with the Dirac-Coulomb Hamiltonian by the Hartree-Fock method and STO-3G basis set. We show the results for two types of expansion functions, which are respectively generated using H and He atoms. We note that, for these atoms in this basis set, there are two orbitals ($N_D = 2$) for electron and positron respectively taking into account the Kramers partners. In Fig. 6.1, all the ($4^4 = 256$) components of $K_{jj,n^a m^b p^c q^d}$ are plotted so that multiple lines are shown for each H and He. Since the imaginary part of $K_{jj,n^a m^b p^c q^d}$ is found to be zero for all the components, the real part is plotted. In the limiting case of $t - u' = 0$, we can analytically evaluate the integral to be zero (see Appendix 6.5). Also, for $t - u' \to \infty$, $K_{jj,n^a m^b p^c q^d}$ becomes zero owing to the Riemann-Lebesgue lemma. We see that our numerical results reproduce these behaviors at the limiting cases. We also notice that the value of $K_{jj,n^a m^b p^c q^d}$ decreases rapidly when $t - u'$ is larger than around 10^{-2}. This can be attributed to the fact that our expansion functions extend over about 1 a.u. and so does the source of the retarded potential. Note that $K_{jj,n^a m^b p^c q^d}(t - u')$ expresses the contribution to the retarded potential at the past time u', $t - u'$ before the present time t. Since the information is transmitted at the speed of light, there should be no contribution from the time before approximately $1/c$, that is, $(t - u') > O(10^{-2})$. This is supported by the result that $K_{jj,n^a m^b p^c q^d}(t - u')$ for He has a peak at smaller $t - u'$ than that of H, which is consistent with the less extended orbital of He than H (the exponent of the He basis set is about 1.9 times larger than that

of H).

The computation of $K_{jE,n^a m^b p^c q^d}$ defined by Eq. (6.28) is performed using the same technique as described above, and the result is shown in Fig. 6.2. Since the real part of $K_{jE,n^a m^b p^c q^d}$ is found to be zero for all the components, the imaginary part is plotted. Fig. 6.2 exhibits a similar pattern to Fig. 6.1, and this can be interpreted in a similar manner to that of $K_{jj,n^a m^b p^c q^d}$ as described above. We, however, have to remember that the integrand of $K_{jE,n^a m^b p^c q^d}$ contains a factor $I_{jE,n^a m^b p^c q^d}(\alpha)$ which diverges at $\alpha = 0$ like a delta function (Eq. (6.47) in Appendix 6.5). This contributes to $K_{jE,n^a m^b p^c q^d}$ as an indefinite constant term which in general depends on the component, but not on the spacetime coordinate. The result shown in Fig. 6.2 omits this possible contribution. We may determine this constant term by looking at other quantity such as the Hamiltonian operator but it is beyond the scope of the current paper.

6.5 Conclusion

In this paper, we have discussed the method to compute the integrals, denoted by K_{jj} and K_{jE}, which appear in the retarded potential term for a real-time simulation based on QED. We have shown that the oscillatory integrals over the infinite interval involved in them can be efficiently performed by the method developed by Ooura and Mori based on the DE formula. Now, we can set almost all the coefficients for the evolution equation of the electron creation and annihilation operators, Eq. (6.26). We, however, also have found that there seems to be an indefinite constant contribution to K_{jE}, which stems from the delta-function-like singularity in its integrand. How we may set the constant is not known at this stage, and we shall look for a way by investigating other quantity such as the Hamiltonian operator or using more sophisticated mathematical technique to treat the singularity.

Even if we find a way to fix the constant and obtain K_{jE}, there will be several issues in solving Eq. (6.26). One of them is a reasonable matrix representation of the creation and annihilation operators. This may be determined by using a method of constructing the basis ket vectors using newly found b-photon, f-electron, and f^c-positron field operators [3]. As they work for interacting theory, we do not have to invoke asymptotic fields to define a Fock space on which the creation and annihilation operators act, and non-perturbative

formulation is possible. Our next task would be to connect $\hat{e}_{n^a}(t)$ in this paper and b-photon, f-electron, and f^c-positron field operators introduced in Ref. [3].

Further issue is that, in addition to the time evolution of the quantum operators, we have to solve the other side of the dual Cauchy problem of QED as mentioned in the introduction. That is, the time evolution of the wavefunctions. In quantum field theory, we have to deal with the infinite series of wavefunctions, each of them representing a certain combination of fixed numbers of electrons, positrons and photons [3]. This is in contrast to the quantum mechanics of point particles, in which the particle number is conserved and only one wavefunction is needed. Such huge increase in the degree of freedom in quantum field theoretic computation would require some reduction techniques for a practical numerical implementation.

Our quantum field theoretic formulation for the real-time simulation based on QED requires a lot of ingredients which differ from those in the quantum mechanics of point particles based on the electrostatic Hamiltonian. In this paper, we have taken one step further to achieve our goal by showing the practical computational method for the integrations in the retarded potential in QED.

Reference

[1] F. Krausz and M. Ivanov, Rev. Mod. Phys. **81**, 163 (2009).

[2] R. Pazourek, S. Nagele, and J. Burgdörfer, Rev. Mod. Phys. **87**, 765 (2015).

[3] A. Tachibana, J. Math. Chem. **53**, 1943 (2015).

[4] N. Nakanishi, Prog. Theor. Phys. **111**, 301 (2004).

[5] M. Abe and N. Nakanishi, Prog. Theor. Phys. **88**, 975 (1992).

[6] A. Tachibana, J. Chem. Phys. **115**, 3497 (2001).

[7] A. Tachibana, Field Energy Density In Chemical Reaction Systems. In *Fundamental World of Quantum Chemistry, A Tribute to the Memory of Per-Olov Löwdin*, E. J. Brändas and E. S. Kryachko Eds., Kluwer Academic Publishers, Dordrecht (2003), Vol. II, pp 211-239.

[8] A. Tachibana, J. Mol. Model. **11**, 301 (2005).

[9] A. Tachibana, J. Mol. Struct. (THEOCHEM), **943**, 138 (2010).

[10] A. Tachibana, Electronic Stress with Spin Vorticity. In *Concepts and Methods in Modern Theoretical Chemistry*, S. K. Ghosh and P. K. Chattaraj Eds., CRC Press, Florida (2013), pp 235-251

[11] K. Ichikawa, M. Fukuda and A. Tachibana, Int. J. Quant. Chem. **113**, 190 (2013)

[12] K. Ichikawa, M. Fukuda and A. Tachibana, Int. J. Quant. Chem. **114**, 1567 (2014)

[13] QEDynamics, M. Senami, K. Ichikawa and A. Tachibana
http://www.tachibana.kues.kyoto-u.ac.jp/qed/index.html

[14] T. Ooura and M. Mori, J. Comput. Appl. Math. **112**, 229 (1999).

[15] T. Ooura, Publ. RIMS, Kyoto Univ. **41**, 971 (2005).

[16] H. Takahashi and M. Mori, Publ. RIMS Kyoto Univ. **9**, 721 (1974).

[17] M. Senami, T. Miyazato, S. Takada, Y. Ikeda, and A. Tachibana, J. Phys.: Conf. Ser. **454**, 012052 (2013).

[18] M. Senami, Y. Ogiso, T. Miyazato, F. Yoshino, Y. Ikeda, and A. Tachibana, Trans. Mat. Res. Soc. Japan **38**, 535 (2013).

[19] M. Senami, S. Takada, and A. Tachibana, JPS Conf. Proc. **1**, 016014 (2014).

[20] S. Weinberg, *The Quantum Theory of Fields: Volume I Foundations*, Cambridge University Press, Cambridge, 1995.

[21] DIRAC, a relativistic ab initio electronic structure program, Release DIRAC12 (2012), written by H. J. Aa. Jensen, R. Bast, T. Saue, and L. Visscher, with contributions from V. Bakken, K. G. Dyall, S. Dubillard, U. Ekström, E. Eliav, T. Enevoldsen, T. Fleig, O. Fossgaard, A. S. P. Gomes, T. Helgaker, J. K. Lærdahl, Y. S. Lee, J. Henriksson, M. Iliaš, Ch. R. Jacob, S. Knecht, S. Komorovský, O. Kullie, C. V. Larsen, H. S. Nataraj, P. Norman, G. Olejniczak, J. Olsen, Y. C. Park, J. K. Pedersen, M. Pernpointner, K. Ruud, P. Sałek, B. Schimmelpfennig, J. Sikkema, A. J. Thorvaldsen, J. Thyssen, J. van Stralen, S. Villaume, O. Visser, T. Winther, and S. Yamamoto (see http://www.diracprogram.org)

[22] W. H. Press, S. A. Teukolsky, W. T. Vetterling, and B. P. Flannery, *Numerical Recipes, Third edition*, Cambridge University Press, New York, 2007.

[23] Ooura's Mathematical Software Packages, T. Ooura
http://www.kurims.kyoto-u.ac.jp/~ooura/index.html

[24] L. E. McMurchie and E. R. Davidson, J. Comput. Phys. **26**, 218 (1978)

APPENDIX A: Molecular integral formulae for retarded potential term

In this appendix, we summarize the gaussian integral formulae to compute retarded potential terms. Specifically, we describe formulae to compute $I_{jj,n^a m^b p^c q^d}(\alpha)$, and $I_{jE,n^a m^b p^c q^d}(\alpha)$, which are respectively defined by Eqs. (6.30), and (6.32). Our formulae and derivation here are based on a method described in Ref. [24], and we mostly follow their notations. Although there are significant overlaps in this section with the appendix of Ref. [12], we reproduce them with the typos fixed for the convenience of the readers.

Since $I_{jj,n^a m^b p^c q^d}(\alpha)$ and $I_{jE,n^a m^b p^c q^d}(\alpha)$ are four-center integrals, we need to compute basic two-electron integrals

$$\begin{aligned}&[NLM|\theta|N'L'M'] \\ &= \left(\frac{\partial}{\partial P_x}\right)^N \left(\frac{\partial}{\partial P_y}\right)^L \left(\frac{\partial}{\partial P_z}\right)^M \left(\frac{\partial}{\partial Q_x}\right)^{N'} \left(\frac{\partial}{\partial Q_y}\right)^{L'} \left(\frac{\partial}{\partial Q_z}\right)^{M'} [000|\theta|000]\,, \end{aligned} \tag{6.33}$$

where

$$[000|\theta|000] = \int d^3\vec{r}\, d^3\vec{s}\, \exp\left(-\alpha_P|\vec{r}-\vec{P}|^2\right) \exp\left(-\alpha_Q|\vec{s}-\vec{Q}|^2\right) \theta(\vec{r},\vec{s}), \tag{6.34}$$

with $\theta(\vec{r},\vec{s})$ being

$$\theta_{jj}(\vec{r},\vec{s};\alpha) \equiv \exp\left(-i\alpha\frac{|\vec{r}-\vec{s}|^2}{c^2}\right), \tag{6.35}$$

for $I_{jj,n^a m^b p^c q^d}(\alpha)$, and

$$\theta^k_{jE}(\vec{r},\vec{s};\alpha) \equiv \int d^3\vec{t}\,\frac{(\vec{s}-\vec{t})^k}{|\vec{s}-\vec{t}|^3} \exp\left(-i\alpha\frac{|\vec{r}-\vec{t}|^2}{c^2}\right), \tag{6.36}$$

for $I_{jE,n^a m^b p^c q^d}(\alpha)$.

In the case of $\alpha \neq 0$, it is shown that

$$[000|\theta_{jj}|000] = \pi^3 B^{-3/2} \exp\left(-\alpha_T|\vec{D}|^2\right), \tag{6.37}$$

$$\left[000|\theta^k_{jE}|000\right] = -4\pi^4 B^{-3/2} F_1(\alpha_T|\vec{D}|^2) D^k, \tag{6.38}$$

where $\vec{D} = \vec{P}-\vec{Q}$, $A = i\alpha/c^2$, $B = A(\alpha_P+\alpha_Q)+\alpha_P\alpha_Q$, $C = \alpha_P\alpha_Q A$, $\alpha_T = (1/\alpha_P + 1/\alpha_Q + 1/A)^{-1} = C/B$, and

$$F_j(T) = \int_0^1 u^{2j} \exp\left(-Tu^2\right) du. \tag{6.39}$$

It is straightforward to differentiate Eqs. (6.37) and (6.38) to derive $[NLM|\theta|N'L'M']$. As for θ_{jj},

$$\begin{aligned}[NLM|\theta_{jj}|N'L'M'] &= \pi^3 B^{-3/2} \exp\left(-\alpha_T |\vec{D}|^2\right) \alpha_T^{\frac{N+L+M+N'+L'+M'}{2}} (-1)^{N+L+M} \\ &\times H_{N+N'}(\alpha_T^{1/2} D_x) H_{L+L'}(\alpha_T^{1/2} D_y) H_{M+M'}(\alpha_T^{1/2} D_z), \end{aligned} \tag{6.40}$$

where $H_n(x)$ is a Hermite polynomial of degree n. As for θ_{jE},

$$\begin{aligned}\left[NLM|\theta^x_{jE}|N'L'M'\right] &= -4\pi^4 B^{-3/2} (-1)^{N'+L'+M'} \\ &\times \left\{ D_x \tilde{R}_{N+N',L+L',M+M'} + (N+N') \tilde{R}_{N+N'-1,L+L',M+M'} \right\}, \end{aligned} \tag{6.41}$$

$$\begin{aligned}\left[NLM|\theta^y_{jE}|N'L'M'\right] &= -4\pi^4 B^{-3/2} (-1)^{N'+L'+M'} \\ &\times \left\{ D_y \tilde{R}_{N+N',L+L',M+M'} + (L+L') \tilde{R}_{N+N',L+L'-1,M+M'} \right\}, \end{aligned} \tag{6.42}$$

$$\begin{aligned}\left[NLM|\theta^z_{jE}|N'L'M'\right] &= -4\pi^4 B^{-3/2} (-1)^{N'+L'+M'} \\ &\times \left\{ D_z \tilde{R}_{N+N',L+L',M+M'} + (M+M') \tilde{R}_{N+N',L+L',M+M'-1} \right\}, \end{aligned} \tag{6.43}$$

where we have defined

$$\tilde{R}_{NLM} = \left(\frac{\partial}{\partial D_x}\right)^N \left(\frac{\partial}{\partial D_y}\right)^L \left(\frac{\partial}{\partial D_z}\right)^M F_1(T), \tag{6.44}$$

with $T = \alpha_T (D_x^2 + D_y^2 + D_z^2)$. For generating a table of all $\tilde{R}_{NLM}$ up to some maximum $N+L+M$, recursion relations discussed in Ref. [24] can be applied. In particular, we can use the recursion relation for the more general integral R_{NLMj},

$$\begin{aligned} R_{NLMj} &= (-\alpha_T^{1/2})^{N+L+M} (-2\alpha_T)^j \\ &\times \int_0^1 u^{N+L+M+2j} H_N(\alpha_T^{1/2} D_x u) H_L(\alpha_T^{1/2} D_y u) H_M(\alpha_T^{1/2} D_z u) e^{-Tu^2} du, \end{aligned} \tag{6.45}$$

through the relation $\tilde{R}_{NLM} = -R_{NLM1}/(2\alpha_T)$. The details of the recursion relations are found in Ref. [24], and our code used in this paper follows their prescriptions.

Let us now consider the case of $\alpha = 0$. The expressions we have derived above for the case of $\alpha \neq 0$, Eqs. (6.37) and (6.38), are finite at $\alpha = 0$. As $\alpha = 0$ implies $\alpha_T = 0$, the right-hand-sides of Eqs. (6.37) and (6.38) respectively become $\pi^3 (\alpha_P \alpha_Q)^{-3/2}$ and $-(4/3)\pi^4 (\alpha_P \alpha_Q)^{-3/2} D^k$. We, however, have to set $\alpha = 0$ before the integration, that is, to use $\theta_{jj}(\vec{r}, \vec{s}; \alpha = 0) = 1$ and $\theta^k_{jE}(\vec{r}, \vec{s}; \alpha = 0) = \int d^3\vec{t} \frac{(\vec{s}-\vec{t})^k}{|\vec{s}-\vec{t}|^3}$. As for θ_{jj}, Eq. (6.34) becomes the product of two overlap integrals, which leads to $(\pi/\alpha_P)^{3/2} \cdot (\pi/\alpha_Q)^{3/2}$, giving the same

result as setting $\alpha = 0$ in the right-hand-side expression of Eq. (6.37). As for θ_{jE}, Eq. (6.34) turns out to be divergent as

$$-4\pi^4(\alpha_P\alpha_Q)^{-3/2}i \times \lim_{\vec{l}\to\vec{0}} e^{-l^2/(4\alpha_Q)}e^{+i\vec{l}\cdot\vec{Q}}\,\frac{l^k}{l^2}. \tag{6.46}$$

Therefore, $I_{jE,n^am^bp^cq^d}(\alpha)$ has a delta-function-like structure as

$$I_{jE,n^am^bp^cq^d}(\alpha) = \bar{I}_{jE,n^am^bp^cq^d}(\alpha) + C_{n^am^bp^cq^d}\,\delta(\alpha), \tag{6.47}$$

where $\bar{I}_{jE,n^am^bp^cq^d}(\alpha)$ is a part constructed using the expression of Eq. (6.38) for whole range of α including $\alpha = 0$, and $C_{n^am^bp^cq^d}$ is an indefinite constant.

APPENDIX B: Analytic computation of $K_{jj,n^am^bp^cq^d}(t-u')$ for $t - u' = 0$

$K_{jj,n^am^bp^cq^d}(t-u')$ is defined by Eq. (6.27) and, when $t - u' = 0$, the integration can be done analytically as follows.

$$\begin{aligned}
K_{jj,n^am^bp^cq^d}(0) &= \int_{-\infty}^{\infty} d\alpha\, I_{jj,n^am^bp^cq^d}(\alpha), && (6.48)\\
&= \sum_{k=1}^{3}\int_{-\infty}^{\infty} d\alpha \int d^3\vec{r}\,d^3\vec{s}\, j^k_{n^am^b}(\vec{r})j^k_{p^cq^d}(\vec{s})\exp\left(-i\alpha\frac{(\vec{r}-\vec{s})^2}{c^2}\right), && (6.49)\\
&= 2\pi c^2\sum_{k=1}^{3}\int d^3\vec{r}\,d^3\vec{s}\, j^k_{n^am^b}(\vec{r})j^k_{p^cq^d}(\vec{s})\delta\left((\vec{r}-\vec{s})^2\right), && (6.50)\\
&= 2\pi c^2\sum_{k=1}^{3}\int d^3\vec{r}\int_0^{\infty} dR\int_0^{\pi} d\theta\int_0^{2\pi} d\phi R^2\sin\theta\, j^k_{n^am^b}(\vec{r})j^k_{p^cq^d}(\vec{r}+\vec{R})\delta\left(R^2\right), && (6.51)
\end{aligned}$$

where we have defined $\vec{R} = \vec{s} - \vec{r}$ and converted the integration over $\vec{s}$ into the integration over the polar coordinate (R, θ, ϕ) centered at $\vec{r}$. Then, this expression becomes zero upon the integration over R. Similarly, we can show $K_{jE,n^am^bp^cq^d}(0) = 0$.

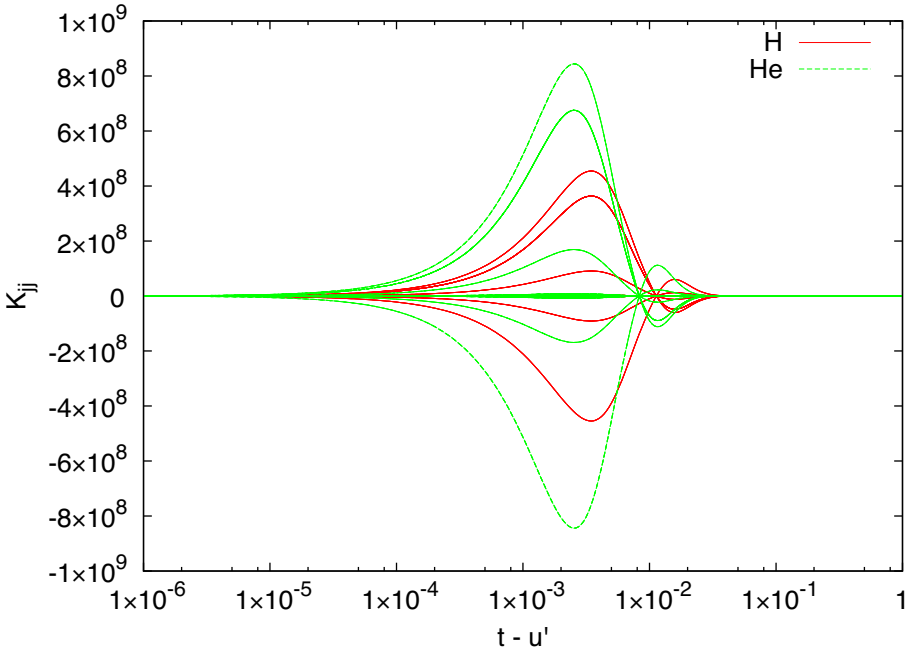

Figure 6.1: The real part of $K_{jj,n^a m^b p^c q^d}$ as a function of $t - u'$. All the components are plotted.

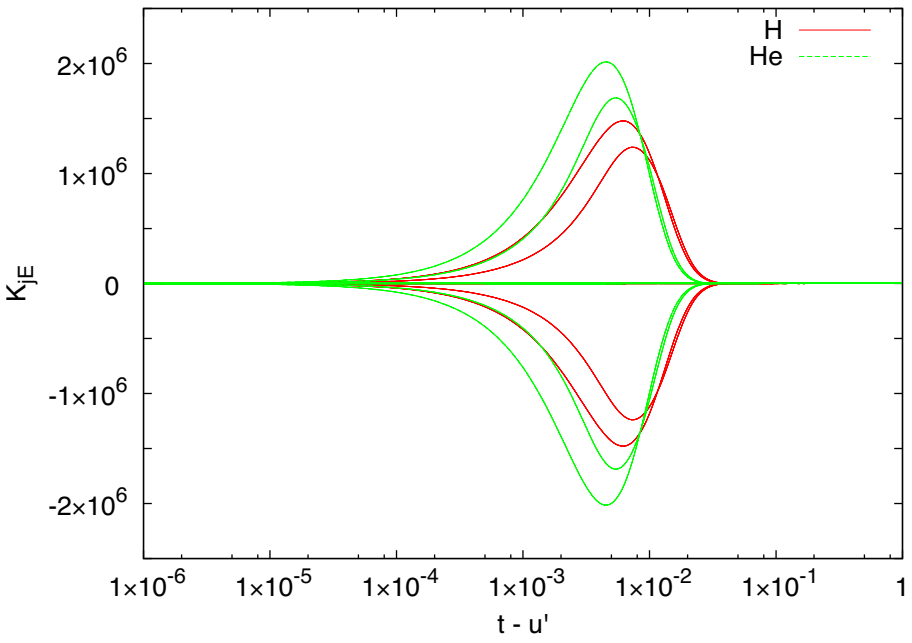

Figure 6.2: The imaginary part of $K_{jE,n^a m^b p^c q^d}$ as a function of $t - u'$. All the components are plotted.

General Conclusion

In this thesis, the local picture of electron spin and the time-evolution simulation method of operators have been studied on the basis of QED.

In Chapter 1, local physical quantities for spin in Li atom and C_6H_6 molecule have been investigated on the basis of the four- and two-component relativistic quantum theory. The cancellation between the nonzero zeta force and spin torque densities has been seen clearly in the singlet ground state of C_6H_6, even though the spin angular momentum density is zero over the whole region. Local physical quantities for each orbital also have been discussed, and it has been found the relativistic interaction can have a great influence on the local physical quantities, even if it has little effect on the orbital energies for a molecule. The relation between the zeta potential and the spatial symmetry of a concerning system has been discussed theoretically to grasp a feature of the zeta potential. The relation has been confirmed by the numerical calculation results. Furthermore, in order to avoid time and cost consuming computations of four-component relativistic wave packets, the formulation of the local physical quantities for spin by two-component relativistic ones has been discussed. It would pave a way to investigate the local physical quantities in large molecular systems.

In Chapter 2, the spin dynamics of the electron has been studied from the viewpoint of the EDM in the framework of the quantum field theory. Calculations of $\mathcal{E}_{\text{eff}}$ in YbF ($^2\Sigma_{1/2}$), BaF ($^2\Sigma_{1/2}$), ThO ($^3\Delta_1$), and HF^+ ($^2\Pi_{1/2}$) have been performed on the basis of RASCI. Moreover, it has been concluded that the large effective electric field is caused by the asymmetric distribution pattern of the small component of the spin angular momentum density. In addition, it has been shown that the local pictures of the spin and torque help us to understand some physical origin of spin phenomena.

In Chapter 3, application examples of the spin vorticity have been discussed. It has been found that half of the spin vorticity, which is introduced naturally as a component of the

electronic momentum density, plays an important role for spin transport phenomena. The generation of the spin vorticity in a local region by using a simple carbon chain attaching both edges to electrodes in the presence of a finite bias voltage has been demonstrated. Furthermore, the dynamical local picture of the spin Hall effect has been proposed on the basis of the quantum spin vorticity theory. These local pictures by the quantum spin vorticity theory would help us to understand spin phenomena in condensed matter and molecular systems from a unified viewpoint.

In Chapter 4 and 5, a method to follow step-by-step time evolution of atomic and molecular systems based on QED has been discussed. Some approximation methods to obtain time differential equations of the electronic density matrix have been described. Under this approximation, some numerical simulations of the time evolution of electron charge density of a hydrogen atom have been carried out, and it has been found that the electron-positron oscillations appear in the charge density of a hydrogen atom and molecule. In our time evolution simulation, the period of the electron-positron oscillations becomes shorter by including the self-energy process. It can be interpreted as the increase in the electron mass due to the self-energy.

In Chapter 6, the method to compute the integrals which appear in the retarded potential term for a space-time resolved simulation based on QED has been discussed. it has been found that the oscillatory integrals over the infinite interval involved in them can be efficiently performed by the method developed by Ooura and Mori on the basis of the double exponential formula.

In the series of these studies, local pictures of electron spin for some applications and a formulation of time-evolution simulation method in QED have been studied theoretically, These would pave a way to clarify time-evolved local pictures of a QED state.

Acknowledgements

I wish to express my gratitude to many people who helped me here. First, I am thankful to Professor Akitomo Tachibana for his guidance, valuable suggestions, discussions, and encouragement. Moreover, I also am grateful to Dr. Masato Senami, and Dr. Kazuhide Ichikawa for their valuable suggestions and discussions. I also thanks Dr. Akinori Fukushima, Dr. Yuji Ikeda, Mr. Takaaki Hara, Mr. Toshihide Miyazato, Mr. Hiroo Nozaki, Mr. Yoji Ogiso, Mr. Soujiro Takada, Mr. Kota Soga, Mr. Kento Naito, and Mr. Koki Taniuchi for their discussions to overcome difficulties. Parts of my studies are supported by the Grant-in-Aid for JSPS Fellows. Finally, I would like to express my gratitude to my parents for their continuing encouragement.

List of Publications

Chapter 1

[1] Masahiro Fukuda, Kota Soga, Masato Senami, and Akitomo Tachibana, "Local Physical Quantities for Spin Based on the Relativistic Quantum Field Theory in Molecular Systems", Int. J. Quant. Chem., published online. [DOI: 10.1002/qua.25102] (2016).

Chapter 2

[2] Masahiro Fukuda, Kota Soga, Masato Senami, and Akitomo Tachibana, "Local spin dynamics with the electron electric dipole moment", Phys. Rev. A **93**, 012518 (2016).

Chapter 3

[3] Masahiro Fukuda, Kazuhide Ichikawa, Masato Senami, and Akitomo Tachibana, "Dynamical picture of spin Hall effect based on quantum spin vorticity theory", AIP Advances **6**, 025108 (2016).

Chapter 4

[4] Kazuhide Ichikawa, Masahiro Fukuda, and Akitomo Tachibana, "Study of Simulation Method of Time Evolution in Rigged QED", Int. J. Quant. Chem., **113**, 190 (2013).

Chapter 5

[5] Kazuhide Ichikawa, Masahiro Fukuda, and Akitomo Tachibana, "Study of Simulation Method of Time Evolution of Atomic and Molecular Systems by Quantum Electrodynamics", Int. J. Quant. Chem., **114**, 1567 (2014).

Chapter 6

[6] Masahiro Fukuda, Kento Naito, Kazuhide Ichikawa, and Akitomo Tachibana, "Computational Method for the Retarded Potential in the Real-time Simulation of Quantum Electrodynamics", Int. J. Quant. Chem., published online. [DOI: 10.1002/qua.25103] (2016).

References

[7] Masahiro Fukuda, Masato Senami, and Akitomo Tachibana, "Spin Torque and Zeta Force in Allene Type Molecules", Advances in Quantum Methods and Applications in Chemistry, Physics, and Biology Progress in Theoretical Chemistry and Physics, Vol. 27; Eds. M. Hotokka, E. J. Brändas, J. Maruani, G. Delgado-Barrio; Springer, Chapter 7, pp. 131-139 (2013).

[8] Masahiro Fukuda, Masato Senami, Yoji Ogiso, and Akitomo Tachibana, "Local Spin Torque Induced by Electron Electric Dipole Moment in the YbF Molecule", AIP Conf. Proc., **1618**, 958 (2014).

[9] Masato Senami, Masahiro Fukuda, Yoji Ogiso, and Akitomo Tachibana, "Torque for Electron Spin Induced by Electron Permanent Electric Dipole Moment", AIP Conf. Proc., **1618**, 954 (2014).

[10] Masahiro Fukuda, Masato Senami, and Akitomo Tachibana, "Local physical quantities for spin in allene type molecules", J. Phys. Soc. Jpn., submitted for publication (2016).

Conference Appearances

- *Study of Simulation Method of Time Evolution in Rigged QED*,
  ○ Kazuhide Ichikawa, Masahiro Fukuda, Akitomo Tachibana,
  The 7th Congress of the International Society for Theoretical Chemical Physics 2011 (ISTCP-VII), Waseda University,Tokyo, Japan, 2-8 September 2011

- *Study of Numerical Simulation Method of Rigged QED* (in Japanese)
  ○Masahiro Fukuda, Kazuhide Ichikawa, Akitomo Tachibana,
  The 5th Annual Meeting of Japan Society for Molecular Science 2011, Hokkaido, Japan, 20–23 September 2011

- *Simulating time evolution in Rigged QED*,
  ○ Kazuhide Ichikawa, Masahiro Fukuda, Akitomo Tachibana,
  Fifth Asian Pacific Conference of Theoretical and Computational Chemistry (APCTCC 5), Novotel Royal Lakeside Rotorua, Rotorua, New Zealand, 9-13 December 2011

- *Numerical Simulation of Spin Dynamics Based on Quantum Electrodynamics* (in Japanese)
  ○Masahiro Fukuda, Kazuhide Ichikawa, Akitomo Tachibana,
  JPS the 67th Annual Meeting, Hyogo, Japan, 24–27 March 2012

- *Time-evolution Simulation of Motion of Nuclei by Rigged QED* (in Japanese)
  ○Kazuhide Ichikawa, Masahiro Fukuda, Akitomo Tachibana,
  The 15th Theoretical Chemistry Symposium, Miyagi, Japan, 24–26 May 2012

- *Numerical Simulation of Spin Dynamics Based on Rigged QED* (in Japanese)
  ○Masahiro Fukuda, Kazuhide Ichikawa, Akitomo Tachibana,
  The 15th Theoretical Chemistry Symposium, Miyagi, Japan, 24–26 May 2012

- *Formulation and simulation of time evolution in rigged QED*,
  ○ Kazuhide Ichikawa, Masahiro Fukuda, Akitomo Tachibana,
  14th International Congress of Quantum Chemistry, Boulder, Colorado, USA, 25-30 June 2012

- *Local spin torque of electron in atoms*,
  ○ Masahiro Fukuda, Masato Senami, Akitomo Tachibana,
  MAterial Simulation in Petaflops era (MASP2012), Tokyo University, Tokyo, Japan, 12-13 July 2012

- *Time evolution method in rigged QED: formulation and simulation*,
  ○ Kazuhide Ichikawa, Masahiro Fukuda, Akitomo Tachibana,
  The 23rd International Conference on Atomic Physics (ICAP 2012), Ecole Polytechnique, Palaiseau, France, 23-27 July 2012

- *Electron spin torque in atoms*,
  ○ Masato Senami, Masahiro Fukuda, Akitomo Tachibana,
  The 17th International Workshop on Quantum Systems in Chemistry and Physics (QCSP-XVIII), the Åbo Akademi University, Turky, Finland, 19-25 August 2012

- *Electron spin torque in transition element atoms*,
  ○ Masato Senami, Masahiro Fukuda, Akitomo Tachibana,
  The conference on Theory and Applications of Computational Chemistry (TACC2012), University of Pavia, Italy, 2-7 September 2012

- *Electron Spin Torque in Transition Metal* (in Japanese)
  Yuji Ikeda, Masato Senami, Akitomo Tachibana,
  The 73rd Autumn Meeting of the Japan Society of Applied Physics, Ehime, Japan, 11–14 September 2012

- *Time evolution of physical quantities in Rigged QED* (in Japanese)
  ○ Kazuhide Ichikawa, Masahiro Fukuda, Akitomo Tachibana,
  The 6th Annual Meeting of Japan Society for Molecular Science 2012, Tokyo, Japan, 18–21 September 2012

- *Theoretical study of electron spin dynamics by Rigged QED simulation* (in Japanese)
  ○Masahiro Fukuda, Kazuhide Ichikawa, Akitomo Tachibana,
  The 6th Annual Meeting of Japan Society for Molecular Science 2012, Tokyo, Japan, 18–21 September 2012

- *Picture of Electron Spin Torque in Atoms and Molecules* (in Japanese)
  ○Masahiro Fukuda, Masato Senami, Akitomo Tachibana,
  Yukawa Institute for Theoretical Physics Workshop "Physics of Quantum Spin Systems", Kyoto, Japan, 12–14 November 2012

- *Contribution of Self Energy of Electron Mass in Rigged QED* (in Japanese)
  ○Kazuhide Ichikawa, Masahiro Fukuda, Akitomo Tachibana,
  The 16th Theoretical Chemistry Symposium, Fukuoka, Japan, 15–17 May 2013

- *Theoretical Studies of Spin Torque Dynamics and Molecular Chirality Based on Rigged QED* (in Japanese)
  ○Masahiro Fukuda, Kazuhide Ichikawa, Akitomo Tachibana,
  The 16th Theoretical Chemistry Symposium, Fukuoka, Japan, 15–17 May 2013

- *Theoretical Study of Rigged QED in Curved Space* (in Japanese)
  ○Hidenori Miyamoto, Masahiro Fukuda, Kazuhide Ichikawa, Akitomo Tachibana,
  The 16th Theoretical Chemistry Symposium, Fukuoka, Japan, 15–17 May 2013

- *Study of Calculation Method of Time evolution in Atoms and Molecules Based on Qusantum Electrodynamics* (in Japanese)
  ○Kazuhide Ichikawa, Masahiro Fukuda, Akitomo Tachibana,
  The 10th Annual Meeting of AMO, Tokyo, Japan, 14–15 June 2013

- *Study of Calculation Method of Time evolution in Atomic and Molecular systems Based on Quantum Electrodynamics* (in Japanese)
  ○ Kazuhide Ichikawa, Masahiro Fukuda, Akitomo Tachibana,
  Yukawa Institute for Theoretical Physics Workshop "Thermal Quantum Field Theory and Their Applications", Kyoto, Japan, 15–17 Augast 2013

- *Effect of vector potential in time evolution simulation of Rigged QED* (in Japanese)
  ○Kazuhide Ichikawa, Masahiro Fukuda, Akitomo Tachibana,

The 7th Annual Meeting of Japan Society for Molecular Science 2013, Kyoto, Japan, 24–27 September 2013

- *Theoretical Study of Time Evolution of Local Quantities in Rigged QED* (in Japanese)
  ○Masahiro Fukuda, Kazuhide Ichikawa, Akitomo Tachibana,
  The 7th Annual Meeting of Japan Society for Molecular Science 2013, Kyoto, Japan, 24–27 September 2013

- *Study of Time Evolution Method of Atomic and Molecular Systems Based on Quantum Electrodynamics* (in Japanese)
  ○Kazuhide Ichikawa, Masahiro Fukuda, Akitomo Tachibana,
  JPS Autumn Meeting, Tokushima, Japan, 25–28 September 2013

- *Time evolution simulation of Rigged QED in Schwarzschild spacetime* (in Japanese)
  ○Hidenori Miyamoto, Masahiro Fukuda, Kazuhide Ichikawa, Akitomo Tachibana,
  The 7th Annual Meeting of Japan Society for Molecular Science 2013, Kyoto, Japan, 24–27 September 2013

- *Spin torque by electron electric dipole moment* (in Japanese)
  ○Yoji Ogiso, Masahiro Fukuda, Masato Senami, Akitomo Tachibana,
  The 7th Annual Meeting of Japan Society for Molecular Science 2013, Kyoto, Japan, 24–27 September 2013

- *Time Evolution of Atomic and Molecular Systems by Rigged QED*,
  ○ Kazuhide Ichikawa, Masahiro Fukuda, Akitomo Tachibana,
  The 5th JCS International Symposium on Theoretical Chemistry, Nara, Japan, 2-6 December 2013

- *Time Evolution Simulation of Electronic Spin Based on Quantum Electrodynamics*,
  ○ Masahiro Fukuda, Kazuhide Ichikawa, Akitomo Tachibana,
  The 5th JCS International Symposium on Theoretical Chemistry, Nara, Japan, 2-6 December 2013

- *Theoretical Study of the Local Torque for the Electron Spin* (in Japanese)
  ○Masahiro Fukuda, Yoji Ogiso, Masato Senami, Akitomo Tachibana,

The 19th Workshop on GateStack Technology and Physics, Shizuoka, Japan, 24–25 January 2014

- *Ab initio calculation of effective electric field for electron EDM experiments*,
  ○ Masahiro Fukuda, Kazuhide Ichikawa, Akitomo Tachibana,
  The 7th International conference on Fundamental Physics Using Atoms (FPUA 2014), Miraican Hall (7F), Miraikan, Odaiba, Tokyo, Japan, 14-16 March 2014

- *Local spin torque induced by electron electric dipole moment in the YbF molecule*,
  Masahiro Fukuda, ○ Masato Senami, Akitomo Tachibana,
  The 10th International Conference of Computational Methods in Sciences and Engineering (ICCMSE2014), Metropolitan Hotel, Athens, Greece, 4-7 April 2014

- *Torque for electron spin induced by electron permanent electric dipole moment*,
  ○ Masato Senami, Masahiro Fukuda, Akitomo Tachibana,
  The 10th International Conference of Computational Methods in Sciences and Engineering (ICCMSE2014), Metropolitan Hotel, Athens, Greece, 4-7 April 2014

- *Calculation of Retardation Potential Term in Four-component Rigged QED* (in Japanese)
  ○Kazuhide Ichikawa, Masahiro Fukuda, Akitomo Tachibana,
  The 17th Theoretical Chemistry Symposium, Nagoya, Japan, 22–24 May 2014

- *Numerical Simulation of Rigged QED under External Electromagnetic fields* (in Japanese)
  ○Masahiro Fukuda, Kazuhide Ichikawa, Akitomo Tachibana,
  The 17th Theoretical Chemistry Symposium, Nagoya, Japan, 22–24 May 2014

- *Time Evolution Simulation of atomic and molecular systems under Curved Space by Four-component Rigged QED* (in Japanese)
  ○Hidenori Miyamoto, Masahiro Fukuda, Kazuhide Ichikawa, Akitomo Tachibana,
  The 17th Theoretical Chemistry Symposium, Nagoya, Japan, 22–24 May 2014

- *Study of Thermalization in Four-component Rigged QED* (in Japanese)
  ○Kento Naito, Masahiro Fukuda, Kazuhide Ichikawa, Akitomo Tachibana,
  The 17th Theoretical Chemistry Symposium, Nagoya, Japan, 22–24 May 2014

- *Study of Effect of nuclear motion in Four-component Rigged QED Simulation* (in Japanese)
  ∘Koki Taniuchi, Masahiro Fukuda, Kazuhide Ichikawa, Akitomo Tachibana,
  The 17th Theoretical Chemistry Symposium, Nagoya, Japan, 22–24 May 2014

- *Spin Torque by Electron Electric Dipole Moment in Molecule* (in Japanese)
  ∘Masahiro Fukuda, Masato Senami, Akitomo Tachibana,
  JPS Autumn Meeting, Aichi, Japan, 7–10 September 2014

- *On the mass renormalization in the 4-component Rigged QED* (in Japanese)
  ∘Kazuhide Ichikawa, Masahiro Fukuda, Akitomo Tachibana,
  The 8th Annual Meeting of Japan Society for Molecular Science 2014, Hiroshima, Japan, 21–24 September 2014

- *Spin Vorticity and Spin Hall Effect* (in Japanese)
  ∘Masahiro Fukuda, Kazuhide Ichikawa, Akitomo Tachibana,
  The 8th Annual Meeting of Japan Society for Molecular Science 2014, Hiroshima, Japan, 21–24 September 2014

- *Study of numerical integration method of retarded potential term in 4-component rigged quantum electrodynamics* (in Japanese)
  ∘Kento Naito, Masahiro Fukuda, Kazuhide Ichikawa, Akitomo Tachibana,
  The 8th Annual Meeting of Japan Society for Molecular Science 2014, Hiroshima, Japan, 21–24 September 2014

- *Time Evolution of Local Quantities in External Electromagnetic Field Based on Rigged QED* (in Japanese)
  ∘Koki Taniuchi, Masahiro Fukuda, Kazuhide Ichikawa, Akitomo Tachibana,
  The 8th Annual Meeting of Japan Society for Molecular Science 2014, Hiroshima, Japan, 21–24 September 2014

- *Effective electric field and spin torque induced by electron electric dipole moment in the YbF molecule* (in Japanese)
  ∘Kota Soga, Masahiro Fukuda, Masato Senami, Akitomo Tachibana,

The 8th Annual Meeting of Japan Society for Molecular Science 2014, Hiroshima, Japan, 21–24 September 2014

- *Effect of electron electric dipole moment on the spin dynamics of the YbF molecule*,
  ○ Kota Soga, Masahiro Fukuda, Masato Senami, Akitomo Tachibana,
  Fourth Joint Meeting of the Nuclear Physics Divisions of the American Physical Society and The Physical Society of Japan, Hilton Waikoloa Village, Hawaii's Big Island, Hawaii, USA, 7-11 October 2014

- *Effective electric field of molecules of observation experiment of electron electric dipole moment*,
  ○ Masahiro Fukuda, Kota Soga, Masato Senami, Akitomo Tachibana,
  Fourth Joint Meeting of the Nuclear Physics Divisions of the American Physical Society and The Physical Society of Japan, Hilton Waikoloa Village, Hawaii's Big Island, Hawaii, USA, 7-11 October 2014

- *Spin Hall Effect and Quantum Spin Vorticity Principle*,
  ○ Masahiro Fukuda, Masato Senami, Kazuhide Ichikawa, Akitomo Tachibana,
  Novel Quantum States in Condensed Matter 2014, Kyoto, Japan, 17-21 November 2014

- *An Analysis Method for Physical Properties of Spintronics Devices by Local Spin Physical Quantities* (in Japanese)
  ○Masahiro Fukuda, Masato Senami, Akitomo Tachibana,
  20th Workshop on GateStack Technology and Physics, Shizuoka, Japan, 29–31 January 2015

- *Theoretical Study of Spin Phenomena Based on Quantum Spin Vorticity Principle* (in Japanese)
  ○Masahiro Fukuda, Masato Senami, Kazuhide Ichikawa, Akitomo Tachibana,
  JPS the 70th Annual Meeting, Tokyo, Japan, 21–24 March 2015

- *Time Evolution in QED: Time Evolution of Operators and Wavefunctions* (in Japanese)
  ○Kazuhide Ichikawa, Masahiro Fukuda, Akitomo Tachibana,
  The 18th Theoretical Chemistry Symposium, Osaka, Japan, 20–22 May 2015

- *Distribution and Origin of Local Spin Torque in Molecules* (in Japanese)
  ○Masahiro Fukuda, Kota Soga, Masato Senami, Akitomo Tachibana,
  The 18th Theoretical Chemistry Symposium, Osaka, Japan, 20–22 May 2015

- *Spin Torque Induced by Exsistence of Electron Electric Dipole Moment in Molecule* (in Japanese)
  ○Kota Soga, Masahiro Fukuda, Masato Senami, Akitomo Tachibana,
  The 18th Theoretical Chemistry Symposium, Osaka, Japan, 20–22 May 2015

- *Numerical Integrals by Double Exponential Formula in Retarded Potential Term in Four-component Rigged QED* (in Japanese)
  ○Ken Inada, Masahiro Fukuda, Kento Naito, Kazuhide Ichikawa, Akitomo Tachibana,
  The 18th Theoretical Chemistry Symposium, Osaka, Japan, 20–22 May 2015

- *Time evolution of Heisenberg operators and wave function in quantum electrodynamics* (in Japanese)
  ○Kazuhide Ichikawa, Masahiro Fukuda, Akitomo Tachibana,
  The 9th Annual Meeting of Japan Society for Molecular Science 2015, Tokyo, Japan, 16–19 September 2015

- *Local picture of relativistic electronic state Based on the spin vorticity principle* (in Japanese)
  ○Masahiro Fukuda, Kota Soga, Masato Senami, Akitomo Tachibana,
  The 9th Annual Meeting of Japan Society for Molecular Science 2015, Tokyo, Japan, 16–19 September 2015

- *Effective electric field and spin torque induced by electron electric dipole moment in molecules* (in Japanese)
  ○Kota Soga, Masahiro Fukuda, Masato Senami, Akitomo Tachibana,
  The 9th Annual Meeting of Japan Society for Molecular Science 2015, Tokyo, Japan, 16–19 September 2015

- *Numerical integration of the retarded potential term in time evolution simulation Based on QED* (in Japanese)
  ○Ken Inada, Masahiro Fukuda, Kento Naito, Kazuhide Ichikawa, Akitomo Tachibana,

The 9th Annual Meeting of Japan Society for Molecular Science 2015, Tokyo, Japan, 16–19 September 2015

- *Local Picture of Spin Based on the Spin Vorticity Theory* (in Japanese)
  ○Masahiro Fukuda, Masato Senami, Akitomo Tachibana,
  Annual Meeting of the Society of Electron Spin Science and Technology Niigata, Japan, 2–4 November 2015

- *Electron Spin Torque and Zeta Force in Molecules* (in Japanese)
  ○Kota Soga, Masahiro Fukuda, Masato Senami, Akitomo Tachibana,
  Annual Meeting of the Society of Electron Spin Science and Technology Niigata, Japan, 2–4 November 2015

- *Effective electric field for electron EDM in heavy polar diatomic molecules* ,
  ○ Masahiro Fukuda, Kota Soga, Masato Senami, Akitomo Tachibana,
  8th International conference on Fundamental Physics Using Atoms (FPUA 2015), Okochi Hall, RIKEN, Wako, Saitama, Japan, November 30 - December 1, 2015

- *Spin torque and zeta force in molecules and magnetic materials*,
  ○ Masato Senami, Masahiro Fukuda, Kota Soga, Akitomo Tachibana,
  Pacifichem 2015, Honolulu, Hawaii, USA, 15-20 December 2015